UNIVERSIDADE DA BEIRA INTERIOR
Ciências

miRNA-29 bioseparation and target delivery strategies for Alzheimer's disease

Patrícia Alexandra Nunes Pereira

Tese para obtenção do Grau de Doutor em
Bioquímica
(3º ciclo de estudos)

Orientadora: Prof.ª Doutora Fani Pereira de Sousa
Co-orientador(a): Prof.ª Doutora Ana Rita Figueiras
Prof. Doutor Ilídio Correia

Covilhã, abril de 2016

"Whether or not your efforts are smiled upon by fate,
what really matters in the end is to be able to say,
I did what I was able to"
Louis Pasteur

Aos meus Pais…

Por todo o amor, apoio incondicional e compreensão

Amo-vos

This work was financed by the Portuguese Foundation for Science and Technology (SFRH/BD/81914/2011) under the program QREN - POPH - Type 4.1 – Advanced Training, cofounded by the European Social Fund and by national funds from the MCTES. Moreover, this work was also supported in the framework of research and development projects (PTDC/EBB-BIO/114320/2009 and EXPL/BBB-BIO/1056/2012) and strategic programs (Pest-C/SAU/UI0709/2011 and Pest-OE/SAU/UI0709/2014) co-founded by the operational program factors of competitiveness – COMPETE (FCOMP-01-0124-FEDER-041068 – EXPL/QEQ-MED/1068/2013) and co-founded by FEDER funds (FCOMP-01-0124-FEDER-027560) of COMPETE.

Final version printed in April of 2016

Acknowledgments

First and foremost, I would like to express my sincere gratitude to my supervisors Professor Fani Sousa, Professor Ana Rita Figueiras and Professor Ilídio Correia, for all the careful guidance, valuable advice and trust. To Professor Fani Sousa my deepest appreciation for her valuable scientific knowledge and experiences shared during the last years. I would like to thanks for encouraging my research and for allowing me to grow as a research scientist. In addition, I am also grateful for believing in me, for her availability, dedication, help, motivation, unconditional support in difficult times, by the endless hours of conversation and especially for her friendship and patience, my very thanks to my " scientific mother "! To my co-supervisor Professor Ana Rita Figueiras my sincerely appreciation for her invaluable support, for the continuous guidance, help, availability, dedication, for all encouragement and especially for her friendship. It was a huge privilege working with you.

I would like to express my sincere gratitude to Professor João Queiroz for all the vast and valuable scientific knowledge that he transmitted me. I am really thankful for the availability, dedication and interest that he demonstrated for my work through the constructive scientific discussions and suggestions made during the development of the same, which were crucial for their success.

I would like to thanks to Professor Carla Cruz for her friendship, availability, help, support and interest demonstrated for my work through the scientific expertise provided, as well as for the trust in me through participation in her scientific projects. I would also like to thanks to Professor Cláudio Maia for the scientific expertise and valuable contribution throughout this thesis. To Professor Luís Passarinha, for his friendship, motivation, help and support, between a coffee and a laugh.

I'm deeply grateful to Fundação para a Ciência e Tecnologia (FCT) for the financial support through my PhD fellowship (SFRH/BD/81914/2011).

I also thank to all the people involved in Health Sciences Research Centre of the University of Beira Interior (CICS-UBI), especially to the Biotechnology and Biomolecular Sciences research group which cooperated in the development of this work. A special acknowledgment to the laboratory technicians Margarida Carrilho and Sofia Duarte that really cooperated for the successful development of this work and, especially for all the friendliness, availability, helpfulness and excellent moments of good humor.

To all my laboratory colleagues, specially Ângela Sousa, Eduarda Coutinho, Rita Martins, Margarida Almeida, Rita Videira, Helena Marcelino, Ana Martinho, Susana Ferreira and Filomena Silva, I would like to acknowledge all these people by their teachings, valuable

technical help, feedback, unspeakable patience, friendship, advice, support on the not so good times and willingness that contributed for this work to move forward. Thanks for all the great moments. Moreover, I am extremely thankful to Joana Tomás, who with her special expertise provided me with invaluable advice and encouragement. Your patience, support, friendship and collaboration were crucial for the success of this work, I sincerely thank you.

A very special thanks to Augusto Pedro, companion and friend, who supported me in good times and bad times, by their critical thinking that contributed significantly to the quality of this work, as well as, by your availability and help whenever I needed. For all your love, affection and friendship, and all the confidence placed in me, by the patience, advices and motivation throughout all the days of intensive work. We managed to overcome more this stage of our lives together, thank you my love.

Por último, e não menos importante, gostaria de agradecer de uma forma muito especial à minha família, por todo o amor, confiança e apoio nos tempos mais difíceis durante a minha formação acadêmica. Aos meus pais, por tornarem isto possível, por toda a vossa bondade e paciência, por me apoiarem sempre sem nunca duvidar e por entenderem as minhas inúmeras ausências. Estou-vos eternamente grata. Esta tese tem o vosso apoio incondicional, amor e carinho. Amo-vos.

Resumo Alargado

A recente descoberta da tecnologia do RNA de interferência tornou-se numa nova ferramenta que permite regular seletivamente o padrão de expressão de um ou mais genes, o que pode ser explorado no âmbito de aplicação terapêutica. Deste modo, os resultados promissores desta nova abordagem têm vindo a reforçar a investigação relacionada com o RNA, avaliando e compreendendo os mecanismos celulares em que está envolvido, com o objetivo de o usar como uma nova classe de produtos bioterapêuticos, de fácil translação e implementação para o âmbito clínico. Na verdade, o mecanismo celular responsável pelo silenciamento da expressão génica apresenta um enorme potencial terapêutico que poderá alterar os tratamentos atualmente disponíveis para diversas patologias, como por exemplo as doenças neurológicas.

Os microRNAs (miRNAs) constituem uma classe de RNAs de baixo peso molecular e, nos últimos anos, têm sido cada vez mais reconhecidos como moléculas endógenas reguladoras em numerosos processos biológicos. Devido à sua especificidade e eficiência, os miRNAs tornaram-se uma das ferramentas mais utilizadas no silenciamento de genes pelo mecanismo de RNA de interferência, uma vez que podem bloquear a síntese de proteínas através da indução da degradação do RNA mensageiro. Assim, os miRNAs podem ser considerados agentes terapêuticos promissores.

Durante a última década, a hipótese de que os miRNAs podem ser usados como biofármacos para regular e controlar várias vias envolvidas no desenvolvimento e progressão da doença de Alzheimer (DA) ganhou consistência, uma vez que estes apresentam um papel crucial em muitas funções neuronais, tais como diferenciação, plasticidade sináptica, formação da memória, e normalmente estão sub-expressos em doentes com esta patologia. A doença de Alzheimer é a forma mais comum de demência e caracteriza-se por uma perda neuronal e sináptica generalizada, que causa um declínio progressivo e irreversível em diversas funções cognitivas. Embora, as causas ainda não sejam completamente compreendidas, sabe-se que esta doença neurodegenerativa está associada ao aparecimento de dois tipos de agregados proteicos, nomeadamente placas extracelulares beta-amiloides (Aβ) e complexos neurofibrilares intraneuronais.

A formação das placas de Aβ resulta da clivagem sequencial da proteína percursora amiloide (APP) pela BACE1 e, posteriormente, pelo complexo gama-secretase dando origem às espécies Aβ tóxicas. Alguns estudos têm descrito uma relação causal entre a expressão do miR-29 e a DA, uma vez que a diminuição dos níveis de expressão da família miR-29 tem sido associada ao aumento da expressão da BACE1 e, consequentemente da formação dos péptidos Aβ em doentes com DA. Desta forma, a utilização do miR-29 pode proporcionar uma estratégia terapêutica eficaz na prevenção, controlo da progressão e tratamento desta patologia.

As terapêuticas baseadas no uso de miRNAs recorrem, na sua maioria, à utilização de miRNAs sintéticos. Embora a síntese de miRNAs possa ser muito eficiente, verifica-se normalmente a presença de contaminantes nas amostras de RNA sintetizado o pode levar à inespecificidade do silenciamento génico. Além disso, por norma, no processo de preparação do RNA sintético é necessário recorrer à utilização de solventes tóxicos, solventes orgânicos e condições desnaturantes, que podem comprometer a qualidade e integridade do produto alvo. Por todos estes motivos, e considerando o objetivo de aplicação terapêutica destes novos produtos biofarmacêuticos, torna-se evidente a necessidade de desenvolver novos processos eficientes ou melhorar as metodologias atualmente empregues para a sua preparação. Assim, um dos desafios mais importantes no desenvolvimento destas estratégias terapêuticas surge com a necessidade de produzir miRNA com elevado grau de pureza e atividade biológica, de modo a satisfazer os requisitos necessários à sua aplicação. Deste modo, uma das estratégias que pode ser aplicada consiste na produção recombinante de biomoléculas utilizando hospedeiros procarióticos.

Desta forma, o objetivo principal do presente trabalho consiste no desenvolvimento e implementação de uma plataforma biotecnológica para a produção e purificação de precursores de miRNAs, em particular o pre-miR-29b (percursor do miR-29), cuja aplicação visa o silenciamento seletivo de vias endógenas diretamente relacionados com DA, nomeadamente a BACE1 e os péptidos Aβ. Paralelamente, serão desenvolvidas e caracterizadas nanopartículas poliméricas para a entrega do pre-miR-29b no citoplasma de células neuronais de forma seletiva e eficaz, de modo a assegurar o sucesso destas administrações.

O sistema de expressão recombinante utilizado permitirá, pela primeira vez, a produção e o isolamento do pre-miR-29b humano na bactéria *Rhodovulum sulfidophilum* (*R. sulfidophilum*) DSM 1374, mantendo a sua atividade biológica. A utilização deste hospedeiro bacteriano é inovadora e vantajosa, devido à sua capacidade invulgar de secretar os ácidos nucleicos para o meio de cultura, bem como devido à ausência de ribonucleases no mesmo, permitindo a obtenção do miRNA de interesse com baixo conteúdo de impurezas bacterianas. A fim de otimizar a produção e acumulação de miRNAs no espaço extracelular, as condições de crescimento foram estudadas, nomeadamente no que diz respeito ao efeito da temperatura e concentração de cloreto de sódio. Os ensaios realizados demonstraram ser possível desenvolver um protocolo para o crescimento aeróbio da bactéria *R. sulfidophilum*, na ausência de luz, a 30ºC, o que resulta num melhoramento do crescimento das células, seguido de um aumento da produção do pre-miR-29b humano. Neste trabalho foi possível atingir uma concentração de pre-miR-29b no meio extracelular de aproximadamente 182 μg/L, após 40 horas de crescimento bacteriano e uma concentração de 358 μg/L de pre-miR-29b intracelular, após 32 horas de fermentação.

Para que seja possível a aplicação terapêutica do pre-miR-29b é necessário ter em conta as exigências estabelecidas pelas agências reguladoras internacionais, que requerem a produção de miRNA com elevada qualidade e atividade biológica. Para assegurar esta condição, foram desenvolvidas novas estratégias de purificação para o pre-miR-29b, baseadas em cromatografia de afinidade. A fim de alcançar a máxima seletividade e especificidade na separação do pre-miRNA de outras biomoléculas do hospedeiro (outras espécies de RNA e proteínas), foram desenvolvidos suportes de afinidade baseados nas interações biológicas que são estabelecidas a nível celular, usando como ligandos de afinidade, aminoácidos básicos como a L-lisina e a L-arginina. Na estratégia de purificação com o aminoácido de L-lisina foi demonstrada pela primeira vez a purificação de pre-miRNA utilizando um gradiente decrescente de concentração de sulfato de amónio em três passos, o que permitiu explorar maioritariamente interações hidrofóbicas. Contudo, a necessidade de aplicar elevadas concentrações de sal pode ser visto como uma desvantagem devido aos custos e ao impacto ambiental associado ao processo, principalmente no que diz respeito à aplicação ao nível industrial. De modo a ultrapassar estas limitações foi usada L-arginina como aminoácido imobilizado. Este estudo demonstrou a possibilidade de purificar o pre-miR-29b utilizando três estratégias diferentes de eluição, nomeadamente concentrações decrescentes de sulfato de amónio e duas condições de eluição moderadas, tais como usando um gradiente crescente de cloreto de sódio e a adição de um agente de competição (arginina) ao tampão de eluição. A versatilidade da matriz de arginina na purificação do pre-miR-29b sugeriu que o mecanismo de interação envolveria uma multiplicidade de interações não-covalentes, que globalmente resultam no bioreconhecimento do RNA de interesse. O reconhecimento bioespecífico e seletivo do pre-miR-29b por estes suportes cromatográficos permitiu a sua purificação e recuperação de forma eficiente, com elevados rendimentos, grau de pureza e integridade, a partir de uma mistura complexa. Além disso, a utilização da cromatografia de afinidade com arginina resultou na eliminação das impurezas associadas à produção recombinante, nomeadamente proteínas e endotoxinas, respeitando os critérios estabelecidos pelas agências reguladoras (por exemplo "Food and Drug Administration" – FDA). Considerando que esta estratégia cromatográfica requer condições suaves de eluição, torna-se um método de purificação mais económico do que a lisina-agarose.

Em paralelo, a ligação do pre-miR-29b aos aminoácidos em estudo foi avaliada por biosensor. Este estudo também permitiu compreender as interações envolvidas entre o pre-miR-29b e as matrizes de lisina- e arginina-agarose, assim como determinar as melhores condições que favorecem o bioreconhecimento e a especificidade de ligação dos aminoácidos ao pre-miR-29b, preservando a sua estabilidade e integridade. Os resultados obtidos neste estudo mostraram a existência de várias interações entre o pre-miR-29b e as matrizes de afinidade com os aminoácidos imobilizados, tais como interações hidrofóbicas, eletrostáticas, catião-π, pontes de hidrogénio e forças de "van der Waals".

Tendo em conta que a estrutura dos suportes cromatográficos está em contínuo desenvolvimento de modo a proporcionar separações rápidas e eficientes, nomeadamente para a purificação de ácidos nucleicos, foi também testado um suporte monolítico na purificação do pre-miR-29b. Esta estratégia que associa a alta capacidade destes suportes com a especificidade e seletividade conferida pelo ligando de agmatina (um derivado da $_{L}$-arginina), permitiu a recuperação do pre-miR-29b com alta eficiência (95%) e com elevado grau de pureza (90%) para posterior aplicação nos ensaios *in vitro*. Além disso, este suporte monolítico revelou elevada capacidade de ligação para o RNA, permitindo uma rápida e eficiente separação do pre-miR-29b, independentemente da taxa de fluxo aplicada. No geral, foi possível desenvolver métodos de purificação simples, robustos, versáteis e de elevada reprodutibilidade, que permitiram minimizar o manuseamento das amostras e evitar o uso de condições desnaturantes e solventes orgânicos, contribuindo para o sucesso das aplicações terapêuticas do RNA.

No entanto, o sucesso das terapêuticas baseadas em miRNAs depende também da capacidade de entrega do miRNA, de forma seletiva e eficiente, aos órgãos-alvo, com a mínima toxicidade. De facto, a entrega cerebral de fármacos é limitada por diversos fatores intrínsecos, nomeadamente a sua rápida degradação quando em contato com os fluidos corporais e a reduzida permeabilidade ao longo da barreira hematoencefálica (BHE). Para ultrapassar estas limitações, vários sistemas de entrega de fármacos não-virais têm sido desenvolvidos e caracterizados, nomeadamente os sistemas poliméricos (poliplexos) que possuem características intrínsecas ideais para a transfecção, proteção e libertação controlada e direcionada de RNA. No presente trabalho, as formulações foram preparadas com polímeros comerciais, tais como quitosano e polietilenimina e demonstraram elevada capacidade de transporte de RNA, apresentando pequenas dimensões e uma forte carga superficial positiva. Além disso, e considerando o campo de aplicação do presente trabalho, estes sistemas devem também ter a capacidade de penetrar a BHE, levando a um aumento da concentração do pre-miRNA no cérebro e, consequentemente uma melhoria da sua ação terapêutica. Deste modo, a fim de potenciar o efeito terapêutico das abordagens baseadas no RNAi no sistema nervoso central, os poliplexos desenvolvidos foram funcionalizados com ligandos específicos, tais como a lactoferrina e o ácido esteárico, os quais são reconhecidos pelos recetores localizados à superfície da BHE. Este estudo revelou que os sistemas de entrega desenvolvidos conseguem penetrar a BHE e assim entregar o pre-miR-29b no cérebro.

Finalmente, avaliou-se a atividade biológica do pre-miR-29b recombinante através da verificação da sua eficiência na regulação dos níveis de expressão dos genes relacionados com a DA, em particular no silenciamento da BACE1 humana, utilizando modelos *in vitro* (linhas de células neuronais). O efeito da administração do pre-miR-29b recombinante foi verificado tanto ao nível da expressão do RNA mensageiro como ao nível da expressão da proteína BACE1, através de RT-qPCR, Western blot e Imunocitoquímica. Os resultados sugerem que o

pre-miR-29b recombinante pode funcionar como biofármaco para a modulação terapêutica dos níveis de BACE1, uma vez que foram atingidos elevados níveis de inibição, ou seja 80% de redução para a expressão da proteína BACE1 e 45% para os níveis dos péptidos beta amiloides, quando comparados com as células não transfectadas e células transfectadas como um RNA não relacionado bem como um miR-29b sintético.

Em suma, a implementação destas metodologias terá um grande impacto na indústria farmacêutica e biotecnológica, fornecendo a base para a utilização de novas formas terapêuticas baseadas na utilização de miRNAs, não apenas para aplicação em doenças neurológicas, mas também para futuros alvos terapêuticos que possam ser de interesse.

Palavras-chave

Doença de Alzheimer; Cromatografia de Afinidade; Direcionamento ao cérebro; Silenciamento Génico; Pre-miR-29b humano; Produção Recombinante; Eficiência de Transfecção; Poliplexos

Abstract

The possibility of selectively alter the expression pattern of a particular gene has been sought by scientists and clinicians for a long time. Nowadays, RNA interference (RNAi)-based technology has become a novel tool for silencing gene expression in cells. In addition, this strategy encloses an enormous therapeutic potential that could change the course of the currently applied treatments in several life threatening pathologies and it is expected that this technology can be translated onto clinical applications in a near future. MicroRNA (miRNA) has become a commonly employed tool for gene silencing, since it prevents protein synthesis by inducing the messenger RNA (mRNA) degradation, with a high specificity degree. Consequently, in the last years, the miRNAs have emerged as biopharmaceuticals to regulate several pathways involved in the insurgence and progression of the Alzheimer's disease (AD), since they might have key regulatory roles in many neuronal functions, such as differentiation, synaptic plasticity and memory formation, and typically they are down-regulated in disease conditions. In the literature there are some studies describing a causal relationship between miR-29 expression and AD, since a loss of miR-29 cluster can contribute to increased beta-amyloid precursor protein-converting enzyme 1 (BACE1) and Amyloid-β (Aβ) levels in sporadic AD patients. Thus, this evidence supports the possibility to use miR-29 as a potential therapeutic target for AD therapy.

In general, miRNA-based therapy relies on the use of synthetic microRNAs. However, these synthesized formulations typically present contaminants that can lead to non-targeted gene silencing, which still restricts the pre-clinical or clinical application of these RNAs. Thus, considering this therapeutic purpose and the global distribution of novel biopharmaceuticals it is necessary to develop efficient processes for their preparation. The development of new strategies for microRNA production with high purity degree and biologically active is extremely required. One of the strategies might be the use of the recombinant production of biomolecules using prokaryotic hosts.

Hence, the present work intends to develop and establish an integrative biotechnological platform to biosynthesize and purify a recombinant miRNA precursor (pre-miR-29b) to act in the selective silencing of endogenous pathways directly related with AD, in particular BACE1 and Aβ. In addition, the success of these therapies also depends upon the ability to selectively and efficiently deliver the pre-miR-29b in the cytoplasmic compartment of neuronal cells, the location where their function is exerted; therefore the development of miRNA delivery systems was also envisioned.

The expression system *Rhodovulum sulfidophilum* (*R. sulfidophilum*) DSM 1374 allowed, for the first time, the production of human pre-miR-29b with a straightforward recuperation of

pre-miR-29b in a single step, maintaining its biological active form. The application of this recombinant bacterial microorganism is innovative and is supported by the unusual capacity of secreting the nucleic acids to the extracellular space and the absence of host ribonucleases in the culture medium. Therefore, it is expected that the secreted miRNA will be devoid of main bacterial associated impurities. Regarding the growth conditions, and conversely to what was previously described for this bacterium, our results showed to be possible to develop an original approach for the aerobic growth of the *R. sulfidophilum*, which results in a cell growth improvement followed by an enhanced production of human pre-miR-29b. The extracellular pre-miR-29b concentration was approximately 182 μg/L, after 40 hours of bacterial growth and the total intracellular pre-miR-29b was of about 358 μg/L, at 32 hours of cell growth.

To further develop a potential therapeutic application, the major interest is not only to produce high quantities of RNA but also to obtain and preserve its biological active form, fulfilling the requirements of regulatory agencies. Hence, to assure that this prerequisite is met it was used a novel and effective purification strategy, based on affinity chromatography, to purify the pre-miR-29b. Therefore, in order to achieve the selectivity towards the target pre-miRNA and the maximum resolution between the pre-miR-29b and other host biomolecules (transfer RNAs and proteins) it was used an affinity support that exploits the same biological interactions that are established within the cell, by using immobilized amino acids ($_{L}$-lysine and $_{L}$-arginine), as specific ligands. The recognition of the pre-miR-29b achieved with these supports, allowed its selective recovery from a complex mixture with high efficiency and high purity. In parallel, the binding of pre-miRNA to these different amino acids was studied by Surface Plasmon Resonance. This information brings important insights concerning the characterization of the pre-miRNA binding onto chromatographic supports. Moreover, it was possible to determine some particular conditions enabling the improvement of the binding specificity of the amino acid ligands used to purify miRNA, preserving the RNA integrity. Taking into account that the structure of the chromatographic supports has been continuously developed to afford rapid and efficient separations, namely for the purification of nucleic acids, it was also tested a monolithic support to purify the pre-miR-29b. The association of the high capacity of these supports with the specificity conferred by the agmatine ligand (a derivative of $_{L}$-arginine) represented a novelty and an advantage to obtain highly pure pre-miR-29b (90%) with a high recovery yield (95%).

The establishment of an effective application of miRNAs is usually constrained by different phenomena, namely their easy degradation when in contact with the body fluids. To overcome this limitation, delivery systems, such as polymeric systems (polyplexes), were developed and characterized in order to encapsulate and protect the pre-miR-29b biopharmaceuticals from degradation, allowing their sustained and targeted release. The formulations prepared with chitosan and polyethylenimine demonstrated high loading

capacity, small sizes and exhibited a strong positive charge on their surface. In addition, considering the application field of this work, the delivery systems should also have the ability to penetrate the Blood-Brain Barrier (BBB), causing an increase of the pre-miRNAs concentration in the brain and, consequently the improvement of the therapeutic effect. Actually, BBB is an intrinsic barrier limiting miRNA therapeutic effect on the central nervous system. Thus, to improve the delivery of pre-miRNA therapeutics in the brain, the polyplexes were functionalized with specific ligands, namely lactoferrin and stearic acid which are recognized by cell surface receptors of BBB.

Finally, it was evaluated the biological activity of the recombinant pre-miR-29b by measuring the efficiency on human BACE1 knockdown, using *in vitro* neuronal cell lines. The effect of recombinant pre-miR-29b administration was verified by both assessing the mRNA and protein human BACE1 levels, by using RT-qPCR, Western blot and Imunocytochemistry. Results suggest that recombinant pre-miR-29b can represent a novel biopharmaceutical product for the therapeutic modulation of human BACE1 levels, because high levels of inhibition were achieved, namely 80% of reduction for BACE1 protein expression and 45% for $A\beta_{42}$ levels. Globally, the implementation of these cutting-edge technologies can have a great impact on the biopharmaceutical industry, providing the basis for the implementation of novel miRNA-based therapeutics, not only for neurological disorders but also for future therapeutic targets that can be of potential interest.

Keywords

Affinity Chromatography; Alzheimer's disease; Brain-targeting; Gene silencing; Human pre-miR-29b; Recombinant Production; Transfection Efficiency; Polyplexes

Thesis Overview

This thesis is structured in four main chapters. The **first chapter** is divided into three sections. The first section of chapter 1 provides a brief explanation concerning the importance and interest to apply microRNAs as biopharmaceuticals, in order to regulate endogenous pathways involved in the emergence and progression of the Alzheimer's disease. This section presents a general introduction to the main issues detailed in sections 2 and 3. The second section consists in a succinct literature review about the relevance of developing and establishing new and integrative approaches to biosynthesize, isolate, purify and deliver the pre-miRNAs molecules, also discussing the main challenges and future directions for the development of miRNA-based therapies for neurodegenerative diseases (Paper I. Current progress on microRNAs-based therapeutics). Lastly, the third section discusses the main issues related with non-coding RNAs purification, the advantages and limitations associated to the current chromatographic methods, as well as the improvements that have been done lately, in order to obtain pure and biologically active samples. This third section is also presented in a paper review form (Paper II. Affinity approaches in RNAi-based therapeutics purification).

The **second chapter** includes the main, as well as, the specific goals established for the development of the present research project.

Afterwards, the **third chapter** consists in the presentation and discussion of the results obtained during this research work, in the form of original research papers organized as follows:

Paper III. Advances in time-course extracellular production of human pre-miR-29b from *Rhodovulum sulfidophilum*

Paper IV. Analysis of pre-miR-29b binding conditions to amino acids by Surface Plasmon Resonance Biosensor

Paper V. New approach for purification of pre-miR-29 using lysine-affinity chromatography

Paper VI. Purification of pre-miR-29 by arginine-affinity chromatography

Paper VII. Pharmaceutical-grade pre-miR-29 purification using an agmatine monolithic support

Paper VIII. Characterization of polyplexes involving small RNA

Paper IX. Recombinant pre-miR-29b for Alzheimer´s disease therapeutics

Paper X. Brain-targeting study of lactoferrin-stearic acid-Chitosan/Polyethylenimine pre-miR-29b-delivery system

To finish, the **fourth chapter** summarizes the concluding remarks obtained during this research work, regarding the development and implementation of cutting-edge technologies to the production, bioseparation and delivery of pre-miRNAs. The impact of the findings here reported on biopharmaceutical industry will also be addressed, discussing the application of these novel approaches based on microRNAs, not only for neurological disorders but also for future therapeutic targets that can be of potential interest. In addition, the future trends of this thesis and additional research work will be also suggested to complement the important findings achieved with this project.

Table of Contents

List of Figures

List of Tables

xxx

List of Abbreviations

3′UTR	3’-Untranslated Regions
5′UTR	5’-Untranslated Regions
AAA	poly(A) tail
Aβ	Amyloid-beta
AD	Alzheimer's Disease
Ago	Argonaute
APH-1	Anterior Pharynx-defective 1
APP	Amyloid Precursor Protein
APOE	Apolipoprotein E
BACE1	β-site Amyloid Precursor Protein-Cleaving Enzyme 1
BBB	Blood-Brain Barrier
C. elegans	*Caenorhabditis elegans*
cDNA	complementary DNA
Cdk5	Cell division protein kinase 5
CircRNAs	Circular RNAs
CS	Chitosan
CSF	Cerebrospinal Fluid
CNS	Central Nervous System
DGCR8	DiGeorge Syndrome Critical Region Gene 8
DNA	Deoxyribonucleic Acid
dsRNA(s)	Double-stranded RNA(s)
E. coli	*Escherichia coli*
EE	Encapsulation Efficiency
EMA	European Medicines Agency
eRNA	Enhancer associated RNAs
FAD	Familial Alzheimer’s disease
FDA	Food and Drug Administration
gDNA	Genomic DNA
GSK3	Glycogen Synthase Kinase 3
GTP	Guanosine Triphosphate
Lf	Lactoferrin
lincRNA	Large Intervening Non-coding RNA
LNA	Locked Nucleic Acid
lncRNA(s)	Long Non-coding RNA(s)
lpaRNA	Promoter-associated long RNAs
MAPT	Microtubule-Associated Protein Tau
miRISC	miRNA-Induced Silencing Complex
miRNA(s) / miR(s)	MicroRNA(s)
MRE	MicroRNA Response Elements
mRNA	Messenger RNA
NATs	Natural Antisense Transcripts
NcRNA(s)	Non-coding RNA(s)
NCSTN	Nicastrin
ND(s)	Neurodegenerative Disease(s)

NFTs	Neurofibrillary Tangles
NMDA receptor	*N*-Methyl-$_D$-Aspartate receptor
nt	Nucleotide
OD_{600}	Optical Density at 600 nm
ORF	Open Reading Frame
PACT	Protein kinase R-activating Protein
PEG	Polyethylene Glycol
PEI	Polyethylenimine
pDNA	Plasmid DNA
PEN 2	Presenilin Enhancer 2
piRNAs	PIWI-Interacting RNAs
PKR	Protein Kinase Receptor
pre-miRNA(s)	Precursor MicroRNA(s)
pri-miRNA(s)	Primary MicroRNA(s)
PSEN	Presenilin
RBP(s)	RNA Binding Protein(s)
R. sulfidophilum	*Rhodovulum sulfidophilum*
RISC	RNA-Induced Silencing Complex
RNA	Ribonucleic Acid
RNAi	RNA Interference
RNAt	Total RNA
RNase(s)	Ribonuclease(s)
RNP	Ribonucleoprotein
rRNA(s)	Ribosomal RNA(s)
ROS	Reactive Oxygen Species
SA	Stearic Acid
SAD	Sporadic Alzheimer's Disease
SELEX	Systematic Evolution of Ligands by Exponential
shRNA	Short Hairpin RNAs
siRNA(s)	Small Interfering RNA(s)
SIRT1	Sirtuin 1
sncRNA(s)	Small Non-coding RNA(s)
snRNA(s)	Small Nuclear RNA(s)
snoRNA(s)	Small Nucleolar RNA(s)
sRNA(s)	Small RNA(s)
SPE	Solid-Phase Extraction
TLRs	Toll-like Receptors
TRBP	Tar RNA-binding Protein
tRNA(s)	Transfer RNA(s)
WHO	World Health Organization

List of Scientific Publications

Papers related with this Thesis

I. Current progress on microRNAs-based therapeutics
P. Pereira, J.A. Queiroz, A. Figueiras, F. Sousa
Submitted for publication (2015)

II. Affinity approaches in RNAi-based therapeutics purification
P. Pereira, J.A. Queiroz, A. Figueiras, F. Sousa
Submitted for publication (2015)

III. Advances in time-course extracellular production of human pre-miR-29b from *Rhodovulum sulfidophilum*
P. Pereira, A.Q. Pedro, J. Tomás, C.J. Maia, J.A. Queiroz, A. Figueiras, F. Sousa
Submitted for publication (2015)

IV. Analysis of pre-miR-29b binding conditions to amino acids by Surface Plasmon Resonance Biosensor
P. Pereira, C. Cruz, J.A. Queiroz, A. Figueiras, F. Sousa
Submitted for publication (2015)

V. New approach for purification of pre-miR-29 using lysine-affinity chromatography
P. Pereira, A. Sousa, J.A. Queiroz, A. Figueiras, F. Sousa
Journal of Chromatography A (2014) 1331: 129-132

VI. Purification of pre-miR-29 by arginine-affinity chromatography
P. Pereira, A. Sousa, J.A. Queiroz, I. Correia, A. Figueiras, F. Sousa
Journal of Chromatography B (2014) 951-952: 16-23

VII. Pharmaceutical-grade pre-miR-29 purification using an agmatine monolithic support
P. Pereira, A. Sousa, J.A. Queiroz, A. Figueiras, F. Sousa
Journal of Chromatography A (2014) 1368: 173-182

VIII. Characterization of polyplexes involving small RNA
P. Pereira, A.F. Jorge, R. Martins, A.C.C. Pais, F. Sousa, A. Figueiras
Journal of Colloid and Interface Science (2012) 387: 84-94

IX. Recombinant pre-miR-29b for Alzheimer´s disease therapeutics
P. Pereira, J. Tomás, J.A. Queiroz, A. Figueiras, F. Sousa
Submitted for publication (2015)

X. Brain-targeting study of lactoferrin-stearic acid-Chitosan/Polyethylenimine pre-miR-29b-delivery system

P. Pereira, J. Tomás, C. Cruz, C. Santos, J.A. Queiroz, A. Figueiras, F. Sousa

In preparation (2015)

Papers not related with this Thesis

I. Polyplexes as Nanovectors for Gene Therapy - Chapter 9

Patrícia Pereira, Fani Sousa, Ana Figueiras

Biotechnology, Nanobiotechnology (2013) Volume 10: 179-223

Published by Studium Press LLC, Houston, USA; ISBN: 1-62699-025-5

II. Purification of pre-miR-29 by a new *O-phospho*-$_L$-tyrosine affinity chromatographic strategy optimized using design of experiments

A. Afonso, P. Pereira, J.A. Queiroz, A. Sousa, F. Sousa

Journal of Chromatography A (2014)1343: 119-127

III. Binding mechanisms for histamine and agmatine ligands in plasmid deoxyribonucleic acid purifications

A. Sousa, P. Pereira, F. Sousa, J.A. Queiroz

Journal of Chromatography A (2014)1366: 110-119

IV. Purification of Membrane-Bound Catechol-*O*-Methyltransferase by Arginine-Affinity Chromatography

A.Q. Pedro, P. Pereira, M.J. Bonifácio, J.A. Queiroz, L.A. Passarinha

Chromatographia (2015) DOI: 10.1007/s10337-015-2970-3

V. Purification of supercoiled G-quadruplex pDNA for *in vitro* transcription

T. Santos, P. Pereira, F. Sousa, J.A. Queiroz, C. Cruz

Submitted for publication (2015)

VI. Stabilization of novel immunoglobulin switch regions G-quadruplexes by naphthalene and quinoline-based ligands

J. Carvalho, J. Ferreira, P. Pereira, E. Coutinho, A. Guédin, P. Nottelet, G.F. Salgado, J.L. Mergny, J.A. Queiroz, F. Sousa, E.J. Cabrita, C. Cruz

Submitted for publication (2015)

VII. Síntese e caracterização do suporte cromatográfico de L-tirosina para purificação de plasmídeos

T. Santos, P. Pereira, F. Sousa, J.A. Queiroz, C. Cruz

Portuguese Patent 108360. Submitted (2015)

List of Scientific Communications

Oral Communications related with this Thesis

I. A biotechnological platform for pre-miRNAs biosynthesis, purification and brain-targeted delivery for Alzheimer's disease
P. Pereira, A.Q. Pedro, J. Tomás, A. Sousa, J.A. Queiroz, A. Figueiras, F. Sousa
MicroBiotec'15 – Congress of Microbiology and Biotechnology 2015. Évora, Portugal

II. Biosynthesis, purification and brain-targeted delivery of pre-miR-29b biopharmaceuticals for Alzheimer's disease therapy
P. Pereira, A.Q. Pedro, J. Tomás, C. Cruz, A. Sousa, C. Maia, J.A. Queiroz, A. Figueiras, F. Sousa
X Annual CICS-UBI Symposium 2015. Covilhã, Portugal

III. Pre-miR-29 biosynthesis and purification for polyplexes-mediated delivery to *in vitro* Alzheimer's disease model
P. Pereira, J. Tomás, A. Sousa, J.A. Queiroz, A. Figueiras, F. Sousa
IX Annual CICS-UBI Symposium 2014. Covilhã, Portugal

IV. Pre-miR-29 purification by amino acids-affinity chromatography
P. Pereira, A. Sousa, J.A. Queiroz, A. Figueiras, F. Sousa
8º Encontro Nacional de Cromatografia 2013. Covilhã, Portugal

Invited Oral Communications related with this Thesis

I. Pre-miR-29b biopharmaceutical for Alzheimer's disease therapy: biosynthesis, purification and targeted delivery
P. Pereira
III Jornadas de Química e Bioquímica 2015. Covilhã, Portugal

II. Pre-miR-29 bioseparation and target delivery strategies for Alzheimer's disease
P. Pereira
V Jornadas Nacionais de Ciências Biomédicas 2014. Covilhã, Portugal

III. Development of new therapeutic strategies for miRNA delivery
P. Pereira, A. Jorge, A.C.C. Pais, F. Sousa, A. Figueiras
I Workshop on Pharmaceutical Technology - "New Drug Delivery Systems" 2012. Coimbra, Portugal

Poster Communications related with this Thesis

I. Biosynthesis of pre-miR-29 for application in neurodegenerative disorders
P. Pereira, C.J. Maia, I.J. Correia, A. Figueiras, F. Sousa
ECCE9 – ECAB2 (9th European Congress of Chemical Engineering and 2nd European Congress of Applied Biotechnology) 2013. The Hague, Netherlands

II. Pre-miR-29 biosynthesis and purification: possible implications in Alzheimer's disease
P. Pereira, A. Sousa, C.J. Maia, J.A. Queiroz, I.J. Correia, A. Figueiras, F. Sousa
MicroBiotec'13 – Congress of Microbiology and Biotechnology 2013. Aveiro, Portugal

III. Exploiting multiple interactions in pre-miR-29 purification by arginine-affinity chromatography
P. Pereira, A. Sousa, I.J. Correia, A. Figueiras, F. Sousa
19th International Symposium on Separation Sciences – New achievements in Chromatography 2013. Porec, Croatia

IV. Improved native pre-miR-29 purification with lysine-affinity chromatography
P. Pereira, A. Sousa, I.J. Correia, A. Figueiras, F. Sousa
19th International Symposium on Separation Sciences – New achievements in Chromatography 2013. Porec, Croatia

V. Structural and functional characterization of polyplexes for small RNA delivery
P. Pereira, A. Jorge, R. Martins, A.C.C. Pais, F. Sousa, A. Figueiras
8th World Meeting on Pharmaceutics, Biopharmaceutics and Pharmaceutical Technology 2012. Istanbul, Turkey

VI. miRNA-29 bioseparation and target delivery strategies for Alzheimer disease
P. Pereira, I.J. Correia, A. Figueiras, F. Sousa
V Jornadas sobre Tecnologia e Saúde 2012. Guarda, Portugal

VII. Characterization of polyplexes containing small RNA
P. Pereira, A. Jorge, A.C.C. Pais, F. Sousa, A. Figueiras
Conference CEF (Center for Pharmaceutical Studies) 2012. Coimbra, Portugal

Oral Communications not related with this Thesis

I. DNA vaccine development for HPV treatment: biotechnological production, purification and *in vitro* application

A.M. Almeida, P. Pereira, J. Tomás, V. Figueiredo, J.A. Queiroz, F. Sousa, A. Sousa

MicroBiotec'15 – Congress of Microbiology and Biotechnology 2015. Évora, Portugal

II. Production and purification of DNA G-quadruplex using pPH600 plasmid

T.A. Santos, P. Pereira, F. Sousa, J.A. Queiroz, C. Cruz

X Annual CICS-UBI Symposium 2015. Covilhã, Portugal

III. Biosynthesis of a G-quadruplex-forming sequence and its stabilization by naphthalene-based ligands

J. Carvalho, J. Ferreira, P. Pereira, E. Coutinho, F. Sousa, E. Cabrita, J.A. Queiroz, C. Cruz

X Annual CICS-UBI Symposium 2015. Covilhã, Portugal

IV. Supercoiled HPV16 E6/E7 plasmid DNA-based vaccine purified by affinity chromatography for *in vitro* transfection studies

A.M. Almeida, P. Pereira, J. Tomás, V. Figueiredo, J.A. Queiroz, F. Sousa, A. Sousa

VIII Jornadas sobre Tecnologia e Saúde 2015. Guarda, Portugal

V. Optimized purification strategy of supercoiled HPV16 E6/E7 plasmid DNA-based vaccine for *in vitro* transfection studies

A.M. Almeida, P. Pereira, J. Tomás, J.A. Queiroz, F. Sousa, A. Sousa

IX Annual CICS-UBI Symposium 2014. Covilhã, Portugal

VI. Pre-miR-29b-1 isolation using a new chromatographic strategy with tyrosine-agarose

A. Afonso, P. Pereira, A. Sousa, F. Sousa

VIII Annual CICS-UBI Symposium 2013. Covilhã, Portugal

Poster Communications not related with this Thesis

I. Biotechnological approach to prepare a DNA vaccine for HPV induced-cervical cancer treatment

A.M. Almeida, P. Pereira, J. Tomás, V. Figueiredo, J.A. Queiroz, F. Sousa, A. Sousa

30th International Papillomavirus Conference 2015. Lisboa, Portugal

II. A breakthrough optimization of *O-phospho*-$_L$-tyrosine affinity chromatography to purify pre-miR-29

A. Afonso, P. Pereira, J.A. Queiroz, A. Sousa, F. Sousa

IX Annual CICS-UBI Symposium 2014. Covilhã, Portugal

III. Pre-miR-29 isolation using a new chromatographic strategy with tyrosine-agarose

A. Afonso, P. Pereira, A. Sousa, F. Sousa

ECCE - ECAB (9th European Congress of Chemical Engineering and 2nd European Congress of Applied Biotechnology) 2013. The Hague, Netherlands

IV. Purification of pre-miR-29 using a new affinity chromatographic strategy optimized by Design of Experiments

A. Afonso, P. Pereira, A. Sousa, J.A. Queiroz, F. Sousa

8º Encontro Nacional de Cromatografia 2013. Covilhã, Portugal

V. Development of an *O-phospho*-$_L$-tyrosine affinity chromatography to purify pre-miR-29 using Design of Experiments

A. Afonso, P. Pereira, J.A. Queiroz, A. Sousa, F. Sousa

V Symposium on Bioengineering 2013. Porto, Portugal

VI. Biosynthesis and purification of siNOX1 for application in neurodegenerative disorders

P. Pereira, C. Maia, I.J. Correia, A. Figueiras, F. Sousa

ESBES - ISPPP (9th European Symposium on Biochemical Engineering Science - 32nd International Symposium on the Separation of Proteins, Peptides and Polynucleotides) 2012. Istanbul, Turkey

Chapter 1

1. Alzheimer's disease and microRNAs

1.1. Introduction

The discovery of RNA interference (RNAi) by Andrew Fire and Craig Mello in the late 1990s, allowed them to win the Nobel Prize in Physiology or Medicine in 2006, and revolutionized the contemporary understanding of gene regulation (Fire *et al.*, 1998). Exogenous double-stranded RNA (dsRNA) was identified in the nematode *Caenorhabditis elegans* (*C. elegans*) as an effector molecule of the RNAi pathway, since this RNA silenced the expression of a homologous target gene by directing degradation of its messenger RNA (mRNA). Moreover, the study demonstrated that the gene silencing was achieved with the administration of only few molecules of dsRNAs and that these molecules were more efficient than the corresponding antisense RNA (Fire *et al.*, 1998). Since then, several studies have demonstrated that RNAi is a well-conserved, endogenous mechanism in several species, including mammals and plants (Chu and Rana, 2007; Lehman, 2010). In mammalian cells, the inhibitory capability of RNA was initially demonstrated by the introduction of shorter dsRNAs, named small interfering RNAs (siRNAs), with perfect sequence complementarity to target mRNA transcripts, which had already been discovered in plants (Chu and Rana, 2007; Dykxhoorn and Lieberman, 2006; Filipowicz *et al.*, 2005; Zamore *et al.*, 2000).

Accordingly, the discovery that genes could be silenced by RNAs allowed the biological understanding of other roles of RNA, which changed from a simple intermediate molecule in the information flux between DNA and proteins to a dynamic and versatile molecule, fundamental in the regulation of genes expression, involved in essential cellular processes of all living systems (Burnett and Rossi, 2012; Ramachandran and Ignacimuthu, 2013).

Currently, RNAi regulates the expression and function of individual genes, involved in pathways or known to be associated with diseases (harmful or unwanted genes). This regulation occurs at the post-transcriptional level through non-coding RNAs molecules (ncRNAs), via sequence-specific degradation or blocking the translation of their target mRNA in most eukaryotic species (Bumcrot *et al.*, 2006; Burnett and Rossi, 2012; Deng *et al.*, 2014; Ramachandran and Ignacimuthu, 2013). RNAi-based technology possesses attractive characteristics to be considered for therapeutic proposes, such as high specificity, efficiency, ability to induce a robust and potent knockdown of the targeted genes and the possibility to promote a long-lasting therapy (the therapeutic effect lasts from days up to weeks), reducing the expenses of medical treatments (Bumcrot *et al.*, 2006; Burnett and Rossi, 2012; Deng *et al.*, 2014; Milhavet *et al.*, 2003). On the other hand, usually, the dosage required of ncRNA therapeutics is low, which can reduce or eliminate the occurrence of undesirable adverse

effects in the patients (Guzman-Villanueva *et al.*, 2012). These breakthroughs clearly encouraged a variety of studies on the mechanisms of gene expression regulation, which led to the emergence of numerous and different types of RNA-based therapeutics that extends the range of targets of the existing pharmacological drugs (Burnett and Rossi, 2012).

NcRNAs are a class of transcripts which, as the name implies, are not translated into proteins. Presently, ncRNAs are recognized as key regulatory molecules in a variety of cellular processes as diverse as development, cell viability, cell cycle regulation, stem cell self-renewal, transposon activity control, differentiation, heterochromatin formation and maintenance of cell integrity by gene silencing pathways, through translational repression or mRNA degradation (Kim, 2005; Svoboda, 2014). A very simplistic classification based on ncRNAs length arbitrarily separates these biomolecules into two groups according to their sizes: the small (<200 nucleotides (nt)) and the long (>200 nt) ncRNAs (Dogini *et al.*, 2014; Gomes *et al.*, 2013). In turn, the small group comprises infrastructural RNAs and regulatory RNAs. The infrastructural RNAs include ribosomal RNA (rRNA), transfer RNA (tRNA), small nuclear RNA (snRNA) and small nucleolar RNA (snoRNA) that are involved in the spliceosomal and translational machinery. On the other hand, regulatory RNAs include microRNAs (miRNAs), siRNAs delivered as synthetic duplexes to the cells, short hairpin RNA (shRNA) and Piwi-interacting RNAs (piRNAs), among others (Chu and Rana, 2007; Dogini *et al.*, 2014; Gomes *et al.*, 2013; Matera *et al.*, 2007). These differ significantly in their biogenesis and mode of action (Kim, 2005; Kim *et al.*, 2009).

Presently, RNAi-based therapies have major implications for basic and biomedical research that can lead to a number of clinical applications, for treating the vast number of human diseases caused by one or few genes, such as viral infections, metabolic diseases, cardiovascular disease, hypertension and stroke, immune dysfunction and autoimmune disorders, distinct types of cancers and neurodegenerative and psychiatric diseases (Gomes *et al.*, 2013; Ramachandran and Ignacimuthu, 2013; Sullenger and Gilboa, 2002).

1.2. Alzheimer's disease

Neurodegenerative diseases (NDs) are a family of disorders of central nervous system (CNS) characterized by a progressive loss of neuronal structure and function, resulting in a motor and cognitive dysfunction (Goodall *et al.*, 2013; Maciotta *et al.*, 2013). For that reason, these disorders do not have cure, once the neurons cannot regenerate on their own after cell death or damage. Some of the most studied NDs include Alzheimer's disease (AD), Parkinson's disease, Huntington's disease, Amyotrophic Lateral Sclerosis and Prion diseases (Junn and Mouradian, 2012; Tabares-Seisdedos *et al.*, 2011).

NDs constitute a serious and growing health problem for our societies because they collectively represent one of the leading causes of disability and mortality. Currently, it is estimated that NDs affect over 30 million people worldwide and that by 2030, this number can reach 66 million people and increase to 115 million by 2050 (Schonrock *et al.*, 2012). As a result, these diseases are associated to higher health care costs, as well as, being a source of severe human suffering (Dunkel *et al.*, 2012). The increased prevalence of these diseases is intimately related with the current trends: the aging of the population due to increased life expectancy which cause more people living long enough to be affected and the continuing lack of progress in identifying effective diagnosis and treatment modalities. All these reasons emphasize the necessity to study novel therapeutic interventions for these incurable diseases (Bertram *et al.*, 2010; Qiu *et al.*, 2009).

Among all dementing disorders, AD is the most prevalent (45-60%) and devastating form of dementia in the elderly and leads to death within 3 to 9 years after appearance of symptoms (Isik, 2010). According to the National Institute on Aging (www.nia.nih.gov/alzheimers), the AD is clinically characterized by loss of memory and eventually by disturbances in reasoning (e.g. trouble handling money), planning and performing activities of daily living, language, and perception (e.g. loss of orientation to time and place), as well as, changes of mood, behavior and personality. Common behavioral symptoms of Alzheimer's include sleeplessness, agitation, anxiety, and depression (Buchman *et al.*, 2013; Sperling *et al.*, 2011; Wilson *et al.*, 2013).

In 2014, it was estimated that more than 5.4 million individuals in the USA have AD and that this number can nearly triplicate, from 5 million to as many as 16 million by 2050, thus significantly increasing social and economical burdens in industrialized countries, where the aging population is increasing every year (Provost, 2010b; Suehs *et al.*, 2013). AD is commonly classified into two types: Sporadic Alzheimer's disease (SAD) or Familial Alzheimer's disease (FAD) (Blennow *et al.*, 2006; Piaceri *et al.*, 2013). SAD reports most AD cases (99%), occurs late in life (65 years), and it can take up to 20 years for the disease to develop. Until now, SAD was only associated with a genetic mutation in the ε4 allele of the apolipoprotein E (APOE) gene, which promotes amyloid-beta (Aβ) deposition and impairs Aβ clearance (Bertram *et al.*, 2010; Bu, 2009; Genin *et al.*, 2011; Hardy and Selkoe, 2002; Piaceri *et al.*, 2013). Presently, sporadic type affects 11% of the population over the age 65 and older, 32% of those over the age 85 and, the vast majority, 82% of the population aged 75 or older. In contrast, FAD typically develops before the age 65 (40-50 years), is a very rare condition (1%) and it is caused by autosomal, dominant mutations in three genes, namely in the amyloid precursor protein (APP) and in the genes of presenilin (PSEN1 and PSEN2), which are linked to Aβ processing by γ-secretase complexes (Blennow *et al.*, 2006; Chen *et al.*, 2013; Citron, 2010; Piaceri *et al.*, 2013). Generally, individuals are diagnosed with FAD when more than one member is affected in more than one generation (Piaceri *et al.*, 2013). Hence, it is fundamental to found a solution to this problem as soon as possible.

AD involves various regions of the brain that control learning, language, thought and memory and results from progressive neuronal loss (death of neurons), arising from often unknown or insufficiently characterized risk factors and causes. Thereby, AD is a highly complex disease that involves hundreds of defective genes distributed across the human genome (genetic factors), in close interaction with other factors such as age (atrophy of certain parts of the brain, inflammation, production of free radicals and mitochondrial dysfunction), family history (heredity), lifestyle factors (education, diet, smoking, substance abuse) and environmental risk factors (chemical exposure) contributing to its development and progression (Bertram *et al.*, 2010; Maes *et al.*, 2009).

Neuropathological hallmarks of AD include extracellular senile plaques (known as amyloid plaques) formed of aggregates of toxic Aβ peptides and intracellular neurofibrillary tangles (NFTs) composed by insoluble hyperphosphorylated tau, a microtubule-associated protein (Blennow *et al.*, 2006; Goedert *et al.*, 1989; Hardy and Selkoe, 2002; Mullane and Williams, 2013). Although the mechanisms of AD remain unclear, it has been hypothesized that it can be associated with abnormal protein metabolism, particularly in the formation and accumulation of the Aβ peptides (Mullane and Williams, 2013; Provost, 2010a; Schonrock *et al.*, 2012).

Amyloid peptide is composed by 40 or 42 amino acids and is generated upon sequential proteolytic cleavage of APP, a transmembrane protein expressed in many tissues and involved in the synaptogenesis, axonal transport, transmembrane signal transduction, cell adhesion and calcium metabolism (Chen *et al.*, 2013; Glenner, 1989a; Glenner, 1989b). The initial step in the "amyloidogenic pathway" is catalyzed by β-secretase (also known as β-site APP-cleaving enzyme 1 (BACE1)), producing a carboxyl-terminal fragment of 99 amino acids (CTF99) and simultaneously the ectodomain of APP is released as soluble APPβ (sAPPβ) (see Figure 1) (Kim *et al.*, 2014; De Strooper, 2010). Posteriorly, the resulting fragment of APP (CTF99) is cleaved by the γ-secretase complex (that is composed by at least four components, namely PSEN1, Nicastrin (NCSTN), Presenilin enhancer 2 (PEN2) and Anterior Pharynx-defective 1 (APH-1)), releasing into the cytoplasm an intracellular domain of APP of approximately 50 amino acids (AICD), and a variety of potentially amyloidogenic Aβ peptides (39-42 amino acids) (Figure 1) (Chen *et al.*, 2013; Ghiso and Frangione, 2002; Kim *et al.*, 2014; Provost, 2010a). In alternative, in the "non-amyloidogenic pathway", APP is initially cleaved by the metalloprotease α-secretase, releasing a soluble APPα ectodomain (sAPPα), and generating at the same time, a carboxyl-terminal fragment of 83 residues (CTF83), which is further processed by γ-secretase, liberating extracellular p3 and the AICD (Ghiso and Frangione, 2002).

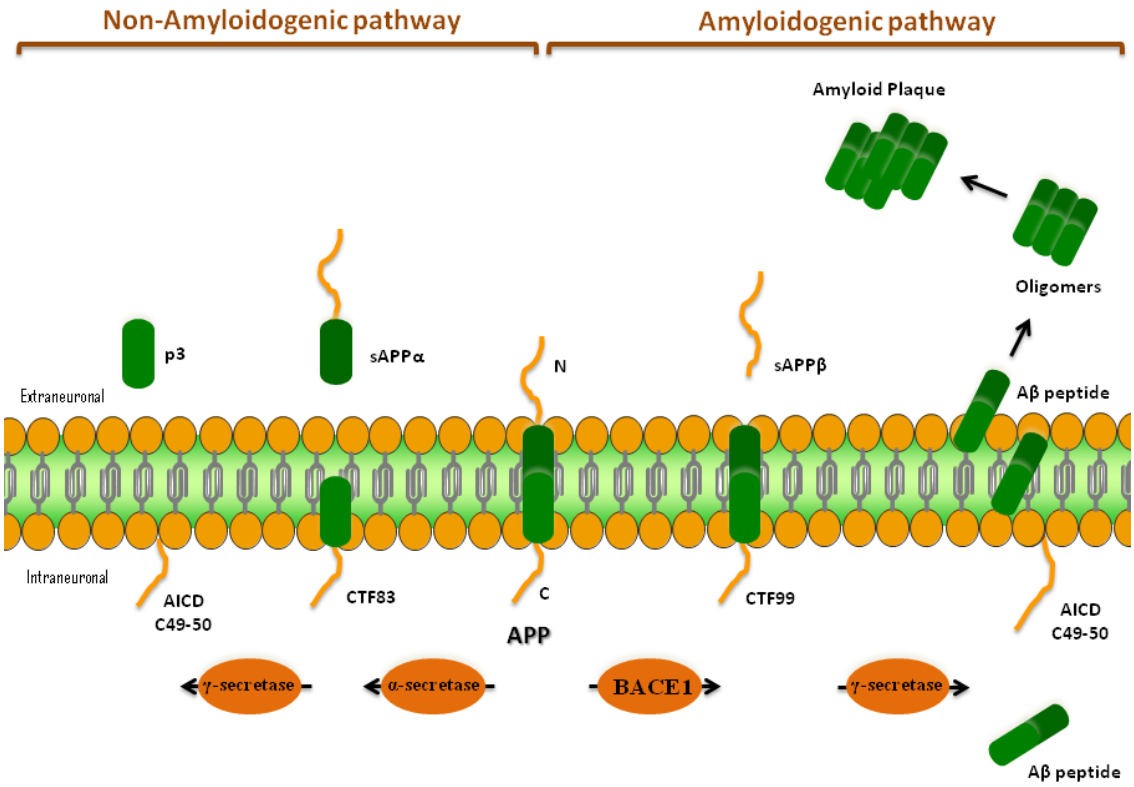

Figure 1 - Amyloidogenic and Non-amyloidogenic pathways for proteolytic processing of APP by α-secretase, BACE1, and γ-secretase.

Abbreviation: APP, amyloid precursor protein; BACE1, β-site APP-cleaving enzyme 1; CTF83/99, carboxyl-terminal fragment of 83/99 amino acids; sAPPα/β, soluble APPα/β.

While γ-secretase produces several Aβ peptides with heterogeneous carboxyl-terminus ranging from 38-43 amino acids, BACE1 is a site-specific protease that cleaves exactly between specific amino-acids of APP. In addition, BACE1 catalyses the first and rate-limiting step in the pathway (Provost, 2010a; Schonrock *et al.*, 2012; Vassar *et al.*, 2009). Consistent with this hypothesis, several research groups have demonstrated that the levels and the activity of BACE1 are elevated in sporadic AD brain, suggesting the possibility that BACE1 overexpression might initiate or accelerate AD. For these reasons, BACE1 has been recognized as a prime drug target for therapeutic inhibition of Aβ production in AD, once the BACE1 inhibition can decrease production of all forms of Aβ peptides (Vassar *et al.*, 2009). Within the variety of Aβ peptide isoforms produced in the CNS, $A\beta_{1\text{-}40}$ is the most predominant form contributing for more than 90% of the total Aβ, whereas $A\beta_{1\text{-}42}$ is the most neurotoxic form and is considered to be primarily responsible for neuronal damage. As mentioned above, amyloid plaques are formed from the gradual accumulation and aggregation of secreted Aβ peptides in oligomers and fibrils in the extracellular space. However, recent studies demonstrated that the accumulation of Aβ occur also within neurons with AD pathogenesis (De Strooper, 2010; Dong *et al.*, 2012).

Although several molecular mechanisms have been implicated in the AD pathology, most evidences indicate that the intraneuronal Aβ accumulation and the amyloid plaques play a pivotal role in the synaptic dysfunction, neuronal death and cognitive dysfunction (Figure 2), which cause neurodegeneration and dementia in a first instance and then leads to AD (Delay *et al.*, 2012; Feng and Feng, 2011; Iyengar *et al.*, 2014; Maciotta *et al.*, 2013; Tan *et al.*, 2013). Many processes are common features in neurodegeneration, namely cellular oxidative stress (overproduction of reactive oxygen species (ROS) and activation of cell death pathways), protein oligomerization and aggregation, deregulation of calcium homeostasis, mitochondrial dysfunction, neuroinflammation, DNA damage and aberrant RNA processing (Borgesius *et al.*, 2011; Goodall *et al.*, 2013; Jeppesen *et al.*, 2011; Qiu *et al.*, 2009). These events initiate pro-apoptotic cascades that activate members of the B-cell lymphoma 2 (Bcl-2) family and lead to the rapid activation of caspases (Feng and Feng, 2011; Maciotta *et al.*, 2013; Van den Hove *et al.*, 2014). In addition to plaques and tangles as histopathological hallmarks, other pathological changes include impaired axonal transport, neuron-glial interactions and reduced synaptic plasticity (Delay *et al.*, 2012). As shown in Figure 2, mechanisms that affect AD pathogenesis involve dysregulation of multiple fundamental cellular pathways, including protein folding and clearance processes. Concluding, in order to develop an AD therapeutic it is essential to understand the principal features of this disease.

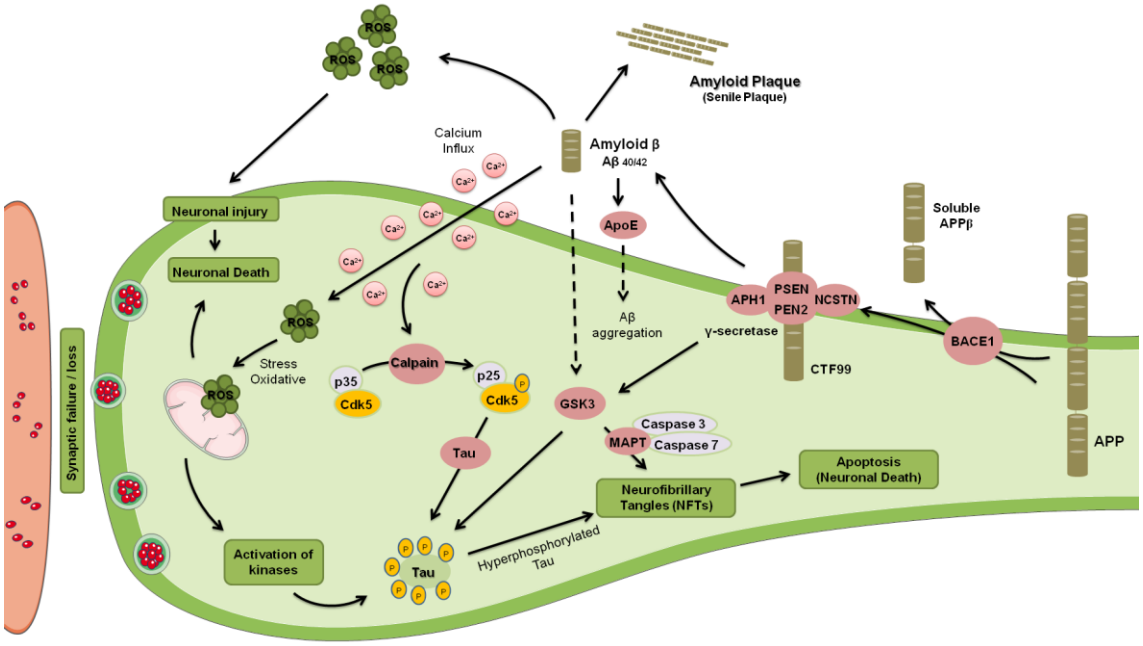

Figure 2 - Alzheimer's disease pathways.

Abbreviations: Aβ, Amyloid-beta; APH-1, Anterior Pharynx-defective 1; APP, Amyloid Precursor Protein; APOE, Apolipoprotein E; Cdk5, Cell division protein kinase 5; GSK3, Glycogen Synthase Kinase 3; MAPT, Microtubule-Associated Protein Tau; NCSTN, Nicastrin; PEN2, Presenilin Enhancer 2; PSEN1, Presenilin 1; ROS, Reactive Oxygen Species.

Many other disorders can be confused with AD, once no specific blood test or imaging test exists for the diagnosis of AD. Thus, AD is currently being diagnosed using a combination of several methods and clinical tools to reach a correct diagnosis, which includes a thorough general medical workup, a neurological exam based in mental status tests (such as tests of memory, problem solving, attention and language) and psychiatric evaluation (to assess mood, anxiety and clarity of thought) (Jack *et al.*, 2011). Furthermore, the diagnosis includes structural imaging of the brain with computed tomography, magnetic resonance imaging, single-photon emission computed tomography or positron emission tomography (Albert *et al.*, 2011; Barthel *et al.*, 2011; McKhann *et al.*, 2011). Nonetheless, brain imaging is not a standard part of the assessment for possible AD since although these methods are good biomarkers, they are also quite expensive. The clinical diagnosis of AD remains difficult and, sometimes the definitive diagnostic is only established by post-mortem confirmation.

In the last few years, several studies have been made to identify the neuropathological, biochemical, and genetic biomarkers of the AD so that the diagnosis could be done as early as possible, even in the absence of obvious symptoms, once AD patients are known to have neuropathology in their brains for over 10 to 20 years before any symptoms occur. Aβ peptides ($A\beta_{40}$ and $A\beta_{42}$, which are more prone to aggregation) and tau/phospho-tau (Thr 181, a common phospho-epitope), in cerebrospinal fluid (CSF), have been widely accepted as robust biomarkers in AD diagnosis (Holtzman, 2011; Tarawneh and Holtzman, 2010). However, the wide variability and inconsistency that exists among different studies and the invasive nature of the procedures required to obtain CSF have been delaying the use of more accurate and efficient biomarkers as a diagnostic tool for AD in the clinical setting (Holtzman, 2011; Ingelson *et al.*, 1999). Finally, the biomarkers also allow following the patient response to the treatment, enabling to elaborate specific regimen changes if a drug is not providing the desired benefit.

Despite the efforts to identify optimal treatment schemes containing one or more drugs, the majority of the currently available options are still largely ineffective due to several reasons. In particular, the molecular pathology of dementia is still poorly understood, the genetic and epigenetic component of dementia is poorly defined, and the understanding of genome-drug interactions is very limited (Cacabelos and Torrellas, 2014). In addition, the drug targets are inappropriated and most treatments are symptomatic, for instance, although patients treated with antipsychotic drugs experience moderate benefits in reducing aggression and psychosis, they are accompanied of serious adverse effects, such as sedation, stroke, movement difficulties (Parkinsonism), thus limiting their routinely use (Cacabelos and Torrellas, 2014). Presently, there are only four drugs approved by the Food and Drug Administration (FDA) available to treat the cognitive problems of Alzheimer's: three are acetylcholinesterase inhibitors (Donepezil (Aricept®), Rivastigmine (Exelon®), Galantamine (Razadyne®) commonly prescribed for mild-to-moderate AD) and the other one (Memantine (Namenda®))

is an *N*-Methyl-$_D$-Aspartate (NMDA) receptor antagonist prescribed for moderate-to-severe AD (Cacabelos and Torrellas, 2014). These drugs can help maintain thinking, memory, and communication skills and help with certain behavioral problems but they do not delay or interrupt AD progression. The most common adverse effects are nausea, hallucinations, confusion, dizziness, headache, fatigue and vomiting.

Although the precise mechanisms responsible for the pathology of AD are still unclear, several convincing evidences suggest that the generation and accumulation of Aβ peptides, in the brain, plays the central role in initiating and development of a complex neurodegenerative cascade, which results in progressive cognitive impairment and dementia (Glenner, 1989a). Hence, the "amyloid cascade" is the most widely discussed and investigated pathway, to find the cause of AD. So the regulation of protein expression levels involved in the Aβ generation process has demonstrated to be important in AD progression. Consequently, the current drug discovery approaches have focused on preventing the formation and aggregation of the Aβ or to facilitate their clearance.

During the past 30 years, the understanding of the genetic and molecular basis of the pathophysiology of this dementia has advanced dramatically; however, limited knowledge of the basic pathogenic mechanisms is a major hurdle in the identification of drug targets and development of therapeutic strategies for this yet incurable disorder. All these reasons highlight the need for the development of innovative and alternative therapeutic strategies to prevent, slow or stop the progression of this disease.

At present, alternative therapeutic strategies focused on the specific gene expression control (mRNA and protein levels) can contribute to the regulation of several neuronal functions, such as differentiation, synaptic plasticity and memory formation (Cacabelos and Torrellas, 2014). Gene therapy is a highly promising therapeutic method for the treatment or prevention of AD, using genetic information. In addition, gene therapy can be more economical and convenient because it provides higher targeting and prolonged action. A possible regulatory mechanism of gene expression in AD is via ncRNAs, designed RNAi mechanism (Cacabelos and Torrellas, 2014). One important class of gene expression regulators is miRNAs. A number of studies, in the last decade, focused on the hypothesis of using miRNAs as biopharmaceuticals to regulate several pathways involved in the insurgence and progression of AD. This idea has gained support, because some miRNAs are differentially expressed in the human brain (including the spinal cord, cerebellum, hypothalamus, hippocampus and cortex) and regulate the expression of genes associated with specific neurodegenerative disorders (Delay *et al.*, 2012; Feng and Feng, 2011; Maciotta *et al.*, 2013; Satoh, 2012; Tan *et al.*, 2013; Tan *et al.*, 2015). Thus, the use of these RNAs can provide an effective therapeutic strategy for AD treatment and diagnosis.

1.3. MicroRNAs as therapeutic products

MiRNAs (miRNAs or miRs) were discovered approximately two decades ago by Ambros and colleagues, when their studies revealed that a small non-coding RNA (sncRNA), lineage-4 (lin-4) regulated the larval development timing of the *C. elegans* (Lee *et al.*, 1993; Wightman *et al.*, 1993). This regulation is accomplished by inhibition of the expression of a protein-coding gene through recognition of complementarity sites in the 3' untranslated region (3'UTR) of lin-14 mRNA (Lee *et al.*, 1993). Accordingly, the discovery of miRNAs has been one of the most fascinating breakthroughs of recent times and, now, miRNAs represent the most extensively studied class of evolutionarily conserved, endogenous, sncRNAs (Satoh, 2010). At present, 1881 miRNAs have been identified in humans and its sequences are available in the official miRNA database (miRBase, www.mirbase.org), a repository of miRNAs from many organisms.

MiRNAs have emerged as pivotal modulators that are directly involved in the regulation of gene expression at the post-transcriptional level via base-pairing interactions between the 5′ end of the miRNA and the 3′UTR of their target mRNA, which results in mRNA translational repression or degradation, depending on the degree of sequence complementarity (Bartel, 2004; Filipowicz *et al.*, 2005; Selbach *et al.*, 2008).

MiRNAs are formed in a multistep biological process involving critical endonucleases. Figure 3 shows the miRNA biogenesis pathway. The great majority of miRNA genes are commonly transcribed as a long primary transcript (usually 1–4 kilobases), known as primary-miRNAs (pri-miRNAs) by RNA polymerase II (Bartel, 2004; Lee *et al.*, 2004). The genomic location of miRNAs genes varies and can be located in intra- and/or inter-genetic regions of the genome and at least 42% are estimated to be expressed in clusters. Like mRNAs, these pri-miRNAs are capped at the 5′ end and polyadenylated at the 3′ end, forming double stranded stem-loop structures, and can be transcribed as autonomous transcription units, or as clusters from a polycistronic transcription unit (Bartel, 2004; Gomes *et al.*, 2013; Junn and Mouradian, 2012). In the nucleus, these primary transcripts, containing the mature miRNA sequence, are recognized by a microprocessor complex (composed by an enzyme ribonuclease III Drosha along with its regulatory subunit, the double-stranded RNA-binding protein called DiGeorge syndrome critical region gene 8 (DGCR8)) that cleaves the base of the stem-loop (~11 nt) (Han *et al.*, 2006). This step produces a long stem-loop precursor of miRNA, with a hairpin secondary structure of approximately 70 to 100 nucleotides, named pre-miRNAs, with two nucleotides overhang at its 3′ end. After nuclear processing by a series of enzymes, the pre-miRNAs are exported to the cytoplasm by a nuclear transport receptor complex, Exportin-5 and its co-factor Ran (the GTP-bound form) that acts by recognizing a 2-3 base pair overhang of the pre-miRNA stem-loop structure (Lund *et al.*, 2004).

Once in the cytoplasm, the pre-miRNAs are further processed and its terminal loop is removed by a complex that contains the cytoplasmic protein Dicer (a ribonuclease III) and its co-

factors TRBP (Tar RNA-binding protein) and PACT (Protein kinase R-activating protein). As a consequence, pre-miRNAs are converted into mature double-stranded miRNAs (miRNA-miRNA* duplexes) of variable length (~19–25 nt) (Nilsen, 2007). After Dicer cleavage, mature miRNAs are associated with Argonaute (Ago) proteins, in particular Ago1 and Ago2, which are core components of RNA-induced silencing complex (RISC). During loading, mature miRNA is unwound in two strands: a single antisense miRNA strand (or guide strand, also referred to as miRNA) and a sense strand (or passenger strand, also referred to as miRNA*) that is released and, subsequently degraded by Ago2-catalysed endonucleolytic cleavage (Figure 3) (Nilsen, 2007). This selection might be determined by the relative thermodynamic stability of the two ends of miRNA duplexes and thus, the strand less stable at the 5' end is loaded into RISC, although in some cases, both strands are incorporated into the RISC.

After the selection of the antisense strand, this is loaded onto the RISC, to form miRNA silencing complex (miRISC) that identifies target mRNA based on sequence complementarity with the miRNA. In animals, the binding between the miRNA strand and their targets RNA transcripts occurs mainly through specific sequences, called the "seed sequence". The "seed" region is composed by 2-8 nt located in 5' end of the miRNA (Bartel, 2009; Gomes *et al.*, 2013). A group of miRNAs that share the same "seed sequence" but differ outside are frequently considered a 'family' of miRNAs and in most, but not all, cases might target the same gene. It is noteworthy that some miRNAs do not have a "seed sequence" complete, instead exhibit 11-12 continuous base pairs in the central region of the miRNA.

MiRNAs usually bind with partial complementarity in the 3'UTRs of its target mRNAs, resulting in the cleavage, de-adenylation or translation inhibition of target mRNAs. As mentioned above, the regulation mechanism of the translation depends on the degree of complementarity between miRNA-target mRNA, resulting in direct cleavage and degradation of mRNA transcripts when there is perfect complementarity or inhibition of protein expression by blocking mRNA translation, in the case of imperfect base pairing (Bartel, 2004; Nilsen, 2007; Selbach *et al.*, 2008; Stark *et al.*, 2005).

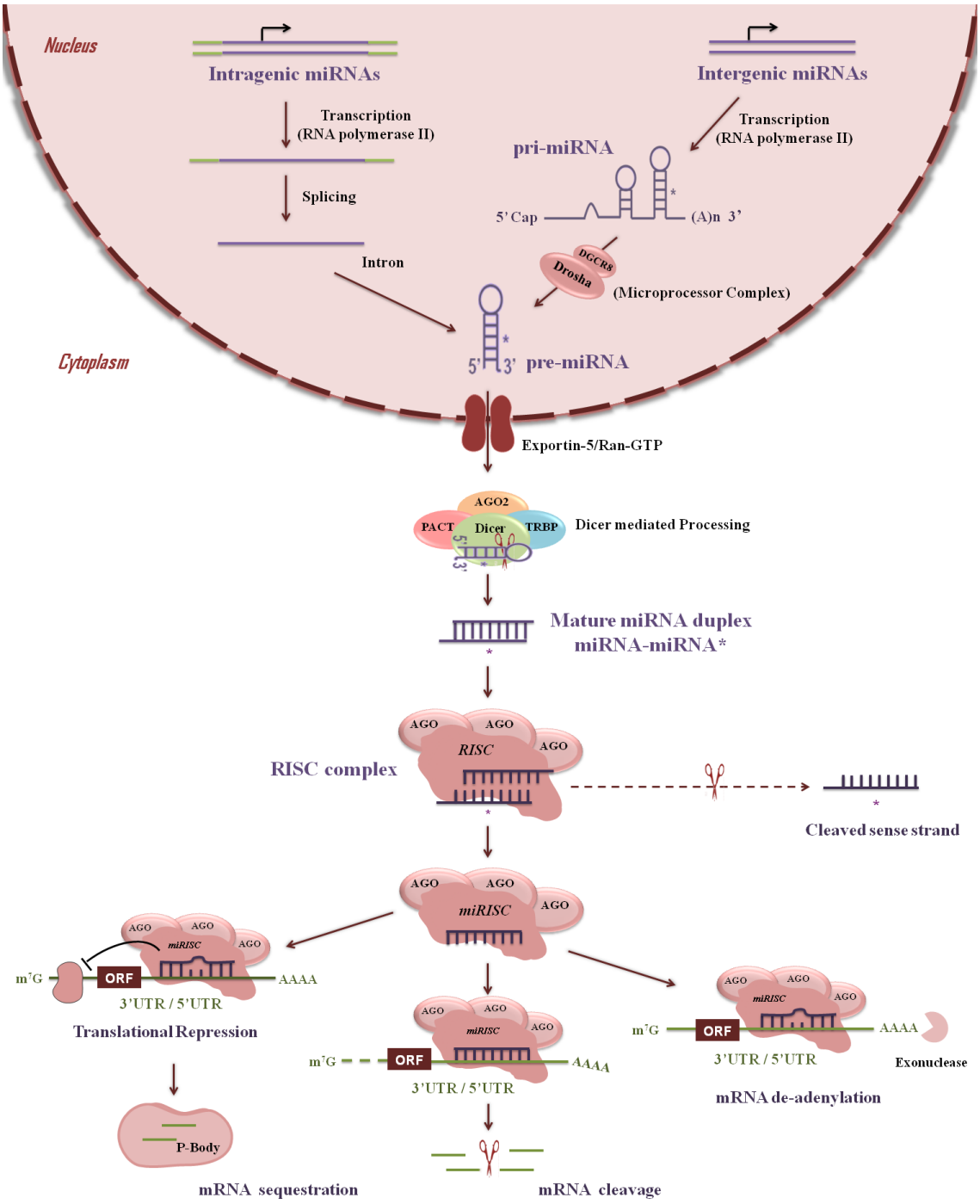

Figure 3 - Biogenesis of microRNAs.

Abbreviations: 3/5′-UTR, 3/5′ Untranslated Region; AAA, poly(A) tail; Ago, Argonaute; DGCR8, DiGeorge syndrome Critical Region gene 8; GTP, Guanosine Triphosphate; miRISC, miRNA-Induced Silencing Complex; mRNA, messenger RNA; miRNA, microRNA; ORF, Open Reading Frame; PACT, Protein kinase R-Activating Protein; pre-miRNA, precursor miRNA; pri-miRNA, primary miRNA; TRBP, Tar RNA Binding Protein.

The target mRNA is enzymatically cleaved, leading to a decrease in the corresponding protein expression. Regulatory subunits within the RISC complex and/or present in the mRNAs (i.e. cytoplasmic ribonucleoprotein complexes, mRNPs) play decisive roles in miRNA-mRNA localization, miRNA responsiveness to cellular signaling and mode of action. These complexes can be directed to polyribosomes in sub-cellular compartments, where miRNA regulates translation, resulting, sometimes, in truncation of the protein (Nilsen, 2007). Alternatively, the resulting translationally blocked mRNAs and miRNA complex can then be sequestered in cytoplasmic processing bodies (termed P-bodies), where untranslated mRNAs are stored and eventually degraded through exonuclease enzymes (Figure 3). On the other hand, specific miRNAs have been shown to destabilize targets by recruiting de-adenylating enzymes, poly(A) nucleases, to help modulate de-adenylation of mRNA and thereby prevent translation.

Therefore, the regulation of gene expression mediated by miRNA is a complex science in eukaryotes and is still an evolving concept, once several molecular mechanisms have been reported, including translational repression, increased mRNA de-adenylation and degradation of the target mRNAs (Bartel, 2004; Gomes *et al.*, 2013; Nilsen, 2007). Although these mechanisms are quite different, the main mode of action of mature miRNA is based on the recognition of specific sites (known as microRNA response elements (MRE)), typically present in the 3'UTRs of their target mRNAs, leading to a decrease in the production of the proteins by cells. Despite, of this binding occurs typically in the 3'UTR of mRNA, some miRNAs can bind specific sites in the 5'UTRs of the mRNA with less frequency and efficiency compared to 3'UTR targeting (Stark *et al.*, 2005).

Overall, the miRNAs can regulate a large proportion of the human transcriptome (up to 60% of all human protein-coding genes) by targeting multiple transcripts. An important feature of these RNAs is that an individual miRNA can regulate up to a few hundred of different mRNA targets and, consequently, can induce multiple effects on the expression of several related gene families, suppressing the expression of multiple and diverse proteins implicated in biological processes (Selbach *et al.*, 2008). On the other hand, multiple miRNAs can regulate the expression of a single target mRNA, and most likely synergistically acting. Despite advances in miRNA discovery, the role of miRNAs in pathophysiologic processes is still in early stages of research. The extensive research in the last decade has implicated miRNAs as master regulators of a variety of physiological and biological processes, including developmental timing, cell cycle, cell proliferation, cell adhesion, apoptosis, cell differentiation, stress response, metabolism, stem cell self-renewal, organ development, hematopoiesis, embryogenesis and neurogenesis (Alvarez-Garcia and Miska, 2005; Bartel, 2004; Bartel, 2009; Kloosterman and Plasterk, 2006). As a result of its efficacy and potential to inhibit the expression of a specific mRNA, coupled with its versatility in several cellular processes, miRNAs might be explored as new therapeutic agents in diseases that have genetic origins, as is the case of AD. In fact, it is expected that miRNAs-based therapeutics will be one of the major classes of therapeutic molecules in the future (Delay *et al.*, 2012; Dessy and

Gorman, 2011; Kocerha *et al.*, 2009; Kosik, 2006; Maes *et al.*, 2009). Not surprisingly, miRNA-targeting therapies are an area of intense interest to pharmaceutical companies, and many of such compounds are now being evaluated in preclinical and clinical trials for a variety of indications, such as cancer and cardiovascular diseases.

1.4. miR-29 in Alzheimer's disease

As mentioned above, over the last years, a growing number of studies have been concentrated in the identification of deregulated proteins and protein-encoding genes involved in the pathogenesis of AD, and, as a result, numerous genes have been identified as targets for therapeutic approaches (see Table 1) (Cacabelos and Torrellas, 2014). Despite their relatively recent discovery, it is already clear that miRNAs might play important regulatory roles in the molecular control of neuronal development, synaptic plasticity (forms the basis of learning and memory), neurotransmission, aging of the brain, and in a variety of physiologically relevant processes in neurodegeneration (Fineberg *et al.*, 2009; Grasso *et al.*, 2014; Klein *et al.*, 2005; Kosik, 2006; Schratt *et al.*, 2006). Consequently, in the past decade, tremendous efforts have been put mainly into identifying miRNAs that are changed in AD, demonstrating that an abundant and particularly diverse source of miRNAs is present in the brain and helping in the characterization of molecular pathways that are deregulated concomitantly to the formation of Tau and amyloid aggregates (Delay *et al.*, 2012; Feng and Feng, 2011; Maciotta *et al.*, 2013; Maes *et al.*, 2009; Satoh, 2012; Tan *et al.*, 2013; Tan *et al.*, 2015; Van den Hove *et al.*, 2014). Nevertheless, it remains difficult to predict whether these changes, like the abnormal expression profiles and dysfunction of brain-enriched miRNAs linked to AD, are a cause or a consequence of the neurodegenerative process and dementia (Du and Pertsemlidis, 2011; Grasso *et al.*, 2014; Kocerha *et al.*, 2009; Nelson *et al.*, 2008; Ullah *et al.*, 2014).

Thus, miRNAs have been intensively investigated as potential diagnostic and prognostic biomarkers, solely or in combination with other AD biomarkers, or also as novel therapeutic agents for AD (Cogswell *et al.*, 2008; Grasso *et al.*, 2014; Kumar *et al.*, 2013). In Table 1 are described some of the de-regulated miRNAs that have been recognized as being involved in the pathological features of AD, as well as their target genes.

Table 1 - Dysregulated microRNAs in Alzheimer's disease (adapted from (Cacabelos and Torrellas, 2014; Delay *et al.*, 2012; Feng and Feng, 2011; Maciotta *et al.*, 2013; Satoh, 2012; Tan *et al.*, 2013; Tan *et al.*, 2015; van den Hove *et al.*, 2014)).

miRNAs	*Trend Status*	*Validated targets*
miR-15a, -16, -34	Up	Bcl-2 (anti-apoptotic factor)
miR-124	Down	APP alternative splicing via PTPB1
miR-9, -15a, -19b, -29a/b-1/c, -107, -124, -195, -298, -328, -485-5p	Down	BACE1
Let-7, miR-15a, -16, -17-5p, -20a, -101, -106a/b, -147, -153, -323, -520c, -644, -655	Down	APP
miR-29a/b-1	Down	NAV3 (Neuron navigator 3), Bim, Bmf, Hrk, Puma
miR-9, -181c	Down	TRIM2, BTBD3, TGFBI
miR-9, -34c, -128	Down/Up	SIRT1 (Sirtuin 1, a de-acetylase that interacts with Tau)
miR-146a	Up	CFH (Complement factor H) and IRAK1 (IL-1 receptor-associated kinase-1)
miR-9	Down	REST (RE-1 silencing transcription factor), BAF53a, Tlx, NF-H (Neurofilament H), Aβ
miR-9, -15, -29a/b-1, -137, -181c	Down	SPT (Serine palmitoyletransferase)
miR-9	Down	PSEN1
miR-34	Up	Cdk4, cyclin D1, Tau
miR-128		ROS
miR-107	Down	CDK6, CFL1, CDK5R1, HIF-1b
miR-132	Down	FOXO3a, Tau via PTBP2 (Polypyrimidine tract-binding protein 2)
miR-9, -15a miR-181c	Down	Hyperphosphorylation of tau via ERK1(Extracellular signal regulated kinase 1) Tau acetylation

Interestingly, several studies showed that there is a set of miRNAs (include miR-9, miR-15, miR-29, miR-106, miR-107 and miR-124) that seems to be specifically altered in the AD brain and they have been associated to different molecular pathways in AD pathogenesis. In particular, the regulation of these miRNAs was correlated with the modulation of the expression and/or processing of AD-related genes, such as APP, BACE1, Aβ peptides deposition, tau protein phosphorylation, SIRT1 and MAPT signaling pathway (which encodes for tau) (see Table 1) (Delay *et al.*, 2012). Indeed, this can represent a significant advance for AD diagnosis and treatment.

The miR-29 remains as one of the most interesting and intriguing miRNA families, once this miRNA has a strong impact on many processes involved in the pathogenesis of the AD (Cogswell *et al.*, 2008). The miR-29 family includes four members: miR-29a, miR-29b-1, miR-29b-2 and miR-29c, and all share identical sequences at nucleotide positions 2-8 of 5' end and the same seed region (Kriegel *et al.*, 2012; Liston *et al.*, 2012).

As mentioned above, the BACE1 protein levels are elevated in AD brains, suggesting that BACE1 dysregulation is directly implicated in AD pathogenesis through the formation of toxic Aβ peptides. Thus, it has been established that reducing BACE1 expression may delay or even reduce AD progression. On the other hand, significant alterations in the expression levels of miR-29 family were found in brains of AD patients, being significantly decreased and displaying abnormally high levels of BACE1 protein (Hebert *et al.*, 2008; Zong *et al.*, 2011). It is tempting to speculate that miR-29 might play an important role in the adult brain. Particularly, the work of Hebert and co-workers, in 2008, showed that the decreased levels of the miR-29a/b-1 cluster were correlated with increased levels of BACE1 expression in patients with SAD (Figure 4) and that the introduction of synthetic miR-29 reduces secretion of Aβ peptides (Hebert *et al.*, 2008).

In addition to its potential role as a major element to silence BACE1 protein expression, it was recently shown that miR-29b can also be used as an inhibitor of neuronal apoptosis. However, the miR-29b is decreased in the AD brain and therefore it loses its ability to inhibit apoptosis. MiR-29b has been identified to target a family of pro-apoptotic regulators, including Bim, Bmf, Hrk and Puma (see Table 1) (Kole *et al.*, 2011; Zhu *et al.*, 2006).

These findings raised the opportunity to use pre-miR-29 in the implementation of a possible protective therapeutic strategy for AD and suggest that BACE1 can be a promising target in the therapeutic of this disease. The use of pre-miRNA instead of the mature miRNA could represent an advantage to the therapeutic process, because, in cellular environment the pre-miRNA is more easily recognized and processing within the cell is more efficient (Tsutsumi *et al.*, 2011). Moreover, the pre-miR-29b structural characteristics, specifically the single chain with approximately 80 nucleotides of which some are unpaired in the 3'overhang, will possibly make easier its production and purification.

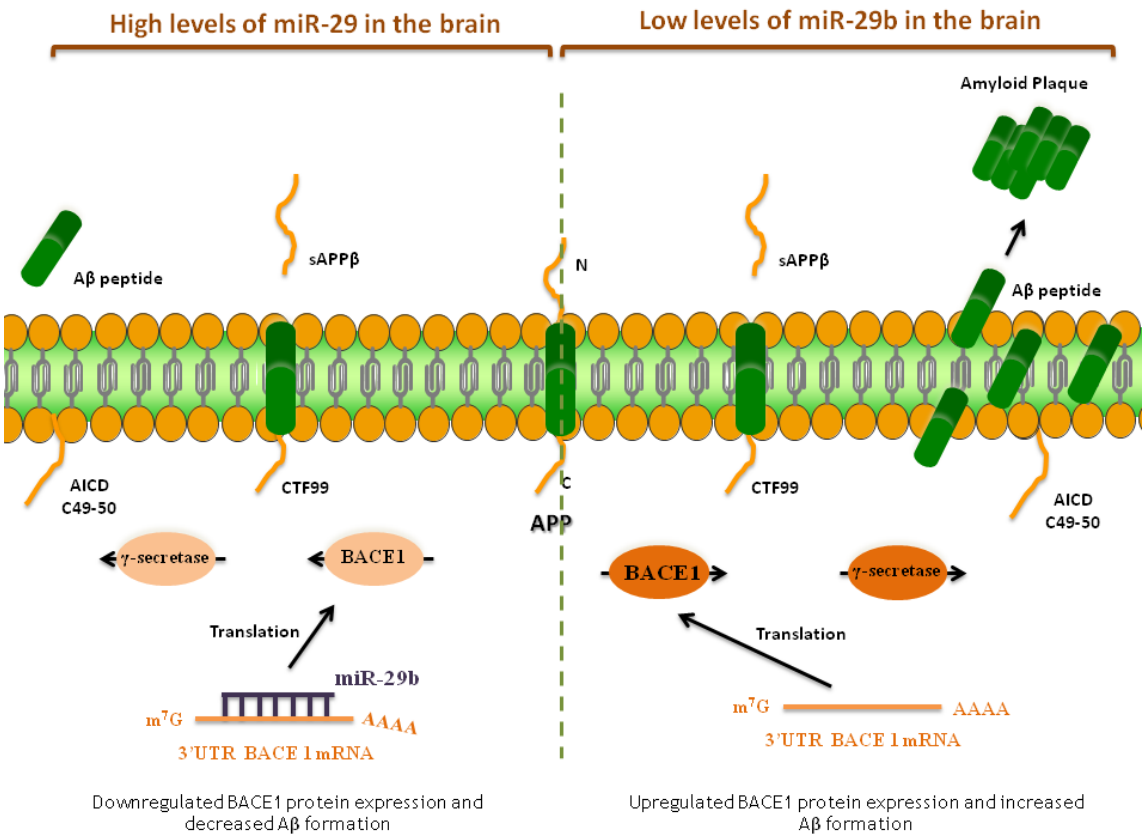

Figure 4 - Pre-miR-29b-1 regulation of BACE1 in Alzheimer's disease.

1.5. References

Albert MS, DeKosky ST, Dickson D, Dubois B, Feldman HH, *et al*. (2011) The diagnosis of mild cognitive impairment due to Alzheimer's disease: recommendations from the National Institute on Aging-Alzheimer's Association workgroups on diagnostic guidelines for Alzheimer's disease. *Alzheimer's & dementia: the journal of the Alzheimer's Association* 7, 270-279.

Alvarez-Garcia I and Miska EA (2005) MicroRNA functions in animal development and human disease. *Development* 132, 4653-4662.

Bartel DP (2004) MicroRNAs: genomics, biogenesis, mechanism, and function. *Cell* 116, 281-297.

Bartel DP (2009) MicroRNAs: target recognition and regulatory functions. *Cell* 136, 215-233.

Barthel H, Gertz HJ, Dresel S, Peters O, Bartenstein P, *et al*. (2011) Cerebral amyloid-beta PET with florbetaben (18F) in patients with Alzheimer's disease and healthy controls: a multicentre phase 2 diagnostic study. *The Lancet. Neurology* 10, 424-435.

Bertram L, Lill CM, Tanzi RE (2010) The genetics of Alzheimer disease: back to the future. *Neuron* 68, 270-281.

Blennow K, de Leon MJ, Zetterberg H (2006) Alzheimer's disease. *Lancet* 368, 387-403.

Borgesius NZ, de Waard MC, van der Pluijm I, Omrani A, Zondag GC, *et al*. (2011) Accelerated age-related cognitive decline and neurodegeneration, caused by deficient DNA repair. *The Journal of neuroscience: the official journal of the Society for Neuroscience* 31, 12543-12553.

Bu G (2009) Apolipoprotein E and its receptors in Alzheimer's disease: pathways, pathogenesis and therapy. *Nature reviews. Neuroscience* 10, 333-344.

Buchman AS, Yu L, Wilson RS, Schneider JA, Bennett DA (2013) Association of brain pathology with the progression of frailty in older adults. *Neurology* 80, 2055-2061.

Bumcrot D, Manoharan M, Koteliansky V, Sah DW (2006) RNAi therapeutics: a potential new class of pharmaceutical drugs. *Nature chemical biology* 2, 711-719.

Burnett JC and Rossi JJ (2012) RNA-based therapeutics: current progress and future prospects. *Chemistry Biology* 19, 60-71.

Cacabelos R and Torrellas C (2014) Epigenetic drug discovery for Alzheimer's disease. *Expert opinion on drug discovery* 9, 1059-1086.

Chen S, Ge X, Chen Y, Lv N, Liu Z, *et al*. (2013) Advances with RNA interference in Alzheimer's disease research. *Drug design, development and therapy* 7, 117-125.

Chu CY and Rana TM (2007) Small RNAs: regulators and guardians of the genome. *Journal of Cellular Physiology* 213, 412-419.

Citron M (2010) Alzheimer's disease: strategies for disease modification. *Nature reviews. Drug discovery* 9, 387-398.

Cogswell JP, Ward J, Taylor IA, Waters M, Shi Y, *et al*. (2008) Identification of miRNA changes in Alzheimer's disease brain and CSF yields putative biomarkers and insights into disease pathways. *Journal of Alzheimer's disease: JAD* 14, 27-41.

Delay C, Mandemakers W, Hebert SS (2012) MicroRNAs in Alzheimer's disease. *Neurobiology of disease* 46, 285-290.

Deng Y, Wang CC, Choy KW, Du Q, Chen J, *et al*. (2014) Therapeutic potentials of gene silencing by RNA interference: principles, challenges, and new strategies. *Gene* 538, 217-227.

Dessy A and Gorman JM (2011) The emerging therapeutic role of RNA interference in disorders of the central nervous system. *Clinical Pharmacology Therapeutics* 89, 450-454.

De Strooper B (2010) Proteases and Proteolysis in Alzheimer Disease: A Multifactorial View on the Disease Process. *Physiological Reviews* 90, 465-494

Dogini DB, Pascoal VD, Avansini SH, Vieira AS, Pereira TC, *et al*. (2014) The new world of RNAs. *Genetics and molecular biology* 37, 285-293.

Dong S, Duan Y, Hu Y, Zhao Z (2012) Advances in the pathogenesis of Alzheimer's disease: a re-evaluation of amyloid cascade hypothesis. *Translational Neurodegeneration* 1, 18

Du L and Pertsemlidis A (2011) Cancer and neurodegenerative disorders: pathogenic convergence through microRNA regulation. *Journal of molecular cell biology* 3, 176-180.

Dunkel P, Chai CL, Sperlagh B, Huleatt PB, Matyus P (2012) Clinical utility of neuroprotective agents in neurodegenerative diseases: current status of drug development for Alzheimer's, Parkinson's and Huntington's diseases, and amyotrophic lateral sclerosis. *Expert opinion on investigational drugs* 21, 1267-1308.

Dykxhoorn DM and Lieberman J (2006) Running interference: prospects and obstacles to using small interfering RNAs as small molecule drugs. *Annual Review of Biomedical Engineering* 8, 377-402.

Feng W and Feng Y (2011) MicroRNAs in neural cell development and brain diseases. *Science China. Life sciences* 54, 1103-1112.

Filipowicz W, Jaskiewicz L, Kolb FA, Pillai RS (2005) Post-transcriptional gene silencing by siRNAs and miRNAs. *Current Opinion in Structural Biology* 15, 331-341.

Fineberg SK, Kosik KS, Davidson BL (2009) MicroRNAs potentiate neural development. *Neuron* 64, 303-309.

Fire A, Xu S, Montgomery MK, Kostas SA, Driver SE, *et al*. (1998) Potent and specific genetic interference by double-stranded RNA in *Caenorhabditis elegans*. *Nature* 391, 806-811.

Genin E, Hannequin D, Wallon D, Sleegers K, Hiltunen M, *et al*. (2011) APOE and Alzheimer disease: a major gene with semi-dominant inheritance. *Molecular psychiatry* 16, 903-907.

Ghiso J and Frangione B (2002) Amyloidosis and Alzheimer's disease. *Advanced drug delivery reviews* 54, 1539-1551.

Glenner GG (1989a) Amyloid beta protein and the basis for Alzheimer's disease. *Progress in clinical and biological research* 317, 857-868.

Glenner GG (1989b) The pathobiology of Alzheimer's disease. *Annual review of medicine* 40, 45-51.

Goedert M, Spillantini MG, Jakes R, Rutherford D, Crowther RA (1989) Multiple isoforms of human microtubule-associated protein tau: sequences and localization in neurofibrillary tangles of Alzheimer's disease. *Neuron* 3, 519-526.

Gomes AQ, Nolasco S, Soares H (2013) Non-coding RNAs: multi-tasking molecules in the cell. *International journal of molecular sciences* 14, 16010-16039.

Goodall EF, Heath PR, Bandmann O, Kirby J, Shaw PJ (2013) Neuronal dark matter: the emerging role of microRNAs in neurodegeneration. *Frontiers in cellular neuroscience* 7, 178.

Grasso M, Piscopo P, Confaloni A, Denti MA (2014) Circulating miRNAs as biomarkers for neurodegenerative disorders. *Molecules* 19, 6891-6910.

Guzman-Villanueva D, El-Sherbiny IM, Herrera-Ruiz D, Vlassov AV, Smyth HD (2012) Formulation approaches to short interfering RNA and MicroRNA: challenges and implications. *Journal of pharmaceutical sciences* 101, 4046-4066.

Han J, Lee Y, Yeom KH, Nam JW, Heo I, *et al*. (2006) Molecular basis for the recognition of primary microRNAs by the Drosha-DGCR8 complex. *Cell* 125, 887-901.

Hardy J and Selkoe DJ (2002) The amyloid hypothesis of Alzheimer's disease: progress and problems on the road to therapeutics. *Science* 297, 353-356.

Hebert SS, Horre K, Nicolai L, Papadopoulou AS, Mandemakers W, *et al*. (2008) Loss of microRNA cluster miR-29a/b-1 in sporadic Alzheimer's disease correlates with increased BACE1/beta-secretase expression. *Proceedings of the National Academy of Sciences of the United States of America* 105, 6415-6420.

Holtzman DM (2011) CSF biomarkers for Alzheimer's disease: current utility and potential future use. *Neurobiology of aging* 32 Suppl 1, S4-9.

Ingelson M, Blomberg M, Benedikz E, Wahlund LO, Karlsson E, *et al*. (1999) Tau immunoreactivity detected in human plasma, but no obvious increase in dementia. *Dementia and geriatric cognitive disorders* 10, 442-445.

Isik AT (2010) Late onset Alzheimer's disease in older people. *Clinical interventions in aging* 5, 307-311.

Iyengar BR, Choudhary A, Sarangdhar MA, Venkatesh KV, Gadgil CJ, *et al*. (2014) Non-coding RNA interact to regulate neuronal development and function. *Frontiers in cellular neuroscience* 8, 47.

Jack CR Jr, Albert MS, Knopman DS, McKhann GM, Sperling RA, *et al*. (2011) Introduction to the recommendations from the National Institute on Aging-Alzheimer's Association workgroups on diagnostic guidelines for Alzheimer's disease. *Alzheimer's & dementia: the journal of the Alzheimer's Association* 7, 257-262.

Jeppesen DK, Bohr VA, Stevnsner T (2011) DNA repair deficiency in neurodegeneration. *Progress in neurobiology* 94, 166-200.

Junn E and Mouradian MM (2012) MicroRNAs in neurodegenerative diseases and their therapeutic potential. *Pharmacology & therapeutics* 133, 142-150.

Kim DH, Yeo SH, Park JM, Choi JY, Lee TH, *et al*. (2014) Genetic markers for diagnosis and pathogenesis of Alzheimer's disease. *Gene* 545, 185-193.

Kim VN (2005) Small RNAs: classification, biogenesis, and function. *Molecules and Cells* 19, 1-15.

Kim VN, Han J, Siomi MC (2009) Biogenesis of small RNAs in animals. *Nature reviews. Molecular cell biology* 10, 126-139.

Klein ME, Impey S, Goodman RH (2005) Role reversal: the regulation of neuronal gene expression by microRNAs. *Current opinion in neurobiology* 15, 507-513.

Kloosterman WP and Plasterk RH (2006) The diverse functions of microRNAs in animal development and disease. *Developmental cell* 11, 441-450.

Kocerha J, Kauppinen S, Wahlestedt C (2009) microRNAs in CNS disorders. *Neuromolecular medicine* 11, 162-172.

Kole AJ, Swahari V, Hammond SM, Deshmukh M (2011) miR-29b is activated during neuronal maturation and targets BH3-only genes to restrict apoptosis. *Genes & development* 25, 125-130.

Kosik KS (2006) The neuronal microRNA system. *Nature reviews. Neuroscience* 7, 911-920.

Kriegel AJ, Liu Y, Fang Y, Ding X, Liang M (2012) The miR-29 family: genomics, cell biology, and relevance to renal and cardiovascular injury. *Physiological genomics* 44, 237-244.

Kumar P, Dezso Z, MacKenzie C, Oestreicher J, Agoulnik S, *et al*. (2013) Circulating miRNA biomarkers for Alzheimer's disease. *PloS one* 8, e69807.

Lee RC, Feinbaum RL, Ambros V (1993) The *C. elegans* heterochronic gene lin-4 encodes small RNAs with antisense complementarity to lin-14. *Cell* 75, 843-854.

Lee Y, Kim M, Han J, Yeom KH, Lee S, *et al*. (2004) MicroRNA genes are transcribed by RNA polymerase II. *The EMBO journal* 23, 4051-4060.

Lehman N (2010) RNA in evolution. *Wiley interdisciplinary reviews. RNA* 1, 202-213.

Liston A, Papadopoulou AS, Danso-Abeam D, Dooley J (2012) MicroRNA-29 in the adaptive immune system: setting the threshold. *Cellular and molecular life sciences: CMLS* 69, 3533-3541.

Lund E, Guttinger S, Calado A, Dahlberg JE, Kutay U (2004) Nuclear export of microRNA precursors. *Science* 303, 95-98.

Maciotta S, Meregalli M, Torrente Y (2013) The involvement of microRNAs in neurodegenerative diseases. *Frontiers in cellular neuroscience* 7, 265.

Maes OC, Chertkow HM, Wang E, Schipper HM (2009) MicroRNA: Implications for Alzheimer Disease and other Human CNS Disorders. *Current genomics* 10, 154-168.

Matera AG, Terns RM, Terns MP (2007) Non-coding RNAs: lessons from the small nuclear and small nucleolar RNAs. *Nature reviews. Molecular cell biology* 8, 209-220.

McKhann GM, Knopman DS, Chertkow H, Hyman BT, Jack CR Jr, *et al*. (2011) The diagnosis of dementia due to Alzheimer's disease: recommendations from the National Institute on Aging-

Alzheimer's Association workgroups on diagnostic guidelines for Alzheimer's disease. *Alzheimer's & dementia: the journal of the Alzheimer's Association* 7, 263-269.

Milhavet O, Gary DS, Mattson MP (2003) RNA interference in biology and medicine. *Pharmacological Reviews* 55, 629-648.

Mullane K and Williams M (2013) Alzheimer's therapeutics: continued clinical failures question the validity of the amyloid hypothesis-but what lies beyond? *Biochemical pharmacology* 85, 289-305.

Nelson PT, Wang WX, Rajeev BW (2008) MicroRNAs (miRNAs) in neurodegenerative diseases. *Brain pathology* 18, 130-138.

Nilsen TW (2007) Mechanisms of microRNA-mediated gene regulation in animal cells. *Trends in genetics: TIG* 23, 243-249.

Piaceri I, Nacmias B, Sorbi S (2013) Genetics of familial and sporadic Alzheimer's disease. *Frontiers in bioscience* 5, 167-177.

Provost P (2010a) Interpretation and applicability of microRNA data to the context of Alzheimer's and age-related diseases. *Aging* 2, 166-169.

Provost P (2010b) MicroRNAs as a molecular basis for mental retardation, Alzheimer's and prion diseases. *Brain research* 1338, 58-66.

Qiu C, Kivipelto M, von Strauss E (2009) Epidemiology of Alzheimer's disease: occurrence, determinants, and strategies toward intervention. *Dialogues in clinical neuroscience* 11, 111-128.

Ramachandran PV and Ignacimuthu S (2013) RNA interference-a silent but an efficient therapeutic tool. *Applied biochemistry and biotechnology* 169, 1774-1789.

Satoh J (2010) MicroRNAs and their therapeutic potential for human diseases: aberrant microRNA expression in Alzheimer's disease brains. *Journal of Pharmacological Sciences* 114, 269-275.

Satoh J (2012) Molecular network of microRNA targets in Alzheimer's disease brains. *Experimental neurology* 235, 436-446.

Schonrock N, Matamales M, Ittner LM, Gotz J (2012) MicroRNA networks surrounding APP and amyloid-beta metabolism-implications for Alzheimer's disease. *Experimental neurology* 235, 447-454.

Schratt GM, Tuebing F, Nigh EA, Kane CG, Sabatini ME, *et al*. (2006) A brain-specific microRNA regulates dendritic spine development. *Nature* 439, 283-289.

Selbach M, Schwanhausser B, Thierfelder N, Fang Z, Khanin R, *et al*. (2008) Widespread changes in protein synthesis induced by microRNAs. *Nature* 455, 58-63.

Sperling RA, Aisen PS, Beckett LA, Bennett DA, Craft S, *et al*. (2011) Toward defining the preclinical stages of Alzheimer's disease: recommendations from the National Institute on Aging-Alzheimer's Association workgroups on diagnostic guidelines for Alzheimer's disease. *Alzheimer's & dementia: the journal of the Alzheimer's Association* 7, 280-292.

Stark A, Brennecke J, Bushati N, Russell RB, Cohen SM (2005) Animal MicroRNAs confer robustness to gene expression and have a significant impact on 3'UTR evolution. *Cell* 123, 1133-1146.

Suehs BT, Davis CD, Alvir J, van Amerongen D, Pharmd NC, *et al*. (2013) The clinical and economic burden of newly diagnosed Alzheimer's disease in a medicare advantage population. *American journal of Alzheimer's disease and other dementias* 28, 384-392.

Sullenger BA and Gilboa E (2002) Emerging clinical applications of RNA. *Nature* 418, 252-258.

Svoboda P (2014) Renaissance of mammalian endogenous RNAi. *FEBS letters* 588, 2550-2556.

Tabares-Seisdedos R, Dumont N, Baudot A, Valderas JM, Climent J, *et al*. (2011) No paradox, no progress: inverse cancer comorbidity in people with other complex diseases. *The Lancet. Oncology* 12, 604-608.

Tan L, Yu JT, Hu N, Tan L (2013) Non-coding RNAs in Alzheimer's disease. *Molecular neurobiology* 47, 382-393.

Tan L, Yu JT, Tan L (2015) Causes and Consequences of MicroRNA Dysregulation in Neurodegenerative Diseases. *Molecular neurobiology* 51, 1249-1262.

Tarawneh R and Holtzman DM (2010) Biomarkers in translational research of Alzheimer's disease. *Neuropharmacology* 59, 310-322.

Tsutsumi A, Kawamata T, Izumi N, Seitz H, Tomari Y (2011) Recognition of the pre-miRNA structure by Drosophila Dicer-1. *Nature structural & molecular biology* 18, 1153-1158.

Ullah S, John P, Bhatti A (2014) MicroRNAs with a role in gene regulation and in human diseases. *Molecular biology reports* 41, 225-232.

Van den Hove DL, Kompotis K, Lardenoije R, Kenis G, Mill J, *et al*. (2014) Epigenetically regulated microRNAs in Alzheimer's disease. *Neurobiology of aging* 35, 731-745.

Vassar R, Kovacs DM, Yan R, Wong PC (2009) The beta-secretase enzyme BACE in health and Alzheimer's disease: regulation, cell biology, function, and therapeutic potential. *The Journal of neuroscience: the official journal of the Society for Neuroscience* 29, 12787-12794.

Wightman B, Ha I, Ruvkun G (1993) Posttranscriptional regulation of the heterochronic gene lin-14 by lin-4 mediates temporal pattern formation in *C. elegans*. *Cell* 75, 855-862.

Wilson RS, Nag S, Boyle PA, Hizel LP, Yu L, *et al*. (2013) Brainstem aminergic nuclei and late-life depressive symptoms. *JAMA psychiatry* 70, 1320-1328.

Zamore PD, Tuschl T, Sharp PA, Bartel DP (2000) RNAi: double-stranded RNA directs the ATP-dependent cleavage of mRNA at 21 to 23 nucleotide intervals. *Cell* 101, 25-33.

Zhu X, Raina AK, Perry G, Smith MA (2006) Apoptosis in Alzheimer disease: a mathematical improbability. *Current Alzheimer research* 3, 393-396.

Zong Y, Wang H, Dong W, Quan X, Zhu H, *et al*. (2011) miR-29c regulates BACE1 protein expression. *Brain research* 1395, 108-115.

Paper I

2. Current progress on microRNAs-based therapeutics

P. Pereira, J. A. Queiroz, A. Figueiras, F. Sousa

(*Submitted for publication*)

Short description: This review provides a general idea of the currently available microRNAs-based therapeutics. Initially, it is presented a comparative overview of the different strategies applied for obtaining microRNAs, either through recombinant biosynthesis from different biological sources or by chemical and enzymatic methods. It is also discussed the methodologies applied for the extraction and isolation of the produced microRNAs. Afterwards, it is summarized the main chromatographic strategies that have been used to purify microRNAs obtained from different sources. Then, the methods currently employed to assess the quality of the recombinant and synthetic microRNAs are also elucidated, as well as general guidelines to obtain microRNAs with clinical-grade quality, intactness and biological activity. Finally, it is also presented and discussed the latest technology for the delivery of microRNAs in the brain, as well as advantages and limitations for their application.

Current progress on microRNAs-based therapeutics

P. Pereira[1], J. A. Queiroz[1], A. Figueiras[1,2], F. Sousa[1]*

[1] *CICS-UBI – Health Sciences Research Centre, University of Beira Interior, Avenida Infante D. Henrique, 6200-506 Covilhã, Portugal;*

[2] *CNC - Center of Neuroscience and Cell Biology, University of Coimbra, Largo Marquês de Pombal, 3004-517 Coimbra, Portugal*

*Corresponding author:
Dr. Fani Sousa
Phone: +351 275 329 074
Fax: +351 275 329 099
E-mail address: fani.sousa@fcsaude.ubi.pt
Postal address: Health Sciences Research Centre, Universidade da Beira Interior, Avenida Infante D. Henrique, 6200-506 Covilhã, Portugal

Contents

Abstract

MicroRNAs-based therapy has recently emerged as a promising strategy in the treatments of neurodegenerative diseases. Thus, in this review, the most recent and important challenges and advances on the development of miRNA therapeutics for brain-targeting are discussed. In particular, this review highlights current knowledge and progress in the field of manufacturing, recovery, isolation, purification and analysis of these therapeutic oligonucleotides. Finally, the available miRNA delivery systems are reviewed and an analysis is presented in what concerns to the current challenges that have to be addressed to ensure their specificity and efficacy. Overall, it is intended to provide a perspective on the future of miRNA-based therapeutics, focusing the biotechnological approach to obtain miRNAs.

Keywords

Biotechnological platform, Delivery systems, Manufacturing, microRNAs-based therapeutics, Neurodegenerative diseases, Purification, Recovery, RNA interference

1. Introduction

Nowadays, microRNAs (miRNAs or miRs) represent the most extensively studied class of non-coding RNAs due their great potential for therapeutic knockdown of disease-causing genes (Satoh, 2010; Soifer et al., 2007). On the other hand, several evidences indicate that some endogenous miRNAs circulate extracellularly steadily and stable in bodily fluids (such as blood serum, plasma, urine, saliva and cerebrospinal fluid (CSF)) and therefore they have also been reported as promising biomarkers (Cogswell et al., 2008; Grasso et al., 2014; Sheinerman and Umansky, 2013).

These RNAs are small, highly-conserved and act as endogenous modulators of gene expression at the post-transcriptional level (reviewed in (Bartel, 2004; Filipowicz et al., 2008; Guo et al., 2010; Selbach et al., 2008)). In a few words, miRNAs mediate the regulation of gene expression through a sequential process involving a long primary miRNA (pri-miRNA) that is cleaved producing a hairpin secondary structure called precursor of miRNA (pre-miRNA). Afterwards, subjected to cytoplasmic processing by a series of enzymes, the pre-miRNA is converted into a mature double-stranded miRNA and, subsequently, the mature miRNA is incorporated into RNA-induced silencing complex (RISC) to regulate the messenger RNA (mRNA) (Bartel, 2004; Gomes et al., 2013; He and Hannon, 2004). The main mechanism of action of mature miRNA is the recognition of specific sites ("seed sequence", 2-8 nucleotides), typically present in the 3'untranslated region (3'UTR) of their target mRNAs. This recognition results in the degradation of mRNA transcripts, when there is perfect complementarity between the 5′ end of the miRNA and selected target mRNA, or translational repression of protein expression by blocking mRNA translation or inducing de-adenylation of mRNA, if imperfect base pairing prevails (Nilsen, 2007; Selbach et al., 2008; Stark et al., 2005). The complexity of the regulation induced by miRNA is also the result of multiple interactions established between miRNAs and their targets, once a single mRNA is targeted by multiple miRNAs, while a single miRNA (or miRNA family) can have effects in the expression of several hundreds of target mRNAs and consequently, is able to regulate the production of multiple and diverse proteins involved in a biological process (Selbach et al., 2008).

As result of the recent and extensive research, miRNAs have been implicated as master regulators of a variety of physiological and cellular processes, such as cell proliferation and differentiation, cell cycle regulation, cellular physiology, cell adhesion, apoptosis, stress response, regulation of signaling pathways and metabolism (Alvarez-Garcia and Miska, 2005; Bartel, 2004, 2009; Kloosterman and Plasterk, 2006). Furthermore, since some miRNAs are expressed in high abundance in the human brain, they are also involved in the regulation of neurobiological functions, namely neurogenesis, aging of the brain, neuronal and dendritic spine development, neurotransmission, synaptic plasticity and self-renewal of neural stem cells (Fineberg et al., 2009; Grasso et al., 2014; Klein et al., 2005; Kosik et al., 2006; Schratt et al., 2006).

As demonstrated by a large number of studies in the last decade, dysregulation of expression levels of miRNAs, as well as their dysfunction in the brain have been associated with the pathogenesis of various diseases of the nervous system, including Alzheimer's disease, Parkinson's disease, Huntington's disease and Amyotrophic Lateral Sclerosis (Du and Pertsemlidis, 2011; Grasso et al., 2014; Kocerha et al., 2009; Nelson et al., 2008; Ullah et al., 2014). The neurodegenerative diseases (NDs) constitute a serious and growing health problem for our societies, being one of the main causes of morbidity and healthcare costs to society. In general, this family of disorders is characterized by a profound and progressive loss of neuronal structure and function in specific parts of the nervous system (such as, cognitive, motor or sensory areas), culminating in a final common pathway of neuronal cell death, arising from often unknown or insufficiently characterized risk factors and causes (Goodall et al., 2013; Maciotta et al., 2013). In fact, there are increasing evidences supporting that NDs are caused by genetic and/or epigenetic alterations to protein-coding genes (Morris et al., 2010; Serretti et al., 2007). The implications of this knowledge for the understanding of the contribution of miRNAs in NDs are the eventual generation of novel targets for therapeutic intervention, which are based on the specific genetic alterations which are directly involved in neurodegenerative pathogenesis, by inhibition of the activity of neurotoxic genes or by molecular activation of neuroprotective pathways (Grasso et al., 2014; Junn and Mouradian, 2012). Thus, the characteristics of miRNAs, as well as, their expression profiling in the NDs has led the advance towards new diagnosis, staging, progression, prognosis/prevention, drug development and response to the treatments of these disorders (Kocerha et al., 2009). Accordingly, miRNAs have recently gained much attention for their roles in neurodegenerative pathogenesis, supporting their potential as targets/drug candidates for the development of novel therapies for application in specific NDs that currently remain very challenging and difficult to overcome. However, the success of these emerging therapeutic strategies depends on the miRNA integrity, the absence of contaminants and its biological activity. Therefore, it is highlighted the importance of the purification procedures in obtaining the final RNA products with quality and quantity compatible with the administration in humans

In this review, it is briefly discussed the key aspects and research trends related to the use of miRNAs in the treatment of NDs, followed by a detailed analysis of the methodologies for their production, isolation, recovery, purification and delivery. Thus, the focus it will be the strategies presently used for miRNA therapy; it will be discussed their use and drawbacks, and the challenges and future directions for development of miRNA-based therapy for NDs.

2. MicroRNAs as therapeutic products

To understand the role of miRNAs in neurological processes, it is mandatory to develop tools to regulate their levels, once NDs may be caused by the loss- or gain-of-function of an individual or family miRNA. The normal function of a miRNA can be efficiently and specifically

restored (miRNA replacement therapy) by synthetic or *in vitro* transcribed mature double-stranded miRNA-like molecules called miRNA mimics (see Figure 1 and Table 1). An alternative approach is the over-expression of exogenous mature miRNAs encoded by plasmids that are processed in eukaryotic cells, by transient or stable transfection or viral transduction of a pri-miRNA transgene, pre-miRNA and pre-miRNA-like short hairpins RNAs (shRNAs) (see Figure 1 and Table 1) (reviewed in (Bumcrot et al., 2006; Junn and Mouradian, 2012; Li and Rana, 2014; Magen and Hornstein, 2014; McDermott et al., 2011; Soifer et al., 2007; van Rooij and Kauppinen, 2014)).

However, when the problem comes from the over-expression of a specific type of miRNA, the inhibition of these miRNAs (miRNA inhibition therapy) can be accomplished through injection of complementary RNA sequence that binds to the miRNA, inactivating and blocking its activity. Thus, the inhibition of miRNA activity can be achieved by the use of small miRNA inhibitors, oligomers, including RNA and DNA analogues, such as various modified anti-sense oligoribonucleotides (anti-sense "anti-miRs"), antagomirs, locked nucleic acid (LNA)-anti-miRNAs, "miRNA sponges" and "miRNA-masks", which are currently being evaluated in preclinical and clinical studies (see Table 1 and Figure 1) (reviewed in (Bumcrot et al., 2006; Junn and Mouradian, 2012; Li and Rana, 2014; Magen and Hornstein, 2014; McDermott et al., 2011; Soifer et al., 2007; van Rooij and Kauppinen, 2014)).

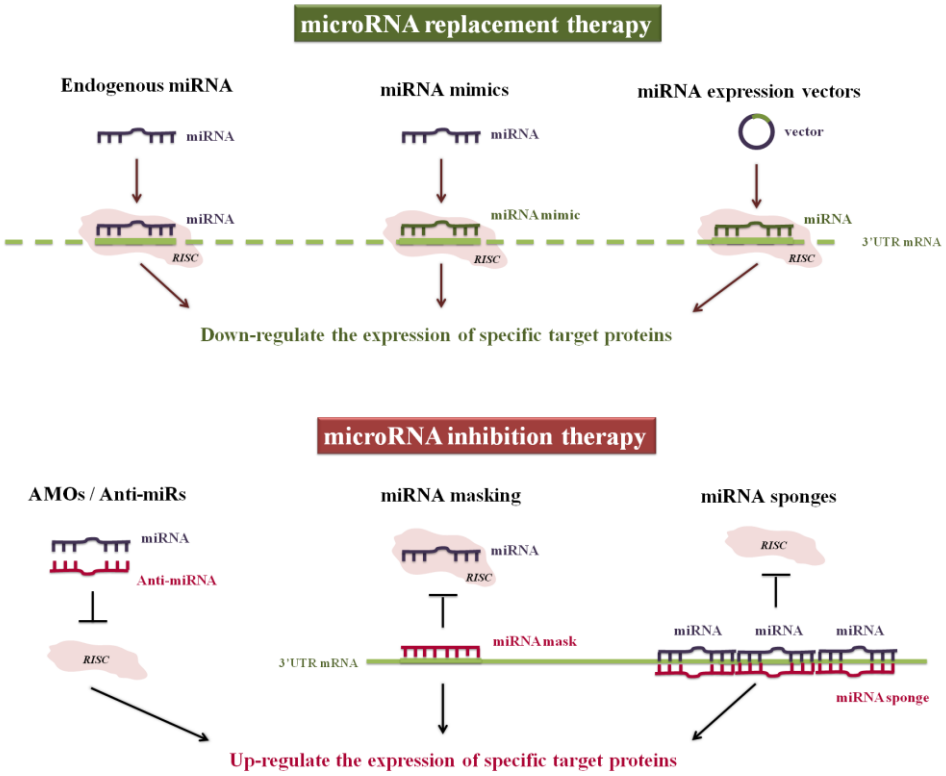

Figure 1 - Schematic representation of microRNA-based therapeutic approaches.

Table 1 - Overview of the available therapeutic strategies for reinstatement or inhibition of microRNAs.

(reviewed in (Bumcrot et al., 2006; Junn and Mouradian, 2012; Li and Rana, 2014; Magen and Hornstein, 2014, McDermott et al., 2011; Soifer et al., 2007; Zhang et al., 2013))

miRNA reinstatement		**Advantages**	**Limitations**
miRNA mimics	-Small, synthetic and chemically modified double-stranded miRNA that are processed into single-strand form inside the cells -They can be loaded into RISC to achieve the downstream inhibition of the target mRNAs	-Mimics the function of endogenous mature or precursor miRNA molecules by direct re-introduction in the cells or tissues -Increases the levels of a miRNA that is lost during disease progression	-Usually conjugated or encapsulated with different *in vivo* delivery system, in order to influence the stability and uptake -Systemic delivery can result in uptake by non-target tissues that normally do not express the miRNA of interest, resulting in potential off-target effects -Mimics can potentially induce a non-specific interferon response through Toll-like receptors
miRNA expression vectors	-Plasmid or viral expression vectors constructed with strong promoters that enable the expression of various species of miRNAs in specific tissues	-Restoration of the expression and function of a specific miRNA -Viral delivery of miRNAs can be optimized to achieve a specific and continuous expression level -Evidences of transduction efficiency and minimal toxicity	-The vector-based miRNA expression systems are generally less efficient because it is necessary to transcribe the DNA to miRNA precursors by the action of RNA polymerases, which implies the delivery to the nucleus -Over-expression of shRNA in rats caused hepatotoxicity, organ failure and death -Argonaute proteins and the pre-miRNA export protein (exportin-5) limit the amount of exogenous miRNA that a cell can tolerate
miRNA inhibiting drugs		**Advantages**	**Limitations**
Antisense oligonucleotides (AMOs), known as anti-miRs	-Synthetic, single-stranded antisense RNA molecules designed to be complementary to the target miRNA -Competitive inhibition between mature miRNAs and their mRNA targets by Watson-Crick binding	-The targeted inhibition of a specific miRNA and subsequent upregulation of target mRNAs can be achieved, as they function by binding to miRNAs inside the RISC -Under physiological conditions, they are generally unable to distinguish between miRNAs within the same family, especially those with identical “seed regions” -Used *in vitro* and *in vivo* to discover gene function, and some AMOs are being tested in clinical trials	-Unmodified anti-miRs are poorly suited to *in vivo* applications because they are incapable of penetrating negatively charged cell membranes and are susceptible to degradation by serum nucleases -Chemical modifications are required to increase resistance to serum nucleases, to enhance their binding affinity, biostability, specificity for the target miRNAs and to improve their entry into the cell -Most of the chemically modified AMOs show limited tissue distribution when administered in the absence of a carrier, and are taken up by the liver and kidney and rapidly excreted in urine

Antagomirs	-A class of chemically modified oligonucleotides (AMOs) which are able to silence endogenous miRNAs -Modified to have a phosphorothioate backbone and a cholesterol group at the 3'-position of the nucleic acid	-Antagomirs are fully complementary to mature miRNAs – competitive inhibition	-Antagomirs are unlikely to be used clinically because the dose required for *in vivo* inhibition is often high (~80 mg per kg) to achieve the same efficacy as other AMO strategies, which increases the risk of off-target effects -Cannot cross the blood–brain barrier, but can penetrate brain cells if injected directly into the brain
Locked Nucleic Acid (LNA) anti-miRs	-Short, single-stranded LNA-modified oligonucleotides -The extraordinary properties of LNA-oligonucleotides enable a reduction in anti-miR size, from 15-16 nucleotides to 8 nucleotides with comparable effects -Addition of an extra methylene bridge connecting the 2'-O atom and the 4'-C atom and 'locks' the ribose ring in a C3'-endo or C2'-endo conformation	-Their small size together with their potency/stability/specificity provided by the LNA modifications, makes delivery possible without vehicle-systems (*in vivo* naked) -Create and enhance high-affinity Watson-Crick binding to target mRNAs and thus exhibit higher thermal stability and superior hybridization with their RNA target molecules	-Only moderate efficiency for miRNA inhibition, possibly because of the tendency of LNA oligonucleotides to form dimers with exceptional thermal stability
"tiny LNAs"	-Modified LNA anti-miRs that are 8 nucleotides long and specifically bind to the 5'-seed sequence	-Can block all members of the same miRNA family or of several miRNAs families that share the same seed region, inducing a consequent upregulation of their direct targets	
'miRNA sponges'	-RNA transcripts with multiple tandem-repeats of miRNA binding sites to block the function of a given endogenous miRNA or a miRNA family -To reproduce the miRNA-mRNA binding, like in the natural setting, a bulge is introduced at position 9-12, which achieve better activity due to increased miRNA retention	-Stably interact with the corresponding miRNA and prevent its interaction with its endogenous target mRNAs -Ability to affect all closely related miRNAs within a family that share overlapping targets -Can be stably integrated into chromosomes, designed to be drug inducible or controlled by promoters whose expression is restricted to a desired cell type, tissue or developmental stage	-Although sponges have been widely used to investigate miRNA function *in vitro*, their utility *in vivo* has been limited to transgenic animals in which the sponge mRNA is over-expressed in target tissues. Interestingly, it seems that some large non-coding RNAs could serve as natural sponges to regulate cellular miRNA availability and lead to upregulation of downstream target genes
miR-Mask	-Single-stranded 2'-*O*'methyl-modified antisense oligonucleotides with locked 5' and 3' ends that are entirely complementary to the miRNA binding sites in the 3'-UTR of the target mRNA	-'Mask' the target mRNA from the endogenous miRNA and thus prevent its suppression -This specific mechanism reduces the off-target effects and is highly target specific	

2.1. MicroRNA manufacturing

As mentioned above, most miRNAs employed in the development of new therapeutic approaches, are manufactured either by enzymatic (*in vitro* transcription) or chemical (via phophoramidite solid-phase chemical synthesis) methods (Beckert and Masquida, 2011; Ling et al., 2013; Milligan et al., 1987; Ponchon and Dardel, 2011; Sherlin et al., 2001). In the last years, new advances in synthetic RNA chemistry were accomplished. Thereafter, the synthesis process has become more efficient, highly effective, and affordable for large scale production of RNA, however, the fidelity of the process is inversely correlated with the length of the oligonucleotide being synthesized (El-Sagheer and Brown, 2010; Ponchon and Dardel, 2007). In addition, the introduction of chemical modifications (see Table 2) in these strategies allows reducing the instability of RNA, as well as their degradation by cellular ribonucleases, increasing the RNA half-life. In turn, this advantage makes difficult to obtain the RNA highly pure and intact (Broderick and Zamore, 2011; Bumcrot et al., 2006; El-Sagheer and Brown, 2010; Li and Rana, 2014; van Rooij and Kauppinen, 2014). Thus, additional purification protocols to remove the contaminants (linearized plasmid DNA template, enzymes, free nucleotides, salts or buffer, short aberrant transcripts, failure in the sequences, among others) derived from the synthesis process have to be employed in the final RNA product (Martins et al., 2014; Milligan et al., 1987). Actually, the presence of these impurities can lead to non-targeted gene silencing, what is commonly associated with a decrease in therapeutic effectiveness and still restrict the implementation of these RNAs onto pre-clinical or clinical applications.

On the other hand, miRNA therapeutics can also be obtained via expression systems of miRNAs encoded by eukaryotic vectors. However, this alternative approach is generally less efficient because it is necessary to transcribe the DNA to RNA (Chen et al., 2007; Huang et al., 2011; Li et al., 2014; Ponchon and Dardel, 2007, 2011) and it is dependent of the action of the RNA polymerase. Thus, considering the rapidly growing interest on these novel biopharmaceuticals, as a result of its potential therapeutic application, novel technologies to improve their manufacturing are currently being pursued. Moreover, the success of any therapeutic will depend on the easy production at large scale, while maintaining maximal product quality and biological activity. For all these reasons, it is required the development of economic and efficient methods for large-scale production of miRNAs.

Table 2 – Chemical modifications used in miRNA modulators.

(reviewed in (Broderick and Zamore, 2011; Bumcrot et al., 2006; El-Sagheer and Brown, 2010; Li and Rana, 2014; van Rooij and Kauppinen, 2014; Zhang et al., 2013)

Chemical Modifications	Features
Phosphorothioate (P=S)	-Exchanges an oxygen atom by a sulfur atom in the phosphate backbone -Inhibits uptake of the passenger strand into the RISC -Promotes binding to serum/plasma proteins, leading to longer serum retention times (half-life), which may induce unwanted side effects, due to reduced clearance by glomerular filtration and urinary excretion -Enhances the resistance to nucleases and cellular uptake -Keeps miRNA silencing function intact -Inhibits coagulation -Can cause cytotoxicity -Activates complement -Improves pharmacokinetic properties, facilitating their delivery into many peripheral tissues *in vivo* -Perhaps a better choice is modification boranophosphate (P=B) instead P=S substitution, which enhances nuclease resistance without causing cytotoxicity or damage to miRNA silencing function
2´-*O*-methyl (2'-*O*-Me)	-Adds a methyl group (-CH_3) to the second carbon of the ribose -Occurs naturally in rRNA and tRNA and is safe -Improves *in vivo* stability in the cytoplasm and increases the resistance to serum nucleases (enhancing half-life) by the closer proximity between the 2´group and 3´phospho-group -Enhances cellular uptake -Minimizes or inhibits the innate immune system activation, as it is a competitive inhibitor of TLR7 -Their introduction into nucleotides within the seed region, can reduce seed region mediated off-target effects without compromising silencing of the intended mRNA -When the sugars of both strands are replaced with 2'-*O*-methyl groups, the duplex loses its silencing ability
2´-Fluoro	-Adds a fluorine atom to the second carbon of the ribose -Increases *in vivo* stability and the resistance to exonucleases by the closer proximity between the 2´group and 3´phospho-group -Decreases nonspecific immune stimulation and off-target effects -Can be introduced through endogenous transcription as opposed to chemical synthesis
2´-*O*-(methoxyethyl) (2'-MOE)	-Adds a methoxy-ethyl group (-C_3H_7O) to the second carbon of the ribose -Increases *in vivo* stability and the resistance against nucleases in the serum by the closer proximity between the 2´group and 3´phospho-group
Cholesterol conjugation	-Addition of cholesterol functionality at the 3'-position of the nucleic acid to generate 'antagomirs' -Enhances serum half-life by binding to serum albumin, improving stability and availability -Enhances the cellular uptake of the modified oligonucleotide by promoting its association with high-density lipoproteins (HDLs) and Low-density lipoproteins (LDL)-that can bind cell surface membrane receptors -Incorporation into HDLs can direct miRNAs to the liver, gut, kidney and steroidogenic organs and LDL-incorporated RNAs are primarily targeted to the liver

2'-O-allylation	-Inhibits activity -Enhances serum half-life
Antibody-conjugated	-The high affinity and binding specificity of antibodies make them attractive vehicles for cell- or tissue-type-specific delivery -Bind multiple miRNAs, creating a particle that bypasses kidney filtration and targets the miRNAs only into cells bearing the cell surface receptor recognized by the antibody -A common approach is to link an RNA-binding protein (e.g. antibody fragment-protamine fusion protein) or domain to Fab fragments isolated from the cell- or tissue-targeting antibody
Locked nucleic acid (LNA) modifications	-LNA is a bicyclic nucleic acid that uses an extra methylene bridge between the 2´-O atom and 4´-C atom also referred to as 2´O-4´C-methylene 'locks' the ribose ring in a C3'-endo or C2'-endo conformation -Prolongs half-life in serum -Inhibits nuclease activity -Without adverse affects on the gene-silencing activity -Displays higher aqueous solubility and increased metabolic stability for *in vivo* delivery and lower toxicity -Reduces the immunostimulatory effects
Folate, various peptides and aptamers	-Help in transport across cellular barriers -Target to specific cells and organs -Improve stability and availability -Frequently associated with impaired function and severe toxicities

Note: P=S, 2'-F and 2'-OMe modifications have been extensively used in clinically tested and FDA approved oligonucleotide drugs.

These issues have spurred a novel interest for recombinant methods using prokaryotic hosts, which allow the production of large amounts of RNA stable structured. So far, only few strategies have emerged to produce stable recombinant miRNAs, namely for the biosynthesis of human mir-27b and human pre-miR-29b, using recombinant bacteria, such as *Escherichia coli* (*E. coli*) and *Rhodovulum Sulfidophilum* (*R. sulfidophilum*) as preferential hosts, respectively (Li et al., 2014; Pereira et al., 2014a). In general, the recombinant approaches comprise several steps, starting with the selection and construction of appropriate expression vectors (Nagao et al., 2014; Ponchon and Dardel, 2011; Suzuki et al., 2010). After the establishment of this step, it is possible to follow to the optimization and selection of the best culture conditions (dissolved oxygen, temperature, stirring speed, pH and medium formulation) for miRNAs production by fermentation (Ponchon and Dardel, 2011). This strategy is usually more cost-effective and simple than the synthesis methods, considering the large-scale production, allowing the costs reduction, but remaining highly efficient.

2.2. MicroRNA isolation

The RNA recovery, either from the recombinant production strategies using prokaryotic hosts or from a biological matrix (e.g. tissue samples, whole organisms, cell cultures, bodily fluids), requires the employment of suitable methodologies for the extraction and isolation of target RNAs. In general, the procedure includes harvesting of cells by centrifugation and ultimately cell lysis to release the molecule of interest, since miRNAs are accumulated in cytoplasmic space (Bernardo et al., 2012; Tan and Yiap, 2009).

Up until now, the most commonly used methods to isolate RNA are the guanidinium thiocyanate-phenol-chloroform extraction and the solid-phase extraction (SPE) (Bernardo et al., 2012; Chomczynski and Sacchi, 2006; Tan and Yiap, 2009; Vomelova et al., 2009). The first method, based on chemical extraction, consists in the disruption of cells using a solution composed by guanidinium thiocyanate, phenol and chloroform (see Figure 2), followed by precipitation (Chomczynski and Sacchi, 2006). This organic extraction can also be carried out using commercial available reagents, such as TRIzol® (Ambion), TRI (Sigma-Aldrich), RiboZol™ (AMRESCO's) and NZYol (Nzytech), which are recommended to isolate intact and pure total RNA with high recovery yield, once endogenous ribonucleases are inactivated by the chaotropic agent used (cationic detergent guanidinium thiocyanate) (Bernardo et al., 2012; Chomczynski and Sacchi, 2006). However, this chemical extraction is extremely toxic, biologically hazardous and conveys health risks, which may strongly compromise the success of several RNA based-procedures in basic and clinical research, due to the use of denaturing agents (guanidinium thiocyanate and β-mercaptoethanol) and organic solvents (alcohols) (Chomczynski and Sacchi, 2006; Tan and Yiap, 2009; Vomelova et al., 2009). Furthermore, this RNA extraction involves multiple and complex processing steps that makes it a time-consuming and laborious protocol.

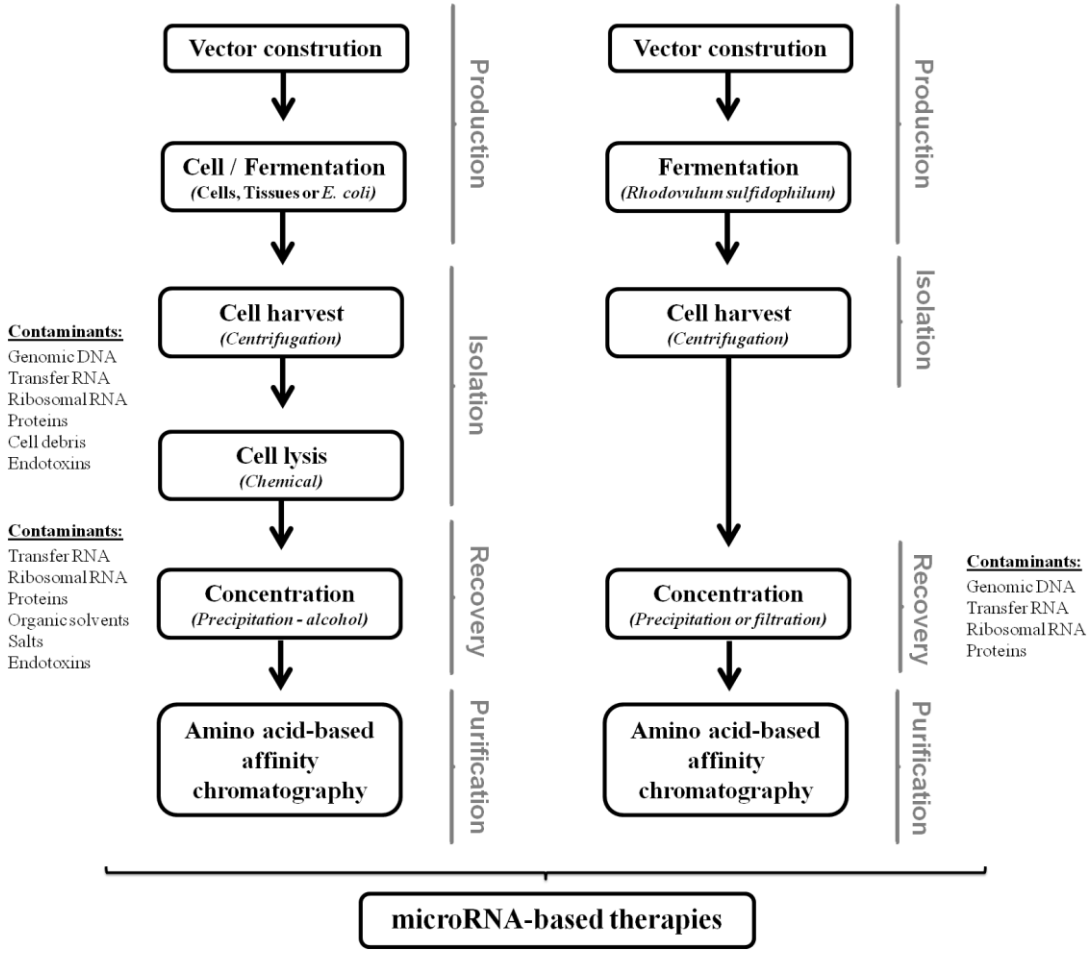

Figure 2 - Flowchart of the main unit operations to be considered during manufacturing process of microRNAs. It is shown a comparison between the most common methodologies for obtaining miRNA from cells, tissues or *E. coli* with the recombinant production methodology in *R. sulfidophilum*. It is also indicated which are the impurities eliminated in each step.

The SPE is an adsorption method based on the ability of RNA to create a hydrogen-binding interaction with specific surfaces, namely silica gel matrix or glass fiber filter (Tan and Yiap, 2009; Vomelova et al., 2009). In general, in the solid-phase extraction, four steps are involved: i) cell lysis employing chemical extraction; ii) RNA adsorption to solid support (with the aid of high pH and salt concentration in the binding buffer); iii) washing; and iv) elution of the desired RNA from the column (Bernardo et al., 2012; Tan and Yiap, 2009; Vomelova et al., 2009). Nowadays, there is a variety of commercially available extraction kits (e.g., Qiagen (miRNeasy Micro Kit), Roche (High Pure miRNA Isolation Kit), Sigma–Aldrich (mirPremier microRNA Isolation Kit), Invitrogen (Ambion® PureLink® miRNA Isolation Kit) and Ambion (mirVana miRNA Isolation kit)), based on SPE or exploiting a magnetic-bead based extraction technology, in order to isolate RNA molecules from different biological sources with high quality, intactness and purity for further analytical or laboratorial applications

(Mraz et al., 2009). These methods significantly reduce sample preparation time, need less manipulation and offer safer and simpler operations, allowing a quick and efficient purification of RNA compared to chemical extraction methods (Bernardo et al., 2012; Tan and Yiap, 2009; Vomelova et al., 2009). However, some limitations are also associated with these procedures, such as, low RNA yields due to the low binding capacity of the cartridges, and sometimes, the RNA isolation is achieved through the use of enzymes, namely DNases that are usually animal-derived and therefore are not accepted by the regulatory agencies due to the adverse effects of their pharmaceutical administrations. It is noted that throughout these extraction processes, several impurities are removed, such as cell debris, genomic DNA (gDNA) and some proteins, but it still remains a large quantity of impurities mixed with the target RNA, namely other small RNAs (sRNAs).

In what concerns to the recovery of RNAs from recombinant hosts, and along with the aforementioned disadvantages, another major issue associated with the cell lysis of the prokaryotic host, *E. coli*, is the release of endotoxins, which can lead to the contamination of the RNA sample (Wei et al., 2007). The importance of removing endotoxins is related to the possibility of these foreign components to originate adverse effects and inflammatory responses to the patients (e.g. symptoms of toxic shock syndrome), if present in quantities higher than those acceptable (Wei et al., 2007). In addition, as *E. coli* expresses several endonucleases, in particular RNases, it can be difficult to maintain the integrity of the target RNA, being always necessary to establish methods to avoid degradation (Wassarman et al., 1999). For all these reasons, an ideal bioprocess must be designed to maximize recovery yield, to reduce the unwanted contaminants (sRNAs, gDNA, proteins, endotoxins, salts, denaturing agents and organic solvents) and to minimize sample transfers. Nonetheless, and considering the therapeutic applications of these products, the major interest is not only to produce high quantities of the target RNA but also to assure its quality, stability, integrity and biological activity, fulfilling the requirements of regulatory agencies.

To accomplish this, an innovative recombinant bacteria, *R. sulfidophilum*, has been recently proposed and used to produce a pre-miRNA. It is non-pathogenic and presents several advantages over *E. coli*, such as the unusual capacity of secretion of the heterologous nucleic acids directly into the culture medium and the absence of detectable host ribonucleases in the culture medium (Ando et al., 2004, 2006; Suzuki et al., 2010). This prokaryotic host can integrate a promising alternative technology, since it allows the recombinant biosynthesis and recovery from the extracellular medium of biologically active miRNAs, circumventing the need of cell lysis that frequently induces RNA denaturation. Besides, this strategy can be highly advantageous regarding the RNA product safety, as it will not stimulate innate immunity because the secreted miRNAs will be devoid of main bacterial associated impurities. Moreover, it is possible to minimize the contamination of the RNA fraction, by recovering the enriched-miRNA extracellular medium, in a specific stage of cell growth (see Figure 2). Indeed, it is expected that the application of this strategy allows suppressing the use of

organic and toxic solvents, and results in an increased RNA recovery yield, drastically reducing the amount and type of impurities present in the RNA extract, prior to purification. Thus, this integrative approach of recombinant production and pre-miRNAs extracellular recovery, is not only innovative but also presents more advantages than the conventional RNA isolation methods, being more economical, efficient, simple and fast in obtaining functional RNA. The recovery and isolation of miRNAs from fermentation broths can be performed using membrane filtration or concentration techniques, designed to eliminate media components and metabolites and recover the target RNAs (Morão et al., 2011; Nunes et al., 2014; Nunes et al., 2012). Figure 2 schematizes the most important steps to be considered during miRNAs manufacturing. It is essential to optimize and improve all unit operations involved in the biotechnological production and recovery of miRNAs, which will comprise a great benefit to the implementation of a new platform on the biopharmaceutical industry, since the primary isolation conditions will also greatly influence the following purification strategy.

2.3. MicroRNA purification

During the last decades, different methods and protocols have been extensively employed for the purification of RNAs obtained either by synthesis or from biological sources, such as preparative denaturing polyacrylamide gel electrophoresis and different chromatographic strategies namely reversed-phase ion-pair liquid chromatography, anion-exchange and size exclusion chromatography, which can be applied either as an isolated or integrated steps (Easton et al., 2010; Kim et al., 2007; Koubek et al., 2013; McCarthy et al., 2009; Noll et al., 2011). Although these methods can be very efficient for the purification of RNA with high resolution, some of these still require time-consuming preparatory steps and are expensive on large scale (Martins et al., 2014). On the other hand, these purification methods can cause structural modifications and degradation of the RNA molecules and may even introduce some contaminants, e.g. acrylamide, lithium metal, ion-pairing agents and organic solvents, related with the method (Easton et al., 2010; Kim et al., 2007; Koubek et al., 2013; Martins et al., 2014; McCarthy et al., 2009; Noll et al., 2011). For these reasons, the RNA product purified by these strategies may require additional treatments to be suitable for the use in analytical and clinical applications, and therefore it is difficult to maintain the stability and biological activity of the target RNA. These challenges associated with RNA purification process, motivate the improvement of the already existing chromatographic techniques or the development of new purification approaches.

In the last years, the downstream strategies based on affinity chromatography have been developed in an attempt to circumvent several challenges in RNA purification (reviewed in (Martins et al., 2014)). Most approaches described in affinity chromatography make use of tags (small sequences that are introduced in the RNA molecules) that bind with high affinity to specific molecules, used as ligands in chromatographic matrices for the selective purification of RNAs from cellular extracts (Di Tomasso et al., 2011, 2012; Pestourie et al.,

2005; Ponchon and Dardel, 2011; Srisawat and Engelke, 2001, Srisawat et al., 2001). In most cases, the tag-RNA complexes can be released from the chromatographic support either by competitive elution or cleavage by a protease that recognizes a specific site that is incorporated along with the affinity tag (Martins et al., 2014; Srisawat and Engelke, 2001; Srisawat et al., 2001). Overall, although these chromatographic methods are rapid, reliable and efficient in obtaining the target RNA with high recovery yields and stability, they still are expensive on large scale and labor intensive (Martins et al., 2014). In addition, the separation procedures with RNA affinity tags make use of enzymes and may induce structural modifications in RNA by the introduction of the tag sequences, which can affect the overall RNA topology (Srisawat and Engelke, 2002; Walker et al., 2008).

A promissory approach to overcome these limitations includes the recent developed affinity chromatographic method using amino acids as specific ligands, which simulates and exploits biological and reversible interactions that occur at the cellular level between amino acids and nucleic acids. The major advantage of this technique relies on the selectivity achieved, resultant from the combination of multiple non-covalent interactions (including electrostatic and hydrophobic interactions, van der Waals forces, cation–π interactions, dipole–dipole forces and hydrogen bonding) between the biospecific ligands (amino acids and derivatives, namely *O-Phospho*-$_{L}$-Tyrosine, $_{L}$-Arginine, $_{L}$-Lysine and Agmatine) and the target RNAs. The interactions can be favored or disfavored by manipulating the binding/elution conditions, such as the temperature, pH and buffer composition (type of salt, ionic strength or presence of competitive agents) (Sousa et al., 2008). The use of amino acids in this chromatographic strategy has the singular ability of purifying nucleic acids with high-selectivity, -specificity, -efficiency, robustness and durability (Lowe et al., 2001; Martins et al., 2014; Sousa et al., 2008). The potential of amino acids-based affinity chromatography to obtain miRNA molecules, in particular the recombinant human pre-miR-29b, from a complex extract, was recently proved (Afonso et al., 2014; Pereira et al., 2014a, 2014b, 2014c).

Although, amino acids immobilized in bead-packed columns showed high selectivity in the purification of miRNAs, these supports present certain restrictions, such as low capacity and flow rates (Arrua and Alvarez Igarzabal, 2011; Pfaunmiller et al., 2013; Sousa et al., 2012). Considering this limitation, an easier, reliable and more robust procedure for miRNA purification was developed, using a monolithic-based strategy, to improve the performance of the biotechnological strategy, while maintaining the efficiency of the method (Pereira et al., 2014c). Overall, the separation of the target miRNA from a crude sample was achieved, with a good recovery yield, high purity level, good integrity and biological activity, due to the fast separation and consequent short contact time with the support (Pereira et al., 2014c). Amongst the several chromatographic strategies implemented for miRNA purification, amino acids-based affinity chromatography allowed an improvement of many technical issues, including the analysis speed, the sensitivity and the separation conditions (use of mild salt conditions instead of organic compounds and enzymes). Furthermore, miRNA is separated in

one single step, improving process economics over other less-selective and time-consuming multi-step procedures (Afonso et al., 2014; Pereira et al., 2014a, 2014b, 2014c).

In accordance, different affinity ligands (amino acids and its derivatives, peptides, complementary oligonucleotides sequences to the target miRNAs, among others) can be characterized and immobilized onto different chromatographic matrices (agarose-based, monoliths, superporous matrices), in order to purify the RNA of interest from host contaminants, thus minimizing non-targeted gene silencing and immunologic responses.

2.4. MicroRNA quality control

RNA purification is a critical step to obtain the product with suitable quality to be applied in several biomedical fields. At present, none regulatory authority (such as Food and Drug Administration (FDA) centre for Drug Evaluation and Research, European Agency for the Evaluation of Medical Products (EMEA) or World Health Organization (WHO)) has formal guidelines available for RNA oligonucleotide products (Martins et al., 2014). Over the years, the scientific community is providing the guidance in the regulatory framework for RNA-based therapies based in the guidelines for plasmid DNA (pDNA) (Ferreira et al., 2000; Stadler et al., 2004).

As previously mentioned, miRNA quality depends on the manufacturing process, the cellular lysis step and the subsequent processes of isolation and purification, which must be carefully designed in order to reduce or eliminate the host impurities without loss or damage of the biological activity of desired RNA. To accomplish this, a strict control of the process and assessment of the remaining impurities on the final sample is crucial, by using several complementary methods (Batkai and Thum, 2014; Chen et al., 2005; McGinnis et al., 2012; Moreno-Moya et al., 2014; Schleef and Schmidt, 2004; Smith et al., 1999; Stadler et al., 2004). Table 3 describes several effective techniques that are commonly applied to evaluate the quality and quantity of purified miRNA, and to verify if the requirements of regulatory authorities are fulfilled. There are also commercially available analyzers to quantify and simultaneously check the integrity of RNA samples (e.g. Bio-Rad Experion, Hercules, CA, or Agilent Bioanalyzer 2100, Santa Clara, CA). The implementation of methodologies able to control RNA quality will be increasingly necessary, especially when the RNA products are finally released to the market. To overcome this issue, convenient, sensitive and straightforward analytical methods have been developed and validated to detect and quantify specific miRNAs in unfractionated total RNA from different biological samples, namely whole blood, plasma, cells and some organs (such as liver, heart, brain, spleen, lungs and kidneys) (reviewed in (Batkai and Thum, 2014)).

Table 3 - Accepted levels of impurities in final pDNA preparation for clinical applications, as recommended by regulatory agencies (adapted from (Batkai and Thum, 2014; Chen et al., 2005; Ferreira et al., 2000; McGinnis et al., 2012; Moreno-Moya et al., 2014; Schleef and Schmidt, 2004; Smith et al., 1999; Stadler et al., 2004)).

Component	Accepted level in final product	Recommended Assay
Host RNA	Undetectable	Agarose gel electrophoresis Polyacrylamide electrophoresis Analytical High-Performance Liquid Chromatography Spectrophotometric Method
Proteins	Undetectable	Micro-BCA (bicinchoninic acid) protein assay Bradford assay SDS-PAGE
Genomic DNA	<2 μg/mg pDNA	Real-time Polymerase Chain Reaction Southern blot Hybridization
Endotoxins	<0.1 EU/μg pDNA	Limulus Amoebocyte Lysate (LAL) assay
miRNA		Polyacrylamide electrophoresis Electrospray ionization mass spectrometry TaqMan-based arrays Reverse-transcriptase polymerase chain reaction Northern blot analysis Nuclease protection analysis Primer extension assay Microarray analysis *In situ* hybridization assay Complementary DNA (cDNA) library construction High-Performance Liquid Chromatography *In Vitro* Translation LC-MS

3. Obstacles to effective microRNA therapeutics

As discussed earlier in this review, the therapeutic application of miRNAs is extremely promising due to the specific and efficient silencing of gene expression, as well as for its simplicity, safety profile and ease of manufacturing. However, some problems must be addressed, namely the extracellular barriers, low bioavailability, rapid enzymatic degradation of miRNA by ubiquitous nucleases found in human serum, rapid renal clearance and phagocytosis by macrophages (Al-Dosari and Gao, 2009; Pathak et al., 2009; Tokatlian and Segura, 2010). Also, the intracellular barriers, such as inefficient cellular uptake and intracellular processing of endosome-targeted RNAs (escape from the endosome, vector unpacking and processing by the RNAi machinery) need to be surpassed before the therapeutic gene arrives at the cytoplasm, allowing an improvement on miRNA pharmacokinetic and pharmacodynamic properties (Al-Dosari and Gao, 2009; Pathak et al., 2009; Tokatlian and Segura, 2010).

3.1. Biological instability

As previously discussed, for the systemic delivery, unmodified naked miRNAs are highly susceptible, due to their rapid degradation by cellular and serum nucleases, resulting in a short half-life in the circulatory system (from several minutes to an hour) (Deng et al., 2014; Gavrilov and Saltzman, 2012). Chemical modifications can increase the RNA stability but are also associated with certain adverse effects, such as decrease on mRNA hybridization, inhibition of coagulation, activation of the complement cascade and cytotoxicity (see Table 2) (reviewed in (Broderick and Zamore, 2011; Bumcrot et al., 2006; Deng et al., 2014; El-Sagheer and Brown, 2010; Li and Rana, 2014; van Rooij and Kauppinen, 2014). For all these reasons, it is still necessary to customize, optimize and/or minimize the chemical modifications, through the identification and modification only of the sites susceptible to degradation.

3.2. Off-target effects

The *in vivo* specificity of miRNAs is based on sequence homology between miRNA and target mRNA. Thus a major challenge in developing miRNAs-based therapeutics remains in the assurance of RNA purity to minimize off-target gene silencing (Deng et al., 2014). Nonetheless, miRNA-based therapeutics can sometimes induce non-specific side effects, i.e., suppression of other non-target genes, which are as critical as effectiveness and duration of miRNA expression or inhibition (as reviewed in (Singh et al., 2011)). The off-target effects can arise through the partial homology of the nucleotides involved in the "seed region" of the endogenous miRNAs, and by effects related with competition of exogenous vectors and/or RNA species and endogenous miRNAs by the incorporation and retention into RISC, resulting in the non-desirable gene silencing (Gavrilov and Saltzman, 2012). Another possible side effect is the saturation of the cellular machinery by miRNA processing, leading to aberrant processing of endogenous miRNAs by the accumulation of toxic precursors (pri-miRNAs, pre-miRNAs, shRNA, stem-loop structures and high expression of miRNA mimics) (Singh et al., 2011; Wang et al., 2011). This saturation interferes with the normal functioning of the cell, not allowing access of the miRNAs in the natural pathway (Ballarin-Gonzalez and Howard, 2012). Most of these undesirable and unspecific effects can be minimized without impairing their silencing capability, with small changes in miRNA sequences (chemical modifications) or by the use of miRNA mimics that are specific enough to distinguish between similar miRNAs. Despite of all the progress that has been made in the miRNAs-based therapeutics, it is still required more basic research on miRNAs to increase the efficacy and significantly reduce and eventually eradicate off-target effects.

3.2. Immune response

Long double-stranded RNA (e.g. vector-mediated expression of shRNAs, viral dsRNAs or other dsRNAs), as well as, siRNAs synthesized *in vitro* can, in some cases, trigger an innate immune

response via interaction with RNA-binding proteins such as Toll-like receptors (TLRs) and protein kinase receptor (PKR) (Ballarin-Gonzalez and Howard, 2012; Deng et al., 2014). The innate immune response is mediated mainly by activation of interferon and pro-inflammatory cytokines, after recognition of immunostimulatory sequence in the RNAs, such as specific GU-rich sequences ("danger motif"), in particular 5'-GUCCUUCAA-3' and 5'-UGUGU-3' (Deng et al., 2014; Gavrilov and Saltzman, 2012). In this manner, there are several parameters determining the stimulation of innate immunity, namely structure and sequence of RNAs, delivery vehicle, delivery route, cell type and species. To minimize these issues, appropriate chemical modifications as well as, the possibility to use miRNA delivery strategies can prevent, decrease and avoid the immunostimulatory properties (see Table 2). Understandably, immunogenicity and toxicity are grounds for concern that must be addressed in developing RNAi for therapeutic use.

4. Delivery Strategies

The major challenge in the development of miRNAs-based therapeutics for clinical applications is the establishment of an effective mode to deliver these molecules to their target cells, specific tissues or organs, in order to exert their function, preventing unwanted side effects. The physicochemical properties of naked miRNAs interfere with their ability to cross the cell membrane by passive diffusion due to their negative charge, hydrophilicity and size (7-20kDa) (Zabner et al., 1995; Zhang et al., 2013). In addition, naked miRNAs are preferentially accumulated by the kidneys and rapidly eliminated into urine within one hour because they are smaller than the size threshold for glomerular filtration.

In the last years, a variety of different and efficient delivery approaches have been developed and applied in gene therapy trials to promote cellular uptake and delivery of RNAs into the cytoplasm of target cells, increasing the accumulation of the therapeutics in the site of interest, increasing the silencing potency, thereby making a given treatment dose more effective. In a simple way, delivery systems can be divided into two categories, viral vectors and non-viral vectors. However, each of these approaches has distinct advantages and disadvantages, which require careful consideration (see Table 4). Initial research focused on the use of viral vectors because these vectors displayed high efficiency at delivering miRNAs, both *in vitro* and *in vivo*, taking advantage of their favorable cell uptake and intracellular trafficking machineries, allowing long-term gene expression (see Table 4) (Mintzer and Simanek, 2009; Robbins et al., 1998; Walther and Stein, 2000). However, the focus has recently changed to the non-viral approaches because of the advantages over viral vectors, such as ability to deliver the exogenous biopharmaceuticals into the cell/tissue-specific, non-immunogenicity, high biocompatibility and low cytotoxicity (De Smedt et al., 2000; Nimesh and Chandra, 2009; Park et al., 2006). In addition, these non-viral vectors offer other advantages such as relatively low production costs, high flexibility and easy quality control,

allowing designing carriers with well-defined structural and chemical properties on a large scale with high reproducibility and simplicity. Thus the potential for large-scale production makes these non-viral vectors increasingly attractive for gene therapy (see Table 4) (Ahn et al., 2002). These vectors are also relatively stable to storage, they can be administered repeatedly with no or little immune response and the dimension of the genetic material they can carry is virtually unlimited. However, they also present some limitations such as the reduced transfection efficiency, due to the cellular barriers and immune defense mechanisms, poor oral bioavailability and instability in circulation (see Table 4).

The non-viral delivery systems include liposomes, lipoplexes, lipid-based delivery systems, polymers, cyclodextrins, dendrimers, polymeric micelles, pluronic block copolymers, exosomes and metallic core nanoparticles, allowing for RNA compacting for systemic delivery (see Table 4) (Chen and Xie, 2012; Cho et al., 2008; Gao and Huang, 2009; Hart, 2010; Kabanov et al., 2002; Mintzer and Simanek, 2009; Morille et al., 2008; Patil and Panyam, 2009; Yin et al., 2014; Zhang et al., 2013).

Consequently, during the last decade a number of polymeric delivery systems, nanoparticles with sizes between 10 and 100 nm, have been developed. These systems should contain a positively charged domain to efficiently bind the miRNAs molecules and facilitate the progression of the transmembrane transport (Al-Dosari and Gao, 2009; Gupta et al., 2005; Hart, 2010; Zabner et al., 1995). In these systems, the miRNAs can be loaded, adsorbed or chemically linked to their surface. The nanoparticle size is a critical factor for effective drug delivery *in vivo*, since nanoparticles should be big enough to avoid fast clearance through the kidney excretion system but small enough to penetrate the target tissue. As mentioned, to be effective and to be considered ideal, there are several aspects to be carefully considered when developing the delivery vehicles, such as, safety, specificity and efficiency of gene transfer; magnitude and duration of expression; immunogenicity and manufacturing (Pathak et al., 2009).

After entry into the target cells, miRNAs still face a number of hurdles before they can exert their gene silencing activity, since non-viral delivery systems are immediately transported into the endocytic vesicles, initially, to the early endosomes where the pH drops to 6 followed by trafficking to late endosomes which are acidified to pH 5-6 (see Figure 3) (Caracciolo et al., 2009; Dominska and Dykxhoorn, 2010; Medina-Kauwe et al., 2005). Once taken up into the endosome, the RNA has to escape in order to avoid subsequent degradation by lysosome (Caracciolo et al., 2009; Dominska and Dykxhoorn, 2010; Medina-Kauwe et al., 2005). Even in the cell cytoplasm, miRNAs remain vulnerable to degradation by intracellular nucleases and still need to be incorporated into RISC with high efficiency, to exert the silencing function (see Figure 3) (Nguyen et al., 2009; Suh et al., 2003).

Table 4 – Barriers to successful *in vivo* delivery of microRNAs using non-viral vectors.

Non-Viral Delivery (Cho et al., 2008; Gao and Huang, 2009; Hart, 2010; Mintzer and Simanek, 2009; Morille et al., 2008; Patil and Panyam, 2009; Zhang et al., 2013)		
Lipid-based delivery systems	**Liposome**	-Consisting of a phospholipid bilayer with an inner aqueous core that contains RNA -Versatility and flexibility in structure -It is an attractive delivery approach because of the biocompatibility of the constituents and facile assembly of the complexes, which requires only mixing and incubation of components -Higher stability in biological fluids and against the enzymatic metabolism -Increase retention in the blood stream -The elimination half-life increased from ~2 min to 6.5 h -Excellent RNA delivery efficiency in multiple cell lines *in vitro* as well as in mice, rats and monkeys -Facilitate efficient internalization of RNA via membrane fusion with the host cell -Are usually heterogeneous in size owing to interactions between water molecules and the hydrophobic groups of lipids -Traditional liposomes have low transfection efficiency into cells due to their lack of surface charges -Highly toxic for *in vivo* applications, nonspecific uptake, and unwanted immune response
	Lipoplexes	-Liposomes that contain cationic lipids driving the interaction between the lipid bilayer and the negatively charged RNA molecules, resulting in a net positive charge that enable the binding to anionic cell surface molecules -The composition of these lipid particles can be tailored to facilitate fusion with the cytoplasm, as well as to promote endosomal release once inside the cell
	Neutral Lipids[1] DOPC; DOPE; DSPC **Cationic lipids**[2] DOTMA; DOGS; DC-Chol; DDAB; DMRIE and DOTAP	-Lipid vectors are presumed to achieve endosome release of RNA through a membrane fusion mechanism -Neutral lipids are non-toxic and do not activate an immune response -Cationic lipids can complex electrostatically with RNAs, enhancing cell entry and protection against serum enzymes -Incorporation of positive charge to increase transfection efficiency must be carefully balanced because it can induce inflammatory effects and unwanted interaction with negatively charged serum proteins, which can lead to opsonization and clearance of the lipocomplex
Biodegradable polymers	Polyethylenimine (PEI) Poly(lactic acid) Poly(lactic-co-glycolic acid) Poly(butylcyanoacrylate) Chitosan (CS) Polylysine Poly(alkylcyanoacrylate) Poly(butylcyanoacrylate)	-High delivery efficacy, biodegradable, biocompatible and non-toxic -Higher stability in biological fluids and protection of the RNA against degradation by RNases -Reduced non-specific biodistribution -Have capacity to encapsulate large amounts of genetic material and co-delivery -Facilitate the cellular uptake via endocytosis -Polymeric vectors commonly use the proton sponge effect to facilitate endosome escape -Can readily be surface-modified to enhance stability, transport properties, targeting or uptake and can be produced in relatively homogeneous sizes (up to 100 nm) -Successfully used to deliver poorly diffused drugs into the brain -Low toxicity and low immunogenicity -Successfully administered to silence target genes *in vitro* and *in vivo*, such as p-glycoprotein in brain endothelial cells -PEI act as a proton sponge that induces the release of RNA to the cytoplasm by osmolysis from the endosome due its high content of protonable amino groups -PEI is a highly efficient cationic polymer since it has numerous amine groups in its structure -PEI showed its dose-dependent cytotoxicity due to non-biodegradability inside cells that results in the formation of aggregates with negatively

		charged intracellular proteins -Use of a high-molecular-weight branched PEI leads to high transfection efficiency but to unfavorable adverse effects such as cellular toxicity -CS is a natural, nonallergic and has mucoadhesive properties, and nuclease resistance -The degradation time of PLGA can be altered from days to years by varying the molecular weight and the lactic acid to glycolic acid ratio of the copolymers -Increase the duration of drug circulation in the blood, which facilitates drug ability to interact with specific molecules expressed on the luminal side of BBB endothelial cells, and consequently to cross the BBB, increasing the uptake of appropriate drugs in the brain safely and effective
Cyclodextrin (CD)	Naturally cyclic oligomers of glucose (oligosaccharides) that are complexed with transferrin	-CD possesses unique structural features, with hydrophilic outer surface and hydrophobic inner cavity -CD containing polymers (CDPs) consist of cationic polymer complexed with RNA and interdigitated with funnel-like cyclodextrin molecules, which, in turn, can be linked to functionalized molecules -CDPs have been investigated intensely in targeted delivery of small therapeutic molecules due to its non-toxicity and not producing immune stimulation even if the RNA cargo contains an immune stimulatory sequence
Polymeric micelles	Polymeric micelles	-Easy to formulate and therefore exist with variable well-defined geometry where insoluble/sparingly soluble bioactive molecules can be incorporated at different sites in micelles -An ideal candidate for brain-targeting delivery -Small particle size that allows escaping from the reticuloendothelial system -Offer protective stability within their hydrophobic core -Flexibility of modification with targeting ligands that can effectively enhance drug solubility and improve drug pharmacokinetics and biodistribution -Require less excipients -High physical stability -Sustained drug release -Self-assembled nanostructures composed of amphiphilic block copolymers can be tuned for RNA delivery by grafting them with amines that can complex RNA -Can act as nanosized structures to solubilize and release hydrophobic drugs
Dendrimers	PAMAM Dendrimers Polypropylenimine Dendrimers	-Ability to control their well-defined structure and molecular weight, shape, degree of branching, flexibility, as well as the “multivalency effect” -Easily modified surface groups -Low polydispersity and high functionality -Improved solubility, pharmacokinetics and biodistribution -High loading capacity and high transfection efficiency -Low toxicity and low immunogenicity -Can also act as a proton sponge, triggering endosomal escape and release RNA into the cytoplasm due its tertiary amine groups inside the repeating backbone structure -Offer a new length scale (~5–10 nm), with significant versatility to incorporate multiple active molecules -Display the ability to cross cell membrane -A number of biologically and pharmacokinetically desirable properties, however, controlled drug release and high drug loading still remain challenge -PAMAM dendrimers require further modifications of their peripheral end groups since the intact structure shows low transfection efficiency -They are cleared rapidly by the bloodstream, preventing ‘long-term’ accumulation in non-targeted organs, such as kidney, lung and liver,

		reducing the potential for side effects -The cytotoxicity of PAMAM increases proportionally with the generation number
Pluronic block copolymer		-Enhance the transport of drugs across *in vitro* models of the BBB, which it is related to the inhibition of P-glycoprotein-mediated efflux -The polymer may have potential as a CNS-targeted delivery system for drugs that are substrates for the P-glycoprotein efflux pump
Exosomes		-Endogenous nanovesicles secreted by several cells and tissues that transport the desired RNAs -The specific targeting of exosomes to the brain following systemic delivery -Ability to escape an immune response (reduced immunogenicity), thus presenting reduced toxicity -The possible effects of nucleic acids and proteins derived from dendritic cells and carried with the exosomes on the target cell need to be further explored
Metallic core nanoparticles	Gold nanoparticles (GNPs)	-Metal cores, such as iron cobalt, iron gold, or iron nickel are coated with various peptides, proteins, antibodies and other biomolecules generating a core-shell structure to which RNA can be externally conjugated through linking molecules such as thiols dextran, cationic polymers or biotin-streptavadin -Ability to be synthesized at diverse sizes, their chemical stability and their unique optical properties -Allow the study of biodistribution upon injection using magnetic resonance imaging or targeting to specific tissues by applying external magnets -*In vivo* toxicity may limit their application
Viral Delivery Systems Reviewed in (El-Aneed, 2004; Mintzer and Simanek, 2009; Robbins et al., 1998; Walther and Stein, 2000)		
Viral	Retrovirus vectors Lentivirus vectors Adenovirus vectors Adeno-associated viruses Herpes simplex viruses	-To express the virulent genome, the virus needs to infect the host cells, thereby inducing prolonged gene silencing -A single administration could lead to durable down-modulation of the targeted pathological protein -High efficiency in *in vivo* delivery because the ability to deliver the gene into the cell is an inherent capacity that they possess -Transient gene silencing -LV and AVV were the most used, as they have the best safety records -Easily eliminated by existing bloodstream antibodies -Can activate coagulation or complement factors to induce mutation in the host genome, which may lead to strong inflammatory reactions -Allergy and infection caused by viruses can be fatal -Their immunogenicity, cytotoxicity and the possibility of mutagenic effects make them risky -The use of these delivery vehicles is mostly moderated in what concerns to their manufacturing and scale-up procedures

[1]**Neutral Lipids:** 1,2-Oleoyl-sn-Glycero-3-phosphocholine (DOPC); 1,2-Dioleoyl-sn-Glycero-3-phosphoethanolamine (DOPE); 1, 2-distearoyl-sn-glycero-3-phosphocholine (DSPC); [2]**Cationic lipids:** N-[1-(2, 3-dioleoyloxy) propyl]-N,N,Ntrimethylammonium chloride (DOTMA), dioctadecylamido glycylspermine (DOGS); 3b[N-(N',N'-dimethylaminoethane)-carbamoyl) cholesterol (DC-Chol); dimethyldioctadecyl-ammonium bromide (DDAB), dimyristyloxypropyl-3-dimethylhydroxyethyl ammonium bromide (DMRIE) and 1-oleoyl-2-[6-[(7-nitro-2-1, 3-benzoxadiazol-4-yl) amino]hexanoyl]-3-trimethylammonium propane (DOTAP)

4.1. Targeting

In the development of miRNAs-based therapies, delivery of miRNAs for the treatment of NDs is intrinsically limited because the delivery of all substances into the brain is tightly regulated by the Blood-Brain Barrier (BBB) (Edwards, 2001). Physiologically, the BBB is a unique structure that separates brain from the rest of the body and their barrier function is due to anatomical features, namely the tight junctions formed between adjacent brain capillary endothelial cells in the brain tissues (see Figure 3) (Alam et al., 2010).

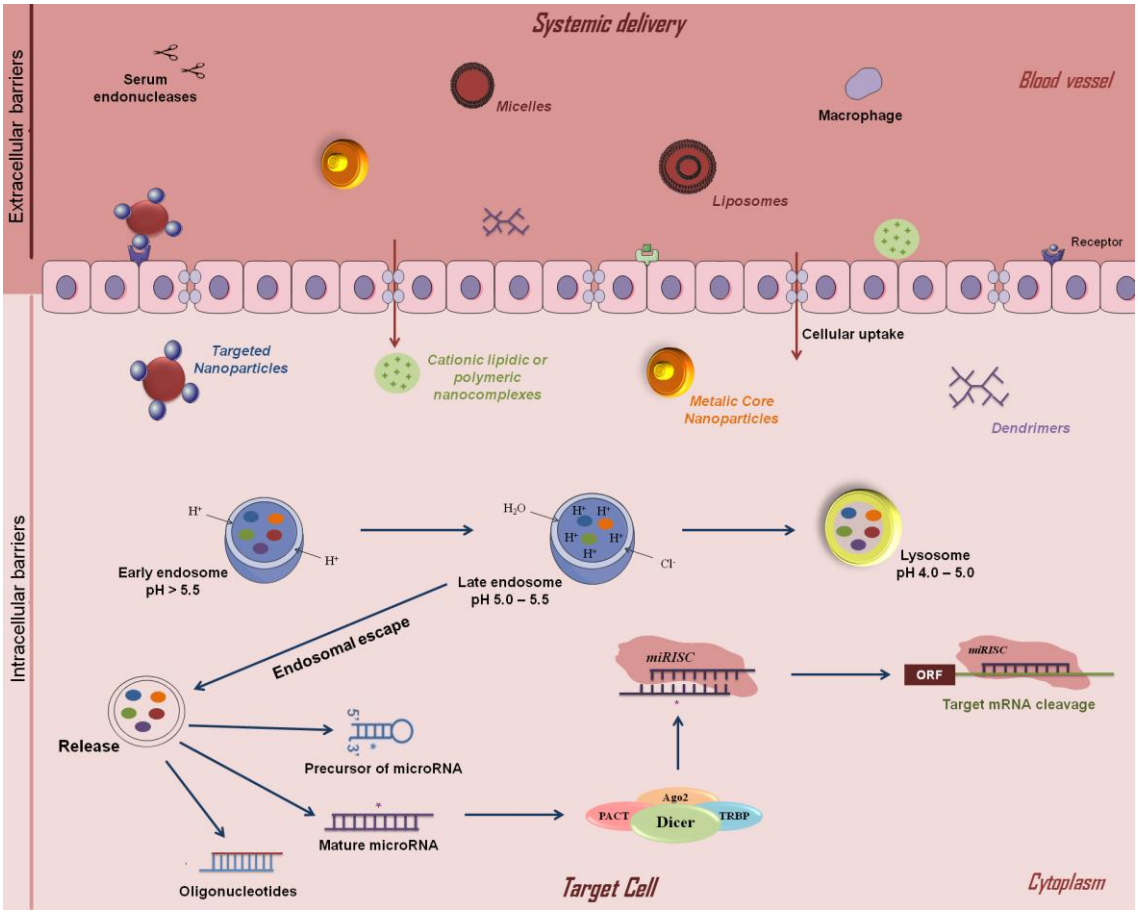

Figure 3 – Main barriers to successful *in vivo* delivery of nucleic acids using non-viral vectors.

This barrier prevents the transport of many harmful substances (foreign organisms, toxic chemicals, hydrophilic drugs and large molecules) present in the systemic blood circulation into the brain and restricts the movement of ions and fluid into the brain (Alam et al., 2010). However, the BBB allows selective access of necessary nutrients (small gaseous agents, glucose, amino acids and small lipophilic molecules) and chemical signaling molecules to the nervous system (Egleton and Davis, 1997). Thus, the BBB controls substance flow in and out of the brain with precision and strictness, ensuring an optimal environment for brain function, making the brain a site of poor permeability to various drugs as well as delivery systems. Another important factor that limits and control the uptake, distribution and efflux of many

drugs in the nervous system are the proteins presents in a variety of drug efflux transporters, such as P-glycoprotein (Kusuhara and Sugiyama, 2001), glucose-related transporters, nucleoside transporters, receptors for transferrin (Descamps *et al.*, 1996, Visser *et al.*, 2004), lactoferrin (Fillebeen et al., 1999), insulin (Frank et al., 1986), leptin, lectins, epidermal growth factor, insulin-like growth factors (Duffy and Pardridge, 1987; Reinhardt and Bondy, 1994), as well as, low-density lipoprotein receptor-related protein (LRP) (Candela et al., 2008; Dehouck et al., 1997), reinforcing BBB function by effectively removing drugs from the brain and pumping them back into blood. Because of this BBB transport restriction mechanism, more than 98% of candidate drugs have been abandoned during their development due to their poor permeability to cross the BBB, in sufficient quantities to produce a therapeutic effect (Pangalos et al., 2007; Pardridge, 2005). These findings are attracting the attention of the pharmaceutical and biotechnology industries.

To accomplish this purpose of targeted delivery, nanoparticles have been modified on the surface with targeting molecules to improve their interactions with the BBB. As mentioned, the surface of the brain endothelial cells of the BBB possess several transport mechanisms mediated by various specific receptors that potentially can be exploited as a means to target drugs to the brain. Small molecules, peptides and proteins, such as angiopep-2 (van Rooy et al., 2011), certain apolipoproteins and lipoproteins (Candela et al., 2008; Kreuter et al., 2002, 2007; Michaelis et al., 2006) directed to low-density lipoprotein receptor (Dehouck et al., 1997) and RVG (rabies virus glycoprotein) (Kim et al., 2013; Son et al., 2011) to GABA receptor have been extensively used as brain-targeting ligands for the development of drug delivery systems to the brain, trying the BBB crossing after intravenous administration. A common drug delivery strategy for targeting cells of interest is the conjugation with proteins, including lactoferrin (Fillebeen et al., 1999), TAT (transactivator of transcription) peptides (Santra et al., 2004) and transferrin (Descamps et al., 1996) that can effectively facilitate the passage of the BBB (Zhang et al., 2012). An alternative strategy to enhance drug delivery to the CNS is the co-administration of a pharmacological modulator or a formulation component, in order to enhance brain penetration of various P-glycoprotein substrates through inhibiting the P-glycoprotein-mediated efflux transport system of a desired therapeutic agent out of the brain as, for example, Pluronic P85 (Batrakova et al., 2001; Yi and Kabanov, 2013).

5. Conclusion and Future trends

MiRNAs are of particular interest in understanding complex disorders, such as NDs, because they can potentially regulate several pathways involved in the insurgence and progression of the disease. Recent developments have suggested that the use of miRNAs as biopharmaceuticals will be possible in a near future and they will become not only important to treat ND, but may also be employed as biomarkers. The biopharmaceutical sector is an important and fast growing part of the wider global pharmaceutical industry, developing healthcare products. However, the development and preparation of biopharmaceuticals poses many technical challenges, including their production, recovery, purification and delivery into the brain, which need to be addressed in order to carry these molecules into clinical trials. Thus, it is necessary the development of effective technologies for miRNAs recombinant production and purification with the intent of obtaining large amounts of highly pure and thus, clinically suitable miRNAs, as an alternative to *in vitro* transcription or chemical synthesis. Within the biotechnological domain, we believe that the integrative approach of extracellular production of stable structured RNA *in vivo* coupled to affinity-based purification using amino acids as ligands will enable the target pre-miRNAs isolation with high efficiency, selectivity, throughput, purity and integrity. The major gain in this field is the possibility to use these methodologies for the preparation of other non-coding RNAs, proving the wide application of the technology, which may have a great impact on biopharmaceutical industry. Furthermore, these approaches could contribute for the establishment of reliable and cost-effective processes, easily adopted by biopharmaceutical industries. In general, this review reports the most recent improvements achieved with the preparation of recombinant miRNAs that meet the required criteria established for clinical application. In addition, another major bottleneck is to achieve a highly targeted delivery of biopharmaceuticals because only then it will be possible to create a significant opportunity to generate new health products useful for diagnosis and treatment of NDs. It is necessary to develop effective brain drug delivery systems that must also be non-invasive, safe, with a low-cost and easy route of administration, for increasing treatment efficacy and patient compliance, reducing societal service burden. The success of these targeted delivery systems preparation will be really impacting since it will open the way for the delivery of numerous drugs to the brain, with relevance not only in AD but also transversal to other neurodegenerative diseases. In fact, the surpass of all issues herein discussed, will lead to the establishment of more cost efficient processes that would reduce the time to application.

6. Acknowledgments

Patrícia Pereira acknowledges the fellowship, SFRH/BD/81914/2011, from FCT (Portuguese Foundation for Science and Technology). The authors also acknowledge the program COMPETE (FCOMP-01-0124-FEDER-041068 – EXPL/QEQ-MED/1068/2013), the FCT project (Pest-OE/SAU/UI0709/2014) and the program Fundo Europeu de Desenvolvimento Regional (FEDER) [COMPETE [FCOMP-01-0124-FEDER-027560]].

7. References

Afonso A, Pereira P, Queiroz JA, Sousa A, Sousa F. Purification of pre-miR-29 by a new O-phospho-l-tyrosine affinity chromatographic strategy optimized using design of experiments. J Chromatogr A 2014;1343:119-27.

Ahn CH, Chae SY, Bae YH, Kim SW. Biodegradable poly(ethylenimine) for plasmid DNA delivery. J Control Release 2002;80:273-82.

Al-Dosari MS, Gao X. Nonviral gene delivery: principle, limitations, and recent progress. AAPS J 2009;11:671-81.

Alam MI, Beg S, Samad A, Baboota S, Kohli K, *et al*. Strategy for effective brain drug delivery. Eur J Pharm Sci 2010;40:385-403.

Alvarez-Garcia I, Miska EA. MicroRNA functions in animal development and human disease. Development 2005;132:4653-62.

Ando T, Suzuki H, Komura K, Tanaka T, Hiraishi A, *et al*. Extracellular RNAs produced by a marine photosynthetic bacterium *Rhodovulum sulfidophilum*. Nucleic Acids Symp Ser (Oxf) 2004:165-6.

Ando T, Suzuki H, Nishimura S, Tanaka T, Hiraishi A, *et al*. Characterization of extracellular RNAs produced by the marine photosynthetic bacterium R*hodovulum sulfidophilum*. J Biochem 2006;139:805-11.

Arrua RD, Alvarez Igarzabal CI. Macroporous monolithic supports for affinity chromatography. J Sep Sci 2011;34:1974-87.

Ballarin-Gonzalez B, Howard KA. Polycation-based nanoparticle delivery of RNAi therapeutics: adverse effects and solutions. Adv Drug Deliv Revi 2012;64:1717-29.

Bartel DP. MicroRNAs: genomics, biogenesis, mechanism, and function. Cell. 2004;116:281-97.

Bartel DP. MicroRNAs: target recognition and regulatory functions. Cell. 2009;136:215-33.

Batkai S, Thum T. Analytical approaches in microRNA therapeutics. J Chromatogr B 2014;964:146-52.

Batrakova EV, Miller DW, Li S, Alakhov VY, Kabanov AV, *et al*. Pluronic P85 enhances the delivery of digoxin to the brain: *in vitro* and *in vivo* studies. J Pharmacol Exp Ther 2001;296:551-7.

Beckert B, Masquida B. Synthesis of RNA by *in vitro* transcription. Methods Mol Biol 2011;703:29-41.

Bernardo BC, Charchar FJ, Lin RC, McMullen JR. A microRNA guide for clinicians and basic scientists: background and experimental techniques. Heart Lung Circ 2012;21:131-42.

Broderick JA, Zamore PD. MicroRNA therapeutics. Gene therapy. 2011;18:1104-10.

Bumcrot D, Manoharan M, Koteliansky V, Sah DW. RNAi therapeutics: a potential new class of pharmaceutical drugs. Nat Chem Biol 2006;2:711-9.

Candela P, Gosselet F, Miller F, Buee-Scherrer V, Torpier G, *et al*. Physiological pathway for low-density lipoproteins across the blood-brain barrier: transcytosis through brain capillary endothelial cells *in vitro*. Endothelium 2008;15:254-64.

Caracciolo G, Caminiti R, Digman MA, Gratton E, Sanchez S. Efficient Escape from Endosomes Determines the Superior Efficiency of Multicomponent Lipoplexes. J Phys Chem B 2009;113:4995-7.

Chen C, Ridzon DA, Broomer AJ, Zhou Z, Lee DH, *et al*. Real-time quantification of microRNAs by stem-loop RT-PCR. Nucleic acids Res 2005;33:e179.

Chen J, Xie J. Progress on RNAi-based molecular medicines. Int J Nanomedicine. 2012;7:3971-80.

Chen S, Ni M, Yu B, Lv T, Lu M, *et al*. Construction and identification of a human liver specific microRNA eukaryotic expression vector. Cell Mol Immunol 2007;4:473-7.

Cho K, Wang X, Nie S, Chen ZG, Shin DM. Therapeutic nanoparticles for drug delivery in cancer. Clin Cancer Res 2008;14:1310-6.

Chomczynski P, Sacchi N. The single-step method of RNA isolation by acid guanidinium thiocyanate-phenol-chloroform extraction: twenty-something years on. Nat Protoc 2006;1:581-5.

Cogswell JP, Ward J, Taylor IA, Waters M, Shi Y, *et al*. Identification of miRNA changes in Alzheimer's disease brain and CSF yields putative biomarkers and insights into disease pathways. J Alzheimers Dis 2008;14:27-41.

De Smedt SC, Demeester J, Hennink WE. Cationic polymer based gene delivery systems. Pharm Res 2000;17:113-26.

Dehouck B, Fenart L, Dehouck MP, Pierce A, Torpier G, *et al*. A new function for the LDL receptor: transcytosis of LDL across the blood-brain barrier. J Cell Biol 1997;138:877-89.

Deng Y, Wang CC, Choy KW, Du Q, Chen J, *et al*. Therapeutic potentials of gene silencing by RNA interference: principles, challenges, and new strategies. Gene. 2014;538:217-27.

Descamps L, Dehouck MP, Torpier G, Cecchelli R. Receptor-mediated transcytosis of transferrin through blood-brain barrier endothelial cells. Am J Physiol 1996;270:H1149-58.

Di Tomasso G, Dagenais P, Desjardins A, Rompre-Brodeur A, Delfosse V, *et al*. Affinity purification of RNA using an ARiBo tag. Methods Mol Biol 2012;941:137-55.

Di Tomasso G, Lampron P, Dagenais P, Omichinski JG, Legault P. The ARiBo tag: a reliable tool for affinity purification of RNAs under native conditions. Nucleic acids Res 2011;39:e18.

Dominska M, Dykxhoorn DM. Breaking down the barriers: siRNA delivery and endosome escape. J Cell Sci. 2010;123:1183-9.

Du L, Pertsemlidis A. Cancer and neurodegenerative disorders: pathogenic convergence through microRNA regulation. J Mol Cell Biol 2011;3:176-80.

Duffy KR, Pardridge WM. Blood-brain barrier transcytosis of insulin in developing rabbits. Brain Res 1987;420:32-8.

Easton LE, Shibata Y, Lukavsky PJ. Rapid, nondenaturing RNA purification using weak anion-exchange fast performance liquid chromatography. RNA. 2010;16:647-53.

Edwards RH. Drug delivery via the blood-brain barrier. Nat Neurosci. 2001;4:221-2.

Egleton RD, Davis TP. Bioavailability and transport of peptides and peptide drugs into the brain. Peptides. 1997;18:1431-9.

El-Aneed A. An overview of current delivery systems in cancer gene therapy. J Control Release 2004;94:1-14.

El-Sagheer AH, Brown T. New strategy for the synthesis of chemically modified RNA constructs exemplified by hairpin and hammerhead ribozymes. Proc Natl Acad Sci U S A 2010;107:15329-34.

Ferreira GN, Monteiro GA, Prazeres DM, Cabral JM. Downstream processing of plasmid DNA for gene therapy and DNA vaccine applications. Trends Biotechnol. 2000;18:380-8.

Filipowicz W, Bhattacharyya SN, Sonenberg N. Mechanisms of post-transcriptional regulation by microRNAs: are the answers in sight? Nat Rev Genet 2008;9:102-14.

Fillebeen C, Descamps L, Dehouck MP, Fenart L, Benaissa M, *et al*. Receptor-mediated transcytosis of lactoferrin through the blood-brain barrier. J Biol Chem 1999;274:7011-7.

Fineberg SK, Kosik KS, Davidson BL. MicroRNAs potentiate neural development. Neuron 2009;64:303-9.

Frank HJ, Pardridge WM, Jankovic-Vokes T, Vinters HV, Morris WL. Insulin binding to the blood-brain barrier in the streptozotocin diabetic rat. J Neurochem 1986;47:405-11.

Gao K, Huang L. Nonviral Methods for siRNA Delivery. Mol Pharm 2009;6:651-8.

Gavrilov K, Saltzman WM. Therapeutic siRNA: principles, challenges, and strategies. Yale J Biol Med 2012;85:187-200.

Gomes AQ, Nolasco S, Soares H. Non-coding RNAs: multi-tasking molecules in the cell. Int J Mol Sci 2013;14:16010-39.

Goodall EF, Heath PR, Bandmann O, Kirby J, Shaw PJ. Neuronal dark matter: the emerging role of microRNAs in neurodegeneration. Front Cell Neurosci 2013;7:178.

Grasso M, Piscopo P, Confaloni A, Denti MA. Circulating miRNAs as biomarkers for neurodegenerative disorders. Molecules. 2014;19:6891-910.

Guo H, Ingolia NT, Weissman JS, Bartel DP. Mammalian microRNAs predominantly act to decrease target mRNA levels. Nature. 2010;466:835-40.

Gupta B, Levchenko TS, Torchilin VP. Intracellular delivery of large molecules and small particles by cell-penetrating proteins and peptides. Adv Drug Deliv Rev 2005;57:637-51.

Hart SL. Multifunctional nanocomplexes for gene transfer and gene therapy. Cell Biol Toxicol 2010;26:69-81.

He L, Hannon GJ. MicroRNAs: small RNAs with a big role in gene regulation. Nat Rev Genet 2004;5:522-31.

Huang Y, Zou Q, Wang SP, Tang SM, Zhang GZ, *et al*. Construction and detection of expression vectors of microRNA-9a in BmN cells. J Zhejiang Univ Sci B 2011;12:527-33.

Junn E, Mouradian MM. MicroRNAs in neurodegenerative diseases and their therapeutic potential. Pharmacol Ther 2012;133:142-50.

Kabanov AV, Batrakova EV, Alakhov VY. Pluronic block copolymers as novel polymer therapeutics for drug and gene delivery. J Control Release 2002;82:189-212.

Kim I, McKenna SA, Viani Puglisi E, Puglisi JD. Rapid purification of RNAs using fast performance liquid chromatography (FPLC). RNA. 2007;13:289-94.

Kim JY, Choi WI, Kim YH, Tae G. Brain-targeted delivery of protein using chitosan- and RVG peptide-conjugated, pluronic-based nano-carrier. Biomaterials. 2013;34:1170-8.

Klein ME, Impey S, Goodman RH. Role reversal: the regulation of neuronal gene expression by microRNAs. Curr Opin Neurobiol 2005;15:507-13.

Kloosterman WP, Plasterk RH. The diverse functions of microRNAs in animal development and disease. Dev Cell. 2006;11:441-50.

Kocerha J, Kauppinen S, Wahlestedt C. microRNAs in CNS disorders. Neuromolecular Med 2009;11:162-72.

Kosik KS. The neuronal microRNA system. Nat Rev Neurosci 2006;7:911-20.

Koubek J, Lin KF, Chen YR, Cheng RP, Huang JJ. Strong anion-exchange fast performance liquid chromatography as a versatile tool for preparation and purification of RNA produced by *in vitro* transcription. RNA. 2013;19:1449-59.

Kreuter J, Hekmatara T, Dreis S, Vogel T, Gelperina S, *et al*. Covalent attachment of apolipoprotein A-I and apolipoprotein B-100 to albumin nanoparticles enables drug transport into the brain. J Control Release 2007;118:54-8.

Kreuter J, Shamenkov D, Petrov V, Ramge P, Cychutek K, *et al*. Apolipoprotein-mediated transport of nanoparticle-bound drugs across the blood-brain barrier. J Drug Target 2002;10:317-25.

Kusuhara H, Sugiyama Y. Efflux transport systems for drugs at the blood-brain barrier and blood-cerebrospinal fluid barrier (Part 1). Drug Discov Today. 2001;6:150-6.

Li MM, Wang WP, Wu WJ, Huang M, Yu AM. Rapid production of novel pre-microRNA agent hsa-mir-27b in *Escherichia coli* using recombinant RNA technology for functional studies in mammalian cells. Drug Metab Dispos 2014;42:1791-5.

Li Z, Rana TM. Therapeutic targeting of microRNAs: current status and future challenges. Nat Rev Drug Discov 2014;13:622-38.

Ling H, Fabbri M, Calin GA. MicroRNAs and other non-coding RNAs as targets for anticancer drug development. Nat Rev Drug Discov 2013;12:847-65.

Lowe CR, Lowe AR, Gupta G. New developments in affinity chromatography with potential application in the production of biopharmaceuticals. J Biochem Biophys Methods. 2001;49:561-74.

Maciotta S, Meregalli M, Torrente Y. The involvement of microRNAs in neurodegenerative diseases. Front Cell Neurosci 2013;7:265.

Magen I, Hornstein E. Oligonucleotide-based therapy for neurodegenerative diseases. Brain Res 2014;1584:116-28.

Maitani Y, Aso Y, Yamada A, Yoshioka S. Effect of sugars on storage stability of lyophilized liposome/DNA complexes with high transfection efficiency. Int J Pharm 2008;356:69-75.

Martins R, Queiroz JA, Sousa F. Ribonucleic acid purification. J Chromatogr A 2014;1355:1-14.

McCarthy SM, Gilar M, Gebler J. Reversed-phase ion-pair liquid chromatography analysis and purification of small interfering RNA. Anal Biochem 2009;390:181-8.

McDermott AM, Heneghan HM, Miller N, Kerin MJ. The therapeutic potential of microRNAs: disease modulators and drug targets. Pharm Res 2011;28:3016-29.

McGinnis AC, Chen B, Bartlett MG. Chromatographic methods for the determination of therapeutic oligonucleotides. J Chromatogr B 2012;883-884:76-94.

Medina-Kauwe LK, Xie J, Hamm-Alvarez S. Intracellular trafficking of nonviral vectors. Gene Ther 2005;12:1734-51.

Michaelis K, Hoffmann MM, Dreis S, Herbert E, Alyautdin RN, *et al*. Covalent linkage of apolipoprotein e to albumin nanoparticles strongly enhances drug transport into the brain. J Pharmacol Exp Ther 2006;317:1246-53.

Milligan JF, Groebe DR, Witherell GW, Uhlenbeck OC. Oligoribonucleotide synthesis using T7 RNA polymerase and synthetic DNA templates. Nucleic Acids Res 1987;15:8783-98.

Mintzer MA, Simanek EE. Nonviral Vectors for Gene Delivery. Chem Rev 2009;109:259-302.

Morão A, Nunes JC, Sousa F, Pessoa de Amorim MT, Escobar IC, *et al*. Ultrafiltration of supercoiled plasmid DNA: Modeling and application. J Mem Sci 2011;378:280-289

Moreno-Moya JM, Vilella F, Simon C. MicroRNA: key gene expression regulators. Fertil Steril 2014;101:1516-23.

Morille M, Passirani C, Vonarbourg A, Clavreul A, Benoit JP. Progress in developing cationic vectors for non-viral systemic gene therapy against cancer. Biomaterials 2008;29:3477-96.

Morris LG, Veeriah S, Chan TA. Genetic determinants at the interface of cancer and neurodegenerative disease. Oncogene 2010;29:3453-64.

Mraz M, Malinova K, Mayer J, Pospisilova S. MicroRNA isolation and stability in stored RNA samples. Biochem Biophys Res Commun 2009;390:1-4.

Nagao N, Suzuki H, Numano R, Umekage S, Kikuchi Y. Short hairpin RNAs of designed sequences can be extracellularly produced by the marine bacterium *Rhodovulum sulfidophilum*. J Gen Appl Microbiol 2014;60:222-6.

Nelson PT, Wang WX, Rajeev BW. MicroRNAs (miRNAs) in neurodegenerative diseases. Brain Pathol 2008;18:130-8.

Nguyen DN, Green JJ, Chan JM, Longer R, Anderson DG. Polymeric Materials for Gene Delivery and DNA Vaccination. Adv Mater 2009;21:847-67.

Nilsen TW. Mechanisms of microRNA-mediated gene regulation in animal cells. Trends Genet 2007;23:243-9.

Nimesh S, Chandra R. Polyethylenimine nanoparticles as an efficient *in vitro* siRNA delivery system. Eur J Pharm Biopharm 2009;73:43-9.

Noll B, Seiffert S, Hertel F, Debelak H, Hadwiger P, *et al*. Purification of small interfering RNA using nondenaturing anion-exchange chromatography. Nucleic Acid Ther 2011;21:383-93.

Nunes C, Sousa A, Nunes JC, Morão A, Sousa F, *et al*. Supercoiled plasmid DNA purification by integrating membrane technology with a monolithic chromatography. J Sep Sci 2014;37:11.

Nunes JC, Morão A, Nunes C, Pessoa de Amorim MT, Escobar IC, *et al*. Plasmid DNA recovery from ferementation broths by a combined process of micro- and ultrafiltration: Modeling and application. J Membr Sci 2012;415-416:24-35.

Pangalos MN, Schechter LE, Hurko O. Drug development for CNS disorders: strategies for balancing risk and reducing attrition. Nat Rev Drug Discov 2007;6:521-32.

Pardridge WM. The blood-brain barrier: bottleneck in brain drug development. NeuroRx 2005;2:3-14.

Park TG, Jeong JH, Kim SW. Current status of polymeric gene delivery systems. Adv Drug Deliv Rev 2006;58:467-86.

Pathak A, Patnaik S, Gupta KC. Recent trends in non-viral vector-mediated gene delivery. Biotechnol J. 2009;4:1559-72.

Patil Y, Panyam J. Polymeric nanoparticles for siRNA delivery and gene silencing. Int J Pharm. 2009;367:195-203.

Pereira P, Sousa A, Queiroz J, Correia I, Figueiras A, *et al*. Purification of pre-miR-29 by arginine-affinity chromatography. J Chromatogr B 2014a;951-952:16-23.

Pereira P, Sousa A, Queiroz J, Figueiras A, Sousa F. New approach for purification of pre-miR-29 using lysine-affinity chromatography. J Chromatogr A 2014b;1331:129-32.

Pereira P, Sousa A, Queiroz JA, Figueiras A, Sousa F. Pharmaceutical-grade pre-miR-29 purification using an agmatine monolithic support. J Chromatogr A 2014c;1368:173-82.

Pestourie C, Tavitian B, Duconge F. Aptamers against extracellular targets for *in vivo* applications. Biochimie. 2005;87:921-30.

Pfaunmiller EL, Paulemond ML, Dupper CM, Hage DS. Affinity monolith chromatography: a review of principles and recent analytical applications. Anal Bioanal Chem 2013;405:2133-45.

Ponchon L, Dardel F. Recombinant RNA technology: the tRNA scaffold. Nat Methods 2007;4:571-6.

Ponchon L, Dardel F. Large scale expression and purification of recombinant RNA in *Escherichia coli*. Methods. 2011;54:267-73.

Reinhardt RR, Bondy CA. Insulin-like growth factors cross the blood-brain barrier. Endocrinology. 1994;135:1753-61.

Robbins PD, Tahara H, Ghivizzani SC. Viral vectors for gene therapy. Trends Biotechnol 1998;16:35-40.

Santra S, Yang H, Dutta D, Stanley JT, Holloway PH, *et al*. TAT conjugated, FITC doped silica nanoparticles for bioimaging applications. Chem commun 2004:2810-1.

Satoh J. MicroRNAs and their therapeutic potential for human diseases: aberrant microRNA expression in Alzheimer's disease brains. J Pharmacol Sci 2010;114:269-75.

Schleef M, Schmidt T. Animal-free production of ccc-supercoiled plasmids for research and clinical applications. J Gene Med 2004;6 Suppl 1:S45-53.

Schratt GM, Tuebing F, Nigh EA, Kane CG, Sabatini ME, *et al*. A brain-specific microRNA regulates dendritic spine development. Nature 2006;439:283-9.

Selbach M, Schwanhausser B, Thierfelder N, Fang Z, Khanin R, *et al*. Widespread changes in protein synthesis induced by microRNAs. Nature 2008;455:58-63.

Serretti A, Olgiati P, De Ronchi D. Genetics of Alzheimer's disease. A rapidly evolving field. J Alzheimers Dis 2007;12:73-92.

Sheinerman KS, Umansky SR. Circulating cell-free microRNA as biomarkers for screening, diagnosis and monitoring of neurodegenerative diseases and other neurologic pathologies. Front Cell Neurosci 2013;7:150.

Sherlin LD, Bullock TL, Nissan TA, Perona JJ, Lariviere FJ, *et al*. Chemical and enzymatic synthesis of tRNAs for high-throughput crystallization. RNA. 2001;7:1671-8.

Singh S, Narang AS, Mahato RI. Subcellular fate and off-target effects of siRNA, shRNA, and miRNA. Pharm Res 2011;28:2996-3015.

Smith GJ, Helf M, Nesbet C, Betita HA, Meek J, *et al*. Fast and accurate method for quantitating *E. coli* host-cell DNA contamination in plasmid DNA preparations. BioTechniques. 1999;26:518-22, 24, 26.

Soifer HS, Rossi JJ, Saetrom P. MicroRNAs in disease and potential therapeutic applications. Mol Ther 2007;15:2070-9.

Son S, Hwang do W, Singha K, Jeong JH, Park TG, *et al*. RVG peptide tethered bioreducible polyethylenimine for gene delivery to brain. J Control Release 2011;155:18-25.

Sousa A, Sousa F, Queiroz JA. Advances in chromatographic supports for pharmaceutical-grade plasmid DNA purification. J Sep Sci 2012;35:3046-58.

Sousa F, Prazeres DM, Queiroz JA. Affinity chromatography approaches to overcome the challenges of purifying plasmid DNA. Trends Biotechnol 2008;26:518-25.

Srisawat C, Engelke DR. Streptavidin aptamers: affinity tags for the study of RNAs and ribonucleoproteins. RNA 2001;7:632-41.

Srisawat C, Engelke DR. RNA affinity tags for purification of RNAs and ribonucleoprotein complexes. Methods 2002;26:156-61.

Srisawat C, Goldstein IJ, Engelke DR. Sephadex-binding RNA ligands: rapid affinity purification of RNA from complex RNA mixtures. Nucleic Acids Res 2001;29:E4.

Stadler J, Lemmens R, Nyhammar T. Plasmid DNA purification. J Gene Med 2004;6 Suppl 1:S54-66.

Stark A, Brennecke J, Bushati N, Russell RB, Cohen SM. Animal MicroRNAs confer robustness to gene expression and have a significant impact on 3'UTR evolution. Cell 2005;123:1133-46.

Suh J, Wirtz D, Hanes J. Efficient active transport of gene nanocarriers to the cell nucleus. Proc Natl Acad Sci U S A 2003;100:3878-82.

Suzuki H, Ando T, Umekage S, Tanaka T, Kikuchi Y. Extracellular production of an RNA aptamer by ribonuclease-free marine bacteria harboring engineered plasmids: a proposal for industrial RNA drug production. Appl Environ Microbiol 2010;76:786-93.

Talsma H, Cherng J, Lehrmann H, Kursa M, Ogris M, *et al*. Stabilization of gene delivery systems by freeze-drying. Int J Pharm 1997;157:233-8.

Tan SC, Yiap BC. DNA, RNA, and protein extraction: the past and the present. J Biomed Biotechnol. 2009;2009:574398.

Tokatlian T, Segura T. siRNA applications in nanomedicine. Wiley Interdiscip Rev Nanomed Nanobiotechnol 2010;2:305-15.

Ullah S, John P, Bhatti A. MicroRNAs with a role in gene regulation and in human diseases. Mol Biol Rep 2014;41:225-32.

van Rooij E, Kauppinen S. Development of microRNA therapeutics is coming of age. EMBO Mol Med 2014;6:851-64.

van Rooy I, Mastrobattista E, Storm G, Hennink WE, Schiffelers RM. Comparison of five different targeting ligands to enhance accumulation of liposomes into the brain. J Control Release 2011;150:30-6.

Visser CC, Stevanovic S, Heleen Voorwinden L, Gaillard PJ, Crommelin DJ, *et al*. Validation of the transferrin receptor for drug targeting to brain capillary endothelial cells *in vitro*. J Drug Target 2004;12:145-50.

Vomelova I, Vanickova Z, Sedo A. Methods of RNA purification. All ways (should) lead to Rome. Folia Biol 2009;55:243-51.

Walker SC, Scott FH, Srisawat C, Engelke DR. RNA affinity tags for the rapid purification and investigation of RNAs and RNA-protein complexes. Methods Mol Biol 2008;488:23-40.

Walther W, Stein U. Viral vectors for gene transfer: a review of their use in the treatment of human diseases. Drugs 2000;60:249-71.

Wang Z, Rao DD, Senzer N, Nemunaitis J. RNA interference and cancer therapy. Pharm Res 2011;28:2983-95.

Wassarman KM, Zhang A, Storz G. Small RNAs in *Escherichia coli*. Trends Microbiol 1999;7:37-45.

Wei Z, Huang W, Li J, Hou G, Fang J, *et al*. Studies on endotoxin removal mechanism of adsorbents with amino acid ligands. J Chromatogr B 2007;852:288-92.

Yi X, Kabanov AV. Brain delivery of proteins via their fatty acid and block copolymer modifications. J Drug Target 2013;21:940-55.

Yin H, Kanasty RL, Eltoukhy AA, Vegas AJ, Dorkin JR, *et al*. Non-viral vectors for gene-based therapy. Nat Rev Genet 2014;15:541-55.

Zabner J, Fasbender AJ, Moninger T, Poellinger KA, Welsh MJ. Cellular and Molecular Barriers to Gene-Transfer by a Cationic Lipid. J Biol Chem 1995;270:18997-9007.

Zhang P, Hu L, Yin Q, Feng L, Li Y. Transferrin-modified c[RGDfK]-paclitaxel loaded hybrid micelle for sequential blood-brain barrier penetration and glioma targeting therapy. Mol Pharm 2012;9:1590-8.

Zhang Y, Wang Z, Gemeinhart RA. Progress in microRNA delivery. J Control Release 2013;172:962-74.

Paper II

3. Affinity approaches in RNAi-based therapeutics purification

P. Pereira, J. A. Queiroz, A. Figueiras, F. Sousa

(*Submitted for publication*)

Short description: This paper is a review that summarizes the most recent and important achievements concerning the application of affinity procedures for the purification of non-coding RNAs (small interfering RNA (siRNAs), PIWI-interacting RNAs (piRNAs), microRNAs (miRNAs) and long non-coding RNAs), considering their therapeutic application. Initially, it is presented an overview of the biogenesis pathways of non-coding RNAs, as well as their therapeutic potential. Then, it is focused the application of immobilized metal ion-affinity chromatography and RNA affinity tags-based chromatography. Moreover, recent investigations using affinity approaches based on chromatographic purification exploiting the biorecognition between amino acids ligands and RNA molecules are discussed. Finally, it is highlighted the potential contribution of these strategies to the future development of new and more robust bioseparation methods.

Affinity approaches in RNAi-based therapeutics purification

P. Pereira[1], J. A. Queiroz[1], A. Figueiras[1,2], F. Sousa[1]*

[1] *CICS-UBI – Health Sciences Research Centre, University of Beira Interior, Avenida Infante D. Henrique, 6200-506 Covilhã, Portugal;*

[2] *CNC - Center of Neuroscience and Cell Biology, University of Coimbra, Largo Marquês de Pombal, 3004-517 Coimbra, Portugal*

*Corresponding author:
Dr. Fani Sousa
Phone: +351 275 329 074
Fax: +351 275 329 099
E-mail address: fani.sousa@fcsaude.ubi.pt
Postal address: Health Sciences Research Centre, Universidade da Beira Interior, Avenida Infante D. Henrique, 6200-506 Covilhã, Portugal

Contents

Abstract

The recent investigation on RNA interference (RNAi) related mechanisms and applications led to an increased awareness of the importance of RNA in biology. Nowadays, RNAi-based technology has emerged as a potentially powerful tool for silencing gene expression, being exploited to develop new therapeutics for treating a vast number of human disease conditions, as it is expected that this technology can be translated onto clinical applications in a near future. This approach makes use of a large number of small (namely short interfering RNAs, microRNAs and PIWI-interacting RNAs) and long non-coding RNAs (ncRNAs), which are likely to have a crucial role as the next generation therapeutics. The commercial and biomedical interest in these RNAi-based therapy applications have fostered the need to develop innovative procedures to easily and efficiently purify RNA, aiming to obtain the final product with high purity degree, good quality and biological activity. Recently, affinity chromatography has been applied to ncRNAs purification, in view of the high specificity. Therefore, this article intends to review the biogenesis pathways of regulatory ncRNAs and also to discuss the most significant and recent developments as well as applications of affinity chromatography in the challenging task of purifying ncRNAs. In addition, the importance of affinity chromatography in ncRNAs purification is addressed and prospects for what is forthcoming are presented.

Keywords

Affinity chromatography; Non-coding RNAs; RNA purification

1. Introduction

In the late 1990s there have been significant advances in biology, in which one of the most important and remarkable discoveries was the new world of RNA interference (RNAi), leading to the use of RNA-based strategies for therapy [1,2]. Accordingly, the discovery that genes could be silenced by RNAs allowed the biological understanding of other roles of RNA, which changed from a simple intermediate molecule between DNA and proteins to a dynamic and versatile molecule, fundamental in the regulation of genes expression, involved in numerous cellular processes of all living organisms [1,3]. RNAi is defined as a highly conserved intracellular mechanism, involving the recognition and post-transcriptional control of specific messenger RNA (mRNA), mediated by non-coding RNAs (ncRNAs), that can result in the silencing gene [3]. NcRNAs are a class of transcripts which, as the name implies, are not translated into proteins, but play important roles in the cellular function. A very simplistic classification based on transcript size, arbitrarily separates these biomolecules into two major groups: the small (sncRNAs, <200 nucleotides (nt) in length) and the long (lncRNAs, from 200 nt to approximately 100 kilobases) non-coding RNAs [4,5]. In turn, the small group comprises infrastructural RNAs and regulatory RNAs. The infrastructural ncRNAs include ribosomal, transfer, small nuclear and small nucleolar RNAs with well-known functions that are involved in the spliceosomal and translational machinery [4]. On the other hand, the regulatory ncRNAs include small interfering RNA (siRNAs), PIWI-interacting RNAs (piRNAs) and microRNAs (miRNAs), among others [4,5]. In the last decade, several studies showed that many of these small ncRNAs have important regulatory functions influencing almost all areas of cellular biology with a wide variety of molecular mechanisms. Another group of ncRNAs comprises the lncRNAs, a highly heterogeneous group of transcripts that are the least well understood ncRNAs [6,7]. They have only recently emerged as a major category of regulatory eukaryotic transcripts and are mostly involved in trafficking of protein complexes, genes and chromosomes to appropriate locations.

Considering the functions attributed to ncRNAs, presently they constitute the most promising class of next generation therapeutics with a great potential to exert a revolutionary effect on modern medicine [8]. However, enthusiasm vanished when it was realized that getting ncRNAs to work as drugs was not as straightforward as originally thought. In addition, the mRNA molecules are also an attractive option in the development of new therapeutic approaches and, therefore, they have emerged as a new class of therapeutics due to the extremely important and fundamental roles that they play in all living cells. The ongoing research in this field includes the creation of vaccines for the treatment of cancer or infectious diseases [9,10].

Synthesized RNAs have become an indispensable tool for biological sciences, namely in structural, biochemical and biophysical studies, as well as in the development of new therapeutic approaches using RNAi technology [11-13]. To date, ncRNAs used for therapeutic

purposes have mostly been produced by chemical or enzymatic (*in vitro* transcription) synthesis [14]. Chemical synthesis is normally used for the generation of short oligoribonucleotides (<50 nt) while *in vitro* transcription can produce longer RNAs. Although these processes can be very efficient, the final RNA products typically present a maximum purity of 90%, what means that, depending on the application objective, additional purification protocols to remove the impurities derived from the synthesis process have to be employed. Most impurities, often referred to as failure sequences, may lead to non-targeted gene silencing, what is commonly associated with a decrease in therapeutic effectiveness and still restrict the implementation of these oligonucleotides onto pre-clinical and clinical applications [14,15].

On the other hand, along with the RNAs obtained from chemical or enzymatic synthesis, the RNAi therapy can also be based in recombinant RNAs obtained after biosynthesis using prokaryotic hosts such as *Escherichia coli* or *Rhodovulum Sulfidophilum* which is usually more cost-effective than the chemical or enzymatic synthesis, considering the large-scale production [14,16-20]. Moreover, most of the biological RNAs have post-transcriptional modifications that may not be reproduced under chemical or enzymatic synthesis and some of the modifications are quite important for their function and structure [21]. However, in this strategy, together with the target RNA that is being heterologous produced, other host RNA species are also produced, highlighting the need for an effective purification protocol to isolate the RNA of interest from other contaminants, thus minimizing non-targeted gene silencing and immunologic responses [14].

Thus, a major challenge in developing RNAi-based therapeutics remains the assurance of RNA purity to minimize off-target gene silencing. During the last decades, different methods have been extensively employed to isolate and/or purify of small RNAs obtained either by *in vitro* transcription or from biological sources, such as denaturing polyacrylamide gel electrophoresis, and some chromatographic techniques namely ion-pairing, reversed-phase, anion-exchange as well as size exclusion chromatography [22-28]. Overall, with these methods, the purification of RNA still remains rather time-consuming, expensive, tedious, difficult to scale up and can cause degradation of the RNA molecules (requirement of toxic solvents and denaturing conditions) [22]. On the other hand, affinity chromatography purification represents a highly efficient strategy for RNA purification because it is very rapid, facilitates the maintenance of RNA stability and can be easily adapted to any molecular weight RNA as well as high-throughput applications [22].

Therefore, the aim of this review is an overview of the current knowledge in the field of affinity purification techniques for ncRNAs purification. Finally, it will bring to discussion the importance to recover pure ncRNAs, in accordance to the guidelines of the regulatory agencies for therapeutic application, with an emphasis on new experimental approaches, using different affinity ligands, such as amino acids and amino acids derivatives.

2. Biogenesis of regulatory non-coding RNAs

The most important mechanistic features of RNAi will be briefly presented here to provide information regarding the physicochemical and molecular characteristics of RNA molecules involved and the type of interaction that is established along the processing.

2.1. Small interfering RNAs

siRNAs are short mediators of RNAi that are originated from repetitive sequences, either sense-antisense pairs or long double-stranded RNAs (dsRNAs) precursors designed specifically to silence expression of target genes (see Table 1) [29]. They can be introduced exogenously into the cell in short form (e.g., synthetic siRNAs) or in the form of long dsRNA molecules [3,30]. After introduction into the cytoplasm, long dsRNAs are recognized and processed by a combination of proteins including Dicer enzyme, ribonuclease (RNase) III, Tar RNA binding protein (TRBP), and PACT into a short dsRNA (siRNA), with phosphate groups at both the 5′ ends along with hydroxyl groups and two nucleotide overhangs at both the 3′ ends [3,5,30,31]. After processing, the siRNA consists of a sense strand and a complementary antisense strand. siRNA duplex is then incorporated into the holoenzymatic complex, RISC (RNA-induced silencing complex), where the strands are separated into the complementary antisense strand (or the guide strand) and the sense strand (or the passenger strand). The sense strand is subsequently degraded and expelled by Argonaute-2 (AGO2) protein, a component of the RISC (as shown in Figure 1) [29,32,33]. Posteriorly, the antisense strand of the siRNA molecule, which is in the RISC complex, serves as a template to recognize a complementary region of the target mRNA sequence, with a fully perfect complementarity. The resulting interaction suppresses the gene expression, leading to the endonucleolytic cleavage of the mRNA, which in-turn inhibits translation to the corresponding protein. After the silencing process, the fragments of the mRNA are released and the RISC is free to bind to another mRNA target and to start a new round of cleavage [5,31,32,34].

As previously mentioned, it is also possible to silence gene expression via the siRNA pathway by direct introduction of chemically synthesized siRNAs or dsRNAs (see Figure 1). When synthetic siRNAs are introduced into cells, they can directly engage with the RNAi machinery, without any processing steps, thus avoiding the Dicer catalyzed reaction [3,30]. However, since the half-life of siRNA is short, a number of methodologies exist to take advantage of using the Dicer machinery to produce siRNA within the cell from precursor siRNA molecules [29,31]. In fact, alternative RNA molecules such as plasmid expressed short hairpin RNAs (shRNA) are the most common (see Table 1) [29,30]. Generally, shRNA is transcribed in the nucleus from an external expression DNA vector (see Figure 1). The hairpin loop is spontaneously formed due to the complementary region, by RNA polymerase II or III. Then, the shRNA transcript is processed by Drosha, an RNase III endonuclease.[3] The resulting pre-shRNA is exported to cytoplasm, where it is recognized by the cellular RNAi machinery and is

processed to form active siRNA by Dicer and incorporated into RISC [30]. In comparison to siRNA, these shRNAs are constantly synthesized in host cells and have many advantages like long-lasting silencing effects as well as easy delivery methods. Moreover, the preparation of a shRNA expression vector costs less than the bulk manufacturing of siRNA [3,29].

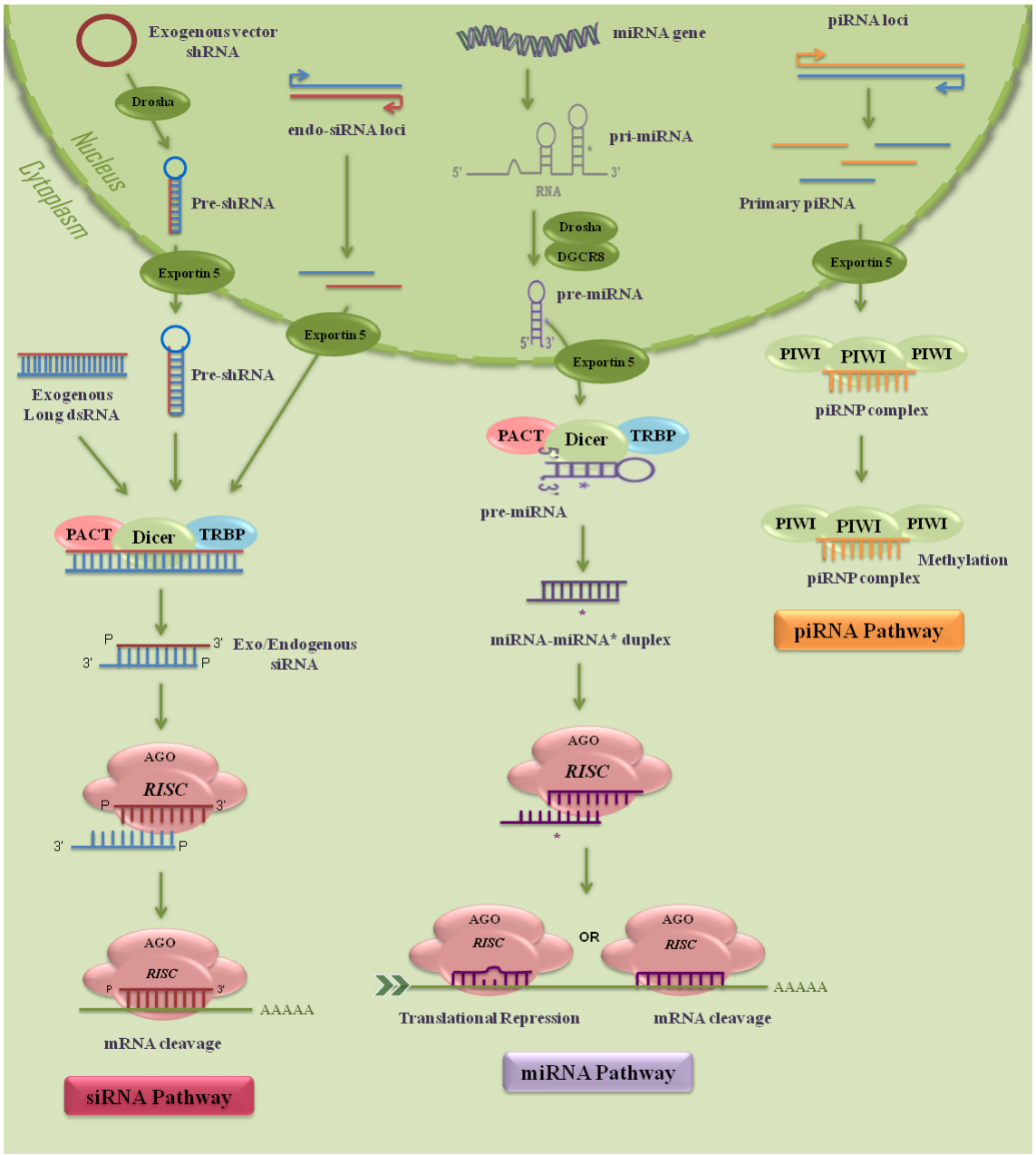

Figure 1 - RNA silencing pathways and their essential components: siRNA; miRNA; piRNA.

2.2. MicroRNAs

MiRNAs are a class of RNAi inducers, codified in the genome that can regulate gene expression at post-transcriptional level by mRNA degradation, translational repression or both mechanisms (see Figure 1) [4,35]. This regulation occurs through a sequential process involving a miRNA precursor (pre-miRNA) and, subsequently, a mature miRNA that is incorporated into RISC to regulate the target mRNA. Thus, most miRNAs are processed from endogenously expressed transcripts [34,36]. RNA polymerase II produces long primary miRNAs transcripts (pri-miRNAs, approximately >100 nt) containing the mature miRNA sequence, which possess a characteristic stem-loop structure and are afterward subjected to processing mechanisms [3,5,33,34]. In the nucleus, these pri-miRNAs transcripts are cleaved by a complex containing both the RNase III endonucleases Drosha and DiGeorge syndrome critical region gene 8 (DGCR8), leading to generation of a corresponding precursor of miRNA (pre-miRNA) [5,36]. The resulting product is RNA of 70-100 ntucleotides in length containing the long hairpin like structure and a two nucleotide overhang at its 3'end [32,33]. The pre-miRNA is then actively transported to the cytoplasm by Exportin-5, a nuclear transport receptor complex. Once in the cytoplasm, the pre-miRNA is further processed, where its loop is removed by a complex that contains the enzyme Dicer, TRBP and PACT [34]. As a consequence, pre-miRNAs are converted into mature miRNAs duplexes (miRNA-miRNA* duplexes, where miRNA is the antisense, or guide strand, and miRNA* is the sense, or passenger strand) (see Table 1) [3,5,32,36,37].

Subsequently, mature miRNAs are associated to Argonaute proteins, in particular AGO1 and AGO2, within the RISC complex. During loading, the sense strand, termed miRNA* is stripped away and targeted for degradation by Argonaute protein [34-36]. In turn, the miRNA antisense strand, called mature miRNA strand, binds to the 3' untranslated regions (3'UTR) of the target mRNA. Hence, the main mode of action of mature miRNA strand is the recognition of specific sites, typically present in the 3'UTR of target mRNA [32,34,35]. This binding results in degradation of mRNA transcripts when perfect base-pairing is present or induction of translational repression by blocking mRNA translation, when not perfectly base pairing prevails [3,5,35,36]. The general processing miRNA pathway is shown in Figure 1.

Indeed, siRNAs and miRNAs are both processed by essentially the same RNAi machinery (Figure 1) due to their similarity in terms of the physicochemical and molecular characteristics (see Table 1). Nevertheless, they differ in the way that they recognize their targets and interact to trigger RNAi. Typically, miRNAs have internal mismatches, creating so-called bulges in the secondary structure, whereas siRNAs usually have complete internal base pairing and no bulging. On the other hand, siRNAs are directed to a particular mRNA target via perfect complementarity, whereas single miRNA can regulate multiple mRNA targets via binding with a number of mismatches [5].

Table 1 - General properties of non-coding RNAs therapeutics.

Class	Mean Size (bp)	Origin	Structure	Biogenesis	Action mechanism	[Ref.]
miRNA	21-25	Endogenous	 Double stranded	Two-step cleavage of hairpin precursors by Drosha and Dicer	Induce translation repression or mRNA degradation	[3,5,33,34]
siRNA	19-25	Exogenous or endogenous	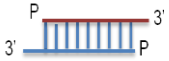 Double stranded	Cleavage of long endogenous dsRNAs by Dicer	Induce mRNA degradation	[3,5,30,31]
shRNA	19-29	Exogenous	 Single stranded	Processed by Dicer to produce siRNA, transcribed by RNA polymerase III	Induce mRNA degradation	[29,30]
piRNA	24-31	Endogenous	 Single stranded	Transcribed from specific genomic loci in primary piRNAs that associate with the PIWI proteins	Can lead to the target RNA molecules degradation	[5,32,34]
lncRNAs	200 to >100 Kb	Endogenous	 Double stranded	Transcribed of primary long non-coding transcripts by RNA polymerase II into smaller non-coding RNAs	Induce translation repression or mRNA degradation	[5,7,38]

2.3. PIWI-interacting RNAs

The piRNAs are a class of sncRNAs widely expressed in different tissues and cell types, in particular in germ line cells of mammals (see Table 1). The name of these ncRNAs results from the fact they associate to the PIWI family of proteins [5,32,34]. However, the intervening factors involved in the piRNAs biogenesis and transcription regulation mechanisms remain to be discovered [5]. Until now, it is only well known that the piRNA biogenesis pathway is very different from that of miRNA and siRNA since it is generated by RNase III-independent pathways that do not involve dsRNA precursors, neither Drosha nor Dicer (Figure 1) [5,32,34]. Mostly, the piRNAs arise from long and single-stranded RNA precursors, derived from intergenic repetitive elements, transposons or large piRNA clusters, which are transported via an unknown mechanism to the cytoplasm [30]. Once in the cytoplasm, they are associated with PIWI subfamily proteins, forming RNA-protein complexes (piRNP complexes) [32,34]. PIWI proteins are responsible for generating the 5′ end of the piRNA, but the nuclease that creates the 3′ end has yet to be identified (Figure 1) [5,32]. On the other hand, these antisense piRNAs can undergo a cycle of amplification, called ping-pong cycle, to generate secondary piRNAs in the cytoplasm [34]. Specifically, in mouse, piRNA-mediated transposon repression, predominantly, happens via DNA methylation [5,32].

2.4. Long non-coding RNAs

LncRNAs represent the most recent breakthrough in the field of RNAi, as pivotal molecules for the regulation of gene expression, since they bind to the mRNA with little or no protein-coding capacity (see Table 1). LncRNAs form a significant part of the eukaryotic transcriptome, regulating the expression of up to 70% of genes, although they are among the least well understood ncRNAs. Many identified lncRNAs are transcribed of primary long non-coding transcripts by RNA polymerase II into sncRNAs [5-7]. Nonetheless, according to their positional location with relation to protein-coding genes, the lncRNAs can be placed into diverse categories, namely sense, antisense, bidirectional, intronic and intergenic. In addition, some studies demonstrated that lncRNAs might also be produced by transcriptional active pseudogenes [5,6,38]. Despite all the efforts, the origins of lncRNAs are not yet clearly defined and understood. Thus, another classification have been used to establish the classes of lncRNA, according with the transcriptional origins, such as promoter-associated long RNAs (lpaRNAs), natural antisense transcripts (NATs), large intervening non-coding RNA (lincRNA), and enhancer associated RNAs (eRNA) [5,7]. The cellular location of lncRNA is also varied and may imply its function, since they can be found in nucleus, cytoplasm, or into specific sub-cellular compartments (p.e. mitochondria) [5,7,38].

The majority of lncRNAs are transcribed from the nuclear genome but some can be generated from mitochondrial genomes. LncRNAs typically have the same structural features as mRNA, including 5'capping, polyadenylated 3' tails and undergo alternative splicing to give rise to the final product. In general, the lncRNAs may be located within nuclear or cytosolic fractions

and may be polyadenylated or non-polyadenylated [5-7,38]. In 2013, it was demonstrated that several lncRNAs can be spliced at their 5' and 3'-ends to give stable circular RNAs (circRNAs) [39]. These circRNAs form an important class of post-transcriptional regulators with unknown function. However, recent data indicated that circRNAs compete with other RNAs for binding by RNA binding proteins (RBPs) or miRNAs, and have function as negative regulators of miRNAs [39]. Therefore, their targets can be either coding or non-coding RNAs, and can positively (concordant regulation) or negatively (discordant regulation) modify the expression or processing of their target genes.

3. Therapeutic potential of regulatory non-coding RNAs

Over the past ten years, a growing number of studies have shown that many of the ncRNAs play important roles in the cellular function, establishing ncRNAs as a promising next-generation therapeutic drug [5,8]. In fact, RNAi-based technology possesses attractive characteristics such as high specificity, efficiency and ability to induce a robust and potent knockdown of the targeted genes. In addition, another advantage of RNAi over other therapies is the possibility to promote a long-lasting therapy (the therapeutic effect lasts from days up to weeks), reducing the expenses of medical treatments. Usually, the dosage required of ncRNA therapeutics is low, which can reduce or eliminate the occurrence of undesirable adverse effects in the patient [33].

For all these reasons, RNAi has become one of the most powerful and widely used tools for the study of gene function/expression. Furthermore, RNAi has also been used to develop new alternative approaches, in order to regulate several pathways involved in the origin and progression of many gene-related diseases [3,5,7,8]. Presently, this biomedical approach is being considered in numerous clinical trials focusing distinct types of cancers, viral infections, metabolic diseases, cardiovascular disease, hypertension and stroke, immune dysfunction and auto-immunity, neurodegenerative and psychiatric diseases [3,5,7,29]. These novel therapies focused on the specific gene expression control can contribute to the regulation of a variety of physiological and biological/cellular processes as diverse as development, cell cycle regulation (DNA repair), proliferation, differentiation, cell adhesion, apoptosis, stress response, metabolism, stem cell self-renewal, embryogenesis and neurogenesis [5-7,38]. The main functions of ncRNAs are summarized in Table 2.

Table 2 – Biological Functions regulated by regulatory non-coding RNAs [5-7,38].

Function	lncRNAs	siRNAs	miRNAs	piRNAs
Genetic Imprinting	✓			
Genome Rearrangement	✓			
Alternative Splicing	✓			
RNA Editing	✓			
Nuclear and cytoplasmic trafficking	✓			
Formation of endogenous siRNAs by NATs	✓			
Protection of the cell/genome against viruses		✓	✓	
mRNA deadenylation / sequestration		✓	✓	
Heterochromatin Formation		✓	✓	✓
Genome Integrity and Stability		✓	✓	✓
Drug resistance		✓	✓	✓
Developmental Robustness				✓
Evolution				✓
Transposon activity Regulation				✓
Genome Reorganization				✓
Telomere Protection Complex				✓
Germ line development				✓
Epigenetic Regulation	✓	✓	✓	
Chromatin Remodeling	✓	✓	✓	
Histone and DNA methylation	✓	✓	✓	
Protein synthesis inhibition	✓	✓	✓	
RNA stability	✓	✓	✓	
Biomarkers	✓	✓	✓	
Maintenance of cell integrity	✓	✓	✓	✓
Transcriptional inhibition (mRNA decay)	✓	✓	✓	✓
Post-transcriptional RNA processing	✓	✓	✓	✓

4. RNAi affinity-chromatography

The promising and successful results of these novel therapeutic approaches reinforced the interest on RNA investigation, which led to an increase in the number of structural, biochemical, biophysical and biomedical studies, allowing the emergence of RNA as a new class of biopharmaceuticals [8,40]. Nowadays, and considering the therapeutic application of these biomolecules, the major interest is not only to produce high quantities of ncRNAs but also to obtain and preserve its good quality and biological activity, fulfilling the requirements of regulatory agencies, such as Food and Drug Administration (FDA), European Medicines Agency (EMA) and World Health Organization (WHO) [22].

In general, purification protocols used for RNA isolation have a number of common requirements, due to the high risk of RNA degradation during the procedure. RNA is an unstable molecule and has a very short half-life once extracted due to the ubiquitous presence of RNA-degrading enzymes (RNases) which are present in biological samples, aqueous buffers, on labware and can be introduced via human handling [41]. Consequently, one of the most important concerns when working on purification of RNA is the adjustment of all working conditions in order to improve the performance of the biotechnological strategy, but always guaranteeing the structural and functional stability of ncRNAs to maintain their biological activity.

Thus, in the last years, the downstream strategies based on affinity chromatography evolved and now represent a highly efficient strategy for RNA purification and have been implemented in order to increase the yields and the selectivity, contributing for the establishment of reliable and economical processes to assure a strict quality in production of therapeutic biomolecules [22,42,43]. In general, these strategies are time-efficient, occur under non-denaturing conditions and can be easily adapted to any molecular weight RNA as well as high-throughput applications. However, they also do present some limitations, particularly in regard to the biological origin of the ligands [44] (see Table 3).

Affinity chromatography is a powerful technique in the development of therapeutically useful products that uses biological agents as specific ligands to analyze, identify and purify RNA on the basis of their biological function or individual chemical structure [22,42,45]. The binding between the target biomolecules and the affinity ligand is specific, selective and reversible. Thereby, this approach simulates and exploits natural biological multiple non-covalent interactions occurring at the cellular level and involved in the molecular recognition of many biological phenomena, for the selective and efficient purification of the target biomolecules [45,46]. Hence, the binding mechanism inherent on the specific biorecognition of the target biomolecule by the specific ligand results from the combination of multiple intermolecular forces, such as electrostatic and hydrophobic interactions, hydrogen bonds and cation–π interactions, as well as van der Waals forces and dipole–dipole forces [43,45,47]. However,

depending on the environmental conditions used, some interactions can be preferentially established than other, becoming more evidenced. This distinctive capacity to establish different types of interactions is a major advantage of this kind of chromatography, resulting in a technique with extremely high selectivity and resolution [22,43,45]. On the other hand, the exploitation of the affinity interactions can trigger new insights not only in isolation strategies but also in many other RNA research fields owing to its implication in molecular recognition phenomena.

In affinity chromatography, the choice of the matrix and conditions to be used will depend on the molecular properties of the target biomolecules and the physicochemical and thermodynamic nature of their molecular interactions. Moreover, the elution of a target biomolecule that is bound to the affinity ligands can be achieved either specifically, using a competitive ligand, or non-specifically, by changing the pH, ionic strength or polarity depending on the matrix used and the chemical characteristics of the biomolecules [22,48]. The addition of a competing agent in the elution buffer, known as biospecific elution, is commonly employed in order to improve the selectivity as well as to get higher elution efficiency [16,49]. The competing agent can bind to the retained target or to the immobilized ligand, depending on their characteristics, thus allowing predicting the interactions that can be involved.

Most ligands used in affinity chromatography such as amino acids, peptides and proteins are of biological origin, although they tend to be fragile, showing low binding capacities. Currently, to address this issue, new strategies have been developed focusing on the search and design of new synthetic molecules to be further employed as affinity ligands [44]. This approach intends to combine the selectivity of natural ligands, with high capacity, robustness, durability and reproducibility of synthetic systems for the purification of biomolecules. Another issue to take into account is the materials typically employed into chromatographic matrices, namely beads, gels or membranes manufactured from raw materials [48,50]. Therefore, the ideal support for the separation and purification of RNA must present diverse characteristics namely high selectivity/specificity and binding capacity, mechanical and chemical stability and low cost. The design of selective ligands and matrices for RNA purification can be complex, time-consuming and expensive, though their implementation into affinity chromatography processes result in significant economic benefits, such as reduction of downstream steps and the improvement of the product quality, therefore justifying the initial investments [43,45,51].

Affinity chromatography can have a widespread application in ncRNAs preparation in view of RNA structural properties (size, charge, hydrophobicity) and versatility in biological function that includes interaction with many molecules in the cell. The stranded nature of RNA (single and double), which is normally involved in RNA recognition due to the high nucleotide bases exposure and accessibility for interactions also influences the purification process [52]. These

properties and features continue to make affinity chromatography a popular method and a useful and important tool in the development of biopharmaceuticals and/or clinical testing. Below it will be discussed different types of affinity chromatography that have been utilized for the purification of ncRNAs. The advantages and limitations of these methodologies applied for the affinity isolation of RNA molecules are discussed in Table 3.

4.1. Boronate affinity chromatography

Since the 1970s, one of the most commonly used affinity techniques in the isolation of RNA molecules is the boronate affinity chromatography (Table 3) [53]. In this affinity technique is exploited one of the few chemical differences between RNA and DNA, the presence of cis-diol groups of ribose sugar at the 3' end of the RNA molecule and their absence in the deoxyribose backbone of DNA [54-57]. Thus, RNA molecules are specifically purified from the mixture of nucleic acids (DNA and RNA) and other biomolecules due to the specific and reversible interaction between diol moieties which are in a cis configuration and the boronate ligands [54-57]. This interaction is dependent on acidic and basic experimental conditions. However, other interactions can also play an important role in the separation of nucleic acids in the boronate affinity methods, namely hydrophobic (due to the phenyl ring present in aromatic boronate ligands), π-π (can also occur with phenyl groups), ionic (due to the negative charge of the active tetrahedral boronate), hydrogen bonding (due to the presence of two hydroxyl groups) and coordination (because the boron atom has an empty orbital, it can serve as an electron receptor for charge transfer interaction) interactions [58]. Several boronate functionalized packed column systems have been developed for the selective separation of RNA from the nucleic acids mixture, including dextran and cellulose derived bipolar 2-[(4-boromophenyl)-methyl]-ethylammonium] ethyl solution polymer system [59], thermo-responsive poly(N-isopropylacrylamide)-co-(vinylphenylboronic acid) [poly(NiPAAm-co-VPBA)] latex particles [60], aminophenyl boronic acid (APBA) modified hydrogel beads [61], monolithic ‘cryogel’ matrices [62] and monolithic silica columns [63].

4.2. RNA affinity tags

In last years, RNA affinity tags have emerged as useful tools for the isolation of RNAs, allowing the development of easy, reliable, fast and more robust procedures for native RNA purification of long constructs produced by *in vitro* transcription methods, providing highly pure RNA preparations (Table 3) [64]. The selection of several oligoribonucleotides sequences functioning as tags for RNA affinity purification (such as, RNA aptamers) with the desired properties and ability to bind specifically and with high affinity to a specific ligand has been performed using the Systematic Evolution of Ligands by Exponential enrichment (SELEX) method [64,65].

To date, a limited number of highly specific RNA affinity tags have already been successfully used for the purification and selective recovery of the tagged RNAs. RNA affinity tags are

based on RNA-protein interactions found in nature and are inserted in the target RNAs molecules, during *in vitro* transcription [14]. Moreover, the tags should bind with high affinity to a ligand that can either be immobilized on a chromatographic matrix or be conjugated to an antibody detection system [14,64]. Thus, the purification of RNAs from cellular extracts is then achieved using an affinity column with a specific RNA-binding protein immobilized, in such a way that the formed complex can be selectively and gently dissociated afterwards (see Figure 2). The protein affinity tags include polyhistidine [66], myc epitope [67], the tandem affinity protein (TAP) tag [68], protein A [69], MS2 coat protein [70], glutathione S-transferase [71], Streptavidin-tag [72-73] and the FLAG epitope [74]. In these strategies, in order to recover the bound RNA of interest it can be used competitive elution (with biotin or dextran) or cleavage by a protease with a recognition site that is incorporated along with the affinity tag [75-78]. In addition, some tagged RNAs do not cleave even after prolonged incubation, presumably due to alternate and unpredictable secondary structures at the cleavage site. Thus, in general, these methods can induce structural modifications in RNA molecules, which can affect the overall topology of the RNA construct, as well as significantly degrade the target biomolecule and compromise the final purification. Generally, the limiting step when is used a known RNA-protein interaction as part of the affinity purification is the inability to efficiently elute or release the purified complex under native conditions since the binding affinity of the known RNA-protein interaction is usually high [73,79,80].

In line with previous expectations, several alternative schemes have been developed for fast non-denaturing purification of RNA transcribed *in vitro*. In 2007, Batey and Kieft developed an affinity-based method that utilizes a MS2 coat protein binding stem–loops as affinity tags at the 3'end of the RNA transcript, which bind to the nickel-affinity matrix via interaction with the hexahistidine-tagged MBP(maltose binding protein)-MS2 coat protein fusion for native RNA purification produced by *in vitro* transcription methods [81]. This RNA tag is preceded by the *glm*S ribozyme sequence which is activated by glucosamine-6-phosphate, removing the tag used at the end of the RNA transcript, to induce the specific elution of the desired RNA [81]. This affinity purification methodology for native RNA purification is robust, rapid and broadly applicable to any RNA of interest, being easily accessible to a wide range of researchers with minimal difficulty. On the other hand, in a recent report, a quick affinity purification procedure was developed for RNAs transcribed with a 3¢-ARiBo tag and shown to provide RNA with exceptionally high purity and yield [82-85]. The ARiBo tag contains the λ boxB RNA and the *glm*S ribozyme, allowing immobilization on glutathione-Sepharose resin via a λ N-GST fusion protein and elution by activation of the *glm*S ribozyme with glucosamine-6-phosphate [84]. The use of RNA tags containing ribozymes has been shown to substantially simplify the procedure, since no additional purification steps other than a buffer exchange are required after the RNA elution. After several matrix washes to remove impurities from the transcription reaction, the RNA of interest is eluted by activation of the self-cleaving ribozyme (see Figure 2) [82-85].

Overall, although these robust affinity purification methodologies can be very efficient for recovering RNA with high quality and quantity, they still are expensive on large scale and labor intensive. Besides, the purification of RNA produced by *in vitro* transcription requires in some cases more than one purification step or the application of denaturing conditions in order to achieve higher RNA enrichments (Table 3) [64,76,86]. Therefore, the challenges associated with RNA purification motivate the improvement of the already existing chromatographic techniques or the development of new purification approaches.

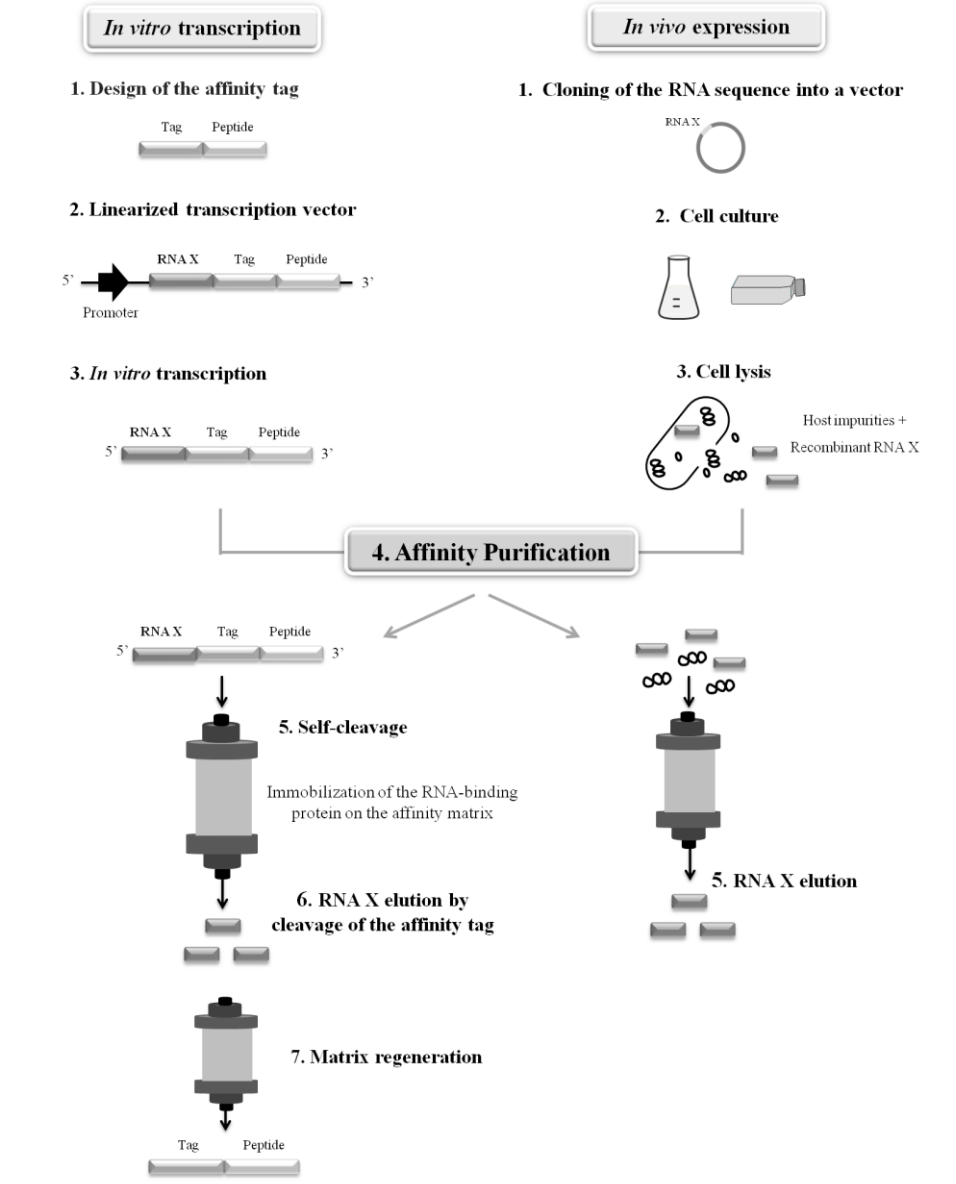

Figure 2 – The general scheme for the native purification of the desired sequence (RNA X) and the amino acids-based affinity chromatography of the recombinant RNA.

Table 3 – Overview of available affinity chromatography methods used in bioseparation of non-coding RNAs therapeutics.

Methods	Target RNA	Advantages	Limitations	[Ref]
Boronate affinity chromatography	tRNAs	-Isolation of RNA molecules from crude cell extracts; -Requires no sample pre-treatment; -High purity and quality of purified RNA, since the steps involved are very fast; -Efficient elimination from genomic DNA; -It is less sensitive to quantitative errors caused by minor fluctuations in reagent pH and ionic strength.	-Non-specific interaction can be avoided by using inert hydrophilic polymers for matrix synthesis; -In some cases, stepwise or gradient elution can give better results; -Sometimes, the column must be washed with 6 M urea prior to washing with the regeneration buffer.	[54-63]
RNA affinity tags	lincRNA shRNA miRNA miRNA-mRNA complex RNA oligonucleotides	-Reliable, rapid and robust methodologies for native RNA purification using affinity tags on inherent biologic interactions; -Broadly applicability to any RNA of interest, making this a useful method to a broad spectrum of the RNA research community; -Allow the production of milligram quantities -Stability of affinity tags; -High recovery and purity due to the specific selection of the tags with high affinities for the resins (high-quality RNA).	-Elution of the complex can be achieved under denaturing conditions or through the use of a competitor oligonucleotide to release the RNP under native conditions, in order to achieve higher RNA enrichments. In addition, in some cases, use of proteases requires additional purification steps to remove the co-eluting enzyme; -Need of several design issues and binding the affinity tags into RNA, which may lead to longer optimization processes (cost and time-demanding); -Requires the screening of appropriate affinity resins to assure the binding only the RNA tags to the matrix; -In some cases, contamination of the target RNA with tag, since the tag is released from the column during the wash and elution steps; -The attached rybozyme may induce the formation of alternative structures on RNA and thus disrupt the correct folding of the ribozyme, with its self-cleaving power disabled; -During the purification process, chemical modifications can lead to structural perturbations that can inhibit complex	[53,64,70,73,75-82,103,104]

			formation or can significantly degrade RNA, an undesirable feature.	
Amino acid-based affinity chromatography	Precursor miRNA rRNAs tRNAs 6S RNA Total RNA	-Isolation of target RNA from crude cell extracts in a single chromatographic step; -Robust methodologies using natural small molecular ligands; -High purity and quality of purified RNA, since the steps involved are very fast; -Purification with high reproducibility; -Efficient elimination of endotoxin, proteins, genomic DNA and single/double-stranded RNAs; -Simplified the workflow integration and miniaturizes sample handling process; -Occur under non-denaturing conditions and can be easily adapted to any molecular weight RNA as well as high-throughput applications.	-The high salt concentrations (namely tyrosine, histidine and lysine amino acids) required for elution of the targets RNAs are the main drawbacks of this approach, especially with regard to biotechnological application since the use of salt is associated with higher costs and environmental impact; -Low recovery yields; -Lower durability of supports.	[16,17,22,87-91]

4.3. Amino acid-based affinity chromatography

In the past few years, a new affinity methodology called amino acid-based affinity chromatography has been successfully developed to efficiently purify different RNA species [22]. Indeed, several studies are already available demonstrating the applicability of amino acids (namely $_{L}$-Arginine, $_{L}$-Histidine, $_{L}$-Lysine and *O-Phospho*-$_{L}$-Tyrosine), as specific affinity chromatographic ligands, in the purification/separation of diverse RNA molecules, such as total RNA, ribosomal RNA, tRNA, 6S RNA and pre-miRNAs (in particular, pre-miR-29b), using conventional particle-based columns (amino acids-agarose matrices) [16,17,87-91]. These results demonstrated the versatility, exceptional ability and the potential of the amino acids to strongly interact with all functional classes of RNA, despite their structural diversity and different folding states, as they are in their native state. Amino acid-based affinity chromatography is a powerful technique that has been used as an improved, very specific and effective bioseparation methodology for the purification of RNA molecules that exploits natural affinity interactions occurring between amino acids and RNA [22,45]. These studies were based on the fact that many several specific interactions exist between proteins and nucleic acids in biological systems, involving particularly basic amino acids [22,45,92,93]. For example, Calnan and co-workers demonstrated that arginine residues are important for specific RNA recognition, even with different conformational rearrangements and that arginine-base interactions have been recognized as the most prevalent interactions in several protein-RNA complexes [93]. Thus, this type of selectivity can be explained on the basis of the biological function or chemical structure of the RNA, which favors the interaction.

In general, the RNA structural features (namely, negative charge of the RNA backbone and single-stranded nature) seem to be relevant for the specific interactions established between the RNA and the amino acids used as immobilized ligands [92,94]. Nonetheless, the high base exposure on RNA species was also suggested to have a crucial role in the RNA recognition and on its distinct retention behavior. Recently, the structural diversity of RNAs was described to be of significant importance in RNA-protein interactions because RNA can exhibit different moieties according to its folding state, for example RNA hairpins and bulges form stable tertiary structures that contributes substantially to their recognition [47,95,96]. On the other hand, the salts used in the chromatographic conditions can also have a profound positive effect on RNA folding as well as on the stability of non-covalent RNA-amino acid interactions during the course of purification, once the salt allows that single-stranded nucleic acid molecules form stable hydrogen bonds between their complementary bases [96,97].

Additionally, this type of selectivity can also be explained in light of the atomic and molecular recognition studies performed on RNA-protein complex structures have predicted preferential interactions/contacts occurring between particular amino acids side chains and specific nucleotides either involving the RNA bases or through a defined conformation of the RNA backbone phosphates (e.g. arginine fork is defined as an interaction between a arginine

and a pair of adjacent phosphates, which mediates specific recognition of RNA structure) [93,98-100]. For instance, several studies have shown that some amino acids, in particular arginine has strongly favored interaction with guanines bases along the bulge and through the continuous stem sequences of the RNA, involving H-bonding [92,93]. In general, these evidences showed that the specific interaction that lead to a biorecognition of different RNA molecules by the amino acids seem to be dependent on the base composition, RNA backbone and RNA conformational rearrangement. Globally, the development of this isolation methodology allowed recovery and efficiently separate of the target RNA while the quality control analysis showed a high efficiency, selectivity and integrity in RNA preparations as well as good purity in what concerns to host RNAs, proteins, genomic DNA and endotoxins (Table 3) [16,17,87-91]. Overall, in a single step, affinity purification can offer several advantages over other less-selective and time-consuming multi-step procedures (see Figure 2).

Although, amino acid ligands immobilized in conventional chromatographic columns of agarose showed high selectivity for RNA purification but a faster and more robust purification method will benefit ncRNAs isolation since it will possibly have important implications in RNA stability. In addition, available conventional columns (particle-based supports) present certain restrictions, namely limitations with the mass transfer, low capacity, gel compressibility and poor pore diffusion leading to high pressure drops and low flow rates application - all of which incur process time and cost [50]. These disadvantages have driven researchers to develop alternative chromatographic supports capable of maintaining the efficiency of the established processes while improving their limitations. One of these new generations is the monolithic supports whose application has been increasing owing to their structural properties [48,50,101,102].

Indeed, monolithic supports present several advantages, namely a huge quantity of accessible binding sites (high binding capacity), high external porosity, high sample distribution and excellent mass transfer properties [48,101]. Moreover, monoliths allow the application of higher flow rates, a very fast separation, short analysis times and purification with high reproducibility both at small and large scales, which reduces the biomolecules degradation due to the shorter contact time with the chromatographic support. Thus, due to their excellent morphological, physicochemical and mechanical properties, monolithic supports have attracted attention for the use in high-throughput separations, coupled to a variety of affinity ligands, both at research and industrial scales. In 2014, our research group showed the possibility of exploring and characterizing the interactions occurring between pre-miR-29b and an agmatine amino acid derivative immobilized into a monolithic disk [49]. As a matter of fact, for the first time, the selectivity, specificity and biorecognition of agmatine ligands was combined with the structural versatility and capacity provided by monolithic supports, as a promising strategy for miRNA purification [49]. Additionally, this monolithic-based strategy represents an advantageous alternative to conventional supports due to the fast separation and consequent short contact time with the chromatographic matrix, ensuring

structural stability of the target molecule (reduces RNA degradation). The successful results obtained in the isolation of several RNA species revealed an efficient affinity methodology to obtain RNA with high purity and good integrity, with potential applicability in several RNA based-procedures in basic and clinical research.

5. Conclusions and Future perspectives

In this review, it was emphasized the potential of affinity chromatography in the RNA purification. As discussed above, in the RNA affinity tags-based chromatography, different tags are introduced into RNA molecules and since they need to be removed before further RNA application, conformational changes can be induced in the target RNAs. In general, these methods are mostly time-consuming, expensive, tedious and the usage of synthetic RNAs also represents a limitation. Thus, there is still an urgent need for high-selectivity, -specificity, -capacity, -reliability and –throughput purification processes, to obtain high quantities of ncRNAs with the demand quality.

From our point of view, amino acid-based affinity chromatography emerges as a particularly promising approach for RNA purification, once it combines the selectivity of a naturally occurring biological interaction with the simplicity of RNA molecule. Thus, in order to achieve the maximum resolution and selectivity between the target RNAs and other host sRNA species, it should be used an affinity support that relies on the same biological interactions that are established within the cell, *i.e.*, by using immobilized amino acids, its derivates, peptides or complementary nucleotide sequences to the target RNAs, as specific ligands. The nucleotide bases complementarity can also be effectively used for ncRNAs trapping onto the column which facilitates their separation. Indeed, since synthetic oligonucleotides can be covalently bound to chromatographic matrices, ncRNAs can be easily captured when the appropriated oligonucleotides is attached to the matrix. Therefore, these new affinity protocols for miRNA isolation can offer advantages over other less-selective and time-consuming multistep procedures and can improve process economics. Moreover, some improvements over other chromatographic techniques are expected because RNA recovery can be achieved under mild elution conditions, rather than using organic or toxic compounds, and the use of enzymes is not necessary. In addition, exploiting the specific and natural affinity interactions between miRNA and the amino acids/peptides/sequences of nucleotides, it is not necessary to modify the recombinant ncRNA in order to bind it to the matrix. Indeed, it is expected that this strategy will allow the recovery of RNAs under their native state and with high integrity, efficiency and purity level. Furthermore, coupling an affinity based bioseparation methodology to its recombinant biosynthesis onto prokaryotic hosts represents an interesting integrated strategy that can be used for ncRNA biosynthesis and purification for further medical or biotechnological applications without the need of using *in vitro* transcribed RNAs. Actually, there are several tools available with some success for producing a large

variety of recombinant RNA using *Escherichia coli* as a host, including cloning vectors and fusion tags (RNA is masked within a stable RNA scaffold, such as tRNA fusions and 5S ribosomal RNA) [14,105]. In order to further develop a therapeutic product based on this approach, the ncRNAs must possess unquestionable biocompatibility features for the potential application in future studies in several RNA research fields, namely in RNA structural and functional studies as well as for application in medical therapies.

6. Acknowledgments

This work was supported by the Portuguese Foundation for Science and Technology (FCT), through the projects EXPL/BBB-BIO/1056/2012, Pest-OE/SAU/UI0709/2014 and FCOMP-01-0124-FEDER-041068 – EXPL/QEQ-MED/1068/2013. Patrícia Pereira acknowledges the fellowship (Ph.D. Grant, Ref SFRH/BD/81914/2011) from FCT. The authors also acknowledge the program Fundo Europeu de Desenvolvimento Regional (FEDER) [COMPETE [FCOMP-01-0124-FEDER-027560]].

7. References

[1] A. Fire, S. Xu, M.K. Montgomery, S.A. Kostas, S.E. Driver, C.C. Mello, Potent and specific genetic interference by double-stranded RNA in *Caenorhabditis elegans*, Nature. 391 (1998) 806-811.

[2] N. Lehman, RNA in evolution, Wiley Interdiscip Rev RNA. 1 (2010) 202-213.

[3] P.V. Ramachandran, S. Ignacimuthu, RNA interference - a silent but an efficient therapeutic tool, Appl Biochem Biotechnol. 169 (2013) 1774-1789.

[4] D.B. Dogini, V.D. Pascoal, S.H. Avansini, A.S. Vieira, T.C. Pereira, I. Lopes-Cendes, The new world of RNAs, Genet Mol Biol. 37 (2014) 285-293.

[5] A.Q. Gomes, S. Nolasco, H. Soares, Non-coding RNAs: multi-tasking molecules in the cell, Int J Mol Sci. 14 (2013) 16010-16039.

[6] X. Shi, M. Sun, H. Liu, Y. Yao, Y. Song, Long non-coding RNAs: a new frontier in the study of human diseases, Cancer Lett. 339 (2013) 159-166.

[7] L.W. Harries, Long non-coding RNAs and human disease, Biochem Soc Trans. 40 (2012) 902-906.

[8] B.A. Sullenger, E. Gilboa, Emerging clinical applications of RNA, Nature. 418 (2002) 252-258.

[9] S. Kreiter, M. Diken, A. Selmi, O. Tureci, U. Sahin, Tumor vaccination using messenger RNA: prospects of a future therapy, Curr Opin Immunol. 23 (2011) 399-406.

[10] S. Pascolo, Vaccination with messenger RNA, Methods Mol Med. 127 (2006) 23-40.

[11] L.G. Scott, M. Hennig, RNA structure determination by NMR, Methods Mol Biol. 452 (2008) 29-61.

[12] J.A. Doudna, Preparation of homogeneous ribozyme RNA for crystallization, Methods Mol Biol. 74 (1997) 365-370.

[13] A. Wittmann, B. Suess, Engineered riboswitches: Expanding researchers' toolbox with synthetic RNA regulators, FEBS Lett. 586 (2012) 2076-2083.

[14] L. Ponchon, F. Dardel, Large scale expression and purification of recombinant RNA in *Escherichia coli*, Methods. 54 (2011) 267-273.

[15] L.D. Sherlin, T.L. Bullock, T.A. Nissan, J.J. Perona, F.J. Lariviere, O.C. Uhlenbeck, S.A. Scaringe, Chemical and enzymatic synthesis of tRNAs for high-throughput crystallization, RNA. 7 (2001) 1671-1678.

[16] P. Pereira, A. Sousa, J. Queiroz, I. Correia, A. Figueiras, F. Sousa, Purification of pre-miR-29 by arginine-affinity chromatography, J Chromatogr B Analyt Technol Biomed Life Sci. 951-952 (2014) 16-23.

[17] R. Martins, J.A. Queiroz, F. Sousa, A new affinity approach to isolate *Escherichia coli* 6S RNA with histidine-chromatography, J Mol Recognit. 23 (2010) 519-524.

[18] L. Huang, J. Lieberman, Production of highly potent recombinant siRNAs in *Escherichia coli*, Nat Protoc. 8 (2013) 2325-2336.

[19] M.M. Li, W.P. Wang, W.J. Wu, M. Huang, A.M. Yu, Rapid production of novel pre-microRNA agent hsa-mir-27b in *Escherichia coli* using recombinant RNA technology for functional studies in mammalian cells, Drug Metab Dispos. 42 (2014) 1791-1795.

[20] N. Nagao, H. Suzuki, R. Numano, S. Umekage, Y. Kikuchi, Short hairpin RNAs of designed sequences can be extracellularly produced by the marine bacterium *Rhodovulum sulfidophilum*, J Gen Appl Microbiol. 60 (2014) 222-226.

[21] S. Dunin-Horkawicz, A. Czerwoniec, M.J. Gajda, M. Feder, H. Grosjean, J.M. Bujnicki, MODOMICS: a database of RNA modification pathways, Nucleic Acids Res. 34 (2006) D145-149.

[22] R. Martins, J.A. Queiroz, F. Sousa, Ribonucleic acid purification, J Chromatogr A. 1355 (2014) 1-14.

[23] L.E. Easton, Y. Shibata, P.J. Lukavsky, Rapid, nondenaturing RNA purification using weak anion-exchange fast performance liquid chromatography, RNA. 16 (2010) 647-653.

[24] S.M. McCarthy, M. Gilar, J. Gebler, Reversed-phase ion-pair liquid chromatography analysis and purification of small interfering RNA, Anal Biochem. 390 (2009) 181-188.

[25] B. Noll, S. Seiffert, F. Hertel, H. Debelak, P. Hadwiger, H.P. Vornlocher, I. Roehl, Purification of small interfering RNA using nondenaturing anion-exchange chromatography, Nucleic Acid Ther. 21 (2011) 383-393.

[26] J. Koubek, K.F. Lin, Y.R. Chen, R.P. Cheng, J.J. Huang, Strong anion-exchange fast performance liquid chromatography as a versatile tool for preparation and purification of RNA produced by *in vitro* transcription, RNA. 19 (2013) 1449-1459.

[27] F.S. Hagen, E.T. Young, Preparative polyacrylamide gel electrophoresis of ribonucleic acid. Identification of multiple molecular species of bacteriophage T7 lysozyme messenger ribonucleic acid, Biochemistry. 13 (1974) 3394-3400.

[28] I. Kim, S.A. McKenna, E. Viani Puglisi, J.D. Puglisi, Rapid purification of RNAs using fast performance liquid chromatography (FPLC), RNA. 13 (2007) 289-294.

[29] A. Gallas, C. Alexander, M.C. Davies, S. Puri, S. Allen, Chemistry and formulations for siRNA therapeutics, Chem Soc Rev. 42 (2013) 7983-7997.

[30] V.N. Kim, Small RNAs: classification, biogenesis, and function, Mol Cells. 19 (2005) 1-15.

[31] K. Gavrilov, W.M. Saltzman, Therapeutic siRNA: principles, challenges, and strategies, Yale J Biol Med. 85 (2012) 187-200.

[32] Y. Huang, J.L. Zhang, X.L. Yu, T.S. Xu, Z.B. Wang, X.C. Cheng, Molecular functions of small regulatory noncoding RNA, Biochemistry (Mosc). 78 (2013) 221-230.

[33] D. Guzman-Villanueva, I.M. El-Sherbiny, D. Herrera-Ruiz, A.V. Vlassov, H.D. Smyth, Formulation approaches to short interfering RNA and MicroRNA: challenges and implications, J Pharm Sci. 101 (2012) 4046-4066.

[34] A. Qurashi, P. Jin, Small RNA-mediated gene regulation in neurodevelopmental disorders, Curr Psychiatry Rep. 12 (2010) 154-161.

[35] T.W. Nilsen, Mechanisms of microRNA-mediated gene regulation in animal cells, Trends Genet. 23 (2007) 243-249.

[36] Y. Zhang, Z. Wang, R.A. Gemeinhart, Progress in microRNA delivery, J Control Release. 172 (2013) 962-974.

[37] J.A. Broderick, P.D. Zamore, MicroRNA therapeutics, Gene Ther. 18 (2011) 1104-1110.

[38] J. Zhu, H. Fu, Y. Wu, X. Zheng, Function of lncRNAs and approaches to lncRNA-protein interactions, Sci China Life Sci. 56 (2013) 876-885.

[39] S. Memczak, M. Jens, A. Elefsinioti, F. Torti, J. Krueger, A. Rybak, L. Maier, *et al.*, Circular RNAs are a large class of animal RNAs with regulatory potency, Nature. 495 (2013) 333-338.

[40] J.C. Burnett, J.J. Rossi, RNA-based therapeutics: current progress and future prospects, Chem Biol. 19 (2012) 60-71.

[41] F. RE, RNA methodologies - Laboratory Guide for Isolation and Characterization, Academic Press, York, USA, 2005.

[42] M. Uhlen, Affinity as a tool in life science, Biotechniques. 44 (2008) 649-654.

[43] A.C. Roque, C.R. Lowe, Affinity chromatography: history, perspectives, limitations and prospects, Methods Mol Biol. 421 (2008) 1-21.

[44] N.E. Labrou, Design and selection of ligands for affinity chromatography, J Chromatogr B Analyt Technol Biomed Life Sci. 790 (2003) 67-78.

[45] F. Sousa, D.M. Prazeres, J.A. Queiroz, Affinity chromatography approaches to overcome the challenges of purifying plasmid DNA, Trends Biotechnol. 26 (2008) 518-525.

[46] C.R. Lowe, A.R. Lowe, G. Gupta, New developments in affinity chromatography with potential application in the production of biopharmaceuticals, J Biochem Biophys Methods. 49 (2001) 561-574.

[47] M. Yarus, J.J. Widmann, R. Knight, RNA-amino acid binding: a stereochemical era for the genetic code, J Mol Evol. 69 (2009) 406-429.

[48] R. Mallik, D.S. Hage, Affinity monolith chromatography, J Sep Sci. 29 (2006) 1686-1704.

[49] P. Pereira, A. Sousa, J.A. Queiroz, A. Figueiras, F. Sousa, Pharmaceutical-grade pre-miR-29 purification using an agmatine monolithic support, J Chromatogr A. 1368 (2014) 173-182.

[50] A. Sousa, F. Sousa, J.A. Queiroz, Advances in chromatographic supports for pharmaceutical-grade plasmid DNA purification, J Sep Sci. 35 (2012) 3046-3058.

[51] B.V. Ayyar, S. Arora, C. Murphy, R. O'Kennedy, Affinity chromatography as a tool for antibody purification, Methods. 56 (2012) 116-129.

[52] P.B. Moore, Structural motifs in RNA, Annu Rev Biochem. 68 (1999) 287-300.

[53] H.L. Weith, J.L. Wiebers, P.T. Gilham, Synthesis of cellulose derivatives containing the dihydroxyboryl group and a study of their capacity to form specific complexes with sugars and nucleic acid components, Biochemistry. 9 (1970) 4396–401.

[54] N. Singh, R.C. Willson, Boronate affinity adsorption of RNA: possible role of conformational changes, J Chromatogr A. 840 (1999) 205–213.

[55] H. Schott, E. Rudloff, P. Schmidt, R. Roychoudhury, H. Koessel, A dihydroxyborylsubstituted methacrylic polymer for the column chromatographic separation of mononucleotides, oligonucleotides, and transfer ribonucleic acid, Biochemistry. 12 (1973) 932-8.

[56] S. Ackerman, B. Cool, J. Furth, Removal of DNA from RNA by chromatography on acetylated N-[N'-(m-dihydroxylborylphenyl)succinamyl]aminoethyl cellulose, Anal Biochem. 100 (1979) 174-8.

[57] M. Rosenberg, P.T. Gilham, The isolation of 3'-terminal polynucleotides from RNA molecules, Biochim Biophys Acta. 246 (1971) 337-40.

[58] X. Liu, W.H. Scouten, Part 1: Boronic Acids as Selective Ligands for Affinity Chromatography, Miscellaneous Methods in Affinity Chromatography. Florida: Taylor and Francis Group (2002).

[59] A. Yurkevich, I. Kolodkina, E. Ivanova, E. Pichuzhkina, Study of the interaction of polyols with polymers containing N-substituted [(4-boronophenyl)methylammonio] groups, Carbohydr Res. 43 (1975) 215–24.

[60] B. Elmas, M.A. Onur, S. Senel, A. Tuncel, Thermosensitive N-isopropylacrylamidevinylphenylboronic acid copolymer latex particles for nucleotide isolation, Colloids Surf A Physicochem Eng Asp. 232 (2004) 253–9.

[61] H. Clcek, Nucleotide isolation by boronic acid functionalized hydrogel beads, J Bioact Compat Polym. 20 (2005) 245–57.

[62] N. Tanaka, H. Kobayashi, H. Ishizuka, H. Minakuchi, K. Nakanishi, K. Hosoya, T. Ikegami, Monolithic silica columns for high efficiency chromatographic separations, J Chromatogr A. 965 (2002) 35–49.

[63] A. Srivastava, A.K. Shakya, A. Kumar, Boronate affinity chromatography of cells and biomacromolecules using cryogel matrices, Enzyme Microb Technol. 51 (2012) 373– 381.

[64] C. Srisawat, D.R. Engelke, RNA affinity tags for purification of RNAs and ribonucleoprotein complexes, Methods. 26 (2002) 156-161.

[65] C. Pestourie, B. Tavitian, F. Duconge, Aptamers against extracellular targets for *in vivo* applications, Biochimie. 87 (2005) 921-930.

[66] J. Porath, Immobilized metal ion affinity chromatography, Protein Expr Purif. 3 (1992) 263–281.

[67] G.I. Evan, G.K. Lewis, G. Ramsay, J.M. Bishop, Isolation of monoclonal antibodies specific for human cmyc proto-oncogene product, Mol Cell Biol. 5 (1985) 3610–3616.

[68] G. Rigaut, A. Shevchenko, B. Rutz, M. Wilm, M. Mann, B. Séraphin, A generic protein purification method for protein complex characterization and proteome exploration, Nat Biotechnol. 17 (1999) 1030–1032.

[69] M. Uhlen, B. Nilsson, B.M. Guss, M. Lindberg, S. Gatenbeck, L. Philipson, Gene fusion vectors based on the gene for staphylococcal protein A, Gene. 23 (1983) 369–378.

[70] J.H. Yoon, S. Srikantan, M. Gorospe, MS2-TRAP (MS2-tagged RNA affinity purification): tagging RNA to identify associated miRNAs, Methods. 58 (2012) 81-87.

[71] P.C. Simons, D.L. Vander Jagt, Purification of glutathione S-transferases by glutathione-affinity chromatography, Methods Enzymol. 77 (1981) 235–237.

[72] T.G. Schmidt, J. Koepke, R. Frank, A. Skerra, Molecular interaction between the Strep-tag affinity peptide and its cognate target, streptavidin, J Mol Biol. 255 (1996) 753–766.

[73] K. Leppek, G. Stoecklin, An optimized streptavidin-binding RNA aptamer for purification of ribonucleoprotein complexes identifies novel ARE-binding proteins, Nucleic Acids Res. 42 (2014) e13.

[74] K.S. Prickett, D.C. Amberg, T.P. Hopp, A calcium-dependent antibody for identification and purification of recombinant proteins, Biotechniques. 7 (1989) 580–589.

[75] C. Srisawat, D.R. Engelke, Streptavidin aptamers: affinity tags for the study of RNAs and ribonucleoproteins, RNA. 7 (2001) 632-641.

[76] C. Srisawat, I.J. Goldstein, D.R. Engelke, Sephadex-binding RNA ligands: rapid affinity purification of RNA from complex RNA mixtures, Nucleic Acids Res. 29 (2001) E4.

[77] K. Wei, F. Yan, H. Xiao, X. Yang, G. Xie, Y. Xiao, T. Wang, *et al.*, Affinity purification of binding miRNAs for messenger RNA fused with a common tag, Int J Mol Sci. 15 (2014) 14753-14765.

[78] U.A. Orom, A.H. Lund, Isolation of microRNA targets using biotinylated synthetic microRNAs, Methods. 43 (2007) 162-165.

[79] C. Gong, M.W. Popp, L.E. Maquat, Biochemical analysis of long non-coding RNA-containing ribonucleoprotein complexes, Methods. 58 (2012) 88-93.

[80] C.F. Flores-Jasso, W.E. Salomon, P.D. Zamore, Rapid and specific purification of Argonaute-small RNA complexes from crude cell lysates, RNA. 19 (2013) 271-279.

[81] R.T. Batey, J.S. Kieft, Improved native affinity purification of RNA, RNA. 13 (2007) 1384-1389.

[82] G. Di Tomasso, P. Lampron, P. Dagenais, J.G. Omichinski, P. Legault, The ARiBo tag: a reliable tool for affinity purification of RNAs under native conditions, Nucleic Acids Res. 39 (2011) e18.

[83] G. Di Tomasso, P. Dagenais, A. Desjardins, A. Rompre-Brodeur, V. Delfosse, P. Legault, Affinity purification of RNA using an ARiBo tag, Methods Mol Biol. 941 (2012) 137-155.

[84] G. Di Tomasso, A. Salvail-Lacoste, J. Bouvette, J.G. Omichinski, P. Legault, Affinity purification of *in vitro* transcribed RNA with homogeneous ends using a 3'-ARiBo tag, Methods Enzymol. 549 (2014) 49-84.

[85] A. Salvail-Lacoste, G. Di Tomasso, B.L. Piette, P. Legault, Affinity purification of T7 RNA transcripts with homogeneous ends using ARiBo and CRISPR tags, RNA. 19 (2013) 1003-1014.

[86] S.C. Walker, F.H. Scott, C. Srisawat, D.R. Engelke, RNA affinity tags for the rapid purification and investigation of RNAs and RNA-protein complexes, Methods Mol Biol. 488 (2008) 23-40.

[87] A. Afonso, P. Pereira, J.A. Queiroz, A. Sousa, F. Sousa, Purification of pre-miR-29 by a new O-*phospho*-l-tyrosine affinity chromatographic strategy optimized using design of experiments, J Chromatogr A. 1343 (2014) 119-127.

[88] P. Pereira, A. Sousa, J. Queiroz, A. Figueiras, F. Sousa, New approach for purification of pre-miR-29 using lysine-affinity chromatography, J Chromatogr A. 1331 (2014) 129-132.

[89] R. Martins, C.J. Maia, J.A. Queiroz, F. Sousa, A new strategy for RNA isolation from eukaryotic cells using arginine affinity chromatography, J Sep Sci. 35 (2012) 3217-3226.

[90] R. Martins, J.A. Queiroz, F. Sousa, Histidine affinity chromatography-based methodology for the simultaneous isolation of *Escherichia coli* small and ribosomal RNA, Biomed Chromatogr. 26(7) 2011 781-8.

[91] D.S. Jones, H.K. Lundgren, F.T. Jay, The separation of ribonucleic acids from *Escherichia coli* on lysin-agarose, Nucleic Acids Res. 3 (1976) 1569-1576.

[92] F. Sousa, C. Cruz, J.A. Queiroz, Amino acids-nucleotides biomolecular recognition: from biological occurrence to affinity chromatography, J Mol Recognit. 23 (2010) 505-518.

[93] B.J. Calnan, B. Tidor, S. Biancalana, D. Hudson, A.D. Frankel, Arginine-mediated RNA recognition: the arginine fork, Science. 252 (1991) 1167-1171.

[94] P. Pereira, C. Cruz, J.A. Queiroz, A. Figueiras, F. Sousa, Analysis of pre-miR-29b binding conditions to amino acids by using a surface plasmon resonance biosensor, Anal Methods. 8 (2016) 205.

[95] J.J. Ellis, M. Broom, S. Jones, Protein-RNA interactions: structural analysis and functional classes, Proteins. 66 (2007) 903-911.

[96] M. Treger, E. Westhof, Statistical analysis of atomic contacts at RNA-protein interfaces, J Mol Recognit. 14 (2001) 199-214.

[97] M.M. Hoffman, M.A. Khrapov, J.C. Cox, J. Yao, L. Tong, A.D. Ellington, AANT: the Amino Acid-Nucleotide Interaction Database, Nucleic Acids Res. 32 (2004) D174-181.

[98] N.M. Luscombe, R.A. Laskowski, J.M. Thornton, Amino acid-base interactions: a three-dimensional analysis of protein-DNA interactions at an atomic level, Nucleic Acids Res. 29 (2001) 2860-2874.

[99] J.D. Puglisi, J.R. Wyatt, I. Tinoco, Jr., Solution conformation of an RNA hairpin loop, Biochemistry. 29 (1990) 4215-4226.

[100] T. Janas, J.J. Widmann, R. Knight, M. Yarus, Simple, recurring RNA binding sites for L-arginine, RNA. 16 (2010) 805-816.

[101] E.L. Pfaunmiller, M.L. Paulemond, C.M. Dupper, D.S. Hage, Affinity monolith chromatography: a review of principles and recent analytical applications, Anal Bioanal Chem. 405 (2013) 2133-2145.

[102] R.D. Arrua, C.I. Alvarez Igarzabal, Macroporous monolithic supports for affinity chromatography, J Sep Sci. 34 (2011) 1974-1987.

[103] L. Ponchon, M. Catala, B. Seijo, M. El Khouri, F. Dardel, S. Nonin-Lecomte, C. Tisne, Co-expression of RNA-protein complexes in *Escherichia coli* and applications to RNA biology, Nucleic Acids Res. 41 (2013) e150.

[104] L. Ponchon, F. Dardel, Recombinant RNA technology: the tRNA scaffold, Nat Methods. 4 (2007) 571-6.

[105] J. Jin, M. Cid, C.B. Poole, L.A. McReynolds, Protein mediated miRNA detection and siRNA enrichment using p19, Biotechniques. 48 (2010) xvii-xxiii.

Chapter 2

Aims of the thesis

Up until now, microRNAs-based gene therapy applications are mainly performed through enzymatically and chemically synthesized microRNAs. However, the presence of contaminants in these synthesized formulations can lead to non-targeted gene silencing, frequently associated with a decrease in therapeutic effectiveness and can still restrict the implementation of these oligoribonucleotides onto pre-clinical and clinical applications. In addition, these current techniques present various limitations in the preparation, isolation and purification of microRNAs, namely by the use of chemical solvents and denaturing conditions.

Thus, the global aim of this work is the development and establishment of an innovative biotechnological platform for the biosynthesis, recovery and purification of the recombinant human pre-miR-29b, to be delivered to neuronal cells using suitable non-viral delivery systems, in order to assure a more effective biological effect in the selective silencing of endogenous pathways involved in the insurgence and progression of the Alzheimer's disease. In particular, this work intends to explore pre-miR-29b as a novel biopharmaceutical to decrease the APP, BACE1 and Aβ expression levels, which could represent a significant advance in terms of treatment of AD. With this work, it is believed that the integrative approach of extracellular production, using *Rhodovulum sulfidophilum* host, and affinity-based purification will enable the preparation of the target pre-miRNA with high efficiency, selectivity, throughput, purity, integrity and biological activity, to be applied in RNA research or RNA therapeutic areas. The high gain in this field is the possibility to use these methodologies for the preparation of other ncRNAs, proving the wideness application of the technology, which may have a great impact on industry, improving workload, process time and economics.

To accomplish the main scope of this thesis, the experimental work will be developed concerning the following tasks:

1. Cloning the human pre-miR-29b sequence in a prokaryotic expression vector, pBHSR1-RM and transformation of the *Rhodovulum sulfidophilum* DSM 1374 host. Development and establishment of the innovative biosynthesis strategy of extracellular pre-miR-29b, testing different growth conditions. Characterization of the intra and extracellular pre-miR-29b production.

2. Characterization of the specificity of the interactions occurring between the amino acids-affinity ligands and microRNA molecules, as well as determination of the influence of several chromatographic conditions in the structure and stability of RNA.

3. Study of the ability of amino acids-based affinity supports, such as lysine-agarose, arginine-agarose and agmatine monolith, in the specific recognition of the intracellular pre-miR-29b. The adequate binding/elution conditions will result from the manipulation of temperature, flow rate and buffer composition (pH, ionic strength, type of salt and presence of competitive agents). These studies will allow the implementation of new methodologies for miRNA purification.

4. Development and characterization of non-viral delivery systems composed by biodegradable polymers, for human pre-miR-29b protection and stabilization, allowing their sustained delivery to the cells. It will be also performed the functionalization of these delivery systems with specific ligands, to be recognized by cell surface receptors of Blood-Brain Barrier, and mediate the delivery of pre-miR-29b to the target cells.

5. Evaluation of the biological activity and efficiency of the pure recombinant pre-miR-29b to regulate the expression of the AD related-genes, namely by inducing the BACE1 knockdown, using *in vitro* neuronal cells lines. These results will be compared with those obtained with the commercially available miR-29b.

Chapter 3

Paper III

Advances in time-course extracellular production of human pre-miR-29b from *Rhodovulum sulfidophilum*

P. Pereira, A. Q. Pedro, J. Tomás, C. J. Maia, J. A. Queiroz, A. Figueiras, F. Sousa

(*Submitted for publication*)

Short description: This paper introduces a novel prokaryotic system for biosynthesis and recovery of recombinant human pre-miR-29b. First, in order to transfer the pre-miR-29b encoding plasmid to *Rhodovulum sulfidophilum* host, the transformation conditions were established. The expression of the human pre-miR-29b was carried out at small-scale in shake-flasks by *Rhodovulum sulfidophilum* cultures. Then, in order to attain high quantities of pre-miR-29b, several fermentation variables (culture media, sodium chloride concentration, aerobic conditions and temperature) were optimized, allowing the establishment of improved growth conditions. Finally, the expression of both intracellular and extracellular recombinant pre-miR-29b was monitored during different fermentation periods, as well as genomic DNA and proteins, major host contaminants that influence the purity of the target biomolecule.

Advances in time-course extracellular production of human pre-miR-29b from *Rhodovulum sulfidophilum*

P. Pereira[1], A. Q. Pedro[1], J. Tomás[1], C. J. Maia[1], J. A. Queiroz[1], A. Figueiras[1,2], F. Sousa[1]*

[1] *CICS-UBI – Health Sciences Research Centre, University of Beira Interior, Avenida Infante D. Henrique, 6200-506 Covilhã, Portugal;*

[2] *CNC - Center of Neuroscience and Cell Biology, University of Coimbra, Largo Marquês de Pombal, 3004-517 Coimbra, Portugal*

*Corresponding author:
Dr. Fani Sousa
Phone: +351 275 329 074
Fax: +351 275 329 099
E-mail address: fani.sousa@fcsaude.ubi.pt
Postal address: Health Sciences Research Centre, Universidade da Beira Interior, Avenida Infante D. Henrique, 6200-506 Covilhã, Portugal

Abstract

The present study reports the successful production of human pre-miR-29b both intra and extracellularly in the marine phototrophic bacterium *Rhodovulum sulfidophilum* using recombinant RNA technology. In a first stage, the optimal transformation conditions (0.1 μg of plasmid DNA, with a heat-shock of 2 min at 35ºC) were established, in order to transfer the pre-miR-29b encoding plasmid to *Rhodovulum sulfidophilum* host. Furthermore, the extracellular recovery of this RNA product from the culture medium was greatly improved, achieving quantities that are compatible with the majority of applications, namely for *in vitro* or *in vivo* studies. Using this system, the extracellular human pre-miR-29b concentration was approximately 182 μg/L, after 40 h of bacterial growth, and the total intracellular pre-miR-29b was of about 358 μg/L, at 32 h. At the end of the fermentation it was verified that almost 87% of cells were viable, indicating that cell lysis is minimized and that the extracellular medium is not highly contaminated with the host intracellular RNases and endotoxins, which is a critical parameter to guarantee the miRNA integrity. These findings demonstrate that pre-miRNAs can be produced by recombinant RNA technology, offering novel clues for the production of natural pre-miRNA agents for functional studies and RNAi-based therapeutics.

Keywords

Extracellular production; Recombinant human pre-miR-29b; *Rhodovulum sulfidophilum*; RNAi technology; Transformation efficiency

Introduction

In the last couple of decades, RNA interference (RNAi)-based technology has become a novel tool for regulating gene expression in eukaryotic cells, since many small RNAs (sRNAs) act as regulators of messenger RNA (mRNA) expression and have shown great potential for therapeutic knockdown of disease-causing genes (Fire *et al*. 1998; Ramachandran and Ignacimuthu 2013). This discovery led to the expectation that RNA molecules, such as ribozymes, small interfering RNAs (siRNAs), short hairpin RNAs (shRNAs), microRNAs (miRNAs) and long non-coding RNAs (lncRNAs) will be major classes of new therapeutic molecules in the near future (Dogini *et al*. 2014; Gomes *et al*. 2013). Amongst RNAi-based therapeutics, miRNAs have recently gained much attention, being investigated as potential drug candidates for application in several disease scenarios that currently remain very challenging and difficult to overcome (Sullenger and Gilboa 2002). In particular, their therapeutic potential can be exploited in gene expression regulation at post-transcriptional level, through degradation/de-adenylation of selected target mRNAs, translational repression or both mechanisms (Nilsen 2007). Briefly, miRNAs mediate post-transcriptional regulation through a sequential process involving a miRNA precursor (pre-miRNA) and, subsequently, a mature miRNA that is incorporated into RNA-induced silencing complex (RISC) to regulate the mRNA translation. Due to the rapidly growing demand for these biopharmaceuticals, various strategies are currently being pursued to improve production in order to achieve higher product titers while maintaining maximal product quality (Ponchon and Dardel 2007; Ponchon and Dardel 2011). Furthermore, economically efficient methods for large-scale production are also required.

Currently, miRNAs-mediated gene silencing is mainly performed through chemically synthesized RNAs, by phosphoamidite chemistry, normally used for the generation of short oligoribonucleotides (Ling *et al*. 2013). In addition to chemical synthesis, RNAs can also be obtained by enzymatic synthesis, for example longer RNAs can be produced by *in vitro* transcription using T7 RNA polymerase (Beckert and Masquida 2011; Milligan *et al*. 1987). Although these methods can be very efficient in producing miRNA, in general, several purification protocols to remove the contaminants (impurities of plasmid DNA template, enzymes, nucleotides, chemicals, salts or buffers, which are indispensable for *in vitro* transcription or chemical synthesis of RNAs) have to be employed (Martins *et al*. 2014; Milligan *et al*. 1987). The presence of these impurities can lead to non-targeted gene silencing, what is commonly associated with a decrease in therapeutic effectiveness and still restrict the implementation of these RNAs onto pre-clinical or clinical trials. On the other hand, the purification methods usually employed can cause degradation of RNA molecules due to the requirement of toxic solvents and the use of denaturing conditions (Martins *et al*. 2014). MiRNA-based therapeutic applications can also be performed via the endogenous expression of miRNAs encoded by viral vectors or plasmids in eukaryotic cells. However, this

alternative approach is generally less efficient because it is necessary to transcribe the DNA to miRNA precursors (Chen *et al*. 2007; Huang *et al*. 2011; Li *et al*. 2014; Ponchon and Dardel 2007; Ponchon and Dardel 2011). Considering the potential therapeutic applications and the mandatory global distribution of these novel therapeutics, it is crucial to develop efficient methods for their preparation. One of the most promising strategies might be the use of recombinant microorganisms to produce the target biomolecules. This approach can reduce the costs and remains highly efficient.

At present, few strategies have emerged to produce stable RNAs, namely a circular RNA aptamer (Umekage and Kikuchi 2009), a "tRNA scaffold" (Ponchon and Dardel 2007) and hsa-mir-27b, using recombinant bacteria, mainly *Escherichia coli (E. coli)* as preferential host (Li *et al*. 2014). Occasionally, modifications of RNA products are required to efficiently obtain the product, such as the addition of flanking sequences in the case of tRNA scaffold, which are then removed by ribonuclease (RNase) H treatment, making the process unsuitable for industrial RNA drug production (Ponchon and Dardel 2007). Moreover, in what concerns to the use of *E. coli* for RNA production, it demands the completion of cell lysis and extraction of nucleic acids, which can be laborious and time-consuming due to the number and complexity of the processing steps (Wassarman *et al*. 1999). Along with the aforementioned disadvantages, another major issue associated with the cell lysis is the release of endotoxins, which can lead to the contamination of the target RNA sample, and, in a last analysis, produce symptoms of toxic shock syndrome if present in sufficient quantities *in vivo* (Wei *et al*. 2007). In addition, as *E. coli* expresses several endonucleases, it can be difficult to maintain the integrity of the target RNA, being always necessary to establish methods to avoid its degradation.

Very recently, the marine phototrophic bacterium *Rhodovulum sulfidophilum (R. sulfidophilum)* was also described as an attractive host for the recombinant production of an artificial RNA model (streptavidin RNA aptamer) (Suzuki *et al*. 2010; Suzuki *et al*. 2011) and shRNAs (Nagao *et al*. 2014). In particular, this bacterium is non-pathogenic and presents several advantages over *E. coli,* such as the capacity of secretion of nucleic acids directly to the culture medium and the absence of detectable host RNases in the extracellular medium (Suzuki *et al*. 2009a; Ando *et al*. 2004; Ando *et al*. 2006). The endogenous RNAs released by *R. sulfidophilum* to the extracellular medium are mainly nonaminoacylated fully mature transfer RNAs (tRNAs) and fragments of 16S and 23S ribosomal RNAs (rRNAs) (Ando *et al*. 2006; Suzuki *et al*. 2009b). In fact, previous works described that both recombinant RNAs (streptavidin RNA aptamer and shRNAs) produced in *R. sulfidophilum* were found not only inside the cells but also in the culture medium (Nagao *et al*. 2014; Suzuki *et al*. 2010; Suzuki *et al*. 2011).

In the present study, for the first time, an alternative strategy for the recombinant biosynthesis and extracellular recovery of biologically active human pre-miR-29b (hsa-pre-

mir-29b) is proposed. The pre-miR-29 target was chosen because it belongs to one of the most interesting miRNA families in humans to date, once this miRNA is involved in several regulatory pathways associated with neurodegenerative diseases and also presenting tumor-suppressing and immune-modulating properties (Alvarez-Garcia and Miska 2005; Du and Pertsemlidis 2011; Hebert *et al*. 2008; Nelson *et al*. 2008). It is expected that this strategy can be highly advantageous regarding the RNA product safety, since it will not stimulate innate immunity, as the secreted miRNAs will be devoid of main bacterial associated impurities. Moreover, after the application of an appropriated purification flowsheet (Fig. 1), the isolation and purification of the target pre-miRNA will be easier and successful. The recovery of miRNAs from the fermentation broth will be performed using membrane filtration or concentration techniques. In fact, the application of this approach can be a promising technology since it suppresses the use of salts and solvents typically used in conventional RNA isolation processes. Overall, an economical and fast method for the production of functional RNA molecules with clinical-grade quality and biological activity is described, which can be applied in basic studies or in therapeutic strategies based on RNAi technology. From this stand point, it seems clear that the establishment of a robust and reliable miRNA extracellular production technology can indeed unlock the possibility of further developing effective therapeutic strategies that rely on the intrinsic gene silencing capacity of these oligonucleotides, presenting major advantages over the currently existing practices.

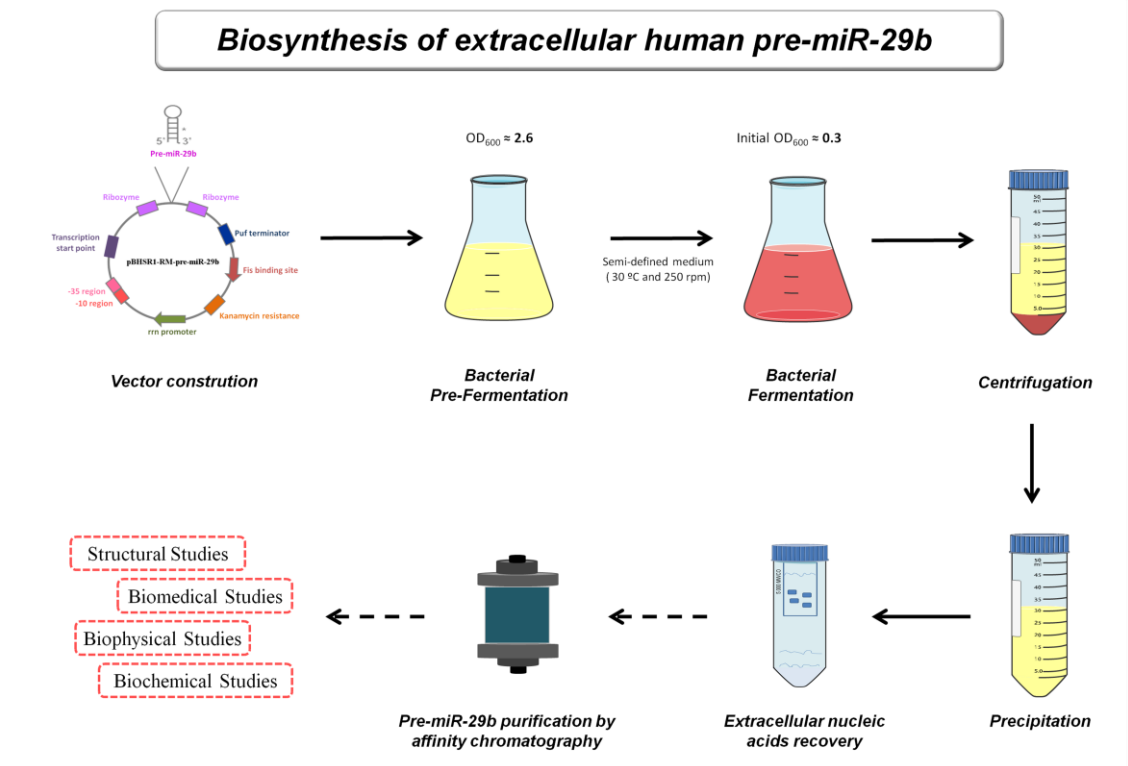

Figure 1 - Schematics of the integrative platform that allows the biosynthesis and extracellular recovery of the recombinant hsa-pre-miR-29b.

Materials and Methods

Materials and Chemicals

Restriction enzymes including *Eco*RI, *Eco*T22I, *Aat*I and *Stu*I were purchased from Thermo Fisher Scientific Inc. (Waltham, MA) and *Xba*I was purchased from New England BioLabs (Ipswich, MA). T4 DNA ligase and pGEM-T easy vector were used as recommended by the manufactures (Promega). DreamTaq DNA polymerase was purchased from Fermentas (Beijing, China). Hyper Ladder I (Bioline, London, UK) was used as DNA molecular weight marker. Primers were synthesized by StabVida (Caparica, Lisbon). The sequence of pre-miRNA was obtained from the miRBase (http://www.mirbase.org/index.shtml).

Bacterial strains and growth conditions

The *R. sulfidophilum* DSM 1374 strain (BCCM/LMG, Belgium) modified with plasmid pBHSR1-RM containing the sequence of human pre-miR-29b was used in this study for pre-miR-29b production. One Shot® TOP10 Chemically Competent *E. coli* (Invitrogen) was used for the propagation of the recombinant plasmid DNA (pDNA). The pGEM-T easy vector was applied for DNA manipulations and the plasmid pBHSR1-RM (a generous gift from Dr. Yo Kikuchi) was used as the expression vector (Nagao *et al*. 2014; Suzuki *et al*. 2011). *E. coli* TOP10 was grown in Luria-Bertani (LB) medium (10.0 g/L tryptone, 5.0 g/L yeast extract and 5.0 g/L sodium chloride (NaCl)) and LB-Agar. In the preliminary results, *R. sulfidophilum* was tested in Nutrient Agar (g per liter of deionized water: beef extract, 1.5; yeast extract, 1.5; peptidic digest of animal tissue, 5.0; NaCl, 5.0 and agar, 15.0), Tryptone Soya Agar (g per liter of deionized water: casein peptone (pancreatic), 15.0; soya peptone, 5.0; NaCl, 5.0 and agar, 15.0) and Mueller Hinton Agar (g per liter of deionized water: beef, dehydrated infusion from, 30.0; casein hydrolysate, 17.5; starch, 1.5 and agar 17.0). *R. sulfidophilum* cells were cultivated in a semi-defined medium, developed in this work, containing (per L of water) tryptone, 10.0 g; polypeptone, 5.0 g; yeast extract, 0.5 g; NaCl, 30.0 g; K_2HPO_4, 4.0 g; KH_2PO_4, 1.0 g; glucose, 50.0 g; $MgSO_4.7H_2O$, 0.2 g; $CaCl_2.2H_2O$, 0.05 g; $(NH_4)_2SO_4$, 1.0 g and 1 mL of trace elements solution (TES). The TES composition was as follows: (5.56 g/L $FeSO_4.7H_2O$, 3.96 g/L $MnCl_2.4H_2O$, 5.62 g/L $CoSO_4.7H_2O$, 0.34 g/L $CuCl_2.2H_2O$, 0.58 g/L $ZnSO_4.7H_2O$, 0.6 g/L H_3BO_3, 0.04 g/L $NiCl_2.6H_2O$ and 0.06 g/L $Na_2MoO_4.2H_2O$ in 0.5 N HCl) (Kim et al. 2000; Silva et al. 2009). For solid media, the MT medium was used (10.0 g/L glucose, 10.0 g/L peptone, 5.0 g/L yeast extract, 20.0 g/L NaCl, 10.0 mg/L $FeSO_4.7H_2O$, 10.0 mg/L $MnSO_4.4H_2O$, 1.0 mg/L $ZnSO_4.7H_2O$, 4.1 g/L $MgCl_2$ and 15.0 g/L agar) (Pedro *et al*. 2011). The medium pH was adjusted to 7.0, with 0.1 M NaOH before autoclaving. When appropriated, media were supplemented with the following antibiotics: for *E. coli*, ampicillin and kanamycin were used with final concentrations of 100 and 20 µg/mL, respectively, while for *R. sulfidophilum*, kanamycin was used at a concentration of 30 µg/mL. Unless otherwise stated, *E. coli* cells were grown at 37ºC and *R. sulfidophilum* growth was carried out at 30ºC under dark-aerobic conditions. Cell growth was monitored by measuring the optical density

(OD) of the culture medium at a wavelength of 600 nm (OD_{600}). Posteriorly, cells were recovered by centrifugation and stored at -20ºC.

Construction of pBHSR1-RM-pre-miR-29b plasmid

Using the plasmid pBHSR1-RM as template (Suzuki *et al*. 2011), a DNA fragment containing the *rrn* promoter, the streptavidin RNA aptamer sequence with flanker ribozyme sequences and *puf* terminator region was amplified by PCR. The sequence primers pBHSR1_Fw and pBHSR1_Rv are shown in Table S1, Supporting Information. The amplified DNA fragment of the pBHSR1-RM was purified and cloned into pGEM-T easy vector. Then, the vector was digested with *Stu*I and *Xba*I, releasing a fragment containing the streptavidin RNA aptamer sequence with flanker ribozyme sequences, and the pGEM-T easy vector was purified from agarose gel with NucleoSpin Gel and PCR Clean-up (Macherey-Nagel). Using the pBHSR1-RM plasmid as template in a PCR reaction, specific primers (pBHSR1-RM_StuI_premiR_511Fw and pBHSR1-RM_XbaI820Rv) flanking the second sequence of hammer head ribozyme and the *puf* terminator region were used to insert and amplify the pre-miR-29b sequence, which was digested by *Stu*I and *Xba*I and cloned into pGEM-T easy vector previously digested. The *Stu*I and *Xba*I sites in the primers are underlined and the pre-miR-29b sequence is a bold (Supporting Information, Table S1). In order to obtain the sequence of pre-miR-29b flanked by hammer ribozymes and *puf* terminator region, the pGEM-T easy vector was digested with *Eco*RI and *Xba*I restriction enzymes and cloned into pBHSR-RM previously digested with the same restriction enzymes. After *E. coli* TOP10 transformation with the vector, several colonies were screened by PCR for the presence of the recombinant plasmid pBHSR1-RM containing the pre-miR-29b sequence, being designated by pBHSR1-RM-pre-miR-29b (Supporting Information, Fig. S1). Therefore, some colonies were inoculated in LB medium and grown at 37ºC and 250 rpm, overnight. From these bacterial cultures, the plasmid pBHSR1-RM-pre-miR-29b was isolated and purified using the NZYMiniprep Kit (NZYtech, Lisbon, Portugal) and digested with *Eco*T22I and *Aat*I to confirm the presence of the pre-miR-29b sequence. Plasmid DNA concentrations were determined by NanoPhotometer (Implen) and sequenced in order to confirm the identity and orientation of the amplicon.

Preparation and Transformation of competent *Rhodovulum sulfidophilum* cells

Growth of *R. sulfidophilum* strain was carried out in 500 mL shake flasks containing 100 mL of semi-defined medium, in a rotary shaker at 30ºC and 250 rpm under aerobic-dark conditions, until the cell suspension reached an OD_{600} of 0.4 and 0.8. These cells were used to prepare competent cells for heat shock method. For this purpose, 50 mL aliquots of cell suspension were centrifuged at 5000 rpm for 10 min at 4ºC. The medium was decanted from the cell pellets and each one was ressuspended in 12.5 mL of ice-cold 100 mM $MgCl_2$. The cells were recovered again at 4000 rpm for 10 min at 4ºC and ressuspended in 50 mL of ice-cold 100 mM $CaCl_2$. The cell suspension was maintained on ice for at least 20-30 min. After this, the bacterial culture was centrifuged at 4000 rpm for 10 min at 4ºC and the pellet was

ressuspended in 1 mL of ice-cold 85 mM $CaCl_2$ containing ice-cold 15% (w/v) glycerol for each 50 mL of original culture. Then, the plasmid pBHSR1-RM-pre-miR-29b was introduced into *R. sulfidophilum* cells by the method of heat shock. To this end, different quantities of plasmid pBHSR1-RM-pre-miR-29b (0.1, 0.5, 1 and 5 µg) were immediately added to 0.1 mL of competent cells (the suspension was left on ice for 10 min), and the heat shock was performed at different temperatures (35 and 42ºC) and incubation periods (1 and 2 min), in order to determine the best conditions. After the heat shock, 200 µL of semi-defined medium was added to the transformation mixture and it was incubated at 30ºC, 250 rpm for 2 h under aerobic-dark conditions to allow the expression of antibiotic resistance gene. The culture was then plated on MT agar plates with kanamycin and incubated aerobically at 30ºC for at least 2 days until the appearance of colonies. For each different condition tested, three independent fermentation runs were performed.

Production of pre-miR-29b in *Rhodovulum sulfidophilum*

Unless otherwise stated, recombinant pre-miR-29b biosynthesis was carried out according to the following protocol. Cells containing the expression construct were grown at 30ºC in MT plates containing kanamycin. Then, colonies were used to inoculate 100 mL of the semi-defined medium, on 500 mL shake flasks. Cells were grown at 30ºC and 250 rpm under dark-aerobic conditions, until the OD_{600} typically reached 2.6. Subsequently, in order to start the fermentation with an initial OD_{600} of 0.3, an aliquot of the pre-fermentation medium was added to 500 mL shake flasks to a total volume of 100 mL. The fermentations were carried out during 72 h. Finally, the cells were harvested by centrifugation (1500 g, 10 min, 4ºC) and stored at -20ºC until use.

Isolation of intracellular and extracellular human pre-miR-29b

The isolation of extracellular nucleic acids was based on the method described by Martins and co-workers (2010) with some modifications (Martins *et al*. 2010). Cultivated cells of *R. sulfidophilum* DSM 1374 were recovered by centrifugation at 10000 g for 10 min at 4ºC, and the supernatant was carefully transferred to an autoclaved tube. The nucleic acids fraction of the supernatant was precipitated by adding 3 volumes of 100% ethanol, 1/20th of 3 M sodium acetate (pH 5.0) and 20 µL of glycogen (30 µg/mL). After incubation overnight, nucleic acids were recovered by centrifugation at 10000 g for 10 min at 4ºC and washed with 75% ethanol. The nucleic acids pellets were air-dried for 10 min at room temperature and solubilized in 0.05% DEPC-treated water and incubated with DNase I (Sigma-Aldrich, St Louis, MO, USA). For the intracellular RNAs recovery, the total RNA was extracted from the collected cells using TRIzol reagent (Invitrogen, Carlsbad, CA, USA) and chloroform, according to the protocol provided by the manufacturer. After centrifugation, the aqueous phase was transferred to new tubes, and the RNA was precipitated with isopropanol and washed with 75% of ethanol. The air-dried total RNA pellet was solubilized in 0.05% DEPC-treated water.

Assessment of recombinant human pre-miR-29b production

RNA samples were quantified and evaluated regarding their purity (260/280 nm ratio) using a NANOPhotometer. The integrity and quality of RNA was assessed by agarose gel electrophoresis. A total of 1 µg of RNA was reverse transcribed into complementary DNA (cDNA) in 20 µL final volume using RevertAid First Strand cDNA Synthesis Kit (Thermo Fisher Scientific Inc.), according to the protocol provided by the manufacturer. For quantitative analysis, the amount of pre-miR-29b produced was determined by reverse transcription-quantitative real-time polymerase chain reaction (RT-qPCR) through amplification of cDNA using a specific probe (Roche, Table 1) on a CFX Connect™ Real-Time PCR Detection System from BioRad. RT-qPCR efficiencies were calculated from the given slopes with MyIQ 2.0 software (BioRad). The calibration curve to determine the pre-miR-29b concentration was constructed by serial dilutions of the pre-miR-29b synthetic sample (Stabvida) in the range of 0.00001 to 0.01 pmol/µL. The quantification of the pre-miR-29b expression was calculated by applying the comparative threshold cycle (C_T) method. A list of primers used for RT-qPCR analysis can be seen in Table 1. RT-qPCRs were performed in a 20 µL mixture containing 5 µL cDNA, 400 nM Fw and Rv primers (Roche), 1× FastStart TaqMan® Probe Master (Roche), 200 nM of UPL Probe (Roche, Table S1, Supporting Information) and water, under the following conditions: 95ºC for 10 min for initial denaturation followed by 40 cycles at 95ºC for 10 s, 60ºC for 30 s and 72ºC for 15 s. Due to the small space between the primers it is only possible to design a probe with a sufficient melting temperature if few Locked Nucleic Acid (LNA) bases are added into the probes sequence. Each sample was run in triplicate, and C_T values were averaged from the triplicates. The final data were averaged from three independent experiments.

Protein analysis

Protein content in each sample was measured by the Pierce BCA Protein Assay Kit (Thermo Fisher Scientific Inc.), according to manufacturer's instructions. Reducing sodium dodecyl sulfate-polyacrylamide gel electrophoresis (SDS-PAGE) was performed, according to the method of Laemmli on a 10% polyacrylamide gel (Laemmli 1970). Samples were denatured by the addition of loading dye followed by incubation at 95ºC for 10 min. Gel was stained by BlueSafe (NZYtech, Lisbon, Portugal). Low molecular weight protein marker (NZYtech, Lisbon, Portugal) was used as a molecular weight standard.

Genomic DNA quantification

The concentration of genomic DNA (gDNA) was obtained by real-time qPCR in an iQ5 Multicolor Real-Time PCR Detection System (BioRad). The primers used in these experiments were 5'-ACACGGTCCAGAACTCCTACG-3' (forward) and 5'-CCGGTGCTTCTTCTGCGGGTAACGTCA-3' (reverse) for the amplification of a 181 bp fragment of the 16S rRNA gene. PCR amplicons were quantified by following changes in fluorescence of the DNA binding dye Maxima® SYBR Green/Fluorescein qPCR Master Mix (Thermo Fisher

Scientific Inc.). The calibration curve to achieve the gDNA concentration was constructed by serial dilutions of the *R. sulfidophilum* gDNA sample (purified with the Wizard® Genomic DNA Purification kit, Promega) in the range of 0.005 to 50 ng/mL. Each sample was run in triplicate, and C_T values were averaged from the triplicate. The final data were averaged from three independent experiments.

Cell viability

At different time points of the culture growth, the cellular cytotoxicity was assessed by the *in vitro* toxicology assay kit using the resazurin dye (Sigma-Aldrich, St Louis, MO, USA), conducted according to the manufacturer's instructions. Briefly, cells were incubated at 37ºC during 2 h with a resazurin dye solution. Following incubation, the resulting pink product was transferred to a 96-well black clear bottom fluorescence plates (Corning® Costar®) and quantified in a spectrofluorometer (Spectramax Gemini XS, Molecular Devices LLC, US), using an excitation/emission wavelength of λ_{ex} = 560 nm and λ_{em} = 590 nm. As a positive control for cytotoxicity, death cells were used after incubation at 75ºC during 30 min, while a blank analysis was performed with complete medium without cells. Each value represents the mean of three independent experiments.

Results

pBHSR1-RM-pre-miR-29b expression vector construction

Hsa-pre-miR-29b was already identified as a target in several diseases, and its sequence was selected in the miRBase, which is the official repository of miRNAs. In this study, the production of the pre-miRNA instead of the mature miRNA is described, since the recognition and processing in the cell are more efficient. Moreover, its structural characteristics, specifically the single chain with ~80 nucleotides of which some are unpaired in the 3'overhang, will possibly facilitate the purification of the target miRNAs (Tsutsumi *et al*. 2011). The hsa-pre-miR-29b sequence was amplified by PCR using specific primers (Supporting Information, Table S1) containing two restrictions sites for *Stu*I and *Xba*I and cloned into the plasmid pBHSR1-RM, previously digested with the same restriction enzymes. For the construction of pBHSR1-RM-pre-miR-29b, the target sequence was cloned in the pBHSR1-RM vector, as it presents two self-cleaving hammerhead ribozyme sequences flanking the target pre-miRNA, allowing its release. As can be observed in Figure S1A, Supporting Information, the electrophoretic analysis of the PCR products obtained from the amplification with the specific primers for hsa-pre-miR-29b shows one band corresponding to the size of the gene of interest cloned into pBHSR1-RM-pre-miR-29b. The recombinant plasmid pBHSR1-RM-pre-miR-29b was also digested with restriction enzymes, namely *Eco*T22I and *Aat*I, to confirm the presence of the cloned hsa-pre-miR-29b sequence. In this electrophoresis, one band corresponding to the size of the gene of interest it is also visible (Supporting Information, Fig. S1B). In addition, the vector was sequenced to confirm the identity and orientation of the target gene produced, being identified as the hsa-pre-miR-29b (Supporting Information, Fig. S1C). After confirming that the isolated positive clone contained the hsa-pre-miR-29b, it was introduced into freshly made competent *R. sulfidophilum* cells by heat shock. Thus, in this work, the recombinant hsa-pre-miR-29b was produced in a genetically modified organism, *R. sulfidophilum* DSM 1374, harboring the plasmid pBHSR1-RM-pre-miR-29b.

Improvement of *Rhodovulum sulfidophilum* transformation conditions

Bacterial transformation is of utmost importance in all aspects of genetic engineering. A small number of chemical and physical methods have been established to introduce exogenous DNA into *R. sulfidophilum* cells, including heat shock with polyethylene glycol 6000 and conjugation with the mobilizing strain *E. coli* S17-1 (Donohue and Kaplan 1991; Nagao *et al*. 2014; Suzuki *et al*. 2010; Suzuki *et al*. 2011). Although these two methods have been tested for *R. sulfidophilum* transformation, so far the *Rhodovulum* genus has not been characterized concerning its optimal transformation conditions. In laboratory, the most widely used methods for artificial bacterial transformation are based on the treatment of the cells with $CaCl_2$ or, alternatively, the electroporation (Donohue and Kaplan 1991). Therefore, in this study, an effective method using $CaCl_2$ for the preparation of competent *R. sulfidophilum* cells it is described. As it is known, there are several factors that affect the bacterial

transformation efficiency, namely the incubation time (1 and 2 min) of bacteria with DNA, the plasmid DNA concentration (0.1 to 5 µg/mL) used in the transformation mixture, the temperature of incubation (35 and 42ºC), and growth phase (OD=0.4 and 0.8). To estimate the effect of the growth phase on the transformation efficiency, *R. sulfidophilum* cells cultured to mid-lag (OD=0.4) and late-lag (OD=0.8) phases were subjected to heat shock. As depicted in Figure 2, when the cells were collected in the mid-lag phase for preparation of competent cells, higher transformation efficiencies were obtained, in comparison to that achieved with the cells collected in late-lag phase. Therefore, as the transformation efficiency of mid-lag recovered bacteria are higher than late-lag phase, this was the condition used for the preparation of competent *R. sulfidophilum* cells. The effect of the plasmid concentration was also evaluated, since it also influences the process transformation efficiency. Thus, different plasmid DNA amounts (from 0.1 up to 5 µg/mL) were employed and the transformation efficiency was determined, as represented in Figure 2. In fact, it is possible to observe that the optimum amount of plasmid DNA was 0.1 µg, since it corresponds to the higher transformation efficiency achieved, $8.22x10^3$ transformants/µg plasmid (Fig. 2A). When the plasmid DNA was increased to 5 µg, the transformation efficiency drastically decreased, because this concentration can be toxic for the bacteria. In general, from all the conditions tested, the highest *R. sulfidophilum* transformation efficiency was obtained using the following conditions: 0.1 µg of plasmid DNA, with a heat-shock of 2 min at 35ºC (Fig. 2). The increase in temperature from 35 to 42ºC also played an important role in the transformation efficiency resulting in a decrease of the transformation efficiency from $8.22x10^3$ to $3.85x10^3$ transformants/µg plasmid (Fig. 2B).

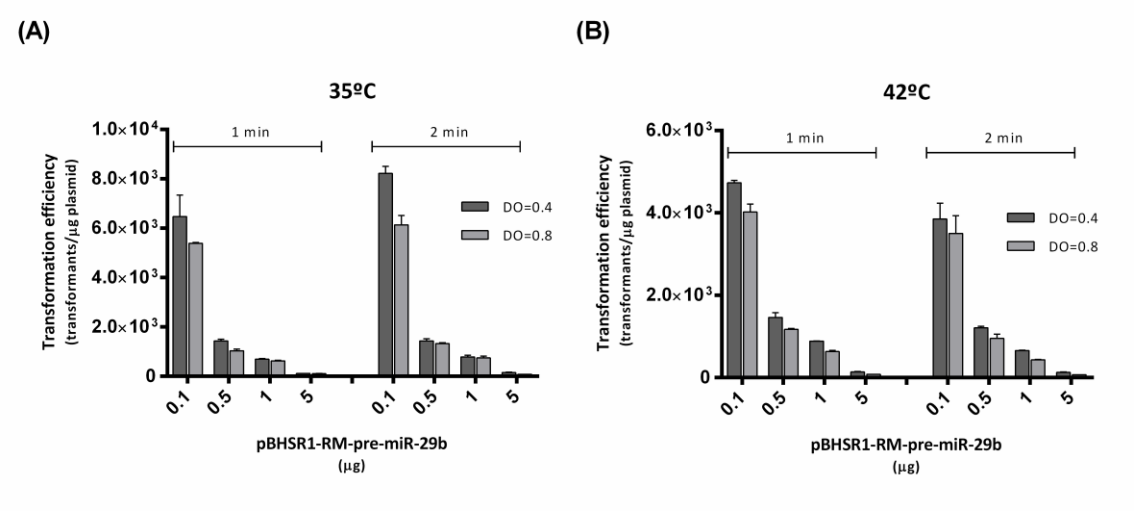

Figure 2 – Effects of growth phase, time incubation, amount of plasmid DNA **(A)** at 35ºC and **(B)** at 42ºC on the transformation efficiency of *R. sulfidophilum* cells. Data shown are mean ± s.d. from triplicate runs.

The effect of temperature and sodium chloride concentration on *Rhodovulum sulfidophilum* growth

In general, the media formulation for culturing *R. sulfidophilum* cells seems to require specific components for the development of a sustainable and successfully upstream stage. Initially, *R. sulfidophilum* growth was tested in aerobic conditions, using different solid culture media commonly applied for bacterial growth, namely Nutrient Agar, Tryptone Soya Agar and Mueller Hinton Agar (see Materials and Methods section). *R. sulfidophilum* growth was only detected with Nutrient Agar medium, indicating that specific components such as sodium chloride and yeast extract are required for *R. sulfidophilum* growth and recombinant hsa-pre-miR-29b biosynthesis (data not shown). Then, in order to define the optimum conditions for bacterial growth and over-expression of the target RNA, several experiments varying the temperature (25 and 30ºC) and sodium chloride concentration (10, 20, 30 and 50 g/L), were carried out, under aerobic conditions. In what concerns to the effect of sodium chloride concentration using Nutrient Broth medium, our results demonstrated that the bacteria hardly grow with 10 g/L NaCl (Fig. 3A), highlighting the requirement of a higher salt concentration for *R. sulfidophilum* growth. On the other hand, using sodium chloride concentrations of 20, 30 and 50 g/L, higher growth rates were achieved. In general, the ideal sodium chloride concentration for higher *R. sulfidophilum* growth was 30 g/L NaCl (Fig. 3A).

Although the optimized concentration of sodium chloride improved the *R. sulfidophilum* growth profile, under aerobic conditions, its growth was not yet optimal, indicating that other compounds such as glucose or polypeptone can be required. Thus, several experiments were performed and the composition of the semi-defined medium adapted from Sankhla and co-workers (Sankhla *et al*. 2010) was evaluated for maximizing *R. sulfidophilum* growth rates (see Materials and Methods section). Considering that the main objective of this work is to produce a microRNA, it is important to mention that the yeast extract, one of the minor components added to the medium, presents RNA traces, which can constitute a contaminant of the target product. Furthermore, after the optimization of the culture medium, it was also evaluated the effect of the temperature (25 and 30ºC) on *R. sulfidophilum* DSM 1374 growth profile, using the semi-defined medium supplemented with 30 g/L of NaCl under aerobic conditions. The time course profiles are shown in Figure 3B, where it is possible to observe that bacterial growth was slightly lower at 25ºC than at 30ºC. Furthermore, Figure 3B shows an initial lag phase of 18 h, followed by a rapid increase in the growth rates at 30ºC where 6.86±0.09 units of OD_{600} was obtained. The temperature selected is within the range of optimum *R. sulfidophilum* growth (30 to 35ºC) as previously reported by other authors (Hansen and Veldkamp 1973). In general, the experiments performed with the aim of understanding the effect of temperature and NaCl concentration on the growth profile of DSM 1374 strain demonstrated that the optimal conditions are 30ºC in semi-defined medium, pH 6.8 (Fig. 3B). In addition, our results suggest that these conditions enable a shorter cultivation time and higher optical densities are achieved (Fig. 3B).

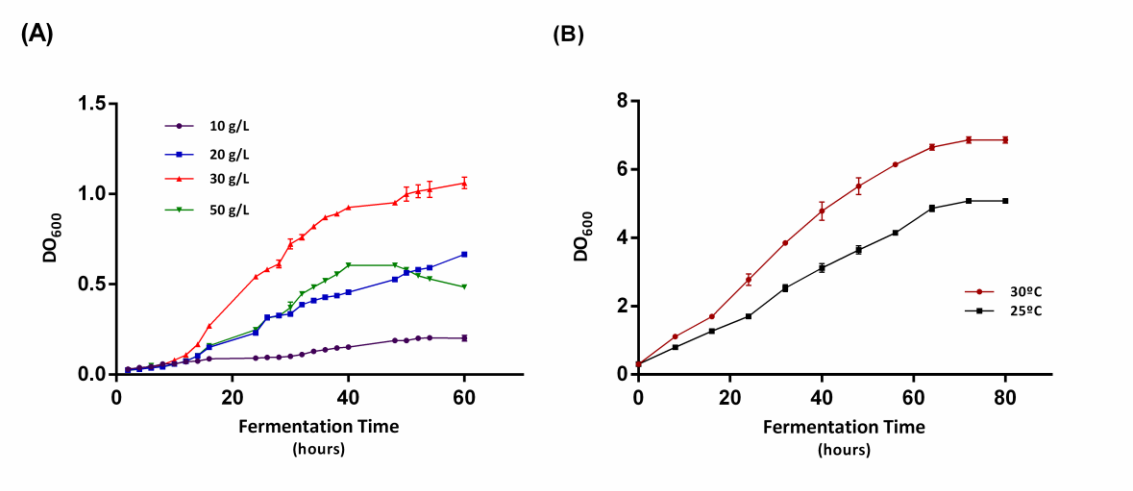

Figure 3 - (A) Effect of sodium chloride concentrations (10, 20, 30 and 50 g/L) on growth of the photosynthetic bacterium *Rhodovulum sulfidophilum* DSM 1374 in Nutrient Broth medium under aerobic conditions, in the dark. The data are the average of three repeats of duplicate cultivations. Bars indicate standard deviation. **(B)** Effect of temperature (25 and 30ºC) on growth of the photosynthetic bacterium *Rhodovulum sulfidophilum* DSM 1374. *R. sulfidophilum* was cultivated in semi-defined medium supplemented with 30 g/L NaCl under aerobic conditions, in the dark. The data are the average of three repeats of duplicate cultivations. Bars indicate standard deviation.

Time course profile of hsa-pre-miR-29b biosynthesis

The cells transformed with the recombinant plasmid expressing the hsa-pre-miR-29b were cultivated under aerobic dark conditions, to clarify the relationship between cell growth and the production of intra and extracellular nucleic acids. First of all, the presence of pre-miR-29b inside the cells was confirmed. Therefore, at various time points of the culture, the cells were recovered by centrifugation and the total RNA was extracted and collected using the phenol/chloroform extraction. The concentration of the intracellular total RNA was estimated by spectrophotometric analysis, measuring the absorbance at 260 and 280 nm. The 260/280 ratio was also determined, which is an indication of the purity of each sample, being achieved a ratio of 2.0, which is often characteristic of a pure RNA preparation (RE 2005). By RT-qPCR using a specific probe, the maximum amount of intracellular pre-miR-29b determined was 358.47±5.48 µg/L of culture, at 32 h of cultivation. On the other hand, to elucidate the relationship between cell growth and the production of extracellular pre-miR-29b, the total extracellular nucleic acids were isolated from the culture medium and analyzed by agarose gel electrophoresis during different periods of cultivation. Figure 4A shows that the nucleic acids profile of the clarified precipitates recovered along the *R. sulfidophilum* cultivation contained different RNA species and fragments of gDNA. The analysis of the electrophoresis (Fig. 4A) revealed the presence of bands with high molecular weight, corresponding to fragments of gDNA (higher than 10000 bp). The 23S and 16S rRNA

bands are also present, with molecular weights between 750 and 1500 bp. In addition, sRNAs are present in sharp bands of low molecular weight (about 200 bp). The results show different contents of extracellular nucleic acids during bacteria growth (Fig. 4A). In order to identify and quantify specifically the pre-miR-29, during 72 h of cultivation (until the stationary phase), the nucleic acids in the culture medium were collected by ethanol precipitation and the resulting fraction was treated with DNase I. The cDNA of the RNA fraction was prepared and subjected to RT-qPCR analysis to detect the pre-miR-29b sequence at various time points of the bacterial growth (Fig. 4B). These results indicated that in fact the self-processed precursor form of the miR-29 (pre-miR-29b) was present in the culture medium. In particular, it was found that the maximum level of extracellular pre-miR-29b obtained in the present study was 181.64±35.78 μg/L of culture (Fig. 4B), and the maximum level of production was observed at 40 h of cultivation (late log phase).

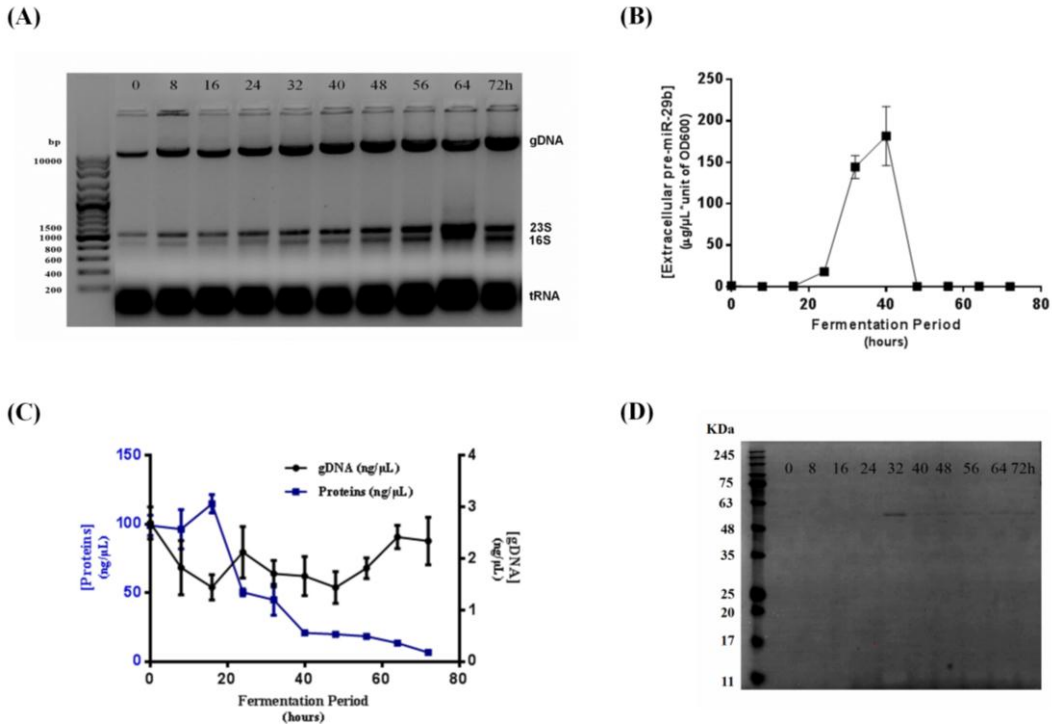

Figure 4 – Extracellular production and release of the human pre-miR-29b, gDNA and proteins into the culture medium. **(A)** Electrophoretic analysis of extracellular nucleic acids. Lanes 0–72 h, cultivation times. Lane M, DNA molecular weight marker. **(B)** The time course of extracellular production of the hsa-pre-miR-29b from the bacteria harboring pBHSR1-RM-pre-miR-29b is shown. The amounts of hsa-pre-miR-29b were measured by quantitative RT-PCR using a specific probe, as described in Materials and Methods (see Table S1, Supporting Information). Error bars indicate the respective standard deviations which were calculated from the results of three independent experiments. **(C)** Production of extracellular gDNA and proteins. **(D)** Electrophoretic analysis of extracellular proteins. Lanes 0–72 h, cultivation times. Lane M, protein molecular weight marker.

As can be seen by Figure 4B, the extracellular pre-miR-29b production increased until 40 h, after which a significant decrease in yield was observed. The time course profile obtained is very similar to the curve of the streptavidin RNA aptamer production which was published by Suzuki and collaborators (Nagao *et al*. 2014; Suzuki *et al*. 2010; Suzuki *et al*. 2011).

Detection of extracellular genomic DNA and proteins

Regarding the potential applicability of this method to obtain recombinant pre-miRNAs, along with the time-course profile of the target RNA biosynthesis, it is also important to evaluate its purity during the fermentation time. Therefore, the levels of gDNA and proteins in the extracellular medium were evaluated during the fermentation period. As discussed above, the purity of the sample is commonly evaluated by the 260/280 nm ratio because it is an indirect method to verify the contamination of nucleic acids with proteins. Nevertheless, a more accurate method was used to verify the protein contamination level. Thus, the protein level in RNA samples was quantified by the micro-BCA method during the cultivation because contaminating protein can be overlooked by spectrophotometric analysis. Figure 4C shows the results for protein quantification in the extracellular RNA fraction, resultant from a culture at 30ºC, 30 g/L NaCl concentration assay. The findings revealed that the proteins level in the extracellular medium was high during the first 32 h of cultivation, with a maximum value of 114.65±6.64 µg/mL at 16h (Fig. 4C). Considering this profile, it is suggested that the initial proteins content can be associated to the presence of complex components in the medium, which can contain residual proteins. Therefore, the proteins of the medium (without bacterial inoculation) were also quantified using the BCA method and a concentration of 93.04±1.43 µg/mL was obtained. As the fermentation time increases, the medium components start to be metabolized by the bacterium and the contribution of the medium to the global protein content slows down. In addition, to identify the profile of the proteins quantified by BCA assay, a SDS-PAGE electrophoresis was also performed (Fig. 4D). These results obtained with SDS-PAGE are in agreement with the results obtained with BCA assay because in the lanes corresponding to 24 h of cultivation, there are no protein bands, indicating that the secretion of proteins by the bacteria is not significant at this point (Fig. 4D). However, it is possible to visualize faint protein bands with molecular weights between 48 and 63 KDa in the samples obtained after 32 h of growth, where the secretion starts to be more significant (Fig. 4D). The time course profile of extracellular gDNA production and secretion to the culture medium at various time points in culture was also determined by quantitative real-time PCR (Fig. 4C). The production of extracellular gDNA showed a similar pattern to bacterial cell growth except that the rapid increase of gDNA production is noticed after 24 h (Fig. 4C).

Cytotoxic profile

Finally, the cellular cytotoxicity during the *R. sulfidophilum* growth was evaluated by resazurin dye and compared with cells treated with heat (positive control). As presented in Figure 5, at 72 h, end of the fermentation, more than 87% of viable cells were obtained, a

value that is acceptable. Thus, as the majority of the cells remain viable, they are contributing to the newly synthesized product and as the cell lysis is minimized, the extracellular medium is not significantly contaminated with the host RNases and other host components.

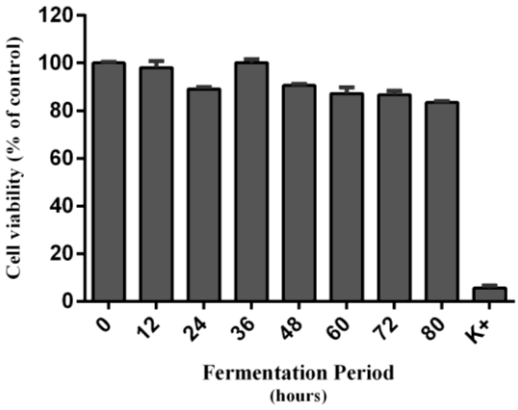

Figure 5 – Cell viability assays during the fermentation time. Heat treated cells were used as positive controls to induce toxicity. Mean percentage values relative to the untreated cells and standard error of the mean in three independent experiments are shown.

Discussion

MicroRNAs have been produced using either prokaryotic or eukaryotic hosts, with eukaryotic expression vectors (Chen *et al*. 2007; Huang *et al*. 2011; Li *et al*. 2014). Although these systems have had complete success, the development of a system capable of producing recombinant miRNAs with increased stability and quality for further applications, such as structural studies or clinical applications, remains a hurdle to overcome. Recent studies have pointed out that *R. sulfidophilum* DSM 1374 has great potential in the production of extracellular RNAs, which can be further applied in structural and biophysical studies and as therapeutic agents in a broad range of diseases (Nagao *et al*. 2014; Suzuki *et al*. 2011). In fact, the use of *R. sulfidophilum* as an alternative host presents a number of advantages over other prokaryotic hosts for obtaining RNAs, namely the unusual ability to secrete heterologous nucleic acids during cell growth and the characteristic of not secrete host RNases to the culture medium, maintaining the integrity and activity of the RNA product. (Ando *et al*. 2004; Ando *et al*. 2006; Nagao *et al*. 2014; Suzuki *et al*. 2010; Suzuki *et al*. 2009b; Suzuki *et al*. 2011). As a result, this strategy allows avoiding time-consuming and laborious RNA extraction methods.

Hence, in this work and for the first time, *R. sulfidophilum* DSM 1374 was successfully applied for the recombinant biosynthesis and isolation of hsa-pre-miR-29b from both the intra and extracellular species. Initially, the optimal conditions (0.1 µg of plasmid DNA, with a heat-shock of 2 min at 35ºC) for transforming *R. sulfidophilum* were determined. The

transformation method developed is advantageous because of its simplicity, low cost, high transformation efficiency (10^3 transformants per µg of plasmid DNA) achieved and the possibility to transfer relatively large segments of DNA. In addition, bacteria prepared by this method can be frozen and stored for future use.

Additionally, the influence of the temperature and sodium chloride concentration in the growth profile of *R. sulfidophilum* cells under aerobic conditions was also addressed. In general, according to the results described in this study, the *R. sulfidophilum* DSM 1374 aerobic cultivation should be performed at 30ºC using semi-defined medium, supplemented with 30 g/L NaCl, under dark-aerobic conditions, since these conditions allowed relatively rapid growth with higher optical densities. In fact, our results showed that cultivation under aerobic conditions was similar to that achieved in anaerobic conditions, previously described in other works (Ando *et al*. 2004; Ando *et al*. 2006; Suzuki *et al*. 2010; Suzuki *et al*. 2009a; Suzuki *et al*. 2009b; Suzuki *et al*. 2011), being possible to reach higher growth rates, higher optical densities and a shorter cultivation time. These results can be explained by the fact that *R. sulfidophilum* DSM 1374 being a facultative phototroph, which is able to grow anaerobically in the presence of light or aerobically in the dark. Despite this feature, this is the first description of RNA production using this bacterium on aerobic conditions.

Therefore, the main purpose of this study was to evaluate the time-course profile of the production of intra and extracellular hsa-pre-miR-29b using *R. sulfidophilum* DSM 1374. The total yield of the pre-miR-29b inside the cells was 358 µg/L of culture at 32 h, which is a quantity almost 17.9 times higher than the value obtained (about 20 µg from 1 L of culture) by Suzuki and co-workers for streptavidin RNA aptamer (Suzuki *et al*. 2010; Suzuki *et al*. 2011). On the other hand, the maximum production of extracellular pre-miR-29b achieved was approximately 182 µg/L of culture. Furthermore, in order to obtain a high production of the extracellular human pre-miR-29b while minimizing the impurities (genomic DNA and proteins), *R. sulfidophilum* DSM 1374 should be cultivated up to 40 h.

The value obtained (182 µg/L) is more than 100 fold higher than those reported in the literature for the production of RNA aptamer and shRNA using this bacterium (Nagao *et al*. 2014; Suzuki *et al*. 2010; Suzuki *et al*. 2011). In accordance to what has been described by other authors, the yield obtained for extracellular streptavidin RNA aptamer was 195 ng/L of culture and 200 ng/L of shRNA, after 70 h of cultivation (stationary phase), using the mutated-*rrn* promoter (Table 1). In another study, a yield of 100 ng/L of culture was obtained under aerobic conditions in the dark. This result can be explained, because the mutated-*rrn* promoter is independent of the FIS protein activation, which is expressed only in early log phase, and allows the transcription even during the late log and stationary phases (Dryden and Kaplan 1993; Suzuki *et al*. 2011). In addition, because the production was observed in the log phase but not in the stationary or the post-stationary phase, it is suggested that the nucleic acids do not originate from the cell autolysis but from active production.

Table 1 - Comparison of growth rates and RNA production yields in *R. sulfidophilum* DSM 1374 under different growth conditions.

Growth Conditions	*Intracellular RNA (µg/L)*	*Extracellular RNA (µg/L)*	*Target RNA*	*Reference*
Anaerobically (25ºC)	7	0.045	RNA aptamer	(Suzuki *et al.* 2010)
Anaerobically (25ºC)	20	0.195	RNA aptamer	(Suzuki *et al.* 2011)
Anaerobically (30ºC)		0.2	shRNA	(Nagao *et al.* 2014)
Aerobically (30ºC)	358	182	pre-miRNA	This study

Globally, the bioprocess optimization here described using *R. sulfidophilum* allows the production and isolation of recombinant extracellular pre-miRNA molecules with high yields as a way to simplify the current extraction methodologies, because this method requires only the cultivation of the bacterium for the product biosynthesis. Thus, the RNAs secretion already represents a significant advantage for the recovery and purification processes, circumventing the need of the lysis procedure that frequently induces RNA denaturation. In addition, it is expected that the application of this strategy allows suppressing the use of organic solvents and extremely toxic chemicals which are employed in conventional RNA isolation techniques and that are biologically hazardous, representing a simplification of the process and allowing an increase in the RNA recovery yield and stability (Fig. 1). The extracellular production is thought to be very beneficial for the future development of an efficient process engineering system for industrial production of RNA drugs. Moreover, the culture volume can be scaled up easily, which is necessary for large-scale industrial preparation. Therefore, it was described a novel, fast and simple process, economically feasible and highly efficient for pre-miRNA isolation. For all these reasons, the approach here proposed for recombinant production of extracellular pre-miRNAs is not only innovative but also presents more advantages in the point-of-view of the potential biological application of miRNAs. Furthermore, it is believed that the pre-miRNAs obtained using this protocol, can be applied in many molecular biology subjects and RNAi-based therapeutics.

Acknowledgments

This work was supported by the Portuguese Foundation for Science and Technology (FCT) through the following projects: EXPL/BBB-BIO/1056/2012 and Pest-OE/SAU/UI0709/2014. Patrícia Pereira and Augusto Pedro acknowledge the fellowships, SFRH/BD/81914/2011 and SFRH/BD/81222/2011, respectively from FCT. The authors would like to thank Prof. Yo Kikuchi (Division of Life Science and Biotechnology, Department of Ecological Engineering, Toyohashi University of Technology) for kindly provide the pBHSR1-RM plasmid.

References

Alvarez-Garcia I, Miska EA (2005) MicroRNA functions in animal development and human disease. Development 132(21):4653-62

Ando T, Suzuki H, Komura K, Tanaka T, Hiraishi A, Kikuchi Y (2004) Extracellular RNAs produced by a marine photosynthetic bacterium *Rhodovulum sulfidophilum*. Nucleic Acids Symp Ser (Oxf)(48):165-6

Ando T, Suzuki H, Nishimura S, Tanaka T, Hiraishi A, Kikuchi Y (2006) Characterization of extracellular RNAs produced by the marine photosynthetic bacterium *Rhodovulum sulfidophilum*. J Biochem 139(4):805-11

Beckert B, Masquida B (2011) Synthesis of RNA by *in vitro* transcription. Methods Mol Biol 703:29-41

Chen S, Ni M, Yu B, Lv T, Lu M, Gong F (2007) Construction and identification of a human liver specific microRNA eukaryotic expression vector. Cell Mol Immunol 4(6):473-7

Dogini DB, Pascoal VD, Avansini SH, Vieira AS, Pereira TC, Lopes-Cendes I (2014) The new world of RNAs. Genet Mol Biol 37(1 Suppl):285-93

Donohue TJ, Kaplan S (1991) Genetic techniques in *rhodospirillaceae*. Methods Enzymol 204:459-85

Dryden SC, Kaplan S (1993) Identification of cis-acting regulatory regions upstream of the rRNA operons of *Rhodobacter sphaeroides*. J Bacteriol 175(20):6392-402

Du L, Pertsemlidis A (2011) Cancer and neurodegenerative disorders: pathogenic convergence through microRNA regulation. J Mol Cell Biol 3(3):176-80

Fire A, Xu S, Montgomery MK, Kostas SA, Driver SE, Mello CC (1998) Potent and specific genetic interference by double-stranded RNA in *Caenorhabditis elegans*. Nature 391(6669):806-11

Gomes AQ, Nolasco S, Soares H (2013) Non-coding RNAs: multi-tasking molecules in the cell. Int J Mol Sci 14(8):16010-39

Hansen TA, Veldkamp H (1973) *Rhodopseudomonas sulfidophila*, nov. spec., a new species of the purple nonsulfur bacteria. Arch Mikrob 92(1):45-58

Hebert SS, Horre K, Nicolai L, Papadopoulou AS, Mandemakers W, Silahtaroglu AN, Kauppinen S, Delacourte A, De Strooper B (2008) Loss of microRNA cluster miR-29a/b-1 in sporadic Alzheimer's disease correlates with increased BACE1/beta-secretase expression. Proc Natl Acad Sci U S A 105(17):6415-20

Huang Y, Zou Q, Wang SP, Tang SM, Zhang GZ, Shen XJ (2011) Construction and detection of expression vectors of microRNA-9a in BmN cells. J Zhejiang Univ Sci B 12(7):527-33

Kim DY, Kim YB, Rhee YH (2000) Evaluation of various carbon substrates for the biosynthesis of polyhydroxyalkanoates bearing functional groups by *Pseudomonas putida*. Int J Biol Macromol 28(1):23-9

Laemmli UK (1970) Cleavage of structural proteins during the assembly of the head of bacteriophage T4. Nature 227(5259):680-5

Li MM, Wang WP, Wu WJ, Huang M, Yu AM (2014) Rapid production of novel pre-microRNA agent hsa-mir-27b in *Escherichia coli* using recombinant RNA technology for functional studies in mammalian cells. Drug Metab Dispos 42(11):1791-5

Ling H, Fabbri M, Calin GA (2013) MicroRNAs and other non-coding RNAs as targets for anticancer drug development. Nat Rev Drug Discov 12(11):847-65

Martins R, Queiroz JA, Sousa F (2010) A new affinity approach to isolate *Escherichia coli* 6S RNA with histidine-chromatography. J Mol Recognit 23(6):519-24

Martins R, Queiroz JA, Sousa F (2014) Ribonucleic acid purification. J Chromatogr A 1355:1-14

Milligan JF, Groebe DR, Witherell GW, Uhlenbeck OC (1987) Oligoribonucleotide synthesis using T7 RNA polymerase and synthetic DNA templates. Nucleic Acids Res 15(21):8783-98

Nagao N, Suzuki H, Numano R, Umekage S, Kikuchi Y (2014) Short hairpin RNAs of designed sequences can be extracellularly produced by the marine bacterium *Rhodovulum sulfidophilum*. J Gen Appl Microbiol 60(6):222-6

Nelson PT, Wang WX, Rajeev BW (2008) MicroRNAs (miRNAs) in neurodegenerative diseases. Brain Pathol 18(1):130-8

Nilsen TW (2007) Mechanisms of microRNA-mediated gene regulation in animal cells. Trends Genet 23(5):243-9

Pedro AQ, Bonifacio MJ, Queiroz JA, Maia CJ, Passarinha LA (2011) A novel prokaryotic expression system for biosynthesis of recombinant human membrane-bound catechol-*O*-methyltransferase. J Biotechnol 156(2):141-6

Ponchon L, Dardel F (2007) Recombinant RNA technology: the tRNA scaffold. Nat Methods 4(7):571-6

Ponchon L, Dardel F (2011) Large scale expression and purification of recombinant RNA in *Escherichia coli*. Methods 54(2):267-73

Ramachandran PV, Ignacimuthu S (2013) RNA interference-a silent but an efficient therapeutic tool. Appl Biochem Biotechnol 169(6):1774-89

RE F (2005) RNA methodologies - Laboratory Guide for Isolation and Characterization, 4th edn. Academic Press, York, USA

Sankhla IS, Bhati R, Singh AK, Mallick N (2010) Poly(3-hydroxybutyrate-co-3-hydroxyvalerate) co-polymer production from a local isolate, *Brevibacillus invocatus* MTCC 9039. Bioresour Technol 101(6):1947-53

Silva F, Passarinha L, Sousa F, Queiroz JA, Domingues FC (2009) Influence of growth conditions on plasmid DNA production. J Microbiol Biotechnol 19(11):1408-14

Sullenger BA, Gilboa E (2002) Emerging clinical applications of RNA. Nature 418(6894):252-8

Suzuki H, Ando T, Umekage S, Tanaka T, Kikuchi Y (2010) Extracellular production of an RNA aptamer by ribonuclease-free marine bacteria harboring engineered plasmids: a proposal for industrial RNA drug production. Appl Environ Microbiol 76(3):786-93

Suzuki H, Daimon M, Awano T, Umekage S, Tanaka T, Kikuchi Y (2009a) Characterization of extracellular DNA production and flocculation of the marine photosynthetic bacterium *Rhodovulum sulfidophilum*. Appl Microbiol Biotechnol 84(2):349-56

Suzuki H, Umekage S, Tanaka T, Kikuchi Y (2009b) Extracellular tRNAs of the marine photosynthetic bacterium *Rhodovulum sulfidophilum* are not aminoacylated. Biosci Biotechnol Biochem 73(2):425-7

Suzuki H, Umekage S, Tanaka T, Kikuchi Y (2011) Artificial RNA aptamer production by the marine bacterium *Rhodovulum sulfidophilum*: improvement of the aptamer yield using a mutated transcriptional promoter. J Biosci Bioeng 112(5):458-61

Tsutsumi A, Kawamata T, Izumi N, Seitz H, Tomari Y (2011) Recognition of the pre-miRNA structure by *Drosophila* Dicer-1. Nat Struct Mol Biol 18(10):1153-8

Umekage S, Kikuchi Y (2009) *In vitro* and *in vivo* production and purification of circular RNA aptamer. J Biotechnol 139(4):265-72

Wassarman KM, Zhang A, Storz G (1999) Small RNAs in *Escherichia coli*. Trends Microbiol 7(1):37-45

Wei Z, Huang W, Li J, Hou G, Fang J, Yuan Z (2007) Studies on endotoxin removal mechanism of adsorbents with amino acid ligands. J Chromatogr B Analyt Technol Biomed Life Sci 852(1-2):288-92

Supporting Information

Figure S1 – (A) Amplification of the hsa-pre-miR-29b DNA sequence from *R. sulfidophilum* harboring pBHSR1-RM-pre-miR-29b, using specific primers (M - DNA maker; Lane 1 – Negative control and Lane 2 - PCR product); **(B)** Characterization of the recombinant plasmid after double digestion with restriction enzymes (M - DNA maker; Lane 1 - pBHSR1-RM-pre-miR-29b digested by *Aat*I and *Eco*T22I); **(C)** Sequencing of the recombinant plasmid pBHSR1-RM-pre-miR-29b.

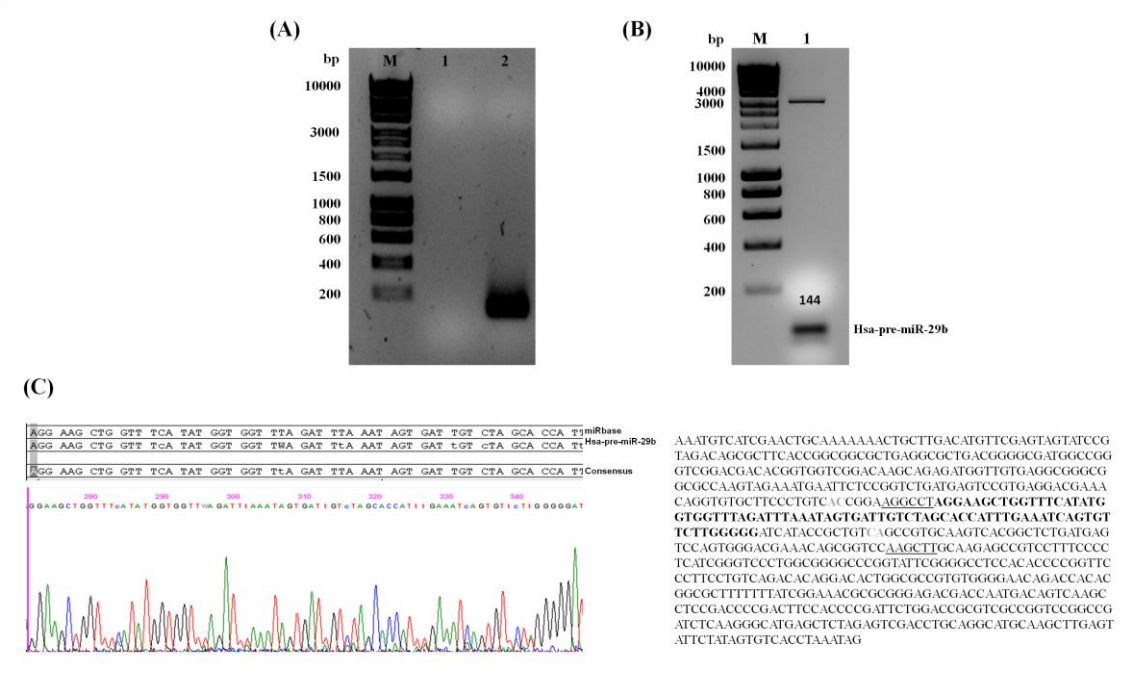

Table S1 – Primers used in this study.

Primer	*Sequence (5'-3')*
pBHSR1-RM_Fw	TGT GTG TTC TTT GGG CGT AA
pBHSR1-RM_Rv	TGT GGA ATT GTG AGC GGA TA
pBHSR1-RM_StuI_premiR_511 Fw	CGA GGC CT**A GGA AGC TGG TTT CAT ATG GTG GTT TAG ATT TAA ATA GTG ATT GTC TAG CAC CAT TTG AAA TCA GTG TTC TTG GGG G**AT CAT ACC GCT GTC AGC CGT GCA AG
pBHSR1-RM_XbaI_820Rv	CAT CTA GAG CTC ATG CCC TTG AGA TCG GCC
pre-miR-29b_Fw	GGA AGC TGG TTT CAT ATG GTG
pre-miR-29b_Rv	CCC CCA AGA ACA CTG ATT TC
Pre-miR-29b_synthetic	CTT CAG GAA GCT GGT TTC ATA TGG TGG TTT AGA TTT AAA TAG TGA TTG TCT AGC ACC ATT TGA AAT CAG TGT TCT TGG GGG
Probe	***Sequence (5'-3')***
pre-miR-29b_Fw	AGG AAG CTG GTT TCA TAT GGT GG
pre-miR-29b_Rv	CAA GAA CAC TGA TTT CAA ATG GTG C
miR-29b_TM	FAM - AGA CAA TCA CTA TTT AAA - BBQ

Note: The underlined letters indicate the restriction enzyme recognition sites.

Paper IV

Analysis of pre-miR-29b binding conditions to amino acids by Surface Plasmon Resonance Biosensor

P. Pereira, C. Cruz, J. A. Queiroz, A. Figueiras, F. Sousa

(*Submitted for publication*)

Short description: This paper characterizes the binding affinity of pre-miR-29b to $_{L}$-arginine and $_{L}$-lysine by Surface Plasmon Resonance. Indeed, this information was obtained under different experimental conditions, in order to mimic the experimental conditions used in chromatographic assays using these amino acids as specific ligands. These results provide relevant information regarding the set of buffers as well as temperature conditions that induce pre-miRNA binding, thereby increasing the selectivity and improving efficient microRNA separation. In addition, in order to verify the effect of these conditions on the interactions and the maintenance of the integrity and stability of the pre-miR-29b molecules, circular dichroism analysis was performed. This study showed the importance of Surface Plasmon Resonance as a technique to assess the most appropriated experimental conditions in future chromatographic experiments.

Analysis of pre-miR-29b binding conditions to amino acids by Surface Plasmon Resonance Biosensor

P. Pereira[1], C. Cruz[1], J. A. Queiroz[1], A. Figueiras[1,2], F. Sousa[1]*

[1] *CICS-UBI – Health Sciences Research Centre, University of Beira Interior, Avenida Infante D. Henrique, 6200-506 Covilhã, Portugal;*

[2] *CNC - Center of Neuroscience and Cell Biology, University of Coimbra, Largo Marquês de Pombal, 3004-517 Coimbra, Portugal*

*Corresponding author:
Dr. Fani Sousa
Phone: +351 275 329 074
Fax: +351 275 329 099
E-mail address: fani.sousa@fcsaude.ubi.pt
Postal address: Health Sciences Research Centre, Universidade da Beira Interior, Avenida Infante D. Henrique, 6200-506 Covilhã, Portugal

Abstract

The aim of this work was to provide binding information between the recombinant pre-miR-29b and $_{L}$-arginine/$_{L}$-lysine by surface plasmon resonance (SPR) and circular dichroism (CD). This information brings important insights concerning the characterization of the microRNA binding onto chromatographic supports using these amino acids as specific ligands. Moreover, it is possible to determine some particular conditions enabling the improvement of the binding specificity of the amino acid ligands used to purify microRNA, preserving their integrity. The binding responses were detectable and reproducible and allowed the determination of the equilibrium dissociation constant (K_D). Considering the binding affinities, it was verified that the pre-miR-29b binds more strongly to L-arginine (K_D between 10^{-6} and 10^{-7}M) than to L-lysine (K_D between 10^{-5} and 10^{-7}M). Remarkably, the results revealed that the ligands possess high affinity to RNA molecules using buffers with low salt concentration and no binding responses were detected with high salt concentrations, suggesting that electrostatic interactions are mainly responsible for ligand-analyte interaction. Above all, this study showed the importance of SPR for future screening of other ligands that, like the ones described herein, can be used to design novel microRNA purification platforms which will have a significant impact in biopharmaceutical-based therapeutics.

Keywords

Amino acid-microRNA interactions; Binding affinities; Circular Dichroism; Recombinant pre-miR-29b; Surface Plasmon Resonance

Introduction

Over the past decade, several hundred small non-coding RNA molecules, known as microRNAs (miRNAs) have emerged as potential biomarkers and drug targets, appearing to be promising to the next generation of diagnostic and therapeutic tools.[1-3] These RNA molecules play important roles in modulating various biological and cellular functions and have potential to treat several pathologies such as cancer, cardiovascular and neurodegenerative diseases. This suggests the use of miRNA as a promising approach in a therapeutic point of view.[4-6] Human pre-miR-29b was chosen for this work because it belongs to one of the most interesting miRNA families identified in humans, being involved in several regulatory actions, namely in tumor-suppressing and immune-modulating processes, as well as in the regulation of pathways of neurodegenerative diseases.[5-7]

Hence, considering the potential therapeutic application and the mandatory global distribution of these novel therapeutics, it is crucial to develop efficient methods for isolation of pharmaceutical grade miRNAs, with high purity degree and biological activity, envisioning their application in gene therapy. Several strategies are available to isolate and purify miRNA molecules chemically synthesized or derived from various biological sources.[8,9] However, these methods make use of denaturing conditions and structural modifications in the RNA molecule can occur, by introduction of tag-sequences. Consequently, these changes can induce RNA conformational alterations which may compromise their activity, in addition, these procedures are expensive and time-consuming.[10,11] More recently, our research group developed an affinity chromatographic method with amino acids as specific ligands, named amino acid–affinity chromatography, applied to efficiently purify different RNA species (total RNA, ribosomal RNA, small RNA, 6S RNA and recombinant pre-miR-29b), on the basis of their biological function or individual chemical structure.[12-17] For these reasons, this chromatographic method can be an attractive approach for the miRNA purification, since it can be successfully employed in the purification of a wide range of biomolecules, based on specific and reversible interactions, simulating natural biological processes that are established within the cell. In addition, affinity chromatography is a selective and reliable technique, offering reduced processing time, and capable of preparing therapeutic biomolecules with the strict quality assurance.[18] However, the problem of finding a suitable ligand in affinity chromatography is not restricted to specificity, but concerns also to the binding strength and the kinetics of the ligand–miRNA interaction. This implies that a ligand with an optimized dissociation constant will facilitate the successful operation of affinity chromatography for miRNA purification.

In the past recent years, Cruz and collaborators applied surface plasmon resonance (SPR) for the analysis of the interaction between plasmid DNA and amino acids ligands.[19-22] This technique provides both equilibrium and kinetic information about intermolecular interactions and is a powerful tool to study the dynamics of nucleic acids–amino acids

interactions and, consequently, to apply this important structural data in the optimization of chromatographic systems.[23-26] According to these considerations, a comparative study was performed to characterize and understand the interactions established between pre-miR-29b and $_{L}$-arginine and $_{L}$-lysine amino acids. For this purpose, we have studied the affinity and the binding responses between pre-miR-29b and $_{L}$-arginine and $_{L}$-lysine immobilized on a surface to mimic the affinity support under different experimental conditions, such as, the composition and ionic strength of the elution, buffer and temperature. This study revealed several interesting characteristics of RNA molecules, including natural affinity interactions that can occur between $_{L}$-arginine and $_{L}$-lysine and pre-miRNA, providing important information that can be further applied in unveiling the miRNA chromatographic behavior in these systems. Furthermore, the experimental data allowed to get binding information to improve pre-miR-29b purification with low sample consumption, using a rapid and automated analysis. Moreover, circular dichroism (CD) was used to evaluate the conformational changes that pre-miR-29b may suffer when exposed to certain experimental conditions. In particular, experimental conditions can influence the interactions established between pre-miRNA and amino acids, as well as the structure of RNA, leading repulsion or neutralization of the biomolecules, or even inducing stabilization or denaturation of the target RNA.

The present work evaluates the conformational changes of pre-miR-29b when exposed to different experimental conditions by circular dichroism (CD) and the binding between the recombinant pre-miR-29b and L-arginine/L-lysine by surface plasmon resonance (SPR) in different buffers, salt conditions, pH and temperature to achieve the best binding/elution conditions.

Materials and Methods

Materials

$_{L}$-arginine–Sepharose 4B gel was acquired from Amersham Biosciences (Uppsala, Sweden) and Lysine-Sepharose 4B was obtained from GE Healthcare Biosciences (Uppsala, Sweden). The guanidinium salt and all the chemicals used in the lysis buffer were obtained from Sigma-Aldrich (St Louis, MO, USA). All buffers used for the chromatographic experiments were freshly prepared with sterilized water pre-treated with 0.05% diethyl pyrocarbonate (DEPC; Sigma-Aldrich, St Louis, MO, USA), filtered through a 0.20 μm pore size membrane (Schleicher Schuell, Dassel, Germany) and degassed ultrasonically. The sodium chloride (NaCl) used was purchased from Panreac (Barcelona, Spain), tris(hydroxymethyl) aminomethane (Tris), HEPES sodium salt and L-arginine were from Sigma-Aldrich (St Louis, MO, USA). L-lysine Hydrochloride was from USB, Acide morpholinopropanesulfonique (MOPS) from Fisher Scientific and, finally, potassium dihydrogen phosphate from Chem-Lab NV (Zedelgem, Belgium). All the materials used in the experiments were RNase-free.

Pre-miR-29b biosynthesis and isolation

The pre-miR-29b used in the experiments was produced by a cell culture of *Rhodovulum sulfidophilum* DSM 1374 strain (BCCM/LMG, Belgium) modified with the pBHSR1-RM plasmid containing the sequence of pre-miR-29b.[27] Growth was carried out at 30ºC under dark-aerobic conditions, using Nutrient Broth medium (1 g/L beef extract; 2 g/L yeast extract; 5 g/L peptone and 30 g/L sodium chloride) supplemented with 30 μg/mL kanamycin. Cells were recovered by centrifugation and stored at -20ºC. Small RNA was extracted using the acid guanidinium thiocyanate-phenol-chloroform extraction method based on the protocol described by Chomczynski and co-workers.[28] Briefly, cells were lysed by adding 5 mL of denaturing cell lysis solution (4 M guanidinium thiocyanate; 25 mM sodium citrate, pH 4.0; 0.5% *N*-laurosylsarcosine and 0.1 M β-mercaptoethanol). After incubating on ice for 10 min, cellular debris, genomic DNA and proteins were precipitated by gently adding and mixing 5 mL of water-saturated phenol and 0.5 mL of 2 M sodium acetate (pH 4.0). The RNA isolation was achieved by adding 1 mL of chloroform/isoamyl alcohol (49:1), and by mixing vigorously until two immiscible phases were obtained. The upper aqueous phase, which contained mostly RNA, was recovered and concentrated by the addition of 5 mL of ice-cold isopropanol. Precipitated molecules were recovered by centrifugation at 10 000 g for 20 min at 4ºC and resuspended in 1.5 mL of lysis solution. It was concentrated again with 1.5 mL of ice-cold isopropanol. After centrifuging for 10 min at 10 000 g (4ºC), the RNA pellet was washed with 7.5 mL of 75% ethanol and incubated at room temperature for 10 min, followed by a 5 min centrifugation at 10 000 g (4ºC). The air-dried RNA pellet was solubilized in 1 mL of 0.05% DEPC-treated water. Finally, 260 and 280 nm absorbance of the samples was measured using Nanodrop spectrophotometer in order to assess RNA quantity and an agarose gel electrophoresis was performed to assess purity.

Pre-miR-29b Purification

Chromatographic experiments were performed in an ÄKTA Avant system with UNICORN 6.1 software (GE Healthcare). A 10 mm diameter x 20 mm long (about 2 mL) column was packed with commercial L-arginine–Sepharose 4B gel. This support is characterized by the manufacturer as a cross-linked 4% beaded agarose matrix with a 12-atom spacer and an extent of labeling between 14 and 20 μmoL/mL. The column was first equilibrated with 0.28 M of NaCl in 10 mM Tris-HCl buffer (pH 8.0). Small RNAs samples (30 μg) were applied onto the column using a 100 μL loop at a flow-rate of 1 mL/min. After the elution of unbound species with 0.28 M of NaCl in 10 mM Tris-HCl buffer (pH 8.0), the ionic strength of the buffer was increased to 0.36 M NaCl in order to elute the pre-miR-29b. The most retained species were finally eluted with 0.5 M NaCl in 10 mM Tris-HCl buffer (pH 8.0), as previously described.[14] The absorbance of the eluate was continuously monitored at 260 nm. All chromatographic runs were performed at 20ºC, by using a specific column containing a water jacket tube connected to a circulating water bath to maintain the temperature. Pre-miR-29b fractions were pooled according to the chromatograms obtained, and were concentrated and desalted with Vivaspin concentrators. Posteriorly, the integrity and purity of pre-miR-29b samples isolated from *R. sulfidophilum* were also analyzed by vertical electrophoresis using an Amersham Biosciences system (GE Healthcare) with 10% polyacrylamide gel supplemented with 8 M urea. Electrophoresis was performed at a running voltage of 125 V for 90 min in TBE buffer, pH 8.3, and samples were previously denatured with 97.5% formamide. Gels were visualized using a UV transilluminator (UVItec, Cambridge) after staining with GreenSafe Premium (NZYTech, Lisbon, Portugal).

SPR measurements

All SPR experiments were performed on a Biacore T200 Biosensor software v 1.0 (Biacore, GE Healthcare, Sweden) using carboxymethylated dextran-coated sensor chips (CM5 research grade). L-arginine and L-lysine (0.2 M in 0.1 M borate buffer, pH 8.5) were immobilized on the CM5 sensor chip surface, to mimic immobilized ligands in affinity chromatographic supports, based on the protocol described by Cruz and co-workers.[19] Briefly, the immobilization of L-arginine and L-lysine was performed through amine coupling chemistry using HBS and 1-ethyl-3-(3-dimethylaminopropyl) carbodiimide (EDC) as a running buffer (7 min, 5 μL/min) in the flow cells 2 and 3, respectively. Flow cell 1 was used as reference control for all experiments, which was treated as the other cells, without amino acids. After immobilization, the surfaces of all flow cells were blocked with 1 M ethanolamine-HCl (pH 8.5), followed by HBS-EP injection to stabilize the baseline. The immobilized density averaging for L-arginine was 245.6 RU and for L-lysine was 242.2 RU. Human pre-miR-29b samples used to collect affinity binding data were prepared by serial dilutions to obtain the desired concentration range (2.5 to 0.0195 μM) with adequate buffers, for each experiment. Duplicate injections of each pre-miR-29b sample were analyzed in random order and a buffer blank was flowed over the L-arginine and L-lysine surface, as well as over the reference surface, at a flow rate of 2 μL/min for 7

min. No regeneration solution was required since all pre-miR-29b solutions were removed from the surface chip during the dissociation time. Thus, equilibrium binding experiments were performed under similar conditions to those used in the affinity chromatography assays (temperature, pH, ionic strength of the buffer and competitive ligand), in order to understand the biomolecular interactions occurring between ligands and pre-miR-29b. Several buffers were studied to determine which are suitable to be used with RNA allowing the establishment of interactions involved in miRNA purification, namely (i) 10 mM Tris-HCl, pH 8.0; (ii) 10 mM and 100 mM HEPES buffer, pH 7.4; (iii) 10 mM and 50 mM phosphate buffer, pH 8.0; (iv) 10 mM MOPS, pH 8.0; (v) 280 mM and 500 mM NaCl in 10 mM Tris-HCl, pH 8.0; (vi) 200 mM NaCl supplemented with 8 mM $_{L}$-arginine in 10 mM Tris-HCl, pH 8.0 and, finally, (vii) 200 mM NaCl supplemented with 10 mM $_{L}$-lysine in 10 mM Tris-HCl, pH 8.0. As previously mentioned, two different temperatures, 4 and 20ºC, were also investigated to address their influence on the interactions. To correct the bulk refractive index background, the signal obtained for the reference surface was subtracted from sensorgrams for the amino acid immobilized on cell surfaces. In addition, subtraction of the blank injection responses (running buffer without pre-miR-29b) was performed prior to each collection of binding data following exactly the same time course as the runs with pre-miR-29b. The equilibrium dissociation constants (K_D) were determined by averaging of the resonance unit values (RU) in the plateau region of the sensorgrams (300 to 400 sec) to an affinity model, $[R_{eq}]=R_{max}-(1/(1+K_D/[A])$, where R_{eq} represents the amount of analyte complexed with the ligand on the surface, [A] is the analyte concentration, and R_{max} is the maximum binding capacity of the surface. R_{max} was also determined by the previous mathematical model. All data processing and analyses were performed in BIAevaluation software v.4.1.

Structural analysis of pre-miR-29b samples by Circular Dichroism (CD)

CD was used to monitor the structural behavior of pre-miR-29b (50 µg/mL) when subjected at different buffer conditions. CD spectra were obtained using a quartz rectangular cell with an optical path length of 0.1 cm at a constant temperature of 25ºC, in a Jasco J-1850 Spectrophotometer (Jasco, Easton, MD, USA). Spectra were recorded from 320 to 215 nm at a scan speed of 10 nm/min and a spectral bandwidth of 1 nm. All measurements were conducted under a constant nitrogen gas flow, to purge the ozone generated by the light source of the instrument. The data were collected in triplicate and the average spectra are presented for each sample after subtraction of the buffer contribution. The CD signal was converted to molar ellipticity. Noise in the data was smoothed using Jasco J-1850 software, including the Fast Fourier transform algorithm, which allows enhancement of most noisy spectra without distorting their peak shape.

Results and Discussion

MiRNAs represents an important target of a wide analysis, particularly relevant, in the diagnostic of several disorders, as well as in basic and applied science research. For this reason, the preparation of highly purified miRNAs in large quantity arises as one of the most important challenges in the development of therapeutic strategies based on the use of miRNAs.[29] In this study, pre-miR-29b biosynthesis was obtained from a cell culture of recombinant *Rhodovulum sulfidophilum* DSM 1374 strain in a standard bacterial culture.[15] However, the RNAs obtained from this culture need to be further purified in order to isolate the target pre-miR-29b from other host sRNAs. Thus, pre-miR-29b isolation was achieved using an increasing sodium chloride gradient in L-arginine-affinity chromatography, as described by Pereira and co-workers.[14] The quality of the pure pre-miR-29b stock solution was examined by polyacrylamide gel electrophoresis, as shown in Fig. 1. In affinity chromatography, elution strategy can be performed either specifically, using a competitive agent, or non-specifically, by changing the pH, ionic strength or polarity of the buffer.

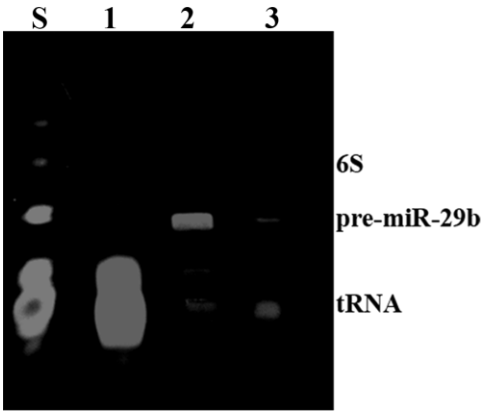

Figure 1 – Polyacrylamide gel electrophoresis analysis of pure pre-miR-29b samples. Lane S, Initial sample; Lanes 1, transfer RNAs; Lane 2, pre-miR-29b; Lane 3, pre-miR-29b plus transfer RNAs.

Hence, this SPR study was developed in order to characterize the interactions between pre-miR-29b and L-arginine and L-lysine as biospecific ligands. For this purpose, changes in the elution buffer composition, ionic strength or temperature were performed in order to observe their effects on biomolecular interactions. The amino acids L-arginine and L-lysine were chosen because they are conserved amino acids in the active center of the Argonaute protein, which is part of the RNA-induced silencing complex (RISC), suggesting that they have an important role in the cellular recognition of the 3' overhang of the pre-miRNA.[30,31] So, it is expected that this biorecognition can be exploited to implement a chromatographic purification methodology for pre-miR-29b. Initially, L-arginine and L-lysine were immobilized on CM5 sensor chip via amine coupling chemistry at pH 8.5 (below their isoelectric point), as

described by Cruz and collaborators.[19] This protocol of immobilization ensures that the guanidine functional groups (ε-amino group) of L-arginine and L-lysine are positively charged and the α-NH_2 group is attached to the reactive ester groups of the chip. All SPR equilibrium data were fitted to a steady state bimolecular interaction model. The SPR binding profile (square-shaped) was identical for all complexes and some were exemplified in Fig. 2.

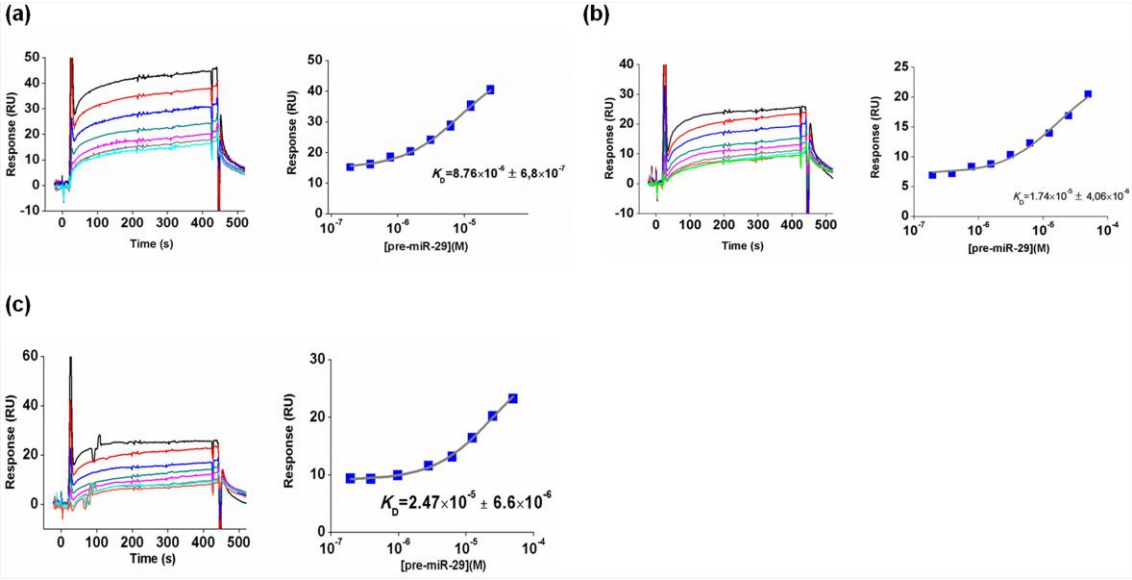

Figure 2 - SPR analysis of pre-miR-29b interaction with L-lysine ligands in different buffers, at 4 and 20ºC. Sensorgrams and equilibrium-binding analysis: (a) 10 mM Tris-HCl buffer (4ºC), (b) 10 mM MOPS (20ºC) and (c) 10 mM HEPES (20ºC).

Biomolecular Interactions between pre-miR-29b and L-arginine

Recently, our research group has demonstrated the potential of the arginine amino acid in the purification of RNA, suggesting that the binding mechanism involves multiple non-covalent interactions with RNA, due to its ability to interact in different conformation arrangements, the length of its side chain, the guanidine functional group and its ability to produce hydrogen bond geometries.[12,17,32] Thereby, since RNA is negatively charged due to the phosphate groups in the backbone, it is easy to predict favorable electrostatic interactions between RNA phosphate groups and L-arginine.

Interestingly, the SPR sensorgrams obtained with L-arginine ligand, present response profiles in shaped of square, indicating rapid dissociation (450 sec), i.e., the binding assays suggest that pre-miR-29b biomolecules interact with the immobilized L-arginine, and that these interactions are reversible. The K_D values are listed in Table 1. At 20ºC, in the range of concentrations tested, SPR responses for L-arginine-pre-miR-29b were obtained in Tris-HCl, NaCl and NaCl supplemented with L-lysine buffers. The equilibrium dissociation constants demonstrate that Tris-HCl (10 mM) promote lower ligand–analyte affinity (K_D =

$5.11x10^{-6}\pm4.4x10^{-7}$ M) when compared with the values obtained for NaCl (K_D = $4.06x10^{-7}\pm3.5x10^{-8}$ M). In fact, in chromatography, the Tris-HCl buffer can be used to promote the retention of total small RNAs onto the L-arginine support, but the application of NaCl in the binding buffer is responsible for the higher selectivity towards the target miRNA. On the other hand, negligible (≤ 5 RU) non-specific binding was detected when using the following buffers: phosphate (10 and 50 mM), HEPES (10 and 100 mM) and MOPS (10 mM), regardless of their concentration, indicating that L-arginine do not interact with pre-miR-29b under these conditions (data not shown).

In contrast, the ionic strength of buffer (10 mM Tris-HCl supplemented with NaCl) has a significant effect on the binding of pre-miR-29b. The SPR response to the pre-miR-29b solution in 500 mM NaCl was very low (< 5 RU), implying that the chromatographic binding and elution of pre-miR-29b may be manipulated with this parameter. In the sensorgrams was notorious the dissociation in the first 100 sec using 500 mM NaCl (data not shown), indicating that the high content of NaCl results in the loss of pre-miR-29b binding. Our results also revealed that when a moderate salt concentration (280 mM NaCl) is used, high binding responses were obtained (K_D = $4.06x10^{-7}\pm3.5x10^{-8}$ M). In general, the affinity of the pre-miR-29b with the L-arginine surface was high ($K_D \geq 10^{-6}$ M) at 20ºC. These results may be correlated with the chromatographic experiments, where the total retention of pre-miR-29b could be achieved using a low concentration of NaCl (280 mM) and high concentrations (500 mM NaCl) lead to its elution.[14] Besides, the salt concentration can also have a positive effect on RNA folding as well as on the stabilization of non-covalent RNA–amino acid interactions during the purification, once the salt allows the single-stranded nucleic acid molecules to form stable hydrogen bonds between their complementary bases. In this case, the chromatographic interaction was promoted by using a low ionic strength buffer and the selective elution of the bound species was achieved by increasing the NaCl concentration.[14] Moreover, it was verified that the pre-miR-29b was eluted at a higher ionic strength, indicating a stronger interaction than other contaminants. We also evaluated the influence of a competing agent (L-arginine and L-lysine) in the buffer, as a way to conclude about the use of these amino acids to promote binding or elution of the pre-miR-29b to the L-arginine ligand. The experiments were carried out using different concentrations, from 8 to 19 mM of L-arginine and 10 to 16 mM of L-lysine in the 200 mM NaCl buffer. However, for the highest concentrations it was not verified the binding of pre-miR-29b to the L-arginine ligand (results not shown). In these experiments, it was only obtained a binding response for the condition of 10 mM of L-lysine in 200 mM NaCl (K_D = $3.53x10^{-6}\pm1.9x10^{-7}$ M), while 8 mM of L-arginine resulted in a negligible (≤ 5 RU) sensor response to the pre-miR-29b solution. This result is in accordance with some evidences obtained in L-arginine-affinity chromatography, once this condition can be used to the pre-miR-29b elution, as it functions as a competitive agent. This behavior can be due to the positive character of these amino acids that promotes the binding of pre-miR-29b to the free amino acid present in the buffer by electrostatic interactions,

inducing the elution of bound pre-miR-29b. Moreover, the results suggest that the elution of bound pre-miR-29b can be more effective when using L-lysine in the buffer. As demonstrated in Table 1, the K_D value for 10 mM L-lysine is higher than the value obtained at 280 mM NaCl, indicating that the affinity of pre-miR-29b to the L-arginine ligand is higher for the 280 mM NaCl condition, and lysine is expected to weaken the interaction.

Considering that RNA is an unstable molecule and has a very short half-life once extracted, the effect of temperature in the miRNA-arginine binding is a critical parameter in RNA purification.[33] In contrary to the results achieved for the temperature of 20ºC, at 4ºC it was only found SPR response for L-arginine and pre-miR-29b using 10 mM Tris-HCl buffer. The dissociation constants for Tris-HCl are of the same order of magnitude at 20 and 4ºC (K_D = $1.34x10^{-6}$±$2.3x10^{-7}$ M), but a slightly higher affinity was found for 4ºC, suggesting stronger interactions at lower temperatures. Non-specific binding (≤ 5 RU) was detected when using the other buffers, regardless their concentration, indicating that no significant interactions occur between pre-miR-29b and L-arginine ligand in these conditions (data not shown). The K_D values obtained are consistent with the chromatographic results previously reported by Pereira and collaborators[14], where the pre-miR-29b retention in the L-arginine-agarose support was higher for the lowest temperature studied (4ºC), suggesting that the temperature is a critical factor in the binding pre-miR-29b.

Summarizing, the affinity order of pre-miR-29b to L-arginine was 280 mM NaCl > 10 mM Tris-HCl ≈ 10 mM L-lysine in 200 mM NaCl, with NaCl promoting the highest affinity for the pre-miR-29b to the L-arginine surface. Hence, this comparative study reinforces the idea that the binding mechanism inherent to the biorecognition between the L-arginine amino acid and pre-miR-29b molecules can result from the combination of several phenomenological interactions such as electrostatic interactions, multiple hydrogen bond and van der Waals forces.[17] Thus, it is reasonable to suggest that the retention of RNA in L-arginine is due to its side chain, which can promote multi contacts with RNA backbone or bases, according to RNA folding.[32,34,35] Additionally, recent studies with saturation transfer difference-nuclear magnetic resonance spectroscopy and SPR reported that guanine polynucleotides interact preferably with L-arginine through the sugar-phosphate backbone.[18,19] Thus, another explanation for these findings is related with pre-miR-29 structural features that seem to be relevant on its distinct retention behavior in the arginine ligand. Pre-miR-29b is a small RNA molecule with a stem-loop shape consisting of two long irregular double-stranded stem regions, which are interrupted by a largely single-stranded internal loop. In addition, along the bulge of pre-miR-29b and through the continuous stem sequences there are several guanines, which were described to interact preferably with arginine. Hence, the nucleotide bases composition and exposure can also favor other biomolecular interactions, responsible for the specificity and biorecognition found in the L-arginine ligand.

Table 1 – Equilibrium analysis of the pre-miR-29.

		Buffers					
		Tris-HCl (10 mM)	**MOPS (10 mM)**	**HEPES (10 mM)**	**NaCl (280 mM)**	**L-arginine (8 mM)**	**L-lysine (10 mM)**
L-arginine	**20ºC**	$5.11\times10^{-6}\pm4.4\times10^{-7}$	-	-	$4.06\times10^{-7}\pm3.5\times10^{-8}$	-	$3.53\times10^{-6}\pm1.9\times10^{-7}$
	4ºC	$1.34\times10^{-6}\pm2.3\times10^{-7}$	-	-	-	-	-
L-lysine	**20ºC**	$3.24\times10^{-7}\pm4.6\times10^{-8}$	$1.74\times10^{-5}\pm4.1\times10^{-6}$	$2.47\times10^{-5}\pm6.6\times10^{-6}$	$9.96\times10^{-7}\pm3.5\times10^{-8}$	$2.08\times10^{-6}\pm4.4\times10^{-7}$	$2.28\times10^{-6}\pm6.3\times10^{-7}$
	4ºC	$8.76\times10^{-6}\pm6.8\times10^{-7}$	$2.31\times10^{-5}\pm3.1\times10^{-6}$	$3.95\times10^{-6}\pm1.5\times10^{-7}$	-	-	-

Biomolecular Interactions between pre-miR-29b and L-lysine

Previous studies have shown that the main interactions occurring between nucleic acids and the L-lysine amino acid are electrostatic, because of its amine groups.[36-38] Moreover, L-lysine has also some characteristics, such as the lateral side chain with significant length and ability to interact with several RNA classes even in different conformational rearrangements, which may produce hydrogen bond geometries, reinforcing the establishment of multiple non-covalent interactions involved in the specific recognition mechanism of nucleic acids.[38] Indeed, besides the multiple interactions (electrostatic interactions, van de Waals forces and hydrogen bonds) that L-lysine can establish with the RNA backbone or with the more exposed bases, several sRNAs can also interact and be recognized by the presence of hydrophobic interactions with the aliphatic portion of L-lysine side chain.[15] Considering this complex biorecognition mechanism, it is important to study the influence of experimental conditions on the interaction occurring between pre-miR-29b and L-lysine amino acid, resulting in different binding affinities. It was verified that pre-miR-29b binds more strongly to L-lysine in 10 mM Tris-HCl and 280 mM NaCl at 20ºC (K_D = 3.24x10^{-7}±4.6x10^{-8} M and K_D = 9.96x10^{-7}±3.5x10^{-8} M, respectively) than in 10 mM HEPES (K_D = 2.47×10^{-5}±6.6×10^{-6} M) or 10 mM MOPS buffers (K_D = 1.74×10^{-5}±4.1×10^{-6} M). In fact, these findings are in agreement with the results reported in the literature, where Tris-HCl buffer is commonly used to promote the binding of RNA to L-lysine. Negligible binding (≤ 5 RU) was detected when the following buffers were used: phosphate (10 mM and 50 mM) and HEPES (100 mM), indicating that pre-miR-29b has no affinity to L-lysine under these conditions. Similarly to the results obtained to L-arginine, the ionic strength of buffer (10 mM Tris-HCl supplemented with NaCl or with amino acids) has an effect on the binding of pre-miR-29b to L-lysine. Our findings demonstrate that when high concentrations of salt (500 mM NaCl) or amino acids are used, no binding responses of pre-miR-29b are observed and, consequently, these conditions can be used for the elution of the target biomolecule in chromatography. The addition of 10 mM of L-lysine in 200 mM NaCl resulted in a binding response characterized by K_D = 2.28x10^{-6}±6.3×10^{-7} M and the supplementation with 8 mM of L-arginine in 200 mM NaCl resulted in a K_D = 2.08x10^{-6}±4.4×10^{-7} M. Although these concentrations of competing agents induce binding of pre-miR-29b, the interaction is weaker when compared with Tris-HCl. Briefly, the affinity order for pre-miR-29b binding to L-lysine was 10 mM Tris-HCl ≈ 280 mM NaCl > 10 mM L-lysine ≈ 8 mM L-arginine in 200 mM NaCl > 10 mM HEPES ≈ 10 mM MOPS, thus Tris-HCl and NaCl buffers induced the greater affinity to L-lysine surface, followed by HEPES and MOPS (Table 1).

In this study it was also evaluated the effect of decreasing the temperature to 4ºC on the binding of pre-miR-29b to the L-lysine surface, comparing with the binding at 20ºC. The binding responses is similar to that obtained at 20ºC, illustrating that the interactions between L-lysine and pre-miR-29b also occur under these conditions. However, some differences were found in K_D values determined at 4ºC (3.24x10^{-7} M to 8.76x10^{-6} M for 10 mM Tris-HCl; 2.47x10^{-5} M to 3.95x10^{-6} M for 10 mM HEPES and 1.74x10^{-5} to 2.31x10^{-5} M for 10 mM

MOPS, at 20 and 4ºC, respectively). In general, the K_D values obtained are consistent with the chromatographic results, which the lowest temperature studied induced higher pre-miR-29b retention onto the L-lysine-agarose support (data not shown). Globally, these results can also be related with the pre-miRNA structure, which presents continuous stem sequences mostly containing guanines that are described to preferentially interact with L-lysine due to hydrogen bonds that are established with one of the donor atoms.[39,40]

Briefly, to compare the salt influence on the binding of pre-miR-29b to the L-arginine and L-lysine surfaces, several buffers were analyzed. In general, the maximum RU signal was higher for the L-lysine than for the L-arginine surface (Fig. 3).

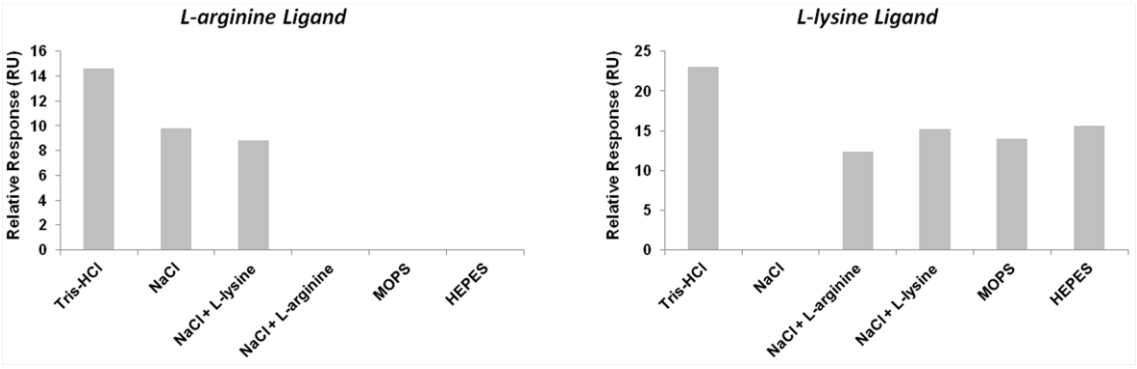

Figure 3 - Relative resonance response (RU) with different running buffers at 450 s after injection of pre-miR-29b at a concentration of 1.25 µM, at 20ºC, in L-arginine and L-lysine surfaces.

The experiments showed a low resonance response level with both surfaces (normalized signal). It was found that the maximum binding between pre-miR-29b and immobilized L-arginine and L-lysine was observed in 280 mM NaCl, followed by 10 mM Tris-HCl, whereas the lowest binding was observed in 200 mM NaCl supplemented with 8 mM L-arginine or 10 mM L-lysine, 10 mM HEPES and 10 mM MOPS (Fig. 3). Thus, our affinity data show that Tris-HCl and NaCl are optimal buffers for interaction assays and distinct buffer environments such as MOPS or HEPES did not enhanced the binding to L-arginine and L-lysine. Overall, these results provide suitable conditions to induce pre-miRNA binding, thereby increasing the selectivity and improving efficient microRNA separation. It was also proved that under these conditions (ionic strength and buffer composition) the electrostatic interactions are favored between the amino positive groups of the L-arginine and L-lysine and the negative phosphate groups of the pre-miR-29b, mainly with guanosine.

These results demonstrated that SPR allows making a screening of ligands that, like the ones described herein, can be used to design and implement novel miRNA purification methods.

Pre-miR-29b structural analysis

Both ligands promoted the biorecognition of pre-miR-29b as well as an effective interaction for most conditions studied. To select the buffer that is able to enhance the pre-miR-29b binding to the amino acids ligands and to evaluate the effect of the different conditions in the pre-miR-29b structural stability, four buffers were analyzed (Tris-HCl, HEPES buffer, MOPS, phosphate buffer) by circular dichroism (CD) spectroscopy. Thus, structural characterization of the pre-miR-29b under different experimental conditions give additional information about the interactions with the ligands and also about the suitable conditions that must be used in chromatographic procedures to purify the target biomolecules while maintaining its stability and biological activity. CD technique offers good resolution, provides sensitive spectra and it has been widely used in structural determination of biomolecules (proteins, nucleic acids, etc.). Quantitative analysis of CD spectra is possible, but, as with any assay, the correct and proper interpretation of the results depends on an accurate understanding of the procedure. The spectra in Figure 4 are given in terms of molar ellipticity thus making it possible to directly compare the intensity of the bands obtained for different samples. CD spectra of the pre-miR-29b show characteristic peaks around 210 nm (negative maximum signal) and 265 nm (positive maximum signal). The comparison with the CD spectrum of established nucleic acids structures confirms that the pre-miRNA possesses a stem-loop structure because the CD spectral pattern typically indicates the B-form RNA duplex.[15,41] Although, CD is not sensible to detect the contamination of other cytosol containing miRNAs, it is sensible to detect the contamination of other biomolecules. However, the pre-miR-29 subjected to this analysis has a purity of 98%, and it is unlikely that the sample is contaminated, being not expected changes in the CD spectra resulting from contamination.

In Figure 4 are shown the CD spectra resulting from the evaluation of pre-miR-29b in four buffers, after an initial 15 min incubation in Tris-HCl buffer (10 mM) and HEPES (10 mM). The CD spectra of the pre-miRNA sample in Tris-HCl and HEPES show typical CD spectrum of RNA, with a positive band at 265 nm and a negative band at 210 nm, similar to the obtained with DEPC water. However, a significant difference in the bands magnitude of the pre-miR-29b spectra was found (Figure 4).

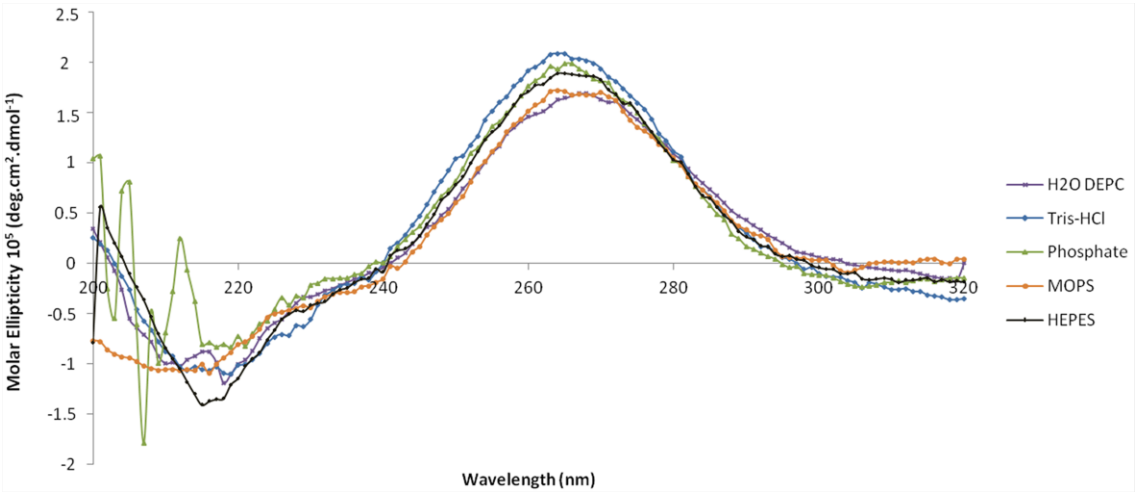

Figure 4 - Circular Dichroism spectra of the pre-miR-29b.

These results are consistent with the responses obtained with SPR, suggesting that Tris-HCl is a valuable choice for promoting pre-miRNA–$_L$-arginine/lysine binding interactions in future applications. In the presence of HEPES or MOPS, the electrostatic interaction between the $_L$-arginine and $_L$-lysine surface and the pre-miR-29b backbone could be more favored, since these buffers at neutral pH are a zwitterionic molecule with a positive charge on one of the protonated nitrogens. This can reduce the repulsive electrostatic interaction between charged phosphate groups of pre-miR-29b, stabilizing the pre-miRNA molecule and favoring the interaction with the amino acids. By analyzing the CD spectra of pre-miR-29b in MOPS (10 mM), it is visible a decrease of intensity of the positive band as well as the negative band. By the CD spectra analysis of Figure 4, it is evident a strong modification in the RNA structure for the phosphate buffer. This data can also justify why pre-miR-29b molecules don't interact with the $_L$-arginine or $_L$-lysine supports in the presence of phosphate buffer due to the increase of the repulsions with the pre-miR-29b backbone. In contrast, in the presence of salt (280 mM NaCl), phosphate groups of the pre-miR-29b backbone are effectively screened by the salt counterions resulting in a more compact and less regular structure. The data obtained from SPR can play an important role in the optimization of chromatographic-based purification processes since it allows the determination of which buffers favor interactions of the target biomolecule with the chromatographic support. Moreover, the conjugation with the CD technique allows the confirmation of which buffers are able to maintain the stability of the miRNA.

Conclusions

The binding affinity quantification between pre-miR-29b and $_L$-arginine and $_L$-lysine surfaces was examined by SPR technique, under different conditions, in order to mimic the immobilized ligand onto an affinity chromatographic support, and to verify the effect of these conditions on the interactions and stability of the molecule. Therefore, several experimental conditions for amino acids ligands-pre-miR-29b binding were characterized, and an optimal set of buffers as well as temperature conditions were defined. Distinct buffers affected the interaction strength with an increased response in presence of Tris-HCl and NaCl. These results provide suitable conditions to induce pre-miRNA binding, thereby increasing the selectivity and improving efficient miRNA separation. The predominant interactions of pre-miR-29b with $_L$-arginine and $_L$-lysine ligands are ionic between the amino positive groups of the $_L$-arginine and $_L$-lysine and the negative phosphate groups of the pre-miR-29b and hydrogen bonds with the more exposed bases, mainly with guanosine. Overall, the present study showed that SPR can be used as a first technique to screen, manipulate, determine and establish the best binding/elution conditions that can lead to an improved performance and selectivity of the chromatographic process. In addition, it was demonstrated that although some conditions used in chromatographic experiments favor multiple interactions between the pre-miR-29b and the respective ligand ($_L$-arginine and $_L$-lysine), these conditions can affect the structural stability of the target molecule. From CD, it was possible to conclude that the biorecognition observed by the pre-miR-29b can be related to the higher availability and base exposition, which confers a different conformational structure of this molecule. Moreover, the highest equilibrium dissociation constants determined by SPR ranged from 10^{-6} to 10^{-7} M to $_L$-arginine and from 10^{-5} to 10^{-7} M to $_L$-lysine, indicating that pre-miR-29b showed high binding affinity on these surfaces. In addition, the results obtained in this study, provide valuable and relevant information that can be further applied in unveiling the miRNA chromatographic behavior in these systems, in order to improve the binding of the pre-miR-29b onto the amino acids-based supports, preserving their structural stability, integrity and activity. In conclusion, it was proved that the association of these two techniques might be a powerful strategy to define the best conditions to be applied in the miRNA purification.

Acknowledgments

This work was supported by the Portuguese Foundation for Science and Technology (FCT), through the projects EXPL/BBB-BIO/1056/2012, Pest-OE/SAU/UI0709/2014 and FCOMP-01-0124-FEDER-041068 – EXPL/QEQ-MED/1068/2013. Patrícia Pereira and Carla Cruz acknowledge the fellowships, SFRH/BD/81914/2011 and SFRH/BPD/100015/2014, respectively from FCT. The authors also acknowledge the program Fundo Europeu de Desenvolvimento Regional (FEDER) [COMPETE [FCOMP-01-0124-FEDER-027560]].

References

1. D. P. Bartel, *Cell*, 2004, **116**, 281-297.
2. J. A. Broderick and P. D. Zamore, *Gene therapy*, 2011, **18**, 1104-1110.
3. A. Eulalio and M. Mano, *Journal of biomolecular screening*, 2015, DOI: 10.1177/1087057115578837.
4. C. L. Bartels and G. J. Tsongalis, *Clinical chemistry*, 2009, **55**, 623-631.
5. M. V. Latronico and G. Condorelli, *Nature reviews. Cardiology*, 2009, **6**, 419-429.
6. P. T. Nelson, W. X. Wang and B. W. Rajeev, *Brain Pathol*, 2008, **18**, 130-138.
7. L. Du and A. Pertsemlidis, *J Mol Cell Biol*, 2011, **3**, 176-180.
8. I. Vomelova, Z. Vanickova and A. Sedo, *Folia biologica*, 2009, **55**, 243-251.
9. M. A. Dineva, L. MahiLum-Tapay and H. Lee, *The Analyst*, 2007, **132**, 1193-1199.
10. L. Ponchon and F. Dardel, *Methods*, 2011, **54**, 267-273.
11. S. C. Walker, F. H. Scott, C. Srisawat and D. R. Engelke, *Methods Mol Biol*, 2008, **488**, 23-40.
12. R. Martins, C. J. Maia, J. A. Queiroz and F. Sousa, *J Sep Sci*, 2012, **35**, 3217-3226.
13. R. Martins, J. A. Queiroz and F. Sousa, *Journal of molecular recognition : JMR*, 2010, **23**, 519-524.
14. P. Pereira, A. Sousa, J. Queiroz, I. Correia, A. Figueiras and F. Sousa, *J Chromatogr B Analyt Technol Biomed Life Sci*, 2014, **951-952**, 16-23.
15. P. Pereira, A. Sousa, J. Queiroz, A. Figueiras and F. Sousa, *J Chromatogr A*, 2014, **1331**, 129-132.
16. R. Martins, J. A. Queiroz and F. Sousa, *Biomedical chromatography : BMC*, 2012, **26**, 781-788.
17. R. Martins, J. A. Queiroz and F. Sousa, *Journal of chromatography. A*, 2014, **1355**, 1-14.
18. F. Sousa, D. M. Prazeres and J. A. Queiroz, *Trends Biotechnol*, 2008, **26**, 518-525.
19. C. Cruz, E. J. Cabrita and J. A. Queiroz, *Anal Bioanal Chem*, 2011, **401**, 983-993.
20. C. Cruz, S. D. Santos, E. J. Cabrita and J. A. Queiroz, *International journal of biological macromolecules*, 2013, **56**, 175-180.
21. C. Cruz, A. Sousa, E. Mota, F. Sousa and J. A. Queiroz, *Int J Biol Macromol*, 2014, **70**, 131-137.
22. C. Cruz, A. Sousa,F. Sousa, J.A. Queiroz, *Anal Methods*, 2013, **5**, 1682-1686.
23. C. T. Campbell and G. Kim, *Biomaterials*, 2007, **28**, 2380-2392.
24. P. S. Katsamba, S. Park and I. A. Laird-Offringa, *Methods*, 2002, **26**, 95-104.
25. B. Nguyen, F. A. Tanious and W. D. Wilson, *Methods*, 2007, **42**, 150-161.
26. J. Hwang and S. Nishikawa, *Journal of biomolecular screening*, 2006, **11**, 599-605.
27. H. Suzuki, S. Umekage, T. Tanaka and Y. Kikuchi, *J Biosci Bioeng*, 2011, **112**, 458-461.
28. P. Chomczynski and N. Sacchi, *Nature protocols*, 2006, **1**, 581-585.
29. D. P. Bartel, *Cell*, 2009, **136**, 215-233.

30. F. V. Rivas, N. H. Tolia, J. J. Song, J. P. Aragon, J. Liu, G. J. Hannon and L. Joshua-Tor, *Nat Struct Mol Biol*, 2005, **12**, 340-349.
31. S. Griffiths-Jones, *Methods Mol Biol*, 2006, **342**, 129-138.
32. J. D. Puglisi, J. R. Wyatt and I. Tinoco, Jr., *Biochemistry*, 1990, **29**, 4215-4226.
33. F. RE, *RNA methodologies - Laboratory Guide for Isolation and Characterization*, Academic Press, York, USA, 4th edn., 2005.
34. B. J. Calnan, B. Tidor, S. Biancalana, D. Hudson and A. D. Frankel, *Science*, 1991, **252**, 1167-1171.
35. T. Janas, J. J. Widmann, R. Knight and M. Yarus, *RNA*, 2010, **16**, 805-816.
36. A. Sousa, F. Sousa and J. A. Queiroz, *J Chromatogr B Analyt Technol Biomed Life Sci*, 2011, **879**, 3507-3515.
37. A. Sousa, F. Sousa and J. A. Queiroz, *J Chromatogr B Analyt Technol Biomed Life Sci*, 2009, **877**, 3257-3260.
38. D. S. Jones, H. K. Lundgren and F. T. Jay, *Nucleic Acids Res*, 1976, **3**, 1569-1576.
39. J. J. Ellis, M. Broom and S. Jones, *Proteins*, 2007, **66**, 903-911.
40. M. M. Hoffman, M. A. Khrapov, J. C. Cox, J. Yao, L. Tong and A. D. Ellington, *Nucleic Acids Res*, 2004, **32**, D174-181.
41. B. Ranjbar and P. Gill, *Chem Biol Drug Des*, 2009, **74**, 101-120.

Paper V

New approach for purification of pre-miR-29 using lysine-affinity chromatography

P. Pereira, A. Sousa, J. A. Queiroz, A. Figueiras, F. Sousa

Journal of Chromatography A. 2014. 1331: 129-132

Short description: This article describes a new strategy employing a lysine-agarose support to efficiently separate recombinant pre-miR-29b from a complex mixture containing small RNAs. Besides this novelty, it is further described for the first time the use of ammonium sulfate in this matrix for the purification of nucleic acids. Overall, it was verified that lysine ligand can promote a specific interaction with the pre-miR-29b, thus favoring its isolation and purification.

Journal of Chromatography A, 1331 (2014) 129–132

Contents lists available at ScienceDirect

Journal of Chromatography A

journal homepage: www.elsevier.com/locate/chroma

Short communication, Col Liquid Chromatography

New approach for purification of pre-miR-29 using lysine-affinity chromatography

Patrícia Pereira [a], Ângela Sousa [a], João Queiroz [a], Ana Figueiras [a,b], Fani Sousa [a,*]

[a] CICS-UBI – Health Sciences Research Centre, University of Beira Interior, Avenida Infante D. Henrique, 6200-506 Covilhã, Portugal
[b] CEF-FFUC – Pharmaceutical Studies Center, Faculty of Pharmacy, University of Coimbra, Pólo das Ciências da Saúde, Azinhaga de Santa Comba, 3000-548 Coimbra, Portugal

ARTICLE INFO

Article history:
Received 18 November 2013
Received in revised form 6 January 2014
Accepted 10 January 2014
Available online 17 January 2014

Keywords:
Affinity chromatography
Lysine-agarose
microRNA
pre-miR-29
RNA purification

ABSTRACT

miRNA-based gene therapy applications require microRNA with high purity degree, good quality and biologically active. Owing to the commercial interest in these approaches, there is a growing interest in the development of innovative procedures to easily and efficiently purify the RNA. Thus, several chromatographic and non-chromatographic methods have been reported to accomplish this purpose, but not all of these strategies allow the efficient separation of miRNAs. The present study describes a new strategy that uses a lysine ligand in affinity chromatography to efficiently separate pre-miR-29 from a small RNAs mixture. The interest on this biomolecule is related to the fact that pre-miR-29 deficiencies or excesses have been associated to a number of clinically important diseases. The retention behaviour of pre-miR-29 was characterized and adjusted to achieve higher specificity in this chromatographic operation, using an ammonium sulfate stepwise gradient. Overall, it was verified that lysine-agarose support can promote a specific interaction with the pre-miR-29 favouring its total separation. The results also suggest that the underlying mechanism involves biorecognition of pre-miR-29 by the lysine ligands, resulting from the occurrence of different elementary interactions, including hydrogen and hydrophobic interactions.

1. Introduction

Currently, microRNA (miRNA) is considered a powerful biological material that is directly involved in performing or controlling many biological functions [1]. Thus, understanding the role of several miRNAs present in cellular processes is critical to develop new diagnosis methods or drugs for comprising and treating illness. Recently, differential expression of miRNAs, in patients with Alzheimer's disease (AD) suggests that they might have key regulatory roles in this neurodegenerative disease [2]. Hebert and collaborators showed that miR-29 is potentially involved in the regulation of β-amyloid precursor protein-converting enzyme 1 (BACE1) expression because *in vitro* studies revealed that miR-29 cluster was significantly decreased in AD patients displaying abnormally high BACE1 protein levels, leading the generation and subsequent accumulation of β-amyloid [3]. These findings raised the possibility to use miR-29 as a potential therapeutic target for AD therapy. In fact, miRNAs play a prominent role in the posttranscriptional regulation of gene expression, since it prevents protein synthesis by inducing the messenger RNA degradation, with a high specificity degree [3]. Nevertheless, to get pre-miR-29 as a suitable product for therapeutic applications it is necessary to guarantee its purity, stability and integrity. Regardless of the principle of RNA isolation used, purification protocols have a number of common requirements, because it is a critical process due to the high risk of RNA degradation during the procedure, by the presence of RNA degrading enzymes, once RNA molecule is very susceptible to chemical and enzymatic degradation [4].

Hence, several kits are commercially available for miRNA isolation from a diverse variety of samples; these methods allow the separation of miRNAs from high molecular weight RNA [4]. Furthermore, there are several chromatographic methods reported in the literature for the purification of the RNAs [5,6]. In these methods, different tags are introduced into RNA molecules, which subsequently have to be released from the chromatographic support by competitive elution or cleaved off by a protease [5,6], which may induce conformational changes in RNA and are expensive procedures. The approach to overcome these limitations includes the recent development, by our research group, of an affinity chromatographic (AC) method with amino acids as specific ligands, applied for plasmid DNA [7–9] and RNA [10] purification allowing an improvement in the purification technologies since this technique exploits natural biological processes of specific recognition of the target biomolecules [11].

In this study, a lysine-agarose support was tested to purify pre-miR-29 from a complex mixture containing small RNAs (sRNAs)

* Corresponding author. Tel.: +351 275 329 074; fax: +351 275 329 099.
E-mail address: fani.sousa@fcsaude.ubi.pt (F. Sousa).

0021-9673/$ – see front matter © 2014 Elsevier B.V. All rights reserved.
http://dx.doi.org/10.1016/j.chroma.2014.01.033

of *Rhodovulum sulfidophilum*. In 1978, Jones et al. [12] employed the lysine ligand to separate RNA species with different molecular weights, using a linear gradient of sodium chloride (NaCl). Building on these considerations, it is interesting to verify if the lysine matrix may contribute to the separation of pre-miR-29 and to understand the interaction mechanism underlying the specificity of the support that allowed a biorecognition of the pre-miR-29. Therefore, this matrix allowed the efficient isolation and purification of pre-miR-29 from the other sRNAs. These findings will strengthen the possibility of using lysine-affinity chromatography as a potential enabling technology in the downstream process of pre-miRNA for therapeutic applications.

2. Materials and methods

2.1. Pre-miR-29 production and purification

The pre-miR-29 used in the experiments was produced by a cell culture of *Rhodovulum sulfidophilum* DSM 1374 strain (BCCM/LMG) modified with the plasmid pBHSR1-RM [13] containing the sequence of pre-miR-29. Growth was carried out at 30 °C, using Nutrient Broth medium (1 g/L beef extract; 2 g/L yeast extract; 5 g/L peptone and 5 g/L NaCl) supplemented with 30 μg/mL kanamycin. sRNA was extracted using the acid guanidinium thiocyanate-phenol-chloroform method based on the protocol described by Martins et al. [10]. Chromatographic experiments were performed in an ÄKTA Avant system with UNICORN 6 software (GE Healthcare). A 10 mm diameter × 20 mm long (about 2 mL) column was packed with Lysine-agarose matrix (GE Healthcare). All solutions were freshly prepared using 0.05% diethyl pyrocarbonate (DEPC)-treated water and were filtered through a 0.20 μm pore size membrane. Chromatographic runs were performed at 20 °C. The column was first equilibrated with 2.0 M of $(NH_4)_2SO_4$ in 10 mM Tris buffer (pH 8.0). sRNAs samples (40 μg) were applied onto the column using a 100 μL loop at a flow-rate of 1 mL/min. After the elution of unbound species, the ionic strength of the buffer was decreased to 1.5 and 1.1 M of $(NH_4)_2SO_4$ and then to 10 mM Tris buffer (pH 8.0). The absorbance of the eluate was continuously monitored at 260 nm. Fractions were pooled according to the chromatograms obtained, and following concentration and desalting with Vivaspin concentrators. The integrity of pre-miR-29 samples was analyzed by vertical electrophoresis with 10% polyacrylamide gel [10].

2.2. PCR analysis

Pre-miR-29 identification was assessed using polymerase chain reaction (PCR). cDNAs synthesis was performed using RevertAid First Strand cDNA Synthesis Kit (Fermentas), according to manufacturer's instructions. A total of 0.5 μg of RNA samples collected from the chromatographic purification process with lysine–agarose column was used to initiate cDNA synthesis, which was denatured for 5 min at 65 °C with 20 pmol of gene-specific primer (5′ GAC AGC GGT ATG ATC CCC CAA 3′). Then, PCR reactions were carried out using 1 μL of cDNA in a 25 μL reaction containing 0.125 U of Supreme DNA polymerase (NZYtech) and 150 nM of each primer. Specific primers for cDNA, designed from RNA database information, were used to amplify a fragment of 145 bp (Fw – GGA AGC TGG TTT CAT ATG GTG and Rv – CCC CCA AGA ACA CTG ATT TC). PCR was conducted as follows: denaturation at 95 °C for 5 min, followed by 40 cycles at 95 °C for 30 s, 63 °C for 30 s and 72 °C for 15 s, and a final elongation step at 72 °C for 5 min. To confirm the presence and purity of amplicons, PCR products were analyzed using 1% agarose gel electrophoresis [14]. The DNA molecular weight marker was obtained from Vivantis Technologies.

3. Results and discussion

In the present study, the applicability of lysine-affinity chromatography in the RNA downstream process was exploited, to purify pre-miR-29 from a sRNA complex mixture. The lysine amino acid was studied due to the fact of being conserved in the active centre of the PAZ domains of the Argonaute proteins, suggesting that it has an important role in the specific recognition of the pre-miRNA after which occurs the degradation of mRNA [15]. In this work, it was produced a pre-miRNA instead of the mature miRNA considering their structural characteristics, specifically the single chain with ~100 nucleotides, being some unpaired in the 3′ overhang, which will possibly facilitate the purification, due to the higher bases exposure [16]. Previous published studies, have shown that the main interactions between nucleic acids [12,17] and the lysine amino acid are ionic, because of its amine groups. Thus, initial experiments were performed to choose the best binding/elution strategy for pre-miR-29 using a gradient of NaCl. However, under these conditions the RNA binding was not effective and the selective purification of pre-miRNA was not possible to be achieved (data not shown). Therefore, a different strategy was used to promote the RNA binding. In a first step, lysine-agarose column was equilibrated with 2 M $(NH_4)_2SO_4$ in 10 mM Tris buffer (pH 8.0). After injection of the 40 μg of pre-miR-29 containing mixture, was obtained a peak (Fig. 1A) where pre-miR-29 was not detected (data not shown). This can result either from the elution of unbound material that presents a lower affinity to the matrix or by the alteration in the ionic strength since the injected RNA sample is dissolved in H_2O. The ionic strength of the buffer was decreased to 1.5 and 1.1 M $(NH_4)_2SO_4$ in 10 mM Tris buffer (pH 8.0) in order to elute specific molecules in a peak 2. The chromatographic run was concluded with a final elution step, using 10 mM Tris buffer (pH 8.0), to recover the strongly bound species. The polyacrylamide gel electrophoresis was used to detect and identify different sRNAs species eluted in each peak and assess of RNA integrity and purity (Fig. 1B). The analysis of electrophoresis revealed that the peak 1 mostly corresponds to the transfer RNA (tRNA) (lane 1), while pre-miR-29 remained bound under the same conditions, being identified in the peak 2 (lane 2). The electrophoretic evaluation of fractions recovered from the peak 3 revealed the presence of other tRNAs (lane 3). Thus, the electrophoresis of all fractions pooled from the chromatographic experiment indicated that the pre-miR-29 eluted in the peak 2 is pure. These findings suggest that the lysine ligand distinguishes and differentially interacts with several RNA species (Fig. 1) further suggesting a specific recognition of the pre-miR-29. Moreover, the pores of the lysine-support are characterized with an exclusion limit of $>2 \times 10^7$ (~872 base pairs), allowing the access of sRNAs molecules (<150 nucleotides and M.W. $\sim 4.8 \times 10^4$) to the immobilized ligands at the beads surface and inside the pores. pre-miR-29 presents the shape of a stem-loop consisting of two long irregular double-stranded stem regions, which are interrupted by a largely single-stranded internal loop. Along the bulge and through the continuous stem sequences there are mostly guanines, which are described to preferentially interact with lysine [18–20] due to hydrogen bonds that are established with one of the donor atoms of the lysine [19]. Thus, an increased retention of pre-miRNA with inserts mainly constituted by guanine will be expected. Likewise, the lysine amino acid has some characteristics, such as the lateral side chain with significant length and ability to interact with several RNA classes even with different conformational rearrangements producing good hydrogen bond geometries, which reinforce the specific recognition mechanism [19]. Between multiple interactions (electrostatic interactions, van de Waals forces and hydrogen bonds) that the lysine can promote with the RNA backbone or with the more exposed bases, several sRNAs can also be recognized by the presence of hydrophobic interactions [18] with the aliphatic

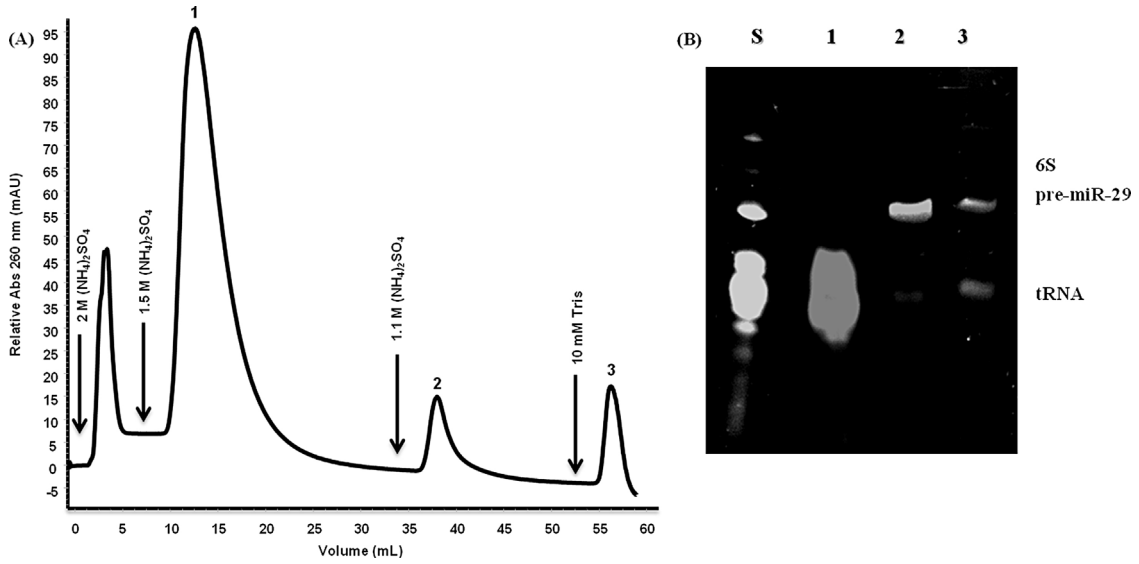

Fig. 1. (A) Chromatographic profile of the pre-miR-29 purification from a sRNA mixture by lysine–agarose chromatography. Elution was performed at 1.0 mL/min by decreasing $(NH_4)_2SO_4$ stepwise gradient from 2 M $(NH_4)_2SO_4$ to 10 mM Tris buffer (pH 8.0), as represented by the arrows. (B) Polyacrylamide gel electrophoresis of samples collected at the column outlet. Fractions corresponding to peaks (1), (2) and (3) are shown in lanes 1-3, respectively. Lane S, sRNA sample injected onto the column.

portion of side chain [17], which can be intensified by the presence of $(NH_4)_2SO_4$. Moreover, the salt concentration can also have a profound positive effect on RNA folding as well as on the stability of non-covalent RNA–amino acid interactions during the course of purification [19,20], once the salt allows that single-stranded nucleic acid molecules form stable hydrogen bonds between their complementary bases.

The conformational stability of the pre-miR-29 secondary structure was assessed using Circular Dichroism (CD) protocol described by Pereira et al. [14] (data not shown). CD spectra of the pre-miR-29 shows characteristic peaks around 210 (negative signal) and 265 nm (positive signal), which, when compared with the CD spectrum of established nucleic acids structures confirm that the pre-miRNA possesses a stem-loop structure that is an intramolecular variant of the B-form and also contains a single-stranded [21]. While the CD spectra of the sRNA shows characteristic features of the A-RNA, a positive band around 260 nm was observed, and a negative signal at 220 nm, with approximately the same intensity. Due to single-stranded, the duplex to stem-loop transition is usually accompanied by CD amplitude reduction when compared with sRNA spectrum. Our results demonstrate that isolation steps involved in the affinity procedure allowed the maintenance of the pre-miRNA stability. Considering the relevance of obtaining pharmaceutical-grade pre-miR-29 is required further characterization of quality parameters by spectrophotometry analysis, estimating the pre-miR-29 concentration (absorbance values at 260 nm) and purity (calculating the 260/280 ratio). The chromatographic process demonstrates an excellent performance in the pre-miR-29 isolation, attaining a significant yield (11.80 ± 0.50 μg) in the peak 2. In addition, pre-miR-29 pure has shown 260/280 ratio of 2.00 ± 0.01, which is often characteristic of a pure RNA preparation [10]. The protein contamination level was assessed by micro-BCA assay (Thermo Fisher Scientific Inc.) in the RNA fractions collected from the chromatographic peaks. This chromatographic strategy provides a reduction of protein level present in the final pre-miR-29 samples (2.613 ± 0.006 ng/μL). As it can be observed from the electrophoretic analysis of the PCR products (Fig. 2), the PCR reaction allowed the amplification of pre-miR-29 cDNA fragments. No further amplification was seen in the control (lane C) or in the peaks 1 (lane 1). The control was made of PCR reaction solutions without cDNA. Therefore, it was verified that the identity of the sRNA isolated from the original population was the pre-miR-29.

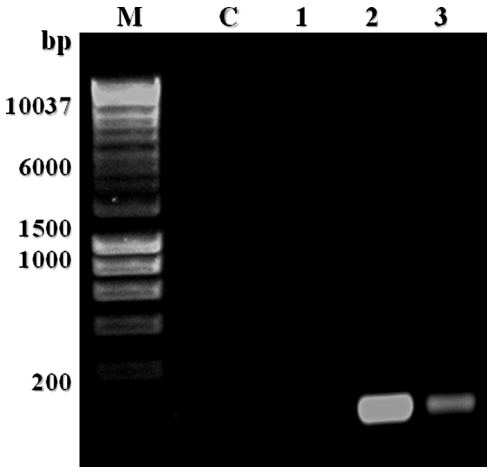

Fig. 2. pre-miR-29 identification by PCR. The agarose gel electrophoretic analysis of PCR products shows amplification of pre-miR-29 cDNA fragments. Lane M, DNA molecular weight marker; lanes C, negative control; lane 1, 2 and 3 corresponding to the three chromatographic peaks, respectively.

These analyses allowed the assessment of RNA quality, indicating that the developed pre-miR-29 isolation methodology can purify the target RNA from different RNA species with high yield, purity and good integrity. Thus, the present data show the development of an AC approach based on natural occurrence interactions, between lysine and RNA species, resulting in the selective purification of pre-miR-29 molecules, in the required conditions for therapeutic applications. These results also demonstrate the versatility of the lysine ligand in the RNA purification, since the pre-miRNA can be purified with $(NH_4)_2SO_4$ but classes of RNAs can also be separated with NaCl [12]. The successful isolation of miRNA species with high purity and quality is a step forward in RNA isolation methodologies and can widely contribute to studies in several RNA research fields.

Acknowledgments

This work was supported by the Portuguese Foundation for Science and Technology (PTDC/EBB-BIO/114320/2009, EXPL/BBB-BIO/1056/2012, PEst-C/SAU/UI0709/2011 and COMPETE:

FCOMP-01-0124-FEDER-027560). Patrícia Pereira and Ângela Sousa acknowledge Ph.D. and Postdoctoral fellowships (SFRH/BD/81914/2011 and SFRH/BPD/79106/2011, respectively). The authors thank Prof. Yo Kikuchi (Toyohashi University of Technology) for kindly provided of pBHSR1-RM plasmid.

References

[1] D.P. Bartel, Cell 116 (2004) 281.
[2] P. Provost, Brain Res. 1338 (2010) 58.
[3] S.S. Hebert, K. Horre, L. Nicolai, A.S. Papadopoulou, W. Mandemakers, A.N. Silahtaroglu, S. Kauppinen, A. Delacourte, B. De Strooper, Proc. Natl. Acad. Sci. U. S. A. 105 (2008) 6415.
[4] I. Vomelova, Z. Vanickova, A. Sedo, Folia Biol. (Praha) 55 (2009) 243.
[5] N. Nonne, M. Ameyar-Zazoua, M. Souidi, A. Harel-Bellan, Nucleic Acids Res. 38 (2010) e20.
[6] N.K. Vo, R.P. Dalton, N. Liu, E.N. Olson, R.H. Goodman, Proc. Natl. Acad. Sci. U. S. A. 107 (2010) 19231.
[7] F. Sousa, D.M. Prazeres, J.A. Queiroz, Biomed. Chromatogr. 23 (2009) 160.
[8] A. Sousa, C.T. Tomaz, F. Sousa, J.A. Queiroz, J. Chromatogr. A 1218 (2011) 8333.
[9] F. Sousa, J.A. Queiroz, J. Chromatogr. A 1218 (2011) 124.
[10] R. Martins, J.A. Queiroz, F. Sousa, Biomed. Chromatogr. 26 (2012) 781.
[11] F. Sousa, D.M.F. Prazeres, J.A. Queiroz, Trends Biotechnol. 26 (2008) 518.
[12] D.S. Jones, H.K. Lundgren, F.T. Jay, Nucleic Acids Res. 3 (1976) 1569.
[13] H. Suzuki, T. Ando, S. Umekage, T. Tanaka, Y. Kikuchi, Appl. Environ. Microbiol. 76 (2010) 786.
[14] P. Pereira, A.F. Jorge, R. Martins, A.A. Pais, F. Sousa, A. Figueiras, J. Colloid Interface Sci. 387 (2012) 84.
[15] F.V. Rivas, N.H. Tolia, J.J. Song, J.P. Aragon, J. Liu, G.J. Hannon, L. Joshua-Tor, Nat. Struct. Mol. Biol. 12 (2005) 340.
[16] A. Tsutsumi, T. Kawamata, N. Izumi, H. Seitz, Y. Tomari, Nat. Struct. Mol. Biol. 18 (2011) 1153.
[17] A. Sousa, F. Sousa, J.A. Queiroz, J. Chromatogr. B Analyt. Technol. Biomed. Life Sci. 877 (2009) 3257.
[18] F. Sousa, C. Cruz, J.A. Queiroz, J. Mol. Recognit. 23 (2010) 505.
[19] M.M. Hoffman, M.A. Khrapov, J.C. Cox, J. Yao, L. Tong, A.D. Ellington, Nucleic Acids Res. 32 (2004) D174.
[20] J.J. Ellis, M. Broom, S. Jones, Proteins 66 (2007) 903.
[21] B. Ranjbar, P. Gill, Chem. Biol. Drug Des. 74 (2009) 101.

Paper VI

Purification of pre-miR-29 by arginine-affinity chromatography

P. Pereira, A. Sousa, J. A. Queiroz, I. Correia, A. Figueiras, F. Sousa

Journal of Chromatography B. 2014. 951-952: 16-23

Short description: The lysine-affinity methodology reported in paper V for recombinant pre-miR-29b purification was successfully developed and implemented. As a matter of fact, although pre-miR-29b was recovered with high purity, it is not compatible with clinical applications, reinforcing the need of implementing more selective methods for the purification of this biomolecule. Thus, in this paper, it is described a new affinity chromatography method using an arginine support to specifically and efficiently purify pre-miR-29b from other small RNA species. Initially, it was characterized the behavior of pre-miR-29b under the influence of different binding/elution conditions, such as increased sodium chloride, arginine or decreased ammonium sulfate stepwise gradients, in order to achieve higher efficiency and selectivity. The results obtained suggest that the underlying mechanism involves biorecognition of pre-miR-29b by the arginine ligand, resulting from the occurrence of different elementary interactions. In the elution strategies using sodium chloride or arginine, an improvement in the final pre-miR-29b yields was obtained, as well as high integrity and purity. Moreover, in this strategy the recovery of the pre-miR-29b was achieved under mild elution conditions in comparison with the ligand lysine.

Journal of Chromatography B, 951–952 (2014) 16–23

Contents lists available at ScienceDirect

Journal of Chromatography B

journal homepage: www.elsevier.com/locate/chromb

Purification of pre-miR-29 by arginine-affinity chromatography

Patrícia Pereira [a], Ângela Sousa [a], João Queiroz [a], Ilídio Correia [a], Ana Figueiras [a,b], Fani Sousa [a,*]

[a] CICS-UBI–Health Sciences Research Centre, University of Beira Interior, Avenida Infante D. Henrique, 6200-506 Covilhã, Portugal
[b] CNC–Center of Neuroscience and Cell Biology, University of Coimbra, Largo Marquês de Pombal, 3004-517 Coimbra, Portugal

ARTICLE INFO

Article history:
Received 23 October 2013
Accepted 14 January 2014
Available online 19 January 2014

Keywords:
Alzheimer's disease
Arginine-affinity chromatography
Multiple interactions
pre-miR-29
Rhodovulum sulfidophilum
RNA purification

ABSTRACT

Recently, differential expression of microRNAs, in patients with Alzheimer's disease (AD) suggests that they might have key regulatory roles in this neurodegenerative disease. Taking into account this fact, several studies demonstrated that the miR-29 is significantly decreased in AD patients, also displaying abnormally high levels of β-site APP-cleaving enzyme 1. Thus, RNA biochemical or structural studies often require a RNA sample that is chemically pure and biologically active. The present work describes a new affinity chromatography method using an arginine support to specifically purify pre-miR-29 from other *Rhodovulum sulfidophilum* small RNA species. Nevertheless, in order to achieve higher efficiency and selectivity, it is essential to characterize the behavior of pre-miR-29 binding/elution. Thus, three different strategies based on increased sodium chloride (280–500 mM), arginine (25 mM) or decreased ammonium sulfate (2–0.1 M) stepwise gradients are described to purify pre-miR-29. In this way, it was proved that well-defined binding/elution conditions are crucial to enhance the purification performance. As a matter of fact, by employing elution strategies using sodium chloride or arginine, an improvement in the final pre-miR-29 yields (96.5 and 56.7%, respectively) was obtained. Moreover, the quality control analysis revealed high integrity in pre-miR-29 preparations as well as high purity (90 and 98%, respectively), demonstrated by the scarce detection of proteins. This improved method takes advantage of its simplicity, significant cost reduction, due to the elimination of some complex operations, and speed for large-scale purification of pre-miRNAs suitable for biochemical and structural studies.

1. Introduction

MicroRNAs (miRNAs) constitute a class of small non-coding regulatory RNAs that act as key regulators of gene expression through a highly conserved intracellular mechanism termed RNA interference, involving the recognition and translational control of specific messenger RNA (mRNA) [1]. MiRNAs are initially transcribed as pri-miRNAs that are processed by Drosha into pre-miRNAs stem-loop. Pre-miRNAs are then exported to the cytoplasm, where their loops are removed by Dicer resulting into mature miRNAs. Finally, miRNA is loaded onto the RNA-induced silencing complex (RISC) toward the target mRNA, resulting primarily in degradation of mRNA transcripts or repression of protein translation, depending on the degree of sequence complementarity [2].

Several studies, over the last decade, have been published concerning the expression of miRNAs in patients with Alzheimer's disease (AD), suggesting that these can play an important role in the regulation of neurodegeneration. One major hallmark of AD is the generation and subsequent accumulation of β-amyloid (Aβ) through sequential cleavage of the β-amyloid precursor protein (APP) by β-site APP-cleaving enzyme 1 (BACE1) and γ-secretase [3,4]. The regulation of the expression levels of proteins involved in this Aβ generation process has demonstrated to be important in AD. Hebert and collaborators showed that the miR-29 is potentially involved in the regulation of APP and BACE1/γ-secretase expression because *in vitro* studies revealed that miR-29 cluster was significantly decreased in AD patients displaying abnormally high BACE1 protein levels [5]. These findings raised the possibility to use miR-29 as a potential therapeutic weapon for AD therapy.

For this reason, RNA represents an important target of a wide collection of laboratory analyses, relevant, particularly, in the

Abbreviations: miRNA, microRNA; RNA, ribonucleic acid; mRNA, messenger RNA; RISC, RNA-induced silencing complex; AD, Alzheimer's disease; Aβ, β-amyloid; APP, β-amyloid precursor protein; BACE1, β-site APP-cleaving enzyme 1; SPE, silica-based solid-phase extraction; PCR, polymerase chain reaction; cDNA, complementary DNA; AC, affinity chromatography; RNases, RNA degrading enzymes; tRNA, transfer RNA; sRNA, small RNA.

* Corresponding author at: Health Sciences Research Centre, Universidade da Beira Interior, Avenida Infante D. Henrique, 6200-506 Covilhã, Portugal.
Tel.: +351 275 329 074; fax: +351 275 329 099.
E-mail address: fani.sousa@fcsaude.ubi.pt (F. Sousa).

1570-0232/$ – see front matter © 2014 Elsevier B.V. All rights reserved.
http://dx.doi.org/10.1016/j.jchromb.2014.01.020

diagnostic of several disorders, as well as in basic research. As a result, RNA purification is a critical first step of a multitude of analytical techniques including real-time quantitative polymerase chain reaction (PCR), microarray analysis, Northern blotting, *in situ* hybridization, *in vitro* translation and cDNA library construction [6]. To provide relevant and reliable results, molecular biology techniques used for such purposes require pure and intact molecules of purified RNA. Consequently, there is a growing demand for commercially available kits (e.g., Exiqon's, Qiagen, Ambion, Promega and Stratagene), which are designed to isolate miRNA molecules from different biological sources with high quality, intactness and purity for further analytical application or scientific need [6]. Most of the existing kits use either silica-based solid-phase extraction (SPE) technology or a magnetic-bead based extraction technology whereby small RNAs (sRNAs) are separated from large RNAs through their capacity to bind to the column [7,8]. Furthermore, there are some chromatographic methods reported in the literature for the purification of the sRNA molecules from high-molecular-weight RNA [9–11] in attempting to overcome the limitations on RNA purification. In these methods, diverse natural or *in vitro* selected RNA aptamers sequences are inserted in RNA molecules [8], which subsequently have to be released from the chromatographic support by competitive elution or cleaved off by a protease, which can affect the overall topology of the recombinant RNA construct [12].

Commonly, miRNA-based therapy applications rely on the use of synthetic miRNAs obtained by *in vitro* transcription and chemical synthesis. Although these methods can be very efficient, they are still expensive to be produced in large scale, limited with respect to the length of oligonucleotides that can be synthesized and labor intensive [12]. In addition, issues associated with the presence of contaminants arising from synthesis still restrict the implementation of these oligonucleotides onto clinical applications, mostly because the presence of impurities may lead to non-targeted gene silencing and are often associated with a decrease in therapeutic effectiveness. Therefore, the requirement for the production of highly purified and clinically suitable miRNAs in large quantity arises as one of the most important challenges in the development of therapeutic strategies based on this technology.

The pursue of highly selective, reliable and economical processes capable of preparing therapeutic biomolecules with the strict quality assurance has been accompanied by an improvement in the downstream strategies that are based on affinity chromatography (AC) [13]. Thus, the development of an affinity-based methodology using amino acids as specific ligands have recently led to an improvement in purification technologies, since this technique exploits natural biological processes such as molecular recognition for the selective purification of target biomolecules [14–18].

Hence, the main goal of this work is to develop new methodologies for the RNA isolation that enable the pre-miR-29 recovery with high integrity and purity, in view of the application in molecular biology procedures, namely for gene expression analysis. To accomplish this purpose, it was explored the possibility of using arginine-AC to selectively isolate the pre-miRNA from *Rhodovulum sulfidophilum*. This bacteria was selected as recombinant host to biosynthesize the pre-miR-29, once it does not produce any detectable ribonucleases (RNases) in the culture medium, maintaining the stability of the RNA produced [19]. Thus, this fact constitutes a great advantage since RNA is an instable molecule due to its susceptibility to nucleases mediated degradation. The method based on arginine-AC can be an attractive approach for the miRNA purification process, since previous results from our research group have demonstrated the potential of this amino acid in the purification of RNA [20] and plasmid DNA [21–23], suggesting that the binding mechanism involves phenomenological interactions like biorecognition between arginine and nucleic acids. In addition, arginine was chosen because it is a conserved amino acid in the active center of the Argonaute protein [24], which is part of the RISC complex. The binding/elution behavior of pre-miR-29 under the influence of different environmental conditions, such as the composition, the ionic strength of the elution buffer, and the temperature were investigated. The study revealed several interesting characteristics of RNA molecules, including their chromatographic behavior and natural interactions that can occur between the arginine support and pre-miRNA. These results support the interest in applying amino acid-based AC to develop new pre-miRNA isolation and purification processes. Therefore, this new affinity protocol for miRNA isolation can offer advantages over other less-selective and time-consuming multistep procedures and can improve process economics. Moreover, some improvements over other chromatographic techniques are expected because RNA recovery can be achieved under mild elution conditions, suggesting the feasibility of exploiting different affinity interactions between amino acids and miRNA to develop an interesting bioseparation methodology.

2. Materials and methods

2.1. Materials

Arginine–Sepharose 4B gel was acquired from Amersham Biosciences, the guanidinium salt and all the chemicals used in the lysis buffer were obtained from Sigma-Aldrich. Other compounds used in the elution buffer were ammonium sulfate ($(NH_4)_2SO_4$) and sodium chloride (NaCl) purchased from Panreac and Tris from Merck. All solutions were freshly prepared using 0.05% diethyl pyrocarbonate (DEPC; Sigma-Aldrich) treated water and the elution buffers were filtered through a 0.20 μm pore size membrane and degassed ultrasonically. The DNA molecular weight marker was obtained from Vivantis Technologies. All the materials used in the experiments were RNase-free.

2.2. Bacterial strain and growth conditions

The pre-miR-29 used in this study was obtained from a cell culture of *R. sulfidophilum* DSM 1374 strain (BCCM/LMG, Belgium) modified with plasmid pBHSR1-RM [19] containing the sequence of pre-miR-29. Growth was carried out in shaker flasks containing 100 mL of Nutrient Broth medium (g per liter of deionized water: beef extract, 1; yeast extract, 2; peptone, 5 and sodium chloride, 5) supplemented with 30 μg/mL kanamycin in a rotary shaker at 30 °C and 250 rpm under dark-aerobic conditions. Cell growth was evaluated by measuring the optical density of the culture medium at a wavelength of 600 nm after dispersing cell flocs by vortexing for 30 s. Cells were recovered by centrifugation and stored at −20 °C.

2.3. Lysis and small RNA isolation

Cells were lyzed and sRNA was extracted using the acid guanidinium thiocyanate-phenol-chloroform method based on the protocol described by Chomczynski and co-workers [25]. Bacterial pellets were resuspended in 5 mL of denaturing cell lysis solution (4 M guanidinium thiocyanate; 25 mM sodium citrate, pH 4.0; 0.5% (m/v) *N*-laurosylsarcosine and 0.1 M β-mercaptoethanol) to perform lysis. After incubating on ice for 10 min, cellular debris, genomic DNA and proteins were precipitated by gently adding and mixing 5 mL of water-saturated phenol and 0.5 mL of 2 M sodium acetate (pH 4.0). The sRNA isolation was achieved by adding 1 mL of chloroform/isoamyl alcohol (49:1), and by mixing vigorously until two immiscible phases were obtained. The upper aqueous phase, which contained mostly RNA, was recovered and

concentrated by the addition of 5 mL of ice-cold isopropanol. Precipitated molecules were recovered by centrifugation at 10,000 × g, for 20 min, at 4 °C and resuspended in 1.5 mL of lysis solution. Molecules were concentrated again with 1.5 mL of ice-cold isopropanol. After centrifuging for 10 min, at 10,000 × g (4 °C), the sRNA pellet was washed with 7.5 mL of 75% ethanol and incubated at room temperature for 10 min, followed by a 5 min centrifugation at 10 000 g (4 °C). The air-dried sRNA pellet was solubilized in 1 mL of 0.05% DEPC-treated water. Finally, 260 and 280 nm absorbance of the samples was measured using Nanodrop spectrophotometer in order to assess sRNA quantity and purity.

2.4. Affinity chromatography

Chromatography was performed in an ÄKTA Avant system with UNICORN 6 software (GE Healthcare). A 10 mm diameter × 20 mm long (about 2 mL) column was packed with commercial L-arginine–Sepharose 4B gel. This support is characterized by the manufacturer as a cross-linked 4% beaded agarose matrix with a 12-atom spacer and an extent of labeling between 14 and 20 μmoL/mL. pre-miR-29 was purified applying three elution strategies, namely by using NaCl, $(NH_4)_2SO_4$ and arginine as competition agent. In the experiments with sodium chloride, after washing out the unbound material with 280 mM NaCl in 10 mM Tris buffer (pH 8.0), the ionic strength of the buffer was stepwise increased to 360 and 500 mM NaCl in 10 mM Tris buffer (pH 8.0). On the other hand, in the experiments with ammonium sulfate, the column was equilibrated with 2.0 M of $(NH_4)_2SO_4$ in 10 mM Tris buffer (pH 8.0). After the elution of unbound species with this condition, the ionic strength of the buffer was stepwise decreased to 1.55 M $(NH_4)_2SO_4$ in 10 mM Tris buffer (pH 8.0). Finally, tightly bound sRNA species were removed by changing the ionic strength to 100 mM of $(NH_4)_2SO_4$ in 10 mM Tris buffer (pH 8.0). The experiments performed with arginine to purify pre-miR-29 molecules were initiated with the equilibration of the column with 280 mM NaCl in 10 mM Tris buffer (pH 8.0) to promote the total retention of pre-miR-29 and then the elution was accomplished by changing to 280 mM NaCl supplemented with 25 mM arginine in 10 mM Tris buffer (pH 8.0). The most retained species were finally eluted with 500 mM NaCl. In the three sets of experiments, sRNAs samples (30 μg) were injected onto the column using a 100 μL loop at a flow-rate of 1 mL/min, which contains 6S RNA, pre-miR-29 and other sRNA, including transfer RNAs. The absorbance of the eluate was continuously monitored at 260 nm. All experiments were performed at 20 °C using a circulating water bath. Fractions were pooled according to the chromatograms obtained, and following concentration and desalting with Vivaspin concentrators, the pools were kept for quantification and further analysis.

2.5. Polyacrylamide electrophoresis

Fractions recovered from the sRNA chromatographic experiment were also analyzed by vertical electrophoresis using an Amersham Biosciences system (GE Healthcare) with 10% polyacrylamide gel. Electrophoresis was carried out at 125 V for 90 min with TBE buffer. sRNA samples were previously denatured with 97.5% formamide and denatured conditions were kept in the gel owing to the presence of 8 M urea. sRNA molecules were stained with ethidium bromide (0.5 mg/mL).

2.6. Protein analysis

Protein residual contamination in pre-miR-29 samples collected from the purification with arginine-agarose support, was measured by using the micro-BCA assay (Thermo Fisher Scientific Inc.), according to manufacturer's instructions. Briefly, the calibration curve was prepared using BSA standards (0.01–0.25 mg/mL). A total of 25 μL of each standard or pre-miR-29 samples were added to 200 μL of BCA reagent in a microplate and incubated for 30 min at 60 °C. The absorbance was measured at 570 nm in a microplate reader.

2.7. PCR analysis

Pre-miR-29 identification was assessed using polymerase chain reaction (PCR) (Biometra). cDNAs synthesis was performed using RevertAid First Strand cDNA Synthesis Kit (Thermo Fisher Scientific Inc.), according to manufacturer's instructions. A total of 0.5 μg of RNA samples collected after the chromatographic purification process with arginine–agarose column was used to initiate cDNA synthesis, which was denatured for 5 min at 65 °C with 20 pmol of gene-specific primer (Supplementary data). Then, PCR reactions were carried out using 1 μL of synthesized cDNAs in a 25 μL reaction containing 0.125 U of Supreme DNA polymerase (NZYtech), 50 mM of magnesium chloride (NZYtech) and 150 nM of each primer. Specific primers for cDNA, whose design was based on a RNA database, were used to amplify a fragment of 145 bp (Supplementary data). The PCR program was carried out as follows: after an initial denaturation at 95 °C for 5 min, 40 cycles consisting of denaturation at 95 °C for 30 s, annealing at 63 °C for 30 s and extension at 72 °C for 15 s, and a final elongation step at 72 °C for 5 min. To confirm the presence and purity of amplicons, PCR products were analyzed by 1% agarose gel electrophoresis (120 V for 35 min) in TAE buffer in the presence of 0.5 μg/mL greensafe (NZYtech).

3. Results

3.1. Effect of ionic strength, elution buffer composition and temperature on pre-miR-29 binding

This study was developed to explore the phenomenological interactions like biorecognition between pre-miR-29 and arginine as a biospecific ligand in AC. In order to establish our method, we changed the elution buffer composition and ionic strength or the experimental temperature and, therefore, evaluated different kinds of interactions between the biospecific ligand and the pre-miR-29. Since RNA is negatively charged due to the phosphate groups in the backbone, it is easy to predict favorable electrostatic interactions between RNA phosphate groups and arginine ligands. However, depending on environmental conditions used, some interactions can be more preferential than other, becoming more evident under specific conditions.

In the studies performed to mainly favor ionic interactions, after binding, the pre-miR-29 elution was achieved with the application of a stepwise gradient increasing the NaCl concentration to 280, 360 and 500 mM, after several optimizations. This strategy is based on previously studied elution pattern of plasmid DNA, in the NaCl concentration range of 200–300 mM, described by our research group [23]. In addition, the potential application of arginine-based chromatography to purify total RNA directly from a clarified lysate has been recently described also by our group [20]. In this case, arginine ligands were able to distinguish and, therefore, interacted differentially with various sRNAs molecules, suggesting a specific recognition for the pre-miR-29. During these experiments, there was a need to strictly control the chromatographic conditions in order to maintain the reproducibility, since a slightly variation in conductivity (salt concentration and/or temperature) affected the sRNA retention. The chromatographic assays initially performed were intended to test the ionic strength effect on sRNA retention. Therefore, Fig. 1A shows the chromatographic profile obtained after the injection of sRNA preparation in the arginine-agarose support.

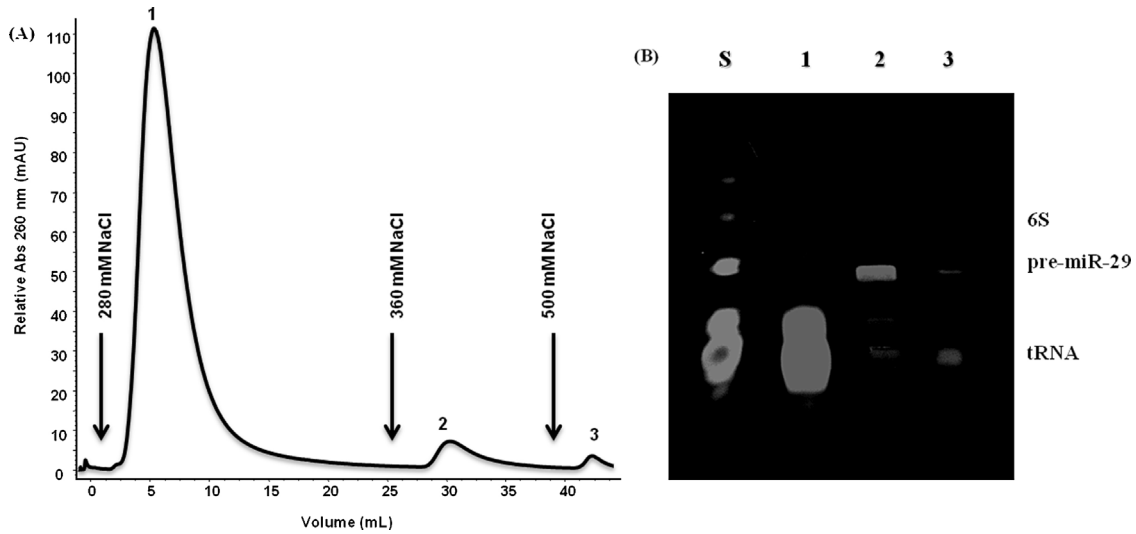

Fig. 1. (A) Chromatographic profile of the pre-miR-29 purification from a sRNA mixture extract by arginine–agarose chromatography. Elution was performed at 1.0 mL/min by stepwise increasing NaCl concentration in the eluent from 280, 360 and 500 mM, as represented by the arrows. (B) Polyacrylamide gel electrophoresis of samples collected at the column outlet. Fractions corresponding to peaks (1), (2) and (3) are shown in lanes 1-3, respectively. Lane S, impure sRNA preparation injected onto the column.

The chromatographic run was initiated at low ionic strength with 280 mM NaCl in 10 mM Tris buffer (pH 8.0). Under these conditions, a first peak of unbound species was obtained. As shown in Fig. 1A, the pre-miR-29 was obtained when the elution step was performed with 360 mM NaCl, being recovered nearly 96.5% of pre-miR-29. The elution of highly bound species was then achieved by increasing the ionic strength of the buffer to 500 mM NaCl. The polyacrylamide gel electrophoresis was used to detect and identify different RNAs species eluting in each peak (Fig. 1B). In Fig. 1B, the electrophoretic profile presented in lanes 1, 2 and 3 corresponds to the samples pooled from the respective peaks in the chromatogram. Hence, the electrophoretic analysis showed that the first peak of unbound species corresponds to the elution of transfer RNA (tRNA) species (Fig. 1B, lane 1), while the second peak mainly refers to pre-miR-29 (Fig. 1B, lane 2) and, finally, the third peak mainly refers to 6S RNA and tRNA species (Fig. 1B, lane 3). These results suggest that pre-miR-29 presents a stronger interaction with the arginine matrix than the majority of tRNA species. The salt concentration (360 mM NaCl) needed to elute bound pre-miR-29 from arginine–agarose matrix (Fig. 1A) is considerably lower than those typically used in different chromatographic techniques, namely in anion-exchange chromatographic supports (higher than 500 mM NaCl) [22] which is an important process advantage.

In order to mainly exploit hydrophobic interactions, a decreasing ammonium sulfate stepwise gradient between 2 and 0.1 M was applied, allowing pre-miR-29 separation. The retention behavior of sRNA molecules in this strategy is in accordance with the results previously described to purify total RNA directly from a clarified lysate [16] or to isolate 6S RNA from a sRNA mixture [17] using histidine as ligand. Fig. 2A shows the chromatographic profile obtained after injection of the sRNA sample. The presence of different peaks in the chromatogram indicates that RNAs present in the sRNA population interact differently with the arginine–agarose support. The higher salt concentration promoted total pre-miR-29 retention. It was observed that tRNA molecules eluted immediately with 1.55 M $(NH_4)_2SO_4$ in 10 mM Tris buffer (pH 8.0). The elution of pre-miR-29 was achieved with 1.1 M $(NH_4)_2SO_4$ in 10 mM Tris buffer (pH 8.0). These results were important to understand the binding behavior of the sRNA mixture and to develop the best purification strategy for pre-miR-29. In fact, the higher salt concentration plays a key role on the pre-miR-29 binding to arginine ligand. Again, a polyacrylamide electrophoresis was used to detect and identify different species eluting in each chromatographic peak (Fig. 2B).

The electrophoretic analysis indicates that the first chromatographic peak (Fig. 2A, peak 1) corresponds to the elution of tRNA (Fig. 2B, lane 1). However, the elution of pre-miR-29 was mainly achieved in the second peak, following the reduction of the ionic strength of the elution buffer (peak 2 and lane 2). Finally, the 6S RNA, pre-miR-29 and other tRNAs species were eluted with 100 mM $(NH_4)_2SO_4$ in 10 mM Tris buffer (pH 8.0), as it was observed in the third chromatographic peak (peak 3 and lane 3).

After identifying the pre-miR-29 retention behavior on the arginine matrix with both elution strategies addressed in this study (NaCl and $(NH_4)_2SO_4$)), the temperature effect on pre-miR-29 stability was also evaluated. In fact, this parameter could also significantly influence pre-miR-29 interactions with the immobilized arginine. Thus, several chromatographic experiments were designed to analyze how the temperature affects the adsorption of pre-miR-29, as well as the other *R. sulfidophilum* sRNA species. Therefore, the water-jacketed column was connected to a circulating water bath to maintain the appropriate temperature (temperature extremes, 4 and 20 °C) in each experiment. As a matter of fact, the results showed an increased retention of all sRNAs species studied with the temperature increase, suggesting that higher temperatures favors the involvement of hydrophobic interactions [26]. This stronger interaction might be due to the fact that bases of the tRNAs are more available to interact with immobilized ligands, because of its single-stranded structure. On the other hand, the pre-miR-29 shows low binding affinity since it has a structure stem-loop. Moreover, for the lowest temperature studied (4 °C), it is observed that the isolated pre-miR-29 retention time is similar to that from the isolated tRNAs (data not shown).

In AC, the elution of a target solute that is bound to the affinity ligands can be achieved through addition of a competing agent in the elution buffer rather than changing the ionic strength, pH, or polarity. Moreover, this methodology is also commonly employed in order to make the elution strategy more selective and biospecific as well as to get higher elution efficiency. The competing agent can bind to the retained target or to the immobilized ligand, depending of their characteristics, thus allowing to predict the interactions that can be involved. In this work, competitive studies were

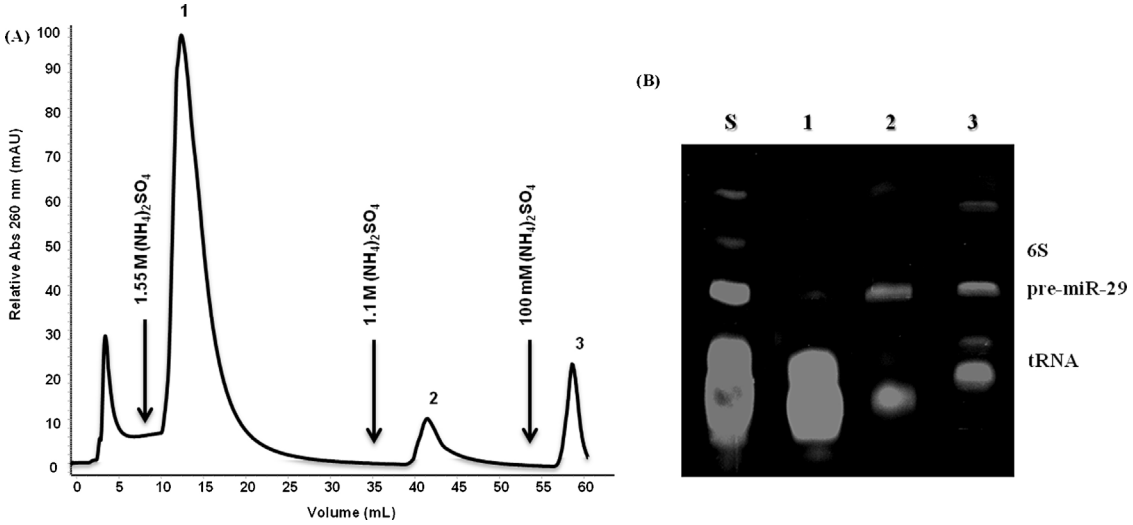

Fig. 2. (A) Chromatogram showing the purification of pre-miR-29 from sRNA population by arginine–agarose chromatography. Elution was performed at 1 mL/min by stepwise decreasing $(NH_4)_2SO_4$ concentration in the eluent from 2 to 0.1 M $(NH_4)_2SO_4$ in 10 mM Tris buffer (pH 8.0). (B) Polyacrylamide gel electrophoresis analysis of samples collected at the column outlet. Fractions corresponding to peaks (1), (2) and (3) are shown in lanes 1–3, respectively. Lane S, impure sRNA sample injected onto the column.

performed by adding 250 mM of arginine to the elution buffer in a stepwise gradient, to exploit specific elution of pre-miR-29 from the column and therefore to evaluate the possibility of reaching higher purification factors, according to the procedure described by Sousa and co-workers for the purification of plasmid DNA [23]. The elution gradients applied were adapted to ensure that the RNA sample is on ideal conditions to bind to the matrix ligands, and to elute only due to the competing agent addition. Thus, the characterization of binding/elution behavior of pre-miR-29 in the arginine–agarose matrix upon addition of arginine is essential. The arginine column was first equilibrated with 280 mM NaCl in 10 mM Tris buffer (pH 8.0) to promote the total retention of pre-miR-29. After sample binding, elution could be carried out by increasing the ionic strength upon NaCl addition. The chromatographic profile presented in Fig. 3A gives an interesting suggestion about the nature of interactions involved in the pre-miR-29 retention to arginine–agarose matrix. Fig. 3A shows the result obtained in an experiment in which pre-miR-29 was first bound to the column with 280 mM NaCl and then eluted by changing to a 280 mM NaCl supplemented with 25 mM arginine (positively charged). In fact, pre-miR-29 recovery was only achieved when the elution buffer containing the arginine amino acid was applied. Summarizing, from the results obtained with this first screening of the pre-miR-29 retention pattern in arginine-based matrix (Fig. 3), it was found that the pre-miR-29 presents a great ability to bind to the matrix, suggesting the establishment of a strong interaction with the support. However, the elution is not difficult to perform and the pre-miR-29 recovery is achieved by using low salt or arginine concentrations. Some experiments were also carried out using other concentrations, from 5 to 30 mM of arginine in the elution buffer but all of the tRNAs species were eluted together with pre-miR-29 (results not shown).

3.2. Pre-miR-29 quality characterization

To ensure the success of the purification methodologies here described, the quality of pre-miRNA preparations was assessed using parameters that are commonly considered, namely spectrophotometry analysis, polyacrylamide gel electrophoresis and total protein quantification [27,28]. Since, the RNA preparations

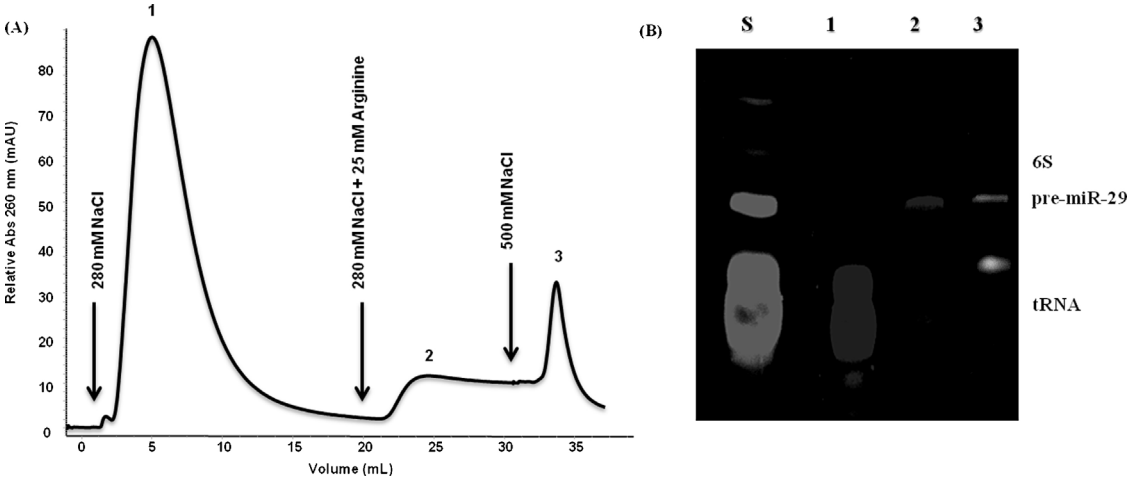

Fig. 3. (A) Separation of pre-miR-29 by arginine–agarose chromatography. Elution was performed at 1 mL/min by stepwise increasing of arginine concentration in the eluent from 25 mM, beginning with 280–500 mM NaCl as represented by the arrows. (B) Polyacrylamide gel electrophoresis analysis of each peak in both experiments is represented in the respective figure. Fractions corresponding to peaks (1), (2) and (3) are shown in lanes 1–3, respectively. Lane S, sRNA sample injected onto the column.

Table 1
Quantitative analysis of purity and yield of pre-miR-29 isolated (peak 2) by arginine–agarose chromatography.

	Elution strategy	sRNA sample (μg)	pre-miR-29 (peak 2) (μg)	Pre-miR-29 Purity (%)	Pre-miR-29 yield (%)	Proteins (ng/μL)
1	NaCl	30	12.40 ± 0.40	90	96.5	4.548 ± 0.007
2	$(NH_4)_2SO_4$	30	8.35 ± 0.61	33	52.8	6.806 ± 0.003
3	Arginine	30	9.33 ± 0.83	98	56.7	ND

should be free of proteins, should maintain the structural integrity, free of enzymatic inhibitors for RT and PCR reactions and free of nucleases [29]. The spectrophotometry analysis allows the estimation of RNA concentration using the absorbance values at 260 and 280 nm, while the purity of each sample was evaluated by calculating the 260/280 ratio. Thus, a ratio of 2.00 ± 0.01 is often characteristic of a pure RNA preparation [27]. However, the protein content is a common impurity in RNA preparations that usually can be omitted in spectrophotometry analysis since it is required a relatively large amount of protein contamination to significantly affect the 260/280 ratio in an RNA solution [27]. Thus, the total protein content was assessed by micro-BCA assay in the RNA fractions collected from the chromatographic peaks. As a result, the protein contamination level was negligible in pre-miR-29 samples (Peak 2 in Fig. 1A, 2A and 3A). The analysis of protein content in the fractions collected along the pre-miR-29 purification gradient revealed that proteins tend to elute more in the first chromatographic steps (data not shown). Therefore, the chromatographic strategies used in these new pre-miRNA isolation methods also provide a reduction of protein contamination in RNA samples, specifically in the competition studies where the proteins were not detected (as shown in Table 1).

Moreover, the electrophoretic analysis (Fig. 1B, 2B and 3B) is an important complementary technique that enables the assessment of RNA integrity. RNA is one of the most difficult materials to separate under chromatographic conditions because it is degraded very quickly in nature and its stabilization is very difficult. Hence, the final RNA integrity is a key factor for the overall success and further application and will depend on maintaining the stability of the sample before separation, throughout the purification process, and also during the recovery of RNA fractions when the separation has been completed. The results demonstrate that the isolation steps involved in the affinity procedure allowed maintaining the pre-miR-29 stability (chemically intact and biologically competent). The application of arginine AC can also be strongly associated with the preserved integrity observed in RNA samples since arginine, owing to its multiplicity of interactions, has been largely associated with stabilizing effects on RNA conformations [26,30,31]. Moreover, electrophoretic analysis allows the visualization of the several sRNA species of a sample in which RNA bands are sharp and clear with a characteristic banding profile, which is crucial to guarantee RNA quality.

The Phoretix 1D software (Nonlinear Dynamics, Newcastle, United Kingdom) was also used as an auxiliary of the electrophoresis polyacrylamide analysis, allowing to control the purity of pre-miR-29 preparations and to determine the yield through the evaluation of the intensity of electrophoresis bands. The quantitative analysis of pre-miR-29 purity throughout the isolation procedure is summarized in Table 1 that presents the concentration of sRNA samples, which were applied in arginine chromatography. Thus, the quality control analysis revealed a high purity (90%) in the final pre-miR-29 RNA preparations obtained with the NaCl elution strategy. Moreover, in the arginine and $(NH_4)_2SO_4$ elution strategies, they were obtained the following purities 98 and 33%, respectively. The chromatographic process demonstrates an excellent performance in the isolation of pre-miR-29, attaining a higher pre-miR-29 yield with the NaCl strategy (96.5%) and a significant recovery with $(NH_4)_2SO_4$ (52.8%) as well as in the competition studies (56.7%), beginning with 30 μg of sRNA (see Table 1). A more accurate identification of pre-miR-29 molecules purified from the sRNA populations with the arginine–agarose matrix was performed by PCR. As it can be observed from the electrophoretic analysis of the PCR products (Fig. 4), by using specific primers for pre-miR-29 cDNA, the PCR reaction allowed the amplification of pre-miR-29. No further amplification was seen in the control (lane 1). The negative control was made of PCR reaction solutions without cDNA. Therefore, it was verified that the identity of the sRNA isolated from the original population was the pre-miR-29.

4. Discussion

In this work, we describe an alternative method to purify miRNA from a complex mixture of total RNA based in the AC, which is the unique technique that simulates and exploits biological interactions allowing the separation of biomolecules on the basis of a specific and reversible contact between the target biomolecules and the specific ligand, which is coupled to a chromatographic matrix [13]. The choice of the matrix and elution conditions to be used will depend on molecular properties of biomolecules and the physicochemical and thermodynamic nature of their molecular interactions [32]. As previously mentioned, elution steps can be performed either specifically, using a competitive ligand, or non-specifically, by changing the pH, ionic strength or polarity of the buffer depending on the matrix used and the chemical characteristics of biomolecules [32]. Our choice was the arginine amino acid because it is considered an excellent ligand since it presents several characteristics that allow the establishment of multiple interactions between itself and nucleic acid molecules, namely its ability to interact in different conformations, the length of its side chain and its ability to produce good hydrogen bond geometries [33]. Furthermore, recent studies emphasized that arginine can be studied as a ligand in AC for RNA purification, since this amino acid is conserved in the active center of the PAZ domains of the Argonaute proteins, suggesting that they have an important role in the specific recognition of the 3′ overhang of the pre-miRNA after which occurs the degradation of the

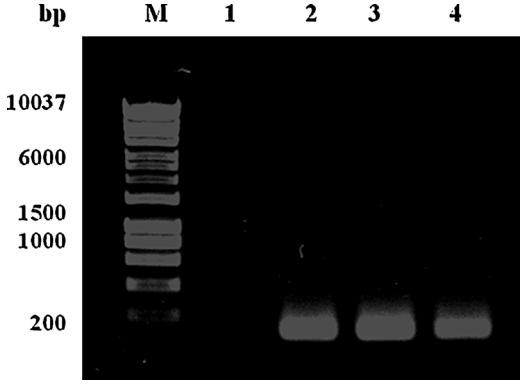

Fig. 4. pre-miR-29 identification by reverse-transcription PCR. The agarose-gel-electrophoretic analysis of PCR products shows amplification of pre-miR-29 cDNA fragments. The negative control had no band intensification. Lane M, DNA molecular weight marker; lanes 1, negative control; lane 2, 3 and 4, second peaks of the three strategies studied (sodium chloride, ammonium sulfate and arginine), respectively.

mRNA [24]. The sequence of pre-miR-29 was sought in the miRBase (http://www.mirbase.org/cgi-bin/mirna_entry.pl?acc=MI0000105) that is the official repository of miRNAs, where known miRNAs are named and stored. However, pre-miRNAs are not described for real sequences, since the predicted stem-loop sequences in the database are not strictly pre-miRNAs, but rather include the pre-miRNA and some flanking sequence from the presumed primary transcript. In this study it was chosen to produce a pre-miRNA instead of the mature miRNA, because of its structural characteristics, specifically the single chain with ~100 nt of which some are unpaired in the 3′ overhang, which will possibly facilitate the purification [34].

In fact, beyond the potential application of arginine-based chromatography to purify pre-miR-29 from *R. sulfidophilum* sRNA mixture described here, this study also demonstrates the possibility of using three different strategies to conduct the pre-miRNA purification. This advantageous methodology reduced the complexity of the general procedure, and examined the applications and selectivity that these elution strategies can have in promote under different environmental conditions. Thus, this purification could be achieved either using an increased NaCl (360 mM), decreased $(NH_4)_2SO_4$ (1.1 M) or arginine (25 mM) stepwise gradients. Comparing the two best elution strategies, using NaCl or arginine to elute bound pre-miR-29 biomolecules, it was verified that the arginine concentration needed to promote elution is lower than the NaCl concentrations. This fact is in accordance with what has been previously described by other authors, because as arginine is monovalent at the pH used, it is equivalent to NaCl in terms of valency; however the conductivity is much lower than for NaCl at identical concentrations [35]. The lower concentration of arginine suggests that its effectiveness is due to other factors than electrostatic effects, involving affinity interactions, although whether the lower conductivity of arginine plays any role in effectiveness as an eluent is not clear [35]. Moreover, this behavior can be due to the positive character of this amino acid that promotes a preferential binding of pre-miR-29 to free arginine present in the buffer by electrostatic interactions, inducing its elution. In a general way, the competition study has shown that the free arginine present in the elution buffer could interact with the pre-miR-29, promoting its biospecific elution of the arginine column, due to the competition with the ligand.

In a general point of view, the strategy with NaCl showed to be ideal for pre-miR-29 purification using a low salt concentration (90% of purity and 96.5% of yield), whereas the strategy with $(NH_4)_2SO_4$ requires high salt concentrations to partially purify pre-miR-29 (33% of purity). On the other hand, the competition studies also demonstrated the possibility of purifying pre-miR-29 with higher purity (98% of purity and 56.7% of yield) when compared with other strategies, even though some pre-miRNA is lost in the next elution step. Thus, if larger amounts of pure pre-miRNA are desired, the strategy that employs NaCl can be used, while if higher purity levels are necessary, the competition strategy is more appropriate. Hence, this comparative study brings more evidences that the binding mechanism inherent on the biorecognition between the arginine amino acid and pre-miR-29 molecules, can result from the combination of several phenomenological interactions such as electrostatic interactions, hydrophobic interactions, (multiple) hydrogen bond interactions, van der Waals forces, dipole–dipole forces, cation–π interactions, etc. [36]. However, depending on environmental conditions established and the amino acid ligands used, some interactions can be more favored than other, becoming more evident under these conditions. In fact, in some molecular recognition studies, arginine is reported as a preferential amino acid to contact with RNA, when the overall negative charge of RNA is considered [36,37]. Additionally, recent studies with saturation transfer difference-nuclear magnetic resonance spectroscopy and surface plasmon resonance biosensor reported that adenine, cytosine, and guanine polynucleotides bind to arginine–agarose support mainly through the sugar-phosphate backbone [38,39]. According to the authors, the negative charge of the biomolecules is important for their interaction with arginine-agarose, nonetheless the base exposure on RNA species was also suggested to have a crucial role in nucleic acid retention [22,23]. Furthermore, the structural diversity of RNAs was recently described to be of significant importance in protein–RNA interactions because RNA can exhibit different moieties according to its folding state [40]. Hence, pre-miR-29 structural features seem to be relevant on its distinct retention behavior with the arginine–agarose matrix. The main explanation for the specific interactions occurring between the pre-miR-29 and the immobilized arginine is the single-stranded nature of RNA, which is normally involved in RNA recognition, due to the high base exposure and availability for interactions. Pre-miR-29 is a sRNA molecule in the shape of a stem-loop or hairpin consisting of two long irregular double-stranded stem regions, which are interrupted by a largely single-stranded internal loop. Along the bulge and through the continuous stem sequences there are mostly guanines, which were described to interact preferably with arginine [13]. Moreover, the arginine support has shown the ability to interact with all RNA classes even with different conformational rearrangements [31]. The multiposition interaction of arginine with RNA sites [26,41] can explain this result. This phenomenon can occur because arginine has two different polar centers with which RNA can strongly associate: at α-carbon group and the guanidinium side chain [36]. Thus, it is reasonable to suppose that the retention of all functional classes of RNA in arginine–agarose matrix is due to arginine side chain, which can promote multicontacts with RNA backbone or RNA bases, according to RNA folding. Overall, it is suggested that although electrostatic interactions could play an important role on RNA retention, the base contact is also involved and modulate some favored interaction and specificity found in arginine–agarose chromatography.

Previous analysis allowed the assessment of RNA quality, indicating that the developed pre-miR-29 isolation methodology can purify the target RNA of different RNA species with high recovery yield, purity and good integrity. In a single step, arginine affinity chromatography offered the pre-miRNA purification from a complex biological mixture, making use of low salt concentrations, rather than organic or toxic compounds, and the use of enzymes is not necessary. The chemical lysis with guanidinium buffers used in this method is extensively described in literature for RNA extraction, including in many commercial kit and reagents, with no significant implications in downstream applications. In conclusion, the present data shows the development of an affinity chromatography approach based on natural occurrence interactions, between arginine and RNA species, aiming the purification of pre-miR-29 molecules. The exploitation of these affinity interactions can trigger new insights not only in isolation strategies but also in many other RNA research fields owing to its implication in molecular recognition phenomena. The successful results obtained with this support reveal an efficient technique to obtain a reproducible and appropriate RNA quality with potential applicability for RNA structural and functional studies and gene therapy.

Acknowledgments

This work was supported by the Portuguese Foundation for Science and Technology (PTDC/EBB-BIO/114320/2009, EXPL/BBB-BIO/1056/2012, COMPETE: FCOMP-01-0124-FEDER-027560 and Pest-C/SAU/UI0709/2011). Patrícia Pereira and Ângela Sousa acknowledge a fellowship (Ph.D. Grant, Ref SFRH/BD/81914/2011 and Postdoctoral Grant, Ref SFRH/BPD/79106/2011, respectively).

The authors would like to thank Prof. Yo Kikuchi (Toyohashi University of Technology) for kindly provided of pBHSR1-RM plasmid.

Appendix A. Supplementary data

Supplementary data associated with this article can be found, in the online version, at http://dx.doi.org/10.1016/j.jchromb.2014.01.020.

References

[1] J.A. Broderick, P.D. Zamore, Gene Ther. 18 (2011) 1104.
[2] M. Selbach, B. Schwanhausser, N. Thierfelder, Z. Fang, R. Khanin, N. Rajewsky, Nature 455 (2008) 58.
[3] K. Bettens, N. Brouwers, S. Engelborghs, H. Van Miegroet, P.P. De Deyn, J. Theuns, K. Sleegers, C. Van Broeckhoven, Hum. Mutat. 30 (2009) 1207.
[4] P. Provost, Brain Res. 1338 (2010) 58.
[5] S.S. Hebert, K. Horre, L. Nicolai, A.S. Papadopoulou, W. Mandemakers, A.N. Silahtaroglu, S. Kauppinen, A. Delacourte, B. De Strooper, Proc. Natl. Acad. Sci. U. S. A. 105 (2008) 6415.
[6] I. Vomelova, Z. Vanickova, A. Sedo, Folia Biol. (Praha) 55 (2009) 243.
[7] R. Boom, C.J. Sol, M.M. Salimans, C.L. Jansen, P.M. Wertheim-van Dillen, J. van der Noordaa, J. Clin. Microbiol. 28 (1990) 495.
[8] S.C. Tan, B.C. Yiap, J. Biomed. Biotechnol. 2009 (2009) 574398.
[9] L.E. Easton, Y. Shibata, P.J. Lukavsky, RNA 16 (2010) 647.
[10] S.M. McCarthy, M. Gilar, J. Gebler, Anal. Biochem. 390 (2009) 181.
[11] N. Nonne, M. Ameyar-Zazoua, M. Souidi, A. Harel-Bellan, Nucleic Acids Res. 38 (2010) e20.
[12] L. Ponchon, F. Dardel, Methods 54 (2011) 267.
[13] F. Sousa, D.M. Prazeres, J.A. Queiroz, Trends Biotechnol. 26 (2008) 518.
[14] A. Sousa, F. Sousa, J.A. Queiroz, J. Chromatogr. B Analyt. Technol. Biomed. Life Sci. 877 (2009) 3257.
[15] A. Sousa, F. Sousa, J.A. Queiroz, J. Sep. Sci. 33 (2010) 2610.
[16] R. Martins, J.A. Queiroz, F. Sousa, Biomed. Chromatogr. 26 (2012) 781.
[17] R. Martins, J.A. Queiroz, F. Sousa, J. Mol. Recognit. 23 (2010) 519.
[18] A. Sousa, C.T. Tomaz, F. Sousa, J.A. Queiroz, J. Chromatogr. A 1218 (2011) 8333.
[19] H. Suzuki, S. Umekage, T. Tanaka, Y. Kikuchi, J. Biosci. Bioeng. 112 (2011) 458.
[20] R. Martins, C.J. Maia, J.A. Queiroz, F. Sousa, J. Sep. Sci. 35 (2012) 3217.
[21] F. Sousa, D.M. Prazeres, J.A. Queiroz, Biomed. Chromatogr. 23 (2009) 160.
[22] F. Sousa, D.M. Prazeres, J.A. Queiroz, J. Gene Med. 11 (2009) 79.
[23] F. Sousa, T. Matos, D.M. Prazeres, J.A. Queiroz, Anal. Biochem. 374 (2008) 432.
[24] F.V. Rivas, N.H. Tolia, J.J. Song, J.P. Aragon, J. Liu, G.J. Hannon, L. Joshua-Tor, Nat. Struct. Mol. Biol. 12 (2005) 340.
[25] P. Chomczynski, N. Sacchi, Nat. Protoc. 1 (2006) 581.
[26] B.J. Calnan, B. Tidor, S. Biancalana, D. Hudson, A.D. Frankel, Science 252 (1991) 1167.
[27] F. RE, RNA Methodologies–Laboratory Guide for Isolation and Characterization, Academic Press, York, USA, 2005.
[28] L.V. Madabusi, G.J. Latham, B.F. Andruss, Methods Enzymol. 411 (2006) 1.
[29] S.A. Bustin, T. Nolan, J. Biomol. Tech. 15 (2004) 155.
[30] F. Jiang, A. Gorin, W. Hu, A. Majumdar, S. Baskerville, W. Xu, A. Ellington, D.J. Patel, Structure 7 (1999) 1461.
[31] J.D. Puglisi, J.R. Wyatt, I. Tinoco Jr., Biochemistry 29 (1990) 4215.
[32] R. Mallik, D.S. Hage, J. Sep. Sci. 29 (2006) 1686.
[33] N.M. Luscombe, R.A. Laskowski, J.M. Thornton, Nucleic Acids Res. 29 (2001) 2860.
[34] A. Tsutsumi, T. Kawamata, N. Izumi, H. Seitz, Y. Tomari, Nat. Struct. Mol. Biol. 18 (2011) 1153.
[35] T. Arakawa, D. Ejima, K. Tsumoto, M. Ishibashi, M. Tokunaga, Protein Expr. Purif. 52 (2007) 410.
[36] M. Yarus, J.J. Widmann, R. Knight, J. Mol. Evol. 69 (2009) 406.
[37] M. Treger, E. Westhof, J. Mol. Recognit. 14 (2001) 199.
[38] C. Cruz, E.J. Cabrita, J.A. Queiroz, J. Chromatogr. A 1218 (2011) 3559.
[39] C. Cruz, E.J. Cabrita, J.A. Queiroz, Anal. Bioanal. Chem. 401 (2011) 983.
[40] J.J. Ellis, M. Broom, S. Jones, Proteins 66 (2007) 903.
[41] T. Janas, J.J. Widmann, R. Knight, M. Yarus, RNA 16 (2010) 805.

Paper VII

Pharmaceutical-grade pre-miR-29 purification using an agmatine monolithic support

P. Pereira, A. Sousa, J. A. Queiroz, A. Figueiras, F. Sousa

Journal of Chromatography A. 2014. 1368: 173-182

Short description: This paper reports, for the first time, a new affinity chromatographic method that combines the structural versatility and high capacity of the monolithic support with the high specificity and selectivity conferred by the agmatine ligand, to efficiently isolate pre-miR-29b from other host small RNAs. Breakthrough experiments were designed to study the effect of different RNA concentrations on the dynamic binding capacity of the monolithic support. Subsequently, different types and concentrations of salt in the loading buffer were tested, allowing the establishment of different interactions, in order to achieve higher efficiency and selectivity to purify pre-miR-29b. The effect of different flow rates on pre-miR-29b separation was also evaluated. This purification strategy presents advantages over other previously published, namely faster separations and shorter contact time, ensuring structural stability of the target molecule, in relation to conventional supports.

Journal of Chromatography A, 1368 (2014) 173–182

Contents lists available at ScienceDirect

Journal of Chromatography A

journal homepage: www.elsevier.com/locate/chroma

Pharmaceutical-grade pre-miR-29 purification using an agmatine monolithic support

Patrícia Pereira [a], Ângela Sousa [a], João A. Queiroz [a], Ana Figueiras [a,b], Fani Sousa [a,*]

[a] CICS – Health Sciences Research Centre, University of Beira Interior, Avenida Infante D. Henrique, 6200-506 Covilhã, Portugal
[b] CNC – Center of Neuroscience and Cell Biology, University of Coimbra, Largo Marquês de Pombal, 3004-517 Coimbra, Portugal

ARTICLE INFO

Article history:
Received 18 June 2014
Received in revised form
14 September 2014
Accepted 27 September 2014
Available online 7 October 2014

Keywords:
Affinity chromatography
Agmatine monolith
pre-miR-29
MicroRNA purification
Small RNA

ABSTRACT

MicroRNA-based therapeutic applications have fostered a growing interest in the development of microRNAs purification processes in order to obtain the final product with high purity degree, good quality and biologically active. The pre-miR-29 deficiency or overexpression has been associated to a number of clinically important diseases, and its therapeutic application can be considered. Monolithic columns emerged as a new class of chromatographic supports used in the plasmid DNA purification platforms, being an interesting alternative to the conventional particle-based columns. Thus, the current work describes, for the first time, a new affinity chromatography method that combines the high selectivity of agmatine ligands with the versatility of monoliths to specifically and efficiently purify pre-miR-29 from other small RNA species and *Rhodovulum sulfidophilum* impurities. The effect of different flow rates on pre-miR-29 separation was also evaluated. Moreover, breakthrough experiments were designed to study the effect of different RNA concentrations on the modified monolithic support binding capacity, being verified that the dynamic binding capacity for RNA molecules is dependent of the feed concentration. In order to achieve higher efficiency and selectivity, three different binding and elution strategies based on increased sodium chloride (1.75–3 M) or arginine (100 mM) and decreased ammonium sulfate (2.4–0 M) stepwise gradients are described to purify pre-miR-29. As a matter of fact, by employing elution strategies using sodium chloride or arginine, an improvement in the final pre-miR-29 yields (97.33 and 94.88%, respectively) as well as purity (75.21 and 90.11%, respectively) were obtained. Moreover, the quality control analysis revealed that the level of impurities (proteins, endotoxins, sRNA) in the final pre-miR-29 sample was negligible. In fact, this new monolithic support arises as a powerful instrument on the microRNA purification to be used in further clinical applications, providing a more rapid and economical purification platform.

1. Introduction

In the past decade, countless species of non-coding RNA, namely ribosomal RNA (rRNA), transfer RNA (tRNA) and a range of smaller like microRNA (miRNA) molecules, have been discovered and deeply studied. Of these, miRNAs molecules attract particular interest due to their essential roles in most cellular processes, as potential biomarkers and drug targets [1,2]. For this reason, RNA represents an important target of a wide range of laboratory analysis, being particularly relevant in the diagnosis of several disorders, as well as in basic and applied research. Hence, RNA quality and purity are prerequisites of a multitude of molecular biology and therapeutic applications [3]. Thereby, RNA purification is important to achieve pure, stable and intact RNA, free from contaminants, including genomic DNA, proteins and organic solvents, once these impurities greatly affect the pharmaceutical and clinical applications [3,4]. This fact greatly contributes to the need to develop novel methods for the rapid and inexpensive isolation and purification of microRNAs.

RNA is an unstable molecule and has a very short half-life once extracted due to the ubiquitous presence of RNA-degrading enzymes (RNases) which are present in biological samples, aqueous buffers, on labware and can be introduced via human handling [5]. To overcome the problems associated with RNA isolation, several strategies are available to isolate and purify miRNA molecules chemically synthesized or derived from various biological sources [3,6]. The purification of RNA molecules is already reported by using preparative denaturing polyacrylamide gel electrophoresis (PAGE),

* Corresponding author at: Centro de Investigação em Ciências da Saúde, Universidade da Beira Interior, Avenida Infante D. Henrique, 6200-506 Covilhã, Portugal. Tel.: +351 275 329 074; fax: +351 275 329 099.
E-mail address: fani.sousa@fcsaude.ubi.pt (F. Sousa).

http://dx.doi.org/10.1016/j.chroma.2014.09.080
0021-9673/

affinity tag-based purification, anion-exchange and size exclusion chromatography [7–11]. These methods make use of enzymes and structural modifications in the RNA molecule by the introduction of tags sequences, which can affect the overall topology of the RNA. In addition, the application of this methodology and RNA modifications is typically limited to sRNAs, smaller than 40 nucleotides [4,12,13]. Overall, and although these purification methods can be very efficient for the recovery of RNA with high quality and quantity, they still are expensive on large scale, labor intensive and only allow the separation of small RNAs (sRNAs) from rRNA. In addition, in most cases the isolation of pure RNA is achieved by a secondary enrichment, either through enzymatic removal of DNA or by a second set of columns specific to miRNA [14].

In the last years, our research group developed a new affinity chromatography approach, named amino acid-affinity chromatography to efficiently purify different RNA species (total RNA, rRNA, sRNA and 6S RNA) [15–17]. This powerful technique is based on the application of amino acids as specific ligands to purify RNA on the basis of their biological function or individual chemical structure [18]. More recently, lysine, tyrosine and arginine amino acids have been successfully applied as affinity ligands for microRNAs purification, particularly in pre-miR-29 isolation, in conventional particle-based columns [19–21]. Amino acid ligands described above showed high selectivity, however a faster and more robust purification method is required due to the structural characteristics of the RNA molecule, including their stability. Monolithic supports have been largely explored in recent years for the separation of large biomolecules owing to their structural properties compared with conventional columns, namely high binding capacity, excellent mass transfer properties and a huge quantity of accessible binding sites [22,23]. Moreover, monoliths allow a very fast separation and purification with high reproducibility both at small and large scales, support higher flow rates and reduced biomolecules degradation due to the shorter contact times with the chromatographic matrix [24].

This work has the purpose of exploring the possibility of using agmatine amino acid derivative as ligand, combined with the multi-functionality of the monolithic support [25–27] to selectively isolate the pre-miRNA from the recombinant *Rhodovulum sulfidophilum* host. Knowing that an agarose based matrix with immobilized arginine amino acid allows an efficient separation of pre-miR-29 [21], it becomes interesting to study a new monolith with agmatine immobilized. Agmatine is a neurotransmitter derived from the decarboxylation of arginine and plays the role of agonist or antagonist of different enzymes involved in several biological mechanisms [28–30]. This study demonstrates for the first time, the use of this amino acid derivative as a chromatographic ligand to purify microRNA. In this way, the aim of the present study is to develop new methodologies for RNA isolation, enabling the pre-miRNA-29 purification with high integrity and purity using monoliths, in view of the application in molecular biology or therapeutic procedures in a short time. Additional chromatographic characterization based on breakthrough experiments is also designed to study the dynamic binding capacity for RNA. The binding behavior of pre-miR-29 under the influence of different environmental conditions, such as the elution buffer composition, or using different flow-rates is also investigated.

2. Materials and methods

2.1. Materials

All buffers used for the chromatographic experiments were freshly prepared with sterilized water pre-treated with 0.05% diethyl pyrocarbonate (DEPC; Sigma–Aldrich, St Louis, MO, USA), filtered through a 0.20 μm pore size membrane (Schleicher Schuell, Dassel, Germany) and degassed ultrasonically. The ammonium sulfate and sodium chloride salts used in these buffers were purchased to Panreac (Barcelona, Spain), tris(hydroxymethyl) aminomethane (Tris) to Merck (Darmstadt, Germany) and agmatine sulfate was from Sigma–Aldrich (St. Louis, MO, USA). Chromatographic experiments were carried out in the 0.34 mL bed volume (average pore size of 1500 nm in diameter) carbonyldiimidazole (CDI) monolith modified with agmatine amino acid derivative, kindly provided by BIA Separations (Ajdovščina, Slovenia). The guanidinium salt and all the chemicals used in the lysis buffer were obtained from Sigma–Aldrich (St Louis, MO, USA). All the materials used in the experiments were RNase-free. The DNA molecular weight marker, Hyper Ladder I, was obtained from Bioline (London, UK) and GreenSafe Premium was purchased to NZYTech (Lisbon, Portugal).

2.2. Pre-miR-29 production and isolation

The pre-miR-29 was obtained from the culture of *Rhodovulum sulfidophilum* DSM 1374 strain (BCCM/LMG, Belgium) modified with the plasmid pBHSR1-RM containing the sequence of pre-miR-29 [31]. Growth was carried out in shaker flasks with capacity of 500 mL containing 100 mL of Nutrient Broth medium (1 g/L beef extract; 2 g/L yeast extract; 5 g/L peptone and 5 g/L sodium chloride) supplemented with 30 μg/mL kanamycin, in a rotary shaker at 30 °C and 250 rpm under dark-aerobic conditions. The small RNA fraction was extracted from bacterial pellets of *Rhodovulum sulfidophilum* by a modified acid guanidinium thiocyanate–phenol–chloroform extraction method, as described by Pereira and co-workers [21]. Briefly, cells were lysed and the small RNA fraction obtained was precipitated with isopropanol. Precipitated molecules were recovered by centrifugation at 15,000 × *g* for 20 min at 4 °C. After centrifuging, the small RNA pellet was washed with 75% ethanol and incubated at room temperature for 10 min, followed by a 5 min centrifugation at 15,000 × *g* (4 °C). The air-dried small RNA pellet was solubilized in 1 mL of DEPC-treated water. Finally, 260 and 280 nm absorbance of the samples was measured using a nanophotometer in order to assess small RNA quantity and purity.

2.3. Chromatographic experiments

The chromatographic experiments were performed in an ÄKTA Avant system with UNICORN 6 software (GE Healthcare, Sweden). For the experiments, agmatine monolithic disk was equilibrated with appropriate loading buffer, as described below, at a flow rate of 1 mL/min. The pre-miR-29 was purified by exploiting three different elution strategies, namely by using sodium chloride (NaCl), ammonium sulfate ($(NH_4)_2SO_4$) and arginine as competition agent. In experiments with ammonium sulfate, the monolith was equilibrated with 2.4 M of $(NH_4)_2SO_4$ in 10 mM Tris–HCl buffer (pH 8). After the elution of unbound species, the ionic strength of the buffer was stepwise decreased to reach the 0 M $(NH_4)_2SO_4$ in 10 mM Tris–HCl buffer (pH 8), to elute of pre-miR-29. On the other hand, in experiments with sodium chloride, after washing out the unbound material with 1.75 M NaCl in 10 mM Tris–HCl buffer (pH 9.5), the ionic strength of the buffer was increased to 3 M NaCl in 10 mM Tris–HCl buffer (pH 9.5). The experiments performed with arginine as a competition agent to purify pre-miR-29 molecules were initiated with the equilibration of the monolith with 1.75 M NaCl in 10 mM Tris–HCl buffer (pH 9.5) to promote the total retention of pre-miR-29 and then the elution was accomplished by changing to 1.75 M NaCl supplemented with 100 mM arginine in 10 mM Tris–HCl buffer (pH 9.5). The most retained species were finally eluted with 3 M NaCl. In the three sets of experiments, sRNAs extracts (30 μg), containing 6S RNA, pre-miR-29 and other sRNA,

including transfer RNAs, were injected onto the column using a 100 μL loop at the same flow-rate. The absorbance of the eluate was continuously monitored at 260 nm. All experiments were performed at room temperature. Fractions were pooled according to the chromatograms obtained, and following concentration and desalting with Vivaspin concentrators (Vivascience), the pools were kept for quantification and further analysis. A posterior study was performed to analyze the effect of different flow-rates (0.5, 1, 2 and 3 mL/min) in the pre-miR-29 purification efficiency using the agmatine monolith.

2.4. Dynamic binding capacity measurement for sRNA

Agmatine monolithic disk was used for the determination of the dynamic binding capacity (DBC) for RNA. These experiments were performed with 1 mL/min of flow rate using different concentrations of the feedstock (0.025, 0.05, 0.075, 0.1, 0.15, 0.20 and 0.25 mg/mL). The support was equilibrated with 10 mM Tris–HCl buffer (pH 8) and thereafter, it was overloaded with the RNA solution under the same equilibrium conditions. DBC was determined by the breakthrough area integration method [32]. Briefly, each breakthrough experiment was derived from a 100% of saturated monolith. Then, the sample volume corresponding to the adsorbed amount of RNA was calculated by numerical integration of the detector response. The area obtained from the filled monolith was subtracted from that for the empty monolith. In this step, the void volume was discounted from the DBC determination. This area is equivalent to the sample volume, which was required to saturate the monolithic support, and can be related with RNA mass that remained bound per milliliter of the support, reflecting the support capacity. Normally, the capacity values are represented at 10, 50 and 100% of the breakthrough that corresponds to 10, 50 and 100% of the column saturation, being calculated in the same way. Finally, the elution of the bound RNA was achieved by increasing the sodium chloride concentration in the mobile phase to 3 M in a stepwise manner.

2.5. Polyacrylamide electrophoresis

Fractions recovered from the sRNA chromatographic experiments were analyzed by vertical electrophoresis using an Amersham Biosciences system (GE Healthcare, Sweden) with 10% polyacrylamide gel. Electrophoresis was carried out at 125 V for 90 min with TBE buffer (0.84 M Tris base, 0.89 M boric acid and 0.01 M EDTA, pH 8.3). sRNA samples were previously denatured with 97.5% formamide and denatured conditions were kept in the gel owing to the presence of 8 M urea. sRNA molecules were visualized in the gel by using the Vilber Lourmat system after staining with ethidium bromide (0.5 mg/mL).

2.6. Protein analysis

Proteins contamination in pre-miR-29 samples collected from the purification with agmatine monolithic support, was measured by using the micro-BCA (bicinchoninic acid) assay (Thermo Fisher Scientific Inc., Rockford, IL, USA), according to manufacturer's instructions. Briefly, the calibration curve was prepared using BSA standards (0.01–0.25 mg/mL). A total of 25 μL of each standard or pre-miR-29 samples was added to 200 μL of BCA reagent in a microplate and incubated for 30 min at 60 °C. Absorbance was measured at 570 nm in a microplate reader.

2.7. Pre-miR-29 identification analysis

Pre-miR-29 identification was confirmed using reverse-transcriptase polymerase chain reaction (RT-PCR). Thus, cDNA synthesis was performed using RevertAid First Strand cDNA Synthesis Kit (Fermentas, Thermo Fisher Scientific Inc.), according to the manufacturer's instructions. A total of 0.5 μg of RNA samples collected after the chromatographic purification process with agmatine monolith was used to initiate cDNA synthesis, which was denatured for 5 min at 65 °C with 20 pmol of gene-specific primers (5′-GACAGC GGT ATG ATC CCC CAA-3′). Then, PCR reactions were carried out using 1 μL of synthesized cDNA in a 25 μL reaction containing 0.125 U of Supreme DNA polymerase (NZYtech, Lisbon, Portugal), 50 mM of magnesium chloride (NZYtech, Lisbon, Portugal) and 150 nM of each primer. Sense (5′-GGA AGCTGG TTT CAT ATG GTG-3′) and antisense (5′-CCC CCA AGA ACA CTG ATT TC-3′) primers were used to amplify a fragment of 145 bp. The PCR program was carried out as follows: denaturation at 95 °C for 5 min, followed by 40 cycles at 95 °C for 30 s, 63 °C for 30 s and 72 °C for 15 s, and a final elongation step at 72 °C for 5 min. To confirm the presence and purity of amplicons, PCR products were analyzed using 1% agarose gel [21].

3. Results and discussion

The purification methods developed to purify microRNAs envisioning therapeutic applications require the use of a chromatographic support able to eliminate impurities, maintaining the structural integrity of the biomolecule. Hence, the present study aims to explore and characterize the interactions occurring between pre-miR-29 and agmatine amino acid derivative immobilized into a monolithic disk, combining, for the first time, the selectivity, specificity and biorecognition of agmatine ligands with the structural versatility and capacity provided by monolithic supports. These supports offer several potential advantages over conventional supports, including higher selectivity and reproducibility and good capacity [17,26,33,34]. The miR-29 target was chosen because it belongs to one of the most interesting miRNA families in humans to date, once this miRNA is involved in several regulatory pathways associated with neurodegenerative diseases and also presenting tumor-suppressing and immune-modulating properties [35–37]. Therefore, the purpose of this work is to describe an alternative method to purify pre-miRNA from a complex mixture of total RNA by affinity chromatography, exploiting the multiple biological interactions which occur between the pre-miR-29 and the agmatine ligand immobilized in monoliths.

3.1. Agmatine monolithic disk

Non-grafted CDI monolith was properly modified with agmatine ligand by BIA Separation (Ajdovščina, Slovenia), and the suitable agmatine ligand immobilization was confirmed through a comparison of the different chromatographic profiles of the new support and the non-grafted CDI monolith (data not shown). Recently, our research group has demonstrated the possibility of using the non-grafted CDI monolith to purify plasmid DNA by using a decreasing stepwise gradient of ammonium sulfate but not using sodium chloride (NaCl) [25,26]. Thereby, the two monolithic disks were equilibrated with 10 mM Tris–HCl buffer (pH 8) at 1 mL/min, and after the injection of 30 μg of sRNA sample, a 15-min linear gradient up to 3 M of NaCl in 10 mM Tris–HCl buffer (pH 8) was established. In the non-grafted CDI monolith, a single peak was rapidly attained in the flow through due to the elution of species with lower affinity. Afterwards, the NaCl linear gradient was established but no species were eluted (data not shown). These results indicated that the non-grafted CDI monolith did not interact with sRNA molecules under the conditions used. The same experiment was conducted in the monolith modified with agmatine ligand. The total retention of sRNA was obtained at 10 mM Tris–HCl buffer (pH 8) and the total

Table 1
Effect of sRNA concentration on 10%, 50% and total dynamic binding capacity of agmatine monolithic disk. The breakthrough experiments were performed on a single monolithic disk, at flow rate of 1 mL/min. The loading sample was sRNA dissolved in 10 mM Tris–HCl buffer (pH 8).

sRNA concentration (mg/mL)	DBC (mg/mL)		
	10%	50%	Total
0.025	0.24	1.04	3.51
0.05	0.71	1.37	4.74
0.075	0.88	1.46	5.90
0.10	1.28	1.63	6.92
0.15	1.98	2.71	7.09
0.20	2.38	3.07	7.59
0.25	2.91	3.22	8.08

elution was verified during the linear gradient by increasing the NaCl concentration in the buffer from 0 to 3 M (data not shown). These results confirmed that the agmatine monolith is chemically different from the non-grafted CDI disk and the agmatine ligands immobilized on the monolith are the ones responsible for sRNA interaction with the support.

3.2. Effect of feed concentration on dynamic binding capacity of sRNA

For a complete characterization of the agmatine monolithic disk, the dynamic binding capacity (DBC) was evaluated, once this parameter is a critical factor for the chromatographic performance. For this purpose, several breakthrough experiments were performed at 1 mL/min, with different sRNA concentrations (0.025–0.25 mg/mL). The results summarized in Table 1 indicate that the total capacity of the agmatine monolithic disk to bind sRNA was higher for the feed concentration of 0.25 mg/mL, where it was found a total capacity of 8.08 mg/mL. By analyzing the data in Table 1, it appears that at 10, 50 and 100% of the breakthrough, the DBC increases with increasing RNA concentrations, thus, it can be argued that the binding capacity is dependent of the RNA concentration. The profile obtained with agmatine monolithic disk is in concordance with other RNA binding profiles described for monoliths, such as CIM IDA monolithic column [38]. Furthermore, these DBC results found for agmatine monolith are very good when compared with other values described for purified baker's yeast RNA, where the CIM IDA monolithic column presented a binding capacity of 1.20 mg/mL, using 1 mg/mL of feed RNA [38]. This comparison suggests that the immobilized agmatine ligand can be responsible for the improvement on the DBC of the monolithic support through the enhancement of the interaction ligand–sRNAs, although the sRNA concentrations used are significantly lower than in the previous study (0.5–2 mg/mL) [38]. These findings can be due to the fact that RNA has a size of 100 nm to over 300 nm in diameter, and monoliths present a larger channel size of 1000–5000 nm allowing full availability of the ligands on the chromatographic support even at low feed concentration of sRNA. Thus, these results indicate that the DBC is dependent of sRNA feed concentration [39]. Overall, these results suggest that a very efficient chromatographic performance for RNA purification using monolithic columns can be achieved if using low RNA feed concentration.

Through the analysis of the isotherm profile, it can be seen that, in the sRNA concentration range studied, the DBC increases from 3 mg/mL to a plateau region, as the RNA concentration (C_{RNA}) increases. Considering the equilibrium binding isotherm data, Fig. 1, it is possible to define a linear and a plateau region. Thus, it is suggested that our data follow the Langmuir model, assuming that the adsorbed molecules have a fixed number of sites on the adsorbent where interactions can occur, and that every adsorption site is energetically equivalent and accepts only one molecule

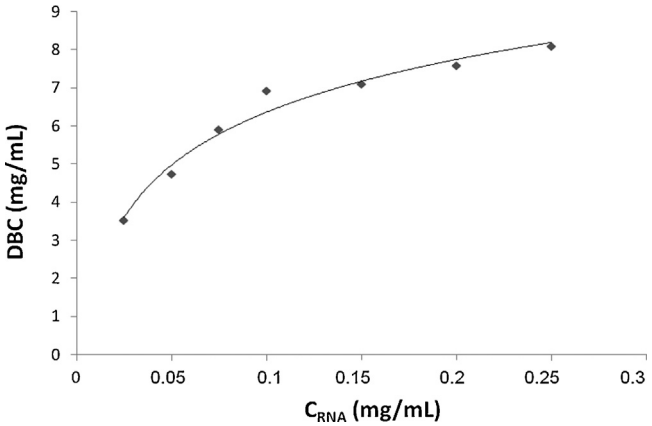

Fig. 1. Adsorption isotherm of sRNA on agmatine monolith.

[40]. At low concentrations (0.025–0.075 mg/mL), RNA is well distributed at the agmatine ligands and the orientation is determined by agmatine ligand–RNA interactions, resulting in a linear shaped curve between RNA adsorbed amounts and mobile phase concentrations. At high concentrations (0.1–0.25 mg/mL), the adsorption sites may become saturated, leading to a curvature of the isotherm into an asymptote. Concentration values of sRNA absorbed above 7 mg/mL are considered in the overloaded zone of the isotherm.

In addition, the dissociation constant (K_d) from adsorption isotherm, which represents the interaction between the sRNA and agmatine monolithic support was also calculated by frontal analysis chromatography, according to what is described by Ruta and co-workers [41]. Through the values at 50% of breakthrough experiments obtained with agmatine monolith at different sRNA concentrations, the K_d value was 2.6×10^{-7} M. A K_d value between 10^{-4} and 10^{-8} M indicates that the risks of irreversible biomolecules adsorption and denaturation are minimized [40]. So, the K_d value obtained, reveals a good affinity interaction between the ligand and RNA, which indicates that agmatine monolith is a good affinity support.

3.3. Effect of elution buffer composition and pH manipulation on pre-miR-29 binding

In affinity chromatography the elution of a target biomolecule can be performed either specifically, through addition of a competing agent in the elution buffer or non-specifically, through changes in the elution buffer composition, namely in type of salt and ionic strength, and pH manipulation depending on the matrix used and the chemical characteristics of target biomolecule [18]. As previously mentioned, in this study the chromatographic behavior of the agmatine monolith interacting with RNA, was evaluated according to the type and salt concentration and pH manipulation. Beforehand, several binding/elution studies were performed in order to determine the best salt concentration range to achieve the binding and elution of the pre-miR-29 (data not shown). Linear and stepwise gradients were tested, and it was determined that the stepwise elution is more suitable to obtain the pre-miR-29 separation, once this strategy allows greater selectivity between the biomolecule in study and contaminants. Moreover, it was verified the possibility to establish an increased NaCl gradient to bind and recover the pre-miR-29. After this preliminary characterization of the pre-miR-29 retention behavior on the agmatine monolith it was evaluated the pH effect on pre-miR-29 stability, in order to determine which pH value should be used in the purification process. In addition, the pH could also significantly influence pre-miR-29 interactions with the immobilized agmatine, given the versatility of this ligand. Thus, several chromatographic experiments, based on ionic-based

Table 2
Effect of pH of mobile phase in the tRNA and pre-miR-29 retention, using 10 mM Tris buffer as loading condition.

pH of mobile phase	tRNA retention	pre-miR-29 retention
6.5	++	++
8.0	+	++
9.5	–	++

From (–) no retention to (++) total retention.

elution conditions, were designed to analyze how the pH ranging between 6.5 and 9.5 affects the retention of pre-miR-29 and other *R. sulfidophilum* sRNA species, considering the pKa of 13 of this ligand [42].

Table 2 summarizes several chromatographic runs performed at different loading conditions (pH and NaCl manipulation), and the relative effect of these conditions on tRNA and pre-miR-29 retention ((–) no retention to (++) total retention). As a matter of fact, the results showed an increased retention of all sRNAs species when the pH of the mobile phase is lower (pH 6.5), suggesting that the decreased pH favors the establishment of stronger electrostatic interactions but also the involvement of multiple non-covalent interactions, namely cation–π interactions, hydrogen bonds, hydrogen π interactions and water mediated bonds. These different types of interaction established between the pre-miR-29 and agmatine ligands can be related with the positive charge (the effective surface charge) of agmatine, considering the fact that at the working pH (between 6.5.and 9.5), agmatine is protonated. In addition, the agmatine is a derivative of arginine amino acid, containing basic guanidinium group and the lack of the carboxyl group, so that both amino acids have very similar structures. Thus, the multiplicity of interactions can also occur because agmatine has one polar center with which RNA can strongly associate. It is reasonable to suppose that the retention of all functional classes of RNA in agmatine monolith is due to the length of agmatine side chain and its ability to produce good hydrogen bond geometries [43,44], which can promote multicontact with RNA backbone or RNA bases, according to RNA folding (RNA conformations) [45–47]. The cation–π interactions can be due to interactions between positive guanidinium group of agmatine and aromatic rings of the nitrogen bases of RNA [17].

Moreover, for the highest pH studied (pH 9.5), it was observed that the pre-miR-29 was more retained than other species from tRNA, because some interactions described above are less favored and therefore only some RNA species bound to the support, as pre-miR-29, whereas other species do not bind. Thus, the pH used for the study, using sodium chloride as elution strategy, was pH 9.5, due to a higher retention of pre-miR-29 and a more pronounced difference between the pre-miR-29 retention and the binding of other RNA species, which allowed exploring the selectivity of the agmatine ligand.

To investigate the retention behavior of the target miRNA in the agmatine monolith, after binding, the pre-miR-29 elution was achieved with the application of a stepwise gradient increasing the NaCl concentration up to 3 M in 10 mM Tris–HCl buffer (pH 9.5). The chromatographic profile of the pre-miR-29 purification from a complex mixture of *R. sulfidophilum* sRNA, using the agmatine monolithic disk, is presented in Fig. 2A. The chromatographic run was initiated with an ionic strength of 1.75 M NaCl in 10 mM Tris–HCl buffer (pH 9.5). After injection of the complex mixture of sRNA, a first peak was obtained with the same salt concentration of the equilibrium buffer, resulting from the elution of unbound species. As shown in Fig. 2A, the ionic strength of elution buffer was increased to 2.5 M of NaCl to elute the pre-miR-29 in a second peak. The elution of highly bound species, mostly tRNAs, was then achieved by increasing the ionic strength of the buffer to 3 M NaCl (peak 3). In this way, this result demonstrates that the agmatine ligands distinguished and differentially interacted with various RNA molecules, suggesting a specific recognition for the pre-miR-29. Thereby, in order to establish a correlation between the different RNAs species present in the mixture, and the peaks in the chromatogram, a polyacrylamide gel electrophoresis (Fig. 2B) was performed, thus the lines 1, 2 and 3 presented in the electrophoretic profile correspond to the samples pooled from the respective peaks in the chromatogram. Hence, electrophoretic analysis revealed that the first peak of unbound species corresponds to the elution of tRNA species (Fig. 2B, lane 1), at lower ionic strength. On the other hand, the elution of the pre-miR-29 only occurs with the increase of ionic strength in the second peak (Fig. 2B, lane 2). Finally, the 6S RNA, pre-miR-29 and other tRNAs species were eluted with 3 M NaCl, as it was observed in the third chromatographic peak (peak 3 and lane 3). These findings suggest that pre-miR-29 presents a stronger interaction with the agmatine monolith than the majority of tRNA species.

Recently, our research group demonstrated the possibility to purify pre-miR-29 using stepwise gradients of NaCl with the arginine–agarose matrix [21] being verified the pre-miR-29 elution at 360 mM of NaCl, while in this study the agmatine monolith

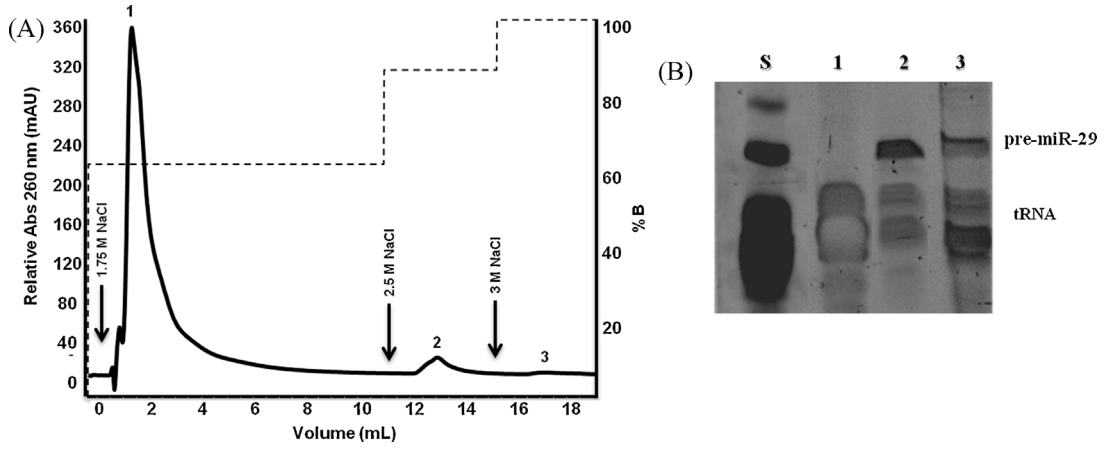

Fig. 2. (A) Chromatographic profile of the pre-miR-29 purification from a sRNA mixture using the agmatine monolithic disk. Elution was performed at 1.0 mL/min by stepwise increasing NaCl concentration in the eluent from 1.75, 2.5 and 3 M, as represented by the arrows. (B) Polyacrylamide gel electrophoresis of samples collected at the column outlet. Fractions corresponding to peaks (1)–(3) are shown in lanes 1–3, respectively. Lane S, impure sRNA preparation injected onto the column.

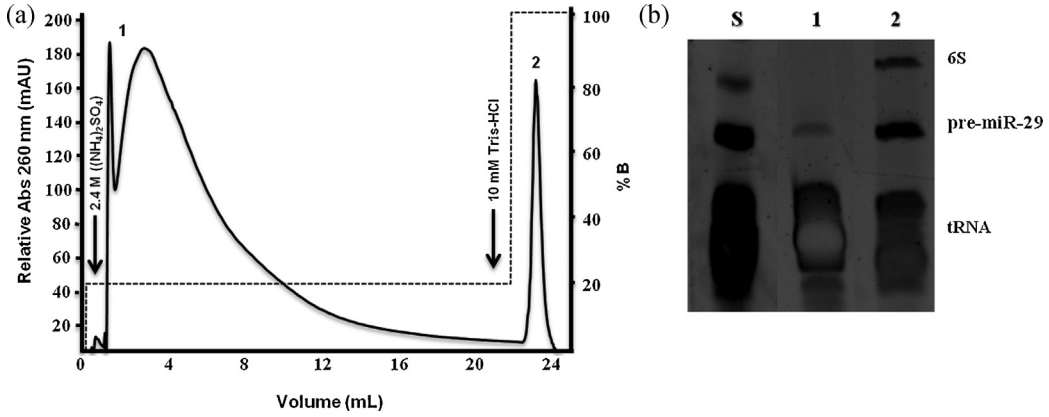

Fig. 3. (A) Chromatogram showing the purification of pre-miR-29 from sRNA population by using the agmatine monolithic disk. Elution was performed at 1 mL/min by stepwise decreasing $(NH_4)_2SO_4$ concentration in the eluent from 2.4 to 0 M $(NH_4)_2SO_4$ in 10 mM Tris buffer (pH 8.0). (B) Polyacrylamide gel electrophoresis analysis of samples collected at the column outlet. Fractions corresponding to peaks (1) and (2) are shown in lanes 1 and 2, respectively. Lane S, impure sRNA sample injected onto the column.

allowed the recovery and purification of pre-miR-29 with 2.5 M of NaCl. In general, this comparative study evidences that the binding mechanism inherent to the biorecognition of pre-miR-29 by the agmatine amino acid derivative is stronger than the interactions established with the arginine amino acid. This phenomenon can result from the combination of multiple elementary interactions such as electrostatic interactions, hydrogen bonds, hydrogen π interactions, water mediated bonds and cation–π interactions, which both ligands may engage through the terminal guanidine group. However, in the agmatine monolith a stronger interaction occurred since the recovery of pre-miR-29 required a higher NaCl concentration. The difference between the ligands is the absence of the carboxyl group in agmatine, which can have two positive effects in the RNA retention. It can prevent repulsion of charged molecules and enables the establishment of additional hydrophobic interactions with the carbon backbone of the ligand. Thus, depending on the environmental conditions established and the amino acid ligands used, some interactions can be more favored than other, becoming more evident under these conditions. In order to prove this hypothesis and mainly exploit hydrophobic interactions, a stepwise gradient by decreasing ammonium sulfate ($(NH_4)_2SO_4$) concentration between 2.4 M and 0 M in 10 mM Tris–HCl buffer (pH 8) was applied. In this case, the agmatine monolith was equilibrated with 2.4 M $(NH_4)_2SO_4$ in 10 mM Tris–HCl buffer (pH 8). After the binding of the sample to the disk, a first elution step designed to elute the tRNA species with lower affinity to the support was carried out with the same salt concentration of the equilibrium buffer, promoting total pre-miR-29 retention (Fig. 3A). The elution of pre-miR-29 was then achieved with a second step by using 0 M $(NH_4)_2SO_4$ in 10 mM Tris–HCl buffer (pH 8) (Fig. 3A). In fact, the high salt concentration plays a key role on the pre-miR-29 binding to agmatine ligand. Again, a polyacrylamide gel electrophoresis was used to detect and identify different species eluting in each chromatographic peak (Fig. 3B). The electrophoretic analysis of the fractions eluting from the agmatine monolith (Fig. 3A) proved that the first peak of unbound material corresponds to the elution of tRNA (Fig. 3B, lane 1), whereas the second peak was mainly attributed to the elution of pre-miR-29 (Fig. 3B, lane 2). The interactions that favor the recognition of pre-miR-29, under hydrophobic elution conditions, can be van der Waals forces and hydrophobic interactions while the main responsible group for the interactions established between pre-miR-29 and agmatine ligand can be the carbon chain of the spacer arm.

The functionality of agmatine ligand to biorecognize the pre-miR-29 under hydrophobic- and ionic-based elution conditions shows the applicability and versatility of this ligand to develop several pre-miR-29 purification strategies due to the multiple interactions involved for each condition. Apart from the structural characteristics of the agmatine ligand, also the pre-miR-29 structural features seem to be relevant on its distinct interaction behavior with the ligand. The main explanation for the specific interactions occurring between the pre-miR-29 and the agmatine amino acid derivative is the single-stranded nature of RNA, which is normally involved in RNA recognition, due to the high base exposure and availability for interactions. Additionally, the negative charge conferred by the phosphate groups in the RNA backbone is important for their interaction with the agmatine monolith, suggesting them to have a crucial role in RNA retention. Likewise, pre-miR-29 is a sRNA molecule with the shape of a stem-loop or hairpin consisting of two long irregular double-stranded stem regions, which are interrupted by a largely single-stranded internal loop [21]. This particular structure may also explain the multiple non-covalent interactions established which are involved in the biomolecular recognition of pre-miR-29 by the agmatine ligand.

In turn, to obtain an elution strategy more selective and biospecific as well as to achieve higher elution efficiency, it was employed a new approach for pre-miR-29 purification using arginine as competitive agent. This agent can bind either to the retained pre-miR-29 or to the immobilized agmatine ligand depending on their characteristics, allowing thus to predict the interactions that can be involved once agmatine is derived of arginine. The competitive studies were performed by adding 250 mM of arginine to the elution buffer in stepwise gradient to exploit specific elution of pre-miR-29 from the agmatine monolith and therefore to evaluate the possibility of reaching higher purification factors. Elution gradients applied were adapted to ensure that the RNA sample is on ideal conditions to bind to the support and be eluted only due to the competing agent. Agmatine monolith was first equilibrated with 1.75 M NaCl in 10 mM Tris–HCl buffer (pH 9.5) to promote the total retention of pre-miR-29. After sample application, a first peak of unbound species was obtained and then the ionic strength was increased upon arginine addition. In this step, 1.75 M of NaCl supplemented with 100 mM arginine in 10 mM Tris–HCl buffer (pH 9.5) was used for the elution of pre-miR-29 in a second peak (Fig. 4A).

These findings are in accordance with previous published results which show that this competition strategy is able to elute bound pre-miR-29 from arginine–agarose column [21]. It is suggested that the major mechanism from which pre-miR-29 is eluted from the agmatine support is the preferential binding of free arginine to the pre-miR-29, an interaction that we believe to be stronger

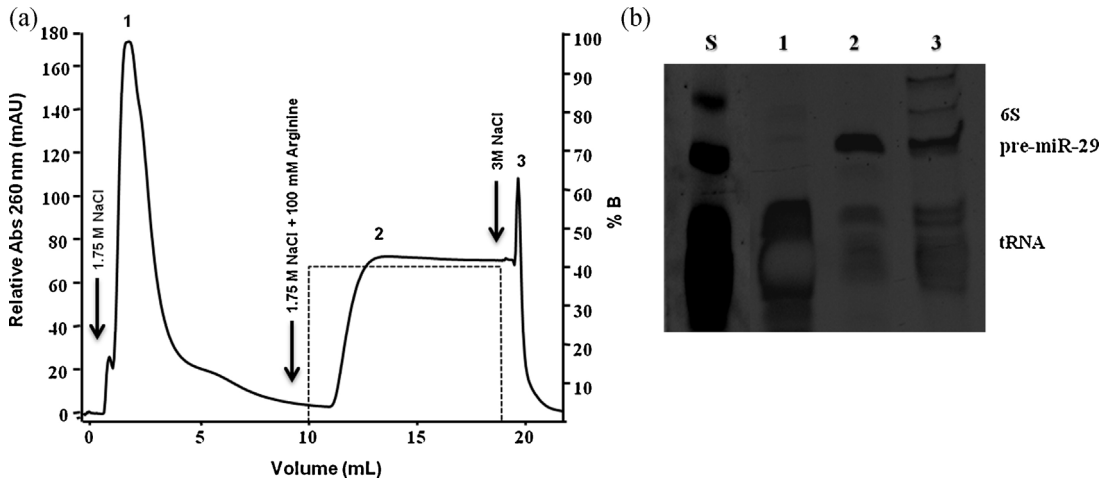

Fig. 4. (A) Separation of pre-miR-29 using agmatine monolithic disk. Elution was performed at 1 mL/min by stepwise increasing of arginine concentration in the eluent to 100 mM as represented by the arrows. (B) Polyacrylamide gel electrophoresis analysis of each peak in both experiments is represented in the respective figure. Fractions corresponding to peaks (1)–(3) are shown in lanes 1–3, respectively. Lane S, sRNA sample injected onto the column.

than the interaction pre-miR-29–agmatine support. In fact, since the arginine is positively charged at the pH in study, electrostatic interactions can possible occur between the pre-miR-29 and the free arginine. However, another mechanism that can explain pre-miR-29 elution is the interaction of free arginine with the agmatine ligand in the immobilized support [48], that could also promote the displacement of bound pre-miR-29. The last peak corresponded to the elution of tRNAs and some residual pre-miR-29 by increasing the ionic strength to 3 M of NaCl. The results of polyacrylamide gel electrophoresis (Fig. 4B) showed that the tRNAs were recovered in the first peak (lane 1), being separated from the pre-miR-29 that was attained in the second peak (lane 2), while other tRNAs and pre-miR-29 were obtained in the third peak (lane 3). As judged by polyacrylamide gel electrophoresis, pre-miR-29 was isolated and suitably purified in the second chromatographic step with high integrity. However, even if some arginine remains in the sample, the structure of pre-miR-29 is not changed, as we have previously studied by circular dichroism (data not shown). Actually, the application of arginine can also be strongly associated with the preserved integrity observed in RNA samples since arginine, owing to its multiplicity for interactions, has been largely associated with stabilizing effects on RNA conformation [17,21].

In a general way, the competition study has shown that the free arginine could promote the pre-miR-29 biospecific elution of the agmatine monolith.

Beyond the potential application of agmatine-based affinity chromatography to purify pre-miR-29 described here, this study also demonstrates the possibility of using three different strategies to achieve the pre-miRNA purification. In fact, the purification of pre-miR-29 was accomplished either using an increased NaCl or decreased $(NH_4)_2SO_4$ gradients or using a competition strategy with arginine supplemented buffer. In addition, this work proves the relevance of the establishment of well-defined binding and elution conditions to enhance the pre-miR-29 purification performance, resulting in an improvement of the final pre-miRNA yields, as this could represent an important impact on therapeutic applications of the purified pre-miR-29. Comparing the elution strategies with NaCl or arginine to elute bound pre-miR-29 biomolecules, it was found that the competition strategy favors the selectivity for pre-miR-29 because the arginine concentration needed to promote elution is lower than the NaCl concentrations. This fact is in accordance with what has been previously described by other authors, because as arginine is monovalent at the pH used, it is equivalent to NaCl in terms of valency; however the conductivity is much lower than for NaCl at identical concentrations [21,49]. This study also allowed the purification of pre-miR-29 in 20 min at a flow-rate of 1 mL/min.

3.4. Effect of flow rate on pre-miR-29 purification

The effect of flow rate on purification of pre-miR-29 was investigated, although no change is expected on the separation selectivity once some studies proved that the molecules separation is flow-independent due to the physical and chemical constitution of monoliths [26,50]. Therefore, to verify the impact of flow rate on purification of pre-miR-29, the same elution gradient previously established for the ideal separation was used. Fig. 5A shows the resulting chromatograms for the separation of pre-miR-29 at the different flow rates from 0.5 to 3 mL/min. The purity of pre-miR-29 separated with different flow rates was followed by electrophoresis as shown in Fig. 5B. Evaluating the chromatograms and the respective electrophoresis, it is clearly evident that no changes have occurred in the separation efficiency of pre-miR-29 for the different flow rates under study, but a significant reduction on the chromatographic run time was verified when higher flow rates were used (Fig. 5A). It is also possible to observe that the chromatograms overlap each other even at the highest applied flow rate of 3 mL/min. In this case the separation was completed in 9 min, which is in accordance with the advantages presented by the monolithic supports, where the chromatographic run was 4 times faster that the time used in conventional matrix of arginine [21].

3.5. Pre-miR-29 characterization

To ensure the success of the pre-miR-29 purification methodologies here described for therapeutic applications it is essential to guarantee the total elimination of impurities such as proteins, assessed by the micro-BCA method and endotoxins evaluated by LAL assay as well as to isolate the pre-miR-29 from other sRNAs species, which may be assured by polyacrylamide gel electrophoresis [5,51]. Moreover, RNA preparations should maintain the structural integrity, free from enzymatic inhibitors for RT and PCR reactions and free from nucleases [52].

The concentration and quality of the pre-miR-29 preparations isolated by the agmatine monolith were evaluated by Phoretix 1D software (Nonlinear Dynamics, Newcastle, United Kingdom) through the evaluation of the intensity of electrophoretic bands. The quantitative analysis of pre-miR-29 throughout the isolation

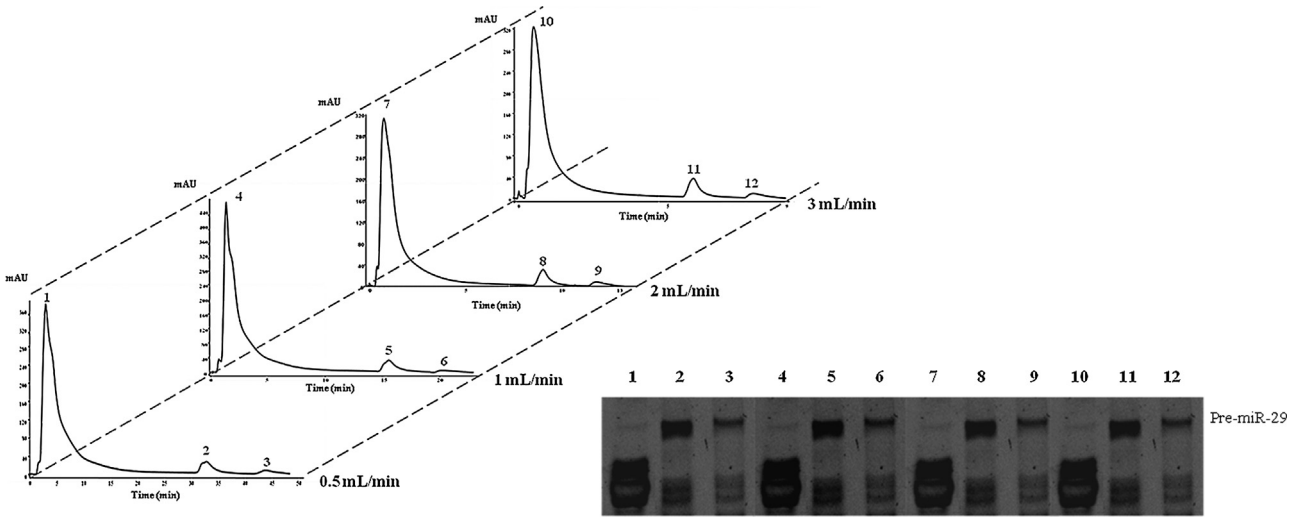

Fig. 5. (A) Effect of flow rate on resolution of pre-miR-29. Experiments were performed in the same salt and gradient conditions applied for the pre-miR-29 purification (presented in Fig. 2) at different flow rates (0.5, 1, 2 and 3 mL/min). (B) The peaks obtained in the chromatographic runs at different flow rates were identified by polyacrylamide gel electrophoresis.

procedure is summarized in Table 3, which presents the purity degree, purification factor and recovery yield of pre-miR-29 sample obtained with the agmatine monolith. In a general point of view, the strategy with NaCl enabled a high recovery (97.33%) of the target miRNA but the purity degree only reached 75.21%, whereas the strategy with $(NH_4)_2SO_4$ allows the recovery of the partially purify pre-miR-29 (35.51% of purity) when the salt concentration is significantly reduced. On the other hand, the competition studies using arginine in the elution buffer, demonstrated the possibility of purifying pre-miR-29 with higher purity (90.11% of purity and 94.88% of yield) in comparison to the other strategies, even though some pre-miRNA is lost in the final elution step. Thus, if larger amounts of pure pre-miRNA are desired, the strategy that employs NaCl can be used, while if higher purity levels are necessary, the competition strategy with arginine is more appropriate [21].

The protein quantification in the purified pre-miR-29 fractions collected from the chromatographic peaks was performed using the micro-BCA assay (Table 3). The analysis of the protein content in the fractions collected along the pre-miR-29 purification gradient revealed that proteins tend to elute more in the first gradient step (data not shown). Therefore, the chromatographic strategies used in these new pre-miRNA isolation methods (peak 2 in Figs. 2A, 3A and 4A) also provide a reduction of protein contamination in RNA samples, specifically in the competition strategy using arginine in the elution buffer, where the protein contamination level was negligible (2.774 ± 0.005 ng/μL), as required for therapeutic applications (Table 3). Endotoxins contamination was assessed using the ToxinSensor™ Chromogenic Limulus Amoebocyte Lysate (LAL) Endotoxin Assay Kit (GenScript, USA, Inc.) according to the manufacturer's instructions. The endotoxins content in the final pre-miR-29 sample indicates a significant reduction of the endotoxins level throughout the chromatographic step with the agmatine monolith, with a purification factor of pre-miR-29 relatively to LPS of 50 times (data not shown). A more accurate identification of pre-miR-29 molecules purified from the sRNA populations with the agmatine monolith was performed by PCR. As it can be observed from the electrophoretic analysis of the PCR products (Fig. 6), by using specific primers for pre-miR-29 cDNA, the PCR reaction allowed the amplification of pre-miR-29. No further amplification was seen in the control (lane 1). The negative

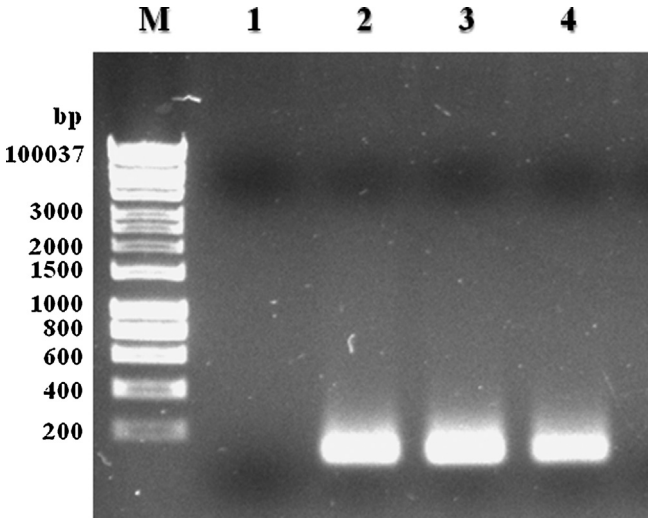

Fig. 6. pre-miR-29 identification by reverse-transcription PCR. The agarose-gel electrophoretic analysis of PCR products shows amplification of pre-miR-29 cDNA fragments. The negative control had no band intensification. Lane M, DNA molecular weight marker; lane 1, negative control; lanes 2, 3 and 4, second peaks of the three strategies under study (sodium chloride, ammonium sulfate and arginine), respectively.

Table 3
Quantitative analysis of purity and recovery yield of pre-miR-29 isolated by agmatine monolithic disk.

Elution strategy	sRNA sample (μg)	Pre-miR-29 purity (%)	Pre-miR-29 yield (%)	Proteins (ng/μL)
NaCl	20	75.21	97.33	3.258 ± 0.001
$(NH_4)_2SO_4$	20	35.51	99.40	5.516 ± 0.006
Arginine	20	90.11	94.88	2.774 ± 0.005

The correlation coefficients of protein calibration curves was 0.9998.
Data are presented as means with SD ($N = 3$).

control was made of PCR reaction solutions without cDNA. Therefore, it was verified the identity of the sRNA isolated from the original population as pre-miR-29.

4. Conclusions

This work combines, for the first time, the structural versatility provided by monolithic supports with the specificity and selectivity of agmatine ligand, as a promising strategy for miRNA purification. Moreover, the characterization of the modified monolith revealed that a maximum binding capacity at 100% breakthrough was 8.08 mg/mL for a RNA concentration of 0.25 mg/mL. The obtained K_d value, 2.6×10^{-7} M, confirms that the agmatine monolith support develops a good affinity interaction with RNA, showing that agmatine monolith is a good affinity chromatographic support. The implementation of agmatine monolithic chromatography for pre-miR-29 purification was based on the development of specific interactions between the pre-miR-29 and agmatine ligands, allowing the removal of other RNA species, as well as the reduction of proteins and endotoxins contaminants, obtaining highly pure pre-miR-29 for therapeutic applications. The type and salt concentration and pH manipulation in the loading buffer allows the establishment of different interactions and consequently different elution strategies. The exploitation of these affinity interactions, resulting from multiple intermolecular forces, namely van der Waals forces, hydrogen bonds, electrostatic and hydrophobic interactions, can trigger new insights not only in isolation strategies but also in many other RNA research fields owing to its implication in molecular recognition phenomena. Additionally, for the pre-miR-29 purification this monolithic support represents an advantageous alternative to conventional supports due to fast separation and consequent short contact time, ensuring structural stability of the target molecule. In conclusion, our approach revealed an efficient technique to obtain pharmaceutical-grade miRNA with high recovery yield, purity and good integrity, which may in a near future be used in RNA structural and functional studies as well as in gene therapy.

Acknowledgments

This work was supported by the Portuguese Foundation for Science and Technology (PTDC/EBB-BIO/114320/2009, EXPL/BBB-BIO/1056/2012, COMPETE: FCOMP-01-0124-FEDER-027560 and Pest-C/SAU/UI0709/2011). The authors also acknowledge the project with Reference CENTRO-07-ST24-FEDER-002014, from "Programa Operacional Regional do Centro 2007-2013 QREN" ("Mais Centro" program). Patrícia Pereira and Ângela Sousa acknowledge fellowships (Ph.D. Grant, Ref SFRH/BD/81914/2011 and Postdoctoral Grant, Ref SFRH/BPD/79106/2011, respectively). The authors would like to thank Prof. Yo Kikuchi (Toyohashi University of Technology) for kindly provide pBHSR1-RM plasmid and to BIA Separations for having kindly provided the agmatine monolithic disk and U. Cernigoj for having made the immobilization of agmatine ligand.

References

[1] D.P. Bartel, MicroRNAs: genomics, biogenesis, mechanism, and function, Cell 116 (2004) 281–297.
[2] J.A. Broderick, P.D. Zamore, MicroRNA therapeutics, Gene Ther. 18 (2011) 1104–1110.
[3] I. Vomelova, Z. Vanickova, A. Sedo, Methods of RNA purification. All ways (should) lead to Rome, Folia Biol. (Praha) 55 (2009) 243–251.
[4] S.C. Tan, B.C. Yiap, DNA RNA, and protein extraction: the past and the present, J. Biomed. Biotechnol. 2009 (2009) 574398.
[5] F. Re, RNA Methodologies – Laboratory Guide for Isolation and Characterization, Academic Press, York, USA, 2005.
[6] M.A. Dineva, L. MahiLum-Tapay, H. Lee, Sample preparation: a challenge in the development of point-of-care nucleic acid-based assays for resource-limited settings, Analyst 132 (2007) 1193–1199.
[7] L.E. Easton, Y. Shibata, P.J. Lukavsky, Rapid, nondenaturing RNA purification using weak anion-exchange fast performance liquid chromatography, RNA 16 (2010) 647–653.
[8] N. Nonne, M. Ameyar-Zazoua, M. Souidi, A. Harel-Bellan, Tandem affinity purification of miRNA target mRNAs (TAP-Tar), Nucleic Acids Res. 38 (2010) e20.
[9] S.M. McCarthy, M. Gilar, J. Gebler, Reversed-phase ion-pair liquid chromatography analysis and purification of small interfering RNA, Anal. Biochem. 390 (2009) 181–188.
[10] J.S. Kieft, R.T. Batey, A general method for rapid and nondenaturing purification of RNAs, RNA 10 (2004) 988–995.
[11] R. Martins, J.A. Queiroz, F. Sousa, Ribonucleic acid purification, J. Chromatogr. A 1355 (2014) 1–14.
[12] L. Ponchon, F. Dardel, Large scale expression and purification of recombinant RNA in *Escherichia coli*, Methods 54 (2011) 267–273.
[13] S.C. Walker, F.H. Scott, C. Srisawat, D.R. Engelke, RNA affinity tags for the rapid purification and investigation of RNAs and RNA–protein complexes, Methods Mol. Biol. 488 (2008) 23–40.
[14] J. Chen, J. Lozach, E.W. Garcia, B. Barnes, S. Luo, I. Mikoulitch, L. Zhou, G. Schroth, J.B. Fan, Highly sensitive and specific microRNA expression profiling using BeadArray technology, Nucleic Acids Res. 36 (2008) e87.
[15] R. Martins, J.A. Queiroz, F. Sousa, Histidine affinity chromatography-based methodology for the simultaneous isolation of *Escherichia coli* small and ribosomal RNA, Biomed. Chromatogr. 26 (2011) 781–788.
[16] R. Martins, J.A. Queiroz, F. Sousa, A new affinity approach to isolate *Escherichia coli* 6S RNA with histidine-chromatography, J. Mol. Recognit. 23 (2010) 519–524.
[17] R. Martins, C.J. Maia, J.A. Queiroz, F. Sousa, A new strategy for RNA isolation from eukaryotic cells using arginine affinity chromatography, J. Sep. Sci. 35 (2012) 3217–3226.
[18] F. Sousa, D.M. Prazeres, J.A. Queiroz, Affinity chromatography approaches to overcome the challenges of purifying plasmid DNA, Trends Biotechnol. 26 (2008) 518–525.
[19] P. Pereira, A. Sousa, J. Queiroz, A. Figueiras, F. Sousa, New approach for purification of pre-miR-29 using lysine-affinity chromatography, J. Chromatogr. A 1331 (2014) 129–132.
[20] A. Afonso, P. Pereira, J.A. Queiroz, A. Sousa, F. Sousa, Purification of pre-miR-29 by a new O-phospho-L-tyrosine affinity chromatographic strategy optimized using design of experiments, J. Chromatogr. A 1343 (2014) 119–127.
[21] P. Pereira, A. Sousa, J. Queiroz, I. Correia, A. Figueiras, F. Sousa, Purification of pre-miR-29 by arginine-affinity chromatography, J. Chromatogr. B: Analyt. Technol. Biomed. Life Sci. 951–952 (2014) 16–23.
[22] A. Strancar, A. Podgornik, M. Barut, R. Necina, Short monolithic columns as stationary phases for biochromatography, Adv. Biochem. Eng. Biotechnol. 76 (2002) 49–85.
[23] A. Podgornik, S. Yamamoto, M. Peterka, N.L. Krajnc, Fast separation of large biomolecules using short monolithic columns, J. Chromatogr. B: Analyt. Technol. Biomed. Life Sci. 927 (2013) 80–89.
[24] A. Sousa, F. Sousa, J.A. Queiroz, Advances in chromatographic supports for pharmaceutical-grade plasmid DNA purification, J. Sep. Sci. 35 (2012) 3046–3058.
[25] A. Sousa, C.T. Tomaz, F. Sousa, J.A. Queiroz, Successful application of monolithic innovative technology using a carbonyldiimidazole disk to purify supercoiled plasmid DNA suitable for pharmaceutical applications, J. Chromatogr. A 1218 (2011) 8333–8343.
[26] A. Sousa, D. Bicho, C.T. Tomaz, F. Sousa, J.A. Queiroz, Performance of a non-grafted monolithic support for purification of supercoiled plasmid DNA, J. Chromatogr. A 1218 (2011) 1701–1706.
[27] A. Sousa, A.M. Almeida, U. Cernigoj, F. Sousa, J.A. Queiroz, Histamine monolith versatility to purify supercoiled plasmid deoxyribonucleic acid from *Escherichia coli* lysate, J. Chromatogr. A 1355 (2014) 125–133.
[28] D. El-Agamy, M. Sharawy, E. Ammar, Agmatine attenuates silica-induced pulmonary fibrosis, Hum. Exp. Toxicol. 33 (2014) 650–660.
[29] N. Kitanaka, J. Kitanaka, F.S. Hall, G.R. Uhl, K. Watabe, H. Kubo, H. Takahashi, K. Tanaka, N. Nishiyama, M. Takemura, Agmatine attenuates methamphetamine-induced hyperlocomotion and stereotyped behavior in mice, Behav. Pharmacol. 25 (2014) 158–165.
[30] N.R. Kotagale, S. Walke, G.P. Shelkar, D.M. Kokare, M.J. Umekar, B.G. Taksande, Agmatine attenuates nicotine induced conditioned place preference in mice through modulation of neuropeptide Y system, Behav. Brain Res. 262 (2014) 118–124.
[31] H. Suzuki, S. Umekage, T. Tanaka, Y. Kikuchi, Artificial RNA aptamer production by the marine bacterium *Rhodovulum sulfidophilum*: improvement of the aptamer yield using a mutated transcriptional promoter, J. Biosci. Bioeng. 112 (2011) 458–461.
[32] A. Jungbauer, O. Kaltenbrunner, Fundamental questions in optimizing ion-exchange chromatography of proteins using computer-aided process design, Biotechnol. Bioeng. 52 (1996) 223–236.
[33] A. Soares, J.A. Queiroz, F. Sousa, A. Sousa, Purification of human papillomavirus 16 E6/E7 plasmid deoxyribonucleic acid-based vaccine using an arginine modified monolithic support, J. Chromatogr. A 1320 (2013) 72–79.
[34] F. Sousa, T. Matos, D.M. Prazeres, J.A. Queiroz, Specific recognition of supercoiled plasmid DNA in arginine affinity chromatography, Anal. Biochem. 374 (2008) 432–434.

[35] M.V. Latronico, D. Catalucci, G. Condorelli, MicroRNA and cardiac pathologies, Physiol. Genomics 34 (2008) 239–242.
[36] P.T. Nelson, W.X. Wang, B.W. Rajeev, MicroRNAs (miRNAs) in neurodegenerative diseases, Brain Pathol. 18 (2008) 130–138.
[37] L. Du, A. Pertsemlidis, Cancer and neurodegenerative disorders: pathogenic convergence through microRNA regulation, J. Mol. Cell Biol. 3 (2011) 176–180.
[38] M.J. Shin, L. Tan, M.H. Jeong, J.H. Kim, W.S. Choe, Monolith-based immobilized metal affinity chromatography increases production efficiency for plasmid DNA purification, J. Chromatogr. A 1218 (2011) 5273–5278.
[39] A. Jungbauer, Chromatographic media for bioseparation, J. Chromatogr. A 1065 (2005) 3–12.
[40] R.E. Boto, P. Almeida, J.A. Queiroz, Thiacarbocyanine as ligand in dye-affinity chromatography for protein purification, Biomed. Chromatogr. 22 (2008) 278–288.
[41] J. Ruta, C. Ravelet, J. Desire, J.L. Decout, E. Peyrin, Covalently bonded DNA aptamer chiral stationary phase for the chromatographic resolution of adenosine, Anal. Bioanal. Chem. 390 (2008) 1051–1057.
[42] D. Grundemann, C. Hahne, R. Berkels, E. Schomig, Agmatine is efficiently transported by non-neuronal monoamine transporters extraneuronal monoamine transporter (EMT) and organic cation transporter 2 (OCT2), J. Pharmacol. Exp. Ther. 304 (2003) 810–817.
[43] B.J. Calnan, B. Tidor, S. Biancalana, D. Hudson, A.D. Frankel, Arginine-mediated RNA recognition: the arginine fork, Science 252 (1991) 1167–1171.
[44] T. Janas, J.J. Widmann, R. Knight, M. Yarus, Simple, recurring RNA binding sites for L-arginine, RNA 16 (2010) 805–816.
[45] F. Jiang, A. Gorin, W. Hu, A. Majumdar, S. Baskerville, W. Xu, A. Ellington, D.J. Patel, Anchoring an extended HTLV-1 Rex peptide within an RNA major groove containing junctional base triples, Structure 7 (1999) 1461–1472.
[46] J.D. Puglisi, J.R. Wyatt, I. Tinoco Jr., Solution conformation of an RNA hairpin loop, Biochemistry 29 (1990) 4215–4226.
[47] M. Yarus, J.J. Widmann, R. Knight, RNA–amino acid binding: a stereochemical era for the genetic code, J. Mol. Evol. 69 (2009) 406–429.
[48] R. Mallik, D.S. Hage, Affinity monolith chromatography, J. Sep. Sci. 29 (2006) 1686–1704.
[49] T. Arakawa, D. Ejima, K. Tsumoto, M. Ishibashi, M. Tokunaga, Improved performance of column chromatography by arginine: dye-affinity chromatography, Protein Exp. Purif. 52 (2007) 410–414.
[50] M.K. Danquah, G.M. Forde, Large-volume methacrylate monolith for plasmid purification. Process engineering approach to synthesis and application, J. Chromatogr. A 1188 (2008) 227–233.
[51] L.V. Madabusi, G.J. Latham, B.F. Andruss, RNA extraction for arrays, Methods Enzymol. 411 (2006) 1–14.
[52] S.A. Bustin, T. Nolan, Pitfalls of quantitative real-time reverse-transcription polymerase chain reaction, J. Biomol. Tech. 15 (2004) 155–166.

Paper VIII

Characterization of polyplexes involving small RNA

P. Pereira, A. F. Jorge, R. Martins, A. A. C. C. Pais, F. Sousa, A. Figueiras

Journal of Colloid and Interface Science. 2012. 387: 84-94

Short description: This paper presents a systematic study of different polymers, such as Polyethylenimine, Chitosan and Poly(allylamine), with different molecular weights, charge densities and backbone structure, to efficiently encapsulate small RNA molecules. The assessment of the biophysical and structural characteristics (such as size, zeta potential, morphology, encapsulation efficiency and protection/stability) of the polymer–small RNA complexes were evaluated and compared, in order to design a successful delivery system for small RNAs. In addition, a rationale for the experimental observations is provided using Monte Carlo simulation for systems with polymers of different lengths and charge densities. The simulations showed that there is an interplay between the size of polymers chains and their charge density that define the degree of condensation for small RNA.

Journal of Colloid and Interface Science 387 (2012) 84–94

Contents lists available at SciVerse ScienceDirect

Journal of Colloid and Interface Science

www.elsevier.com/locate/jcis

Characterization of polyplexes involving small RNA

Patrícia Pereira [a], Andreia F. Jorge [b], Rita Martins [a], Alberto A.C.C. Pais [b], Fani Sousa [a], Ana Figueiras [a,c,*]

[a] CICS-UBI – Health Sciences Research Centre, University of Beira Interior, Avenida Infante D. Henrique, 6200-506 Covilhã, Portugal
[b] Department of Chemistry, University of Coimbra, Rua Larga, 3004-535 Coimbra, Portugal
[c] CEF-FFUC – Pharmaceutical Studies Center, Faculty of Pharmacy, University of Coimbra, Pólo das Ciências da Saúde, Azinhaga de Santa Comba, 3000-548 Coimbra, Portugal

ARTICLE INFO

Article history:
Received 11 May 2012
Accepted 31 July 2012
Available online 21 August 2012

Keywords:
Polyplexes
Small RNA
Polyethylenimine
Chitosan
Poly(allylamine)

ABSTRACT

The purpose of the present study is to provide a tool for an efficient design and synthesis of non-viral vectors for small RNA delivery. The effects of properties of the polycation, such as molecular weight, charge density and backbone structure, to polyplex structure and physicochemical behavior were systematically evaluated. The condensing agents, polyethylenimine (PEI), chitosan (CS) and poly(allylamine) (PAA) were added to sRNA molecules at different N/P ratio. The efficiency of encapsulation and protection of sRNA, as well as polyplex size, zeta potential and morphology were followed and compared. The results show that PEI/sRNA polyplexes display a small size and positive zeta potential. However, for low molecular weights, this polycation is unable to protect sRNA in the presence of a decompacting agent. With chitosan, sRNA is efficiently compacted at high N/P ratios. The CS/sRNA complexes display small sizes, ca. 200 nm, positive surface charge and also good stability. Finally, the PAA/sRNA polyplexes were found to be the smallest at low N/P ratios, displaying a good encapsulation efficiency and high stability. A rationale for the experimental observations is provided using Monte Carlo simulation for systems with polycations of different length and charge density. The simulations showed that there is an interplay between the size of polycation chains and its charge density that define the degree of condensation for sRNA.

1. Introduction

Gene therapy has gained significant attention over the past two decades as a promising approach for a future therapeutic strategy in clinical applications. Gene therapy is important not only for the treatment of diseases caused by genetic defects, but also in the development of methods for treatment and prevention of a wide range of acquired disorders that include severe combined immunodeficiency, cystic fibrosis, rheumatoid arthritis and Parkinson's disease, as well as an alternative to the traditional chemotherapy used in treating cancer [1–4].

Over recent years, the importance of RNA in numerous biological processes has increased substantially. Small RNAs (sRNAs) are being increasingly recognized as crucial regulatory molecules in all organisms. The specificity and the potency of sRNAs suggest that they might become therapeutic agents, especially in interference RNA strategies [5–7]. Free therapeutic genes can be enzymatically degraded by ubiquitous nucleases resulting in a short half-life in the blood. For that reason they show poor cellular uptake when delivered in aqueous solutions, and insufficient tissue bioavailability, which has stimulated the development of carrier systems for gene delivery [1,8,9]. The gene carriers include viral systems such as retrovirus and adenovirus or non-viral systems, including cationic polymers, cationic lipids, peptides and dendrimers [10,11]. The polycations are a promising alternative to compact RNA for systemic delivery because of their low cytotoxicity, low immunogenicity, high stability, biocompatibility, and unrestricted gene materials size. In addition, potential safety benefits make these compounds increasingly attractive for gene therapy [4,12–14]. Moreover, non-viral vectors present relatively low cost production and high flexibility, allowing to design carriers with well-defined structural and chemical properties [1].

Cationic polymers can efficiently condense RNA molecules into nanometer range complexes, commonly via protonated amine groups that promote the electrostatic interaction with the negatively charged phosphate groups in RNA [15]. They may also provide a positively charged surface in the complex. One of the obstacles for an efficient gene transfection is crossing the negatively charged cell membrane, and net positive charge of the polyplexes promotes electrostatic interaction with the overall negative charge of the cell membrane and prevents particle aggregation [14–16]. In addition, the size of the polyplexes should be between 50 and 200 nm for efficient internalization by endocytic processes, and once inside the cell, they should dissociate to release the sRNAs from the vector system for their respective functions [17–19].

* Corresponding author. Address: Centro de Investigação em Ciências da Saúde, Universidade da Beira Interior, Avenida Infante D. Henrique, 6200-506 Covilhã, Portugal. Fax: +351 275 329 099.
E-mail address: rfigueiras@fcsaude.ubi.pt (A. Figueiras).

0021-9797/$ - see front matter © 2012 Elsevier Inc. All rights reserved.
http://dx.doi.org/10.1016/j.jcis.2012.07.088

Due to the increased interest in these systems, a large number of natural and synthetic polymers have been synthesized and characterized. Polyethylenimine (PEI), a polycationic polymer has emerged as one of the most promising candidates for the development of efficient gene delivery vectors [12]. The complexes PEI-nucleotide show high stability, controllable size, adjustable unpackaging properties in cells, and flexibility for addition of moieties that target specific entities on cell membranes and intracellular structures [20]. In particular, PEI has potential as a RNA carrier due to its superior transfection efficiency which may facilitate endosomal escape after entering the cells as it acts as a "proton sponge" during acidification of the endosome [13,21]. Chitosan (CS) is also considered to be a good candidate to integrate gene delivery systems. CS presents beneficial qualities such as low toxicity, low immunogenicity, excellent biodegradability, biocompatibility, as well as a high positive charge that can easily form polyelectrolyte complexes with negatively charged nucleotides through electrostatic interactions [2,9,22]. Recently, poly(allylamine) (PAA), a synthetic cationic polymer having high density of primary amino groups, has drawn considerable attention as a non-viral gene delivery system [23]. PAA carries a strong positive charge, which enables it to bind and package negatively charged sRNA. It is a polymer extensively used in the formulation of biocompatible films, nanomaterials and for cell encapsulation.

In the present work, a systematic study of different polymers, PEI, CS and PAA, with different molecular weights and charge densities is performed. The aim of this study is to compare the performance of these different polycations on sRNA condensation, with the subsequent assessment of the biophysical and structural characteristics (such as size, zeta potential, morphology and complex stability) of the polymer–sRNA complexes, in order to design a successful delivery system for sRNA.

2. Experimental section

2.1. Materials

Five different polycations were used. CS low molecular weight (LMW) (M_w = 50–190 kDa; degree of deacetylation in the 75–85% range), CS medium molecular weight (MMW) (M_w = 190–310 kDa, degree of deacetylation in the 75–85% range), PEI-LMW with M_w = 1.3 kDa, 50 wt% in H_2O and PAA of 17 kDa, 20 wt% in H_2O were obtained from Sigma–Aldrich (St. Louis, MO, USA). PEI high molecular weight (HMW) of M_w = 10 kDa was purchased from Polysciences, Inc. (Warrington, PA). Guanidinium salt and all the chemicals used in the lysis buffer were obtained from Sigma (St. Louis, MO, USA). All solution were freshly prepared using 0.05% diethyl pyrocarbonate (DEPC) treated water. DEPC was purchased from Fluka (Sigma). Fetal bovine serum (FBS) was purchased from Biochrom and heparin (25,000 IU for 5 mL) was obtained from Winthrop.

2.2. sRNA samples

sRNA samples used in this study were isolated from *Escherichia coli* DH5α based on the protocol described by Martins and coworkers (2010), in which an acid guanidinium thiocyanate–phenol–chloroform method is used [24]. Briefly, cells were lysed and the nucleic acid fraction obtained was precipitated with isopropanol. The precipitate was recovered by centrifugation at 16,000*g* for 20 min at 4 °C. After centrifuging, the sRNA pellets were air-dried for 5 min at room temperature and their solubilization was performed in 200 μL of 0.05% DEPC-treated water. Finally, the optical density of the samples was determined using a Nanophotometer to assess sRNA quantity and purity.

2.3. Polyplex formation

All the polyplexes were formulated using the method of simple complexation between molar concentrations of positive charge, present in the protonated amine groups of polycation (N), and the negative charge of the phosphate groups of RNA (P) [3,8]. To determine specific N/P ratios, the mass of 325 Da corresponding to one phosphate group on sRNA was used. Moreover, over the pH used in this study, sRNA displays an approximately constant anionic charge density, with the pK_a of the respective phosphate group close to 1.5 [25]. The calculation of the positive charges was made in accordance with the pK_a values and molecular weight of each polycation (Table 1). sRNA stock solution was prepared by sRNA dissolution in sodium acetate buffer (0.1 M sodium acetate/0.1 M acetic acid, pH 4.5), up to a final concentration of 25 μg/mL. The sRNA concentration was determined by UV absorbance at 260 nm. A solution of 40 μg/mL of RNA will have an absorbance of 1 [26]. The polycation stock solutions were also prepared in sodium acetate buffer pH 4.5 in a concentration of 10 mg/mL. Preliminary experiments were performed to identify the concentration range where the polyplexes are formed. A fixed volume of polycation solution (100 μL) of variable concentration was added to a sRNA solution (400 μL). The final concentration of sRNA was equal to 20 μg/mL (60.6 μM) and was kept constant in all the methods used for the characterization of the formed complexes. Particles were obtained by addition of cationic polymer solution to sRNA solution and immediately vortexed at maximum speed for 30 s. All the samples were subsequently left for equilibration at room temperature for 60 min.

2.4. Circular dichroism (CD)

CD was used to monitor the RNA behavior when subjected to different pH values. CD spectra were obtained using a 0.2 cm path length quartz rectangular cell at a constant temperature of 25 °C, in a Jasco 1850 spectrophotometer. Spectra were recorded from 215 to 320 nm at a scan speed of 10 nm/min and a bandwidth of 1 mm. Three spectra were accumulated and averaged for each sample. The final sRNA concentration was 100 μg/mL. All measurements were conducted under a constant gas flow, to purge the ozon generated by the light source of the instrument. The CD signal was converted to molar ellipticity, smoothed with a Jasco Fast Fourier transform algorithm.

2.5. Gel agarose sRNA assays

A series of polycation/sRNA polyplexes in different ratios were prepared as described above. The samples (20 μL) were analyzed by horizontal electrophoresis using 0.8% of agarose gels (Hoefer, San Francisco, CA, USA). The electrophoresis was carried out in Tris–acetic acid (TAE) buffer in DEPC-treated water (40 mM Tris base, 20 mM acetic acid and 1 mM EDTA, pH 8.0) and run at 90 V for 50 min. The bands corresponding to sRNA and polycation/sRNA complexes were visualized under ultraviolet light after staining the gels with ethidium bromide (0.5 μg/mL) or 5 μL of a 10,000× solution of Gelstar. The gels were imaged using a Vilber Lourmat system (ILC Lda, Lisbon, Portugal).

2.6. Scanning electron microscopy (SEM)

The morphological characteristics of the polyplexes were visualized with a scanning electron microscopy (SEM) (Hitachi S-2700, Tokyo, Japan). Briefly, one drop of the solution containing the polyplex samples was placed on the surface of cover glasses and stored at 37 °C overnight. Subsequently, the samples were

Table 1
Main characteristics of PEI-LMW, PEI-HMW, CS-LMW, CS-MMW and PAA.

Polymer	Molecular weight (MW)[a]	Monomer charge density (e)[a]	Nominal DD[b] (%)	Determined DD[c] (%)	pK_a [ref]
PEI-LMW	1300	11^+	–	–	9.26 [15]
PEI-HMW	10,000	3^+	–	–	8.5 [45]
CS-LMW	50,000–190,000	1^+	75–85	83.14 ± 0.39	6.5 [15]
CS-MMW	190,000–310,000	1^+	75–85	73.86 ± 0.61	6.5 [15]
PAA	17,000	1^+	–	–	8.5 [46]

[a] e is the elementar charge.
[b] Provided by the manufacturer.
[c] Determined by 1DUVS. The data represent the mean and standard error of at least three separate measurements (mean ± SD).

then sputter coated with gold using an Emitech K550 Sputtering Coater (London, England) for 3 min at 30 mA.

2.7. Particle size and zeta potential measurements

The mean particle diameter of the polyplexes and polydispersion index were determined by dynamic light scattering (photon correlation spectroscopy, PCS) using an N5 Particle Analyzer (Beckman Coulter Inc., USA). Particle diameters of the freshly prepared complexes were measured at 25 °C, and data were collected at 90° scattering angle. The time-averaged autocorrelation functions were transformed into intensity-weighted distributions of the apparent hydrodynamic diameter using the available Malvern PCS software 6.20. The surface charges (zeta potential) of the polyplexes were determined by laser Doppler electrophoresis using a Zetasizer Nano ZS (Malvern Instruments Ltd., UK), at 25 °C. The average values of size and zeta potential were calculated with the data obtained from three measurements ± SD.

2.8. Determination of sRNA encapsulation efficiency

The sRNA encapsulation efficiency (EE) was calculated from the determined free sRNA concentration in the supernatant recovered after particle centrifugation (15,000g, 20 min, 25 °C). The amount of unbound sRNA was determined by UV–Vis analysis (Shimadzu UV–Vis 1700 spectrophotometer) at 260 nm. Supernatant recovered from unloaded polycation (without sRNA) was used as a blank. Three repetitions of this procedure were performed for each system. The encapsulation efficiency was calculated as

$$\mathrm{EE}\ (\%) = [(\text{Total sRNA amount} - \text{sRNA supernatant amount})/\text{Total sRNA amount}] \times 100$$

2.9. Polyplexes: release profile and protection of sRNA

Protection and release profile of the sRNA present in the polyplexes were also assessed. All the polyplexes were resuspended in PBS buffer, pH 7.4. The protection experiments were carried out by incubation of 12.5 μL of polyplexes with 1.5 μL of RNase solution (10 and 100 μg/mL) for 1 h at 37 °C or with 10% of fetal bovine serum (FBS) for 30 and 60 min at 37 °C. To characterize the release of the encapsulated sRNA, samples were incubated with a series of heparin solutions (0.01, 0.1, 0.5 and 1 IU/mL of heparin), prepared by diluting aliquots of a heparin stock solution (10 IU/mL). The polyplex solutions (10 μL) were incubated with 10 μL of each concentration for 1 h at 37 °C.

2.10. Molecular modeling

An estimation of size and charge density of all polycations used was carried out resorting to the Avogadro package [27], using the UFF force field [28]. The structure of all polycations was established considering at least ten monomers. The average distance between charged groups, d_{AB}, and also the average size per monomer were established, considering the structure of each monomer as given by the manufacturer.

2.11. Monte Carlo simulation

The systems studied in this work were modeled in a coarse-grain approach, where all ions and chain monomers are considered as charged hard-spheres and the solvent is considered as a continuum with a dielectric permittivity of water. We modeled a titration of a polyanion with 100 negative charged beads, with oppositely charged polyplexes with variable chain lengths and charge densities. The four different systems are listed in Table 2. The notation corresponding to the length of the polycation chain and corresponding charge density (e.g. Short-HCD) is used. The charge density varies between low (LCD), moderate (MCD) and high (HCD). The charge ratio, N/P, between polyanion and polycation were kept constant, equal to unity, for all systems considered. It is given by

$$\mathrm{N/P} = \frac{z_{mon,PC} N_{mon,PC} N_{PC}}{z_{mon,PA} N_{mon,PA}}$$

where Z_{mon} is the charge of monomers, N_{mon} is the number of monomers in each chain and N is the number of polycation chains in the system. The subscript PC and PA correspond to polycation and polyanion, respectively. The linear charge density, d_z, of the polycation chains was calculated as,

$$d_z = \frac{N_{mon,PC} Z_{mon,PC}}{(N_{mon,PC} - 1) R_0}$$

and taking R_0 as the bead-bead separation. A more extensive description of this method can be seen in previous work by some of the authors [29]. In the present work, the hard sphere radius of polyanion beads was 2.7 Å and of positive beads of polycation 2 Å. A reference distance between connected monomers of 6.5 Å was imposed for the negative chain, 5.6 Å for the polycations. The harmonic force constant and angular force constant used was 0.4 N m^{-1} and 1.7 × 10^{-24} J deg^{-2}, respectively. The polyelectrolyte backbones correspond to semi-flexible polymers, in terms of

Table 2
Systems simulated in the present work. In all cases, a negative polyelectrolyte with 100 charged beads of unit charge was present.

Systems	Number of positive chains	Number of beads/chain	Charge per bead
Short-HCD	5	20	1
Intermediate-LCD	8	50	0.25
Intermediate-MCD	4	50	0.5
Long-LCD	2	200	0.25

intrinsic persistence length. Considering also the electrostatic effects, the values of the persistence length, in the presence of the respective counterions only, is 28 Å for the polyanion, and ca. 22 Å for the polycations, irrespective of the chain length. For each system, Metropolis Monte Carlo simulations were performed in the canonical ensemble using the Molsim package [30]. The efficiency of the simulations was improved by taking concerted moves in the chain particles. These included translation as a whole and slithering [31]. The rate of acceptance of single particle moves for the polyanion was 33% for a simulation of a compact polyplex (system Short-HCD), while translation and slithering warranted levels of acceptance of 4% and 39%, respectively. In general, all remaining systems yielded higher values for the polyanion. The polycation moves resulted in significantly higher rates of acceptance: 44%, 32% and 38% for the single particle, translation as a whole and slithering, respectively, also in system Short-HCD. Again, the remaining systems displayed higher acceptance ratios for the polycations backbone.

3. Results and discussion

3.1. Structural characteristics of the polycations

From the structures of different polycations with optimized conformation, it is possible to determine the average size and charge density of the respective monomers (Fig. 1). Also, considering the molecular weight of each monomer and the corresponding average chain molecular weight, it is possible to estimate the number of monomers per chain, $N_{mon,PC}$. The linear charge density was calculated similarly to what was described for the Monte Carlo simulation but $z_{mon,PC}$ is the number of charges in each monomer (see Table 1) and R_0 is the length per monomer. Table 3 summarizes the results obtained from simple molecular mechanics calculations in gas phase. It should be stressed that these are rough estimates, in which the groups are not protonated to avoid the necessity of a solvent, and aim at facilitate the link between the experimental and theoretical approaches. Chitosan chains display the highest chain length, but the lowest charge density. The highest charge density is, as expected, obtained for PEI polymers. In this case, and due to the fact that these polycations are branched, it is more difficult to establish the total chain length. This is especially important in the case of PEI, 10 kDa, in which the branching is random. PAA presents an intermediate size and chain length. Further details will be discussed in the next sections.

Table 3
Estimates from molecular mechanics of the average length per monomer, average length per chain and charge density of each of the polycations used in the present work.

Polycations	Averaged measurements per chain		
	Length per monomer (Å)	Length per chain (Å)	Charge density (e/Å)[a]
PAA	3.4	810	0.29
CS-LMW	5.4	3627	0.19
CS-MMW	5.4	6347	0.19
PEI-LMW	24.9	62.3	0.44
PEI-HMW	9.3	–	0.32

[a] e is the elementar charge.

3.2. Assessment of sRNA stability in different solutions

The conformational stability of the sRNA secondary structure was assessed at different solutions (H_2O–DEPC and acetate buffer, pH 4.5) using CD (Fig. 2). The CD spectra of the sRNA in H_2O–DEPC is very similar and show characteristic features of the A-RNA [32]. For sRNA in H_2O–DEPC, a positive band around 260 nm was observed, and a negative signal at 220 nm, with approximately the same intensity. On the other hand, the sRNA spectrum in acetate buffer at pH 4.5 depicts a decrease in the value of the molar ellipticity of the positive band (260 nm) and maintains the negative signal at 220 nm. These results show that isolated RNA is sensitive to the buffer used, since the respective CD spectrum is different in acetate buffer and in water. This indicates that the sRNA structure is altered at lower pH.

To check on RNA integrity, further techniques were used. Spectrophotometry analysis (Nanophotometer) measuring absorbance

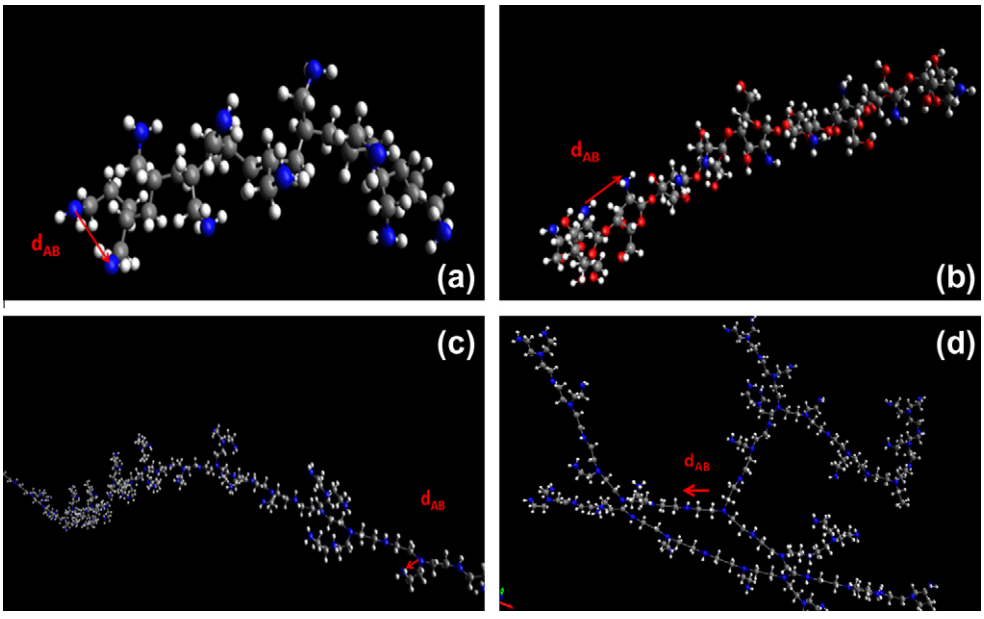

Fig. 1. Optimized geometries (UFF) of polycations in gas phase, (a) PAA and (b) CS, (c) PEI, 1.2 kDa and (d) PEI 10 kDa. Each polycation contains not less than 10 monomers. The average distance between the ionizable species (blue) was performed by considering the distance, d_{AB}, and subsequent distances determined following the nearest ionizable group. (For interpretation of the references to color in this figure legend, the reader is referred to the web version of this article.)

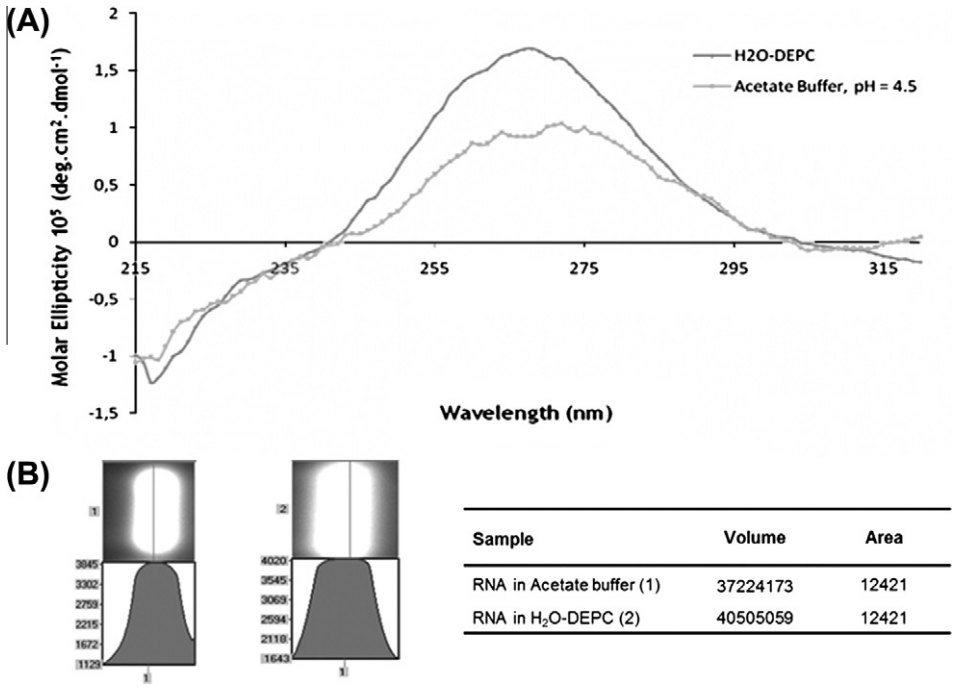

Sample	Volume	Area
RNA in Acetate buffer (1)	37224173	12421
RNA in H_2O-DEPC (2)	40505059	12421

Fig. 2. CD spectra of *E. coli* sRNA in the H_2O–DEPC and acetate buffer at pH 4.5. The data shown in this CD spectrum are the average from three independent measurements.

at 260 and 280 nm [26] were conducted. The nucleic acid concentration was estimated using the absorbance values at 260 nm, while the integrity of each sample was determined by calculating the 260/280 ratio. The spectrophotometric data show that RNA in H_2O–DEPC displays a high degree of integrity as extracted from the absorbance ratio, $A_{260/280} = 2.017 \pm 0.046$, value which is in close agreement with the reference ratio 2.0 ± 0.1 [26]. A similar value is obtained for RNA in acetate buffer, $A_{260/280} = 1.979 \pm 0.057$. Electrophoresis analysis is an important complementary technique that also enables to assess RNA integrity [26]. For that purpose, the UVIband—1D gel analysis software (Uvitec, Cambridge, UK) is used as an auxiliary of the agarose electrophoresis allowing the determination of the intensity of sRNA bands. Fig. 2B shows the semiquantitative analysis of the intensity of sRNA bands in H_2O–DEPC and acetate buffer. The value of peak volume obtained was 40,505,059, which indicates that the intensity of sRNA in H_2O–DEPC band is slightly higher than the intensity of sRNA in acetate buffer (37,224,173). Together, these results demonstrate that there is a small decrease of RNA integrity, but it remains stable at pH 4.5 (Fig. 2B).

However, there is no consensus on the precise nature of the changes that occur in RNA conformation when the pH is lowered, and how pH influences the sRNA degree of ionization. Biologically, hybridization occurs naturally in acidic conditions and promotes the neutralization of the condensed phosphate molecules [33]. *In vitro*, this occurs with a pH below 5 and can result in depurination, base pair protonation, adenine, uracil, and cytosine unstacking, and thus degradation of RNA [33].

3.3. UV and agarose gel electrophoresis

In order to determine the optimal complexation conditions, it is necessary to evaluate the degree of binding between sRNA and polycation at different N/P ratios. The polycations were mixed with sRNA at several ratios for the formation of sRNA–polycation particles (polyplexes) in acetate buffer at pH 4.5 [14]. The pH 4.5 value was chosen because it is located within the range of pH values (4–6) that has been attributed to the endo/lysosomal compartment [34]. Moreover, at this pH, the amine groups of polycations in study are protonated and act as a cationic polyelectrolyte that can interact with the negatively charged sRNA. In Table 1, it is possible to observe that the polycations possess pK_a values higher than those of the RNA phosphate groups. The degree of compaction between sRNA and all polycations in study are analyzed by gel agarose electrophoresis (Fig. 3) and by UV spectrometry (Fig. 4). In preliminary studies, N/P ratio values in the range of 0.625–50 were studied for all the selected polycations (data not shown). In this range, an intermediate region was found for each polycation, where most of the sRNA molecules are partially condensed, followed by complete condensation of the sRNA at higher concentrations of polycation.

Regarding the PEI, it was observed that the bands corresponding to free sRNA in the PEI-LMW/sRNA complex were not observed when the polymer was present at the N/P ratio above 3, (Fig. 3A). In accordance with the results obtained from electrophoresis, 100% of sRNA loading efficiency was achieved at the N/P ratio 3–4 and, at this point, sRNA is completely complexed with PEI-LMW (Fig. 4). In the case of the PEI-HMW/sRNA complex (Fig. 3B), no suppression of sRNA was identified in those complexes with N/P ratios of 1.25–2.5, while sRNA migration in complexes with N/P ratios higher than 2.5 was not observed. These results were also observed in the encapsulation studies, in which 97% of the sRNA loading efficiency was obtained, for the 3–3.5 N/P ratios (Fig. 4). In comparison, the two PEIs in study display subtle differences in the sRNA condensation. In general, however, PEI-HMW seems to be more efficient in sRNA condensation. It is known that polycations with higher charge densities promote the strongest binding with RNA [10, 12, 32, 33]. However, it should be stressed that the degree of compaction depends also on the size of the positive chains, and on their number, for a constant charge ratio [35]. In Table 3 are listed the main differences between these two polycations in terms of size and charge density. It is observed that the charge density of PEI-LMW is higher than that of PEI-HMW, but the chain is longer and the degree of branching is higher in PEI-HMW. Some previous studies have also pointed out that a branched structure may promote a more efficient interaction with sRNA, when

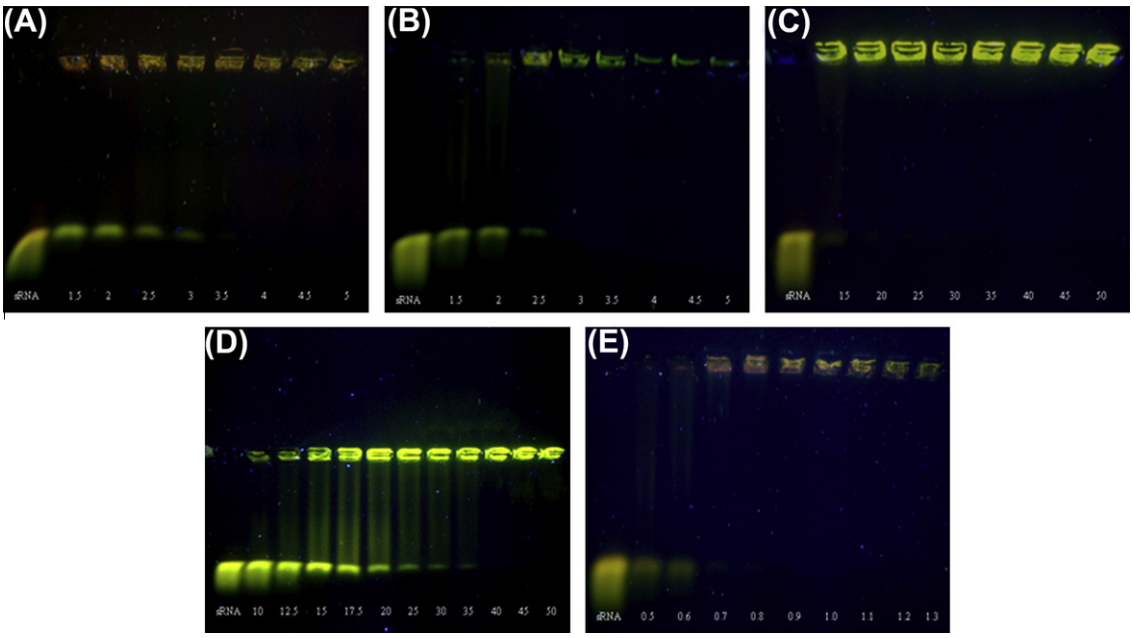

Fig. 3. Binding efficiency of sRNA/polymer polyplexes at various N/P ratios. (A) sRNA/PEI-LMW (1300 Da), (B) sRNA/PEI-HMW (10 kDa), (C) sRNA/CS-LMW (50–190 kDa), (D) sRNA/CS-MMW (190–310 kDa) and (E) sRNA/PAA (17 kDa). The first lane of the gel corresponds to free sRNA. The numbers in each lane indicate the N/P ratios values. Each experiment was performed of three times.

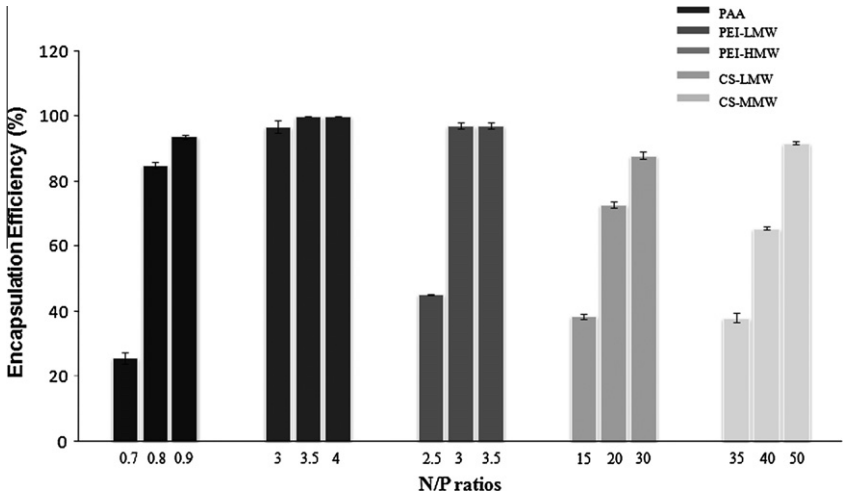

Fig. 4. Encapsulation efficiency of the polyplexes obtained from different polymers. The mean results and standard deviations (vertical lines in figure) of three independent measurements are presented (mean ± SD are given, three repetitions each).

compared to a linear polymer structure, which may be beneficial for the packaging of sRNA [36,37].

In a second set of experiments, we have used two types of chitosan polymers. The characteristics of the different commercial chitosan (CS-LMW and CS-MMW) used in this work are shown in Table 1. MW and DD are the molecular weight and the deacetylation degree, respectively. The DD was measured by a first derivative UV-spectroscopy (1DUVS) method, using a Shimadzu 1700 UV–vis spectrophometer [38]. The DD values represent the percentage of deacetylated primary amine groups along the molecular chain, which subsequently determines the positive charge density when chitosan is dissolved in acidic conditions (pH ~ 5.5) [38]. In the presence of CS-LMW at an N/P ratio of 15–25, sRNA migrated along the gel, which indicates the presence of non-complexed sRNA (Fig. 3C). For higher N/P ratios, around 30, the presence of polyplexes in the wells (neutralized sRNA) is observed, suggesting sRNA is fully complexed. In the case of CS-MMW at N/P ratios of 10–35, sRNA also migrated into the gel but at a N/P ratio above 35 the sRNA is neutralized (Fig. 3D). In Fig. 3D, it is possible to observe that, at the N/P ratio 20–45, some polyplexes move in the direction of the anode, that is, some polyplexes present an excess of positive charge. It was clear that the efficiency of the polycation condensation and the charge distribution inside the polyplex is known to depend on the distance between the charges in the condensing agent. This reflects the fact that both linear charge density and the relative number of chains of the condensing agent are important factors in the condensation behavior. Overcharging effects have been previously observed in similar systems, and overcharging is favored in situations where a concentrated solution of polycation is added to the polyanion solution [39,40].

Finally in the presence of PAA, sRNA complexation starts at very low values of the N/P ratio. This condensation becomes more

marked at N/P = 0.7 and N/P = 0.8, where most sRNA molecules are complexed, as extracted from the intensity decrease of the band that corresponds to free sRNA (Fig. 3E). The results obtained for PAA/sRNA encapsulation are in agreement with those from agarose gel electrophoresis, where a 25.6% of sRNA loading efficiency was achieved at the N/P ratio of 0.7 and the highest N/P ratio was 85% for an N/P ratio of 0.8 (Fig. 4). These observations indicate that this polycation, which possesses an intermediate size and charge density, as compared with the others used in this work, is very efficient in sRNA condensation. An illustration from the molecular mechanics calculations (see Fig. 1) suggests that the charges of the PAA are more accessible than those in the PEI chains. Also, a high degree of charge matching between PAA and sRNA [41] is a definite possibility. In fact, charges in PAA are separated by ca. 3.4 Å (Table 3) yielding a charge density close to that of sRNA.

3.4. Structural properties

The physical properties such as size and surface charge that influence cellular interactions and polyplex biodistribution were also determined. The results of zeta potential and size of polyplexes are shown in Table 4. In general, an increase in the charge of the complexes, for all systems in study, is observed upon the addition of polymers. The size of sRNA, in the absence of polycation, is 325 nm in diameter. The initial size of the sRNA molecules is reduced when the N/P ratio increases, up to a minimum value, after which the chains tend to expand again. It is also observed that the lowest size of the complexes obtained with CS is slightly higher than that obtained with the PEI chains. In turn, PAA reaches the lowest size value. Also, PAA complexes at 0.6, 0.7, 0.8 and 0.9 N/P ratios are smaller than 150 nm, which is considered the size limit for nonspecific endocytosis via clathrin-coated pits [42]. In the case of PEI and PAA it is seen that the zeta potential increases gradually, from negative to positive values (Table 4). The complexes formed with sRNA and the two PEIs at N/P ratio of 2.5 displayed small negative zeta potentials. These results are in accordance with the results obtained in the electrophoresis (Fig. 3) and in the encapsulation studies (Fig. 4) at the N/P ratio 2.5, indicating that, at this point, RNA is not fully complexed with the polycation. These results may be due to the fact that most of the positively charged PEI chains in sRNA/PEI complexes were closely covered with the strongly anionic RNA. For CS chains, the zeta potential values are positive also in the region where condensation occurs. These correspond to a higher N/P ratio values than for the other polymers. In this range, the zeta potential value is almost constant in the case of CS-LMW, and is only slightly increasing for CS-HMW. As noted, PEI and CS promote sRNA condensation at very different N/P ratios. This can be ascribed to the marked difference of charge density between these two classes (see Table 3). However, comparable sizes and surface charges are obtained in the condensation regions. Again, PAA, that possesses an intermediate size and charge densities, leads to the smaller complexes.

Table 4
Average zeta potential and size at various N/P ratios of sRNA and polycation (PEI-LMW, PEI-HMW, CS-LMW, CS-MMW and PAA). The values of zeta potential and size were calculated with the data obtained from three independent measurements (mean ± SD, $n = 3$).

N/P ratios	Zeta potential ± SD (mV)		Size ± SD (nm)	
	PEI-LMW	PEI-HMW	PEI-LMW	PEI-HMW
2.5	−11 ± 1	−3 ± 0.4	254 ± 22	371 ± 18
3	12 ± 1	32 ± 2	198 ± 11	144 ± 2
3.5	19 ± 1	32 ± 1	144 ± 7	154 ± 2
4	21 ± 2	30 ± 2	171 ± 1	168 ± 1
5	24 ± 1	27 ± 2	232 ± 12	265 ± 2
	CS-LMW	CS-MMW	CS-LMW	CS-MMW
15	28 ± 1	23 ± 0.2	215 ± 5	298 ± 4
20	29 ± 0.4	26 ± 0.2	158 ± 5	243 ± 11
30	27 ± 1	27 ± 1	157 ± 7	193 ± 2
35	29 ± 1	28 ± 0.4	182 ± 10	172 ± 4
40	28 ± 1	29 ± 1	237 ± 20	178 ± 1
	PAA			
0.5	−14 ± 1	182 ± 6		
0.6	−8 ± 3	116 ± 7		
0.7	1 ± 0.3	98 ± 16		
0.8	17 ± 2	86 ± 11		
0.9	25 ± 0.4	122 ± 5		

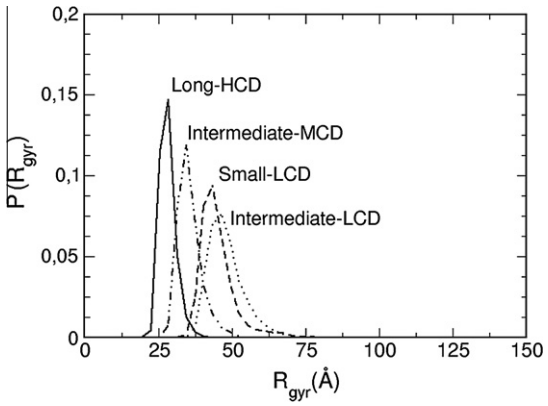

Fig. 5. Probability distributions for the radius of gyration, P(Rgyr), for the polyanion. The labels indicate the correspondent system.

Monte Carlo simulations (Table 2) were performed to explain the trends observed (see Fig. 5). In the simulation, a charge ratio close to 1 corresponds to the existence of neutral complexes. The focus of the simulation is to assess the influence of charge density and size of polymer in the polyanion compaction. As such, the shorter chains possess a higher charge density, and in the longer ones, the charge density is decreased, so as to mimic the differences between the polycations used in the experimental part. It is observed that, while the highest density chains promote the higher degree of compaction, for a constant linear charge density (LCD), the longer chains are the more effective. This means that, in some cases, a decrease in linear charge density may be compensated by an increase in size, in what concerns compaction efficiency. This is consistent with the experimental observations, in which chitosan (long and intermediate-LCD), longer but less densely charged, attains a similar degree of compaction of that attained by PEI (Short-HCD and Intermediate-MCD). Also, PEI is more densely charged but shorter than the more efficient PAA. Naturally, these observations should also take into account more detailed structural aspects, leading to charge matching of charge accessibility, as referred above. The importance of charge density and charge localization has been also emphasized in the interaction of oppositely charged microgel-peptide systems [43].

The simulation also shows additional structural differences in the polyplexes, apart from those observed in the distribution of the radii of gyration (Fig. 5). In the presence of the polycation with longer chain length, the polyanion is neutralized and totally surrounded by the oppositely charged chains (Fig. 6). On the other hand, with shorter and highly charged polycation chains, the polyanion is condensed but more exposed to the outside. These observations can suggest an explanation for the positive charge of all CS-sRNA polyplexes studied, which is higher than that found for the remaining systems.

SEM was used to determine the morphology of the particles obtained with the different polycations. Independently of the polycation used, polyplexes displayed a very well defined spherical and uniform morphology (Fig. 7A–E).

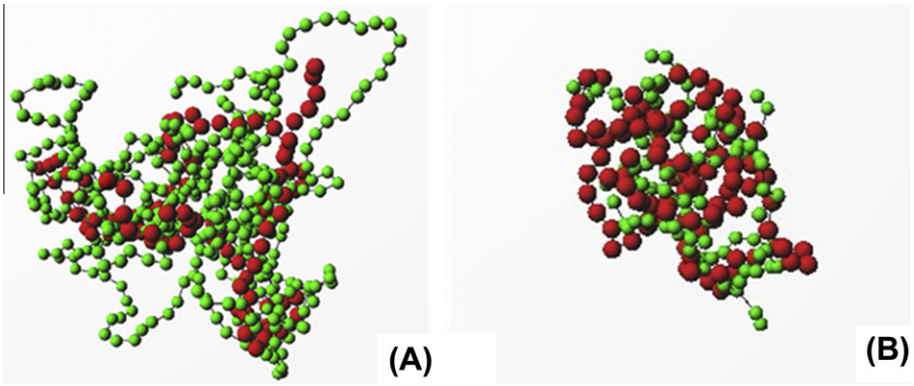

Fig. 6. Representative snapshots showing distinct conformations of polycation (green) and polyanion (red) at N/P = 1. (a) System Long-LCD and (b) system Short-HCD. (For interpretation of the references to color in this figure legend, the reader is referred to the web version of this article.)

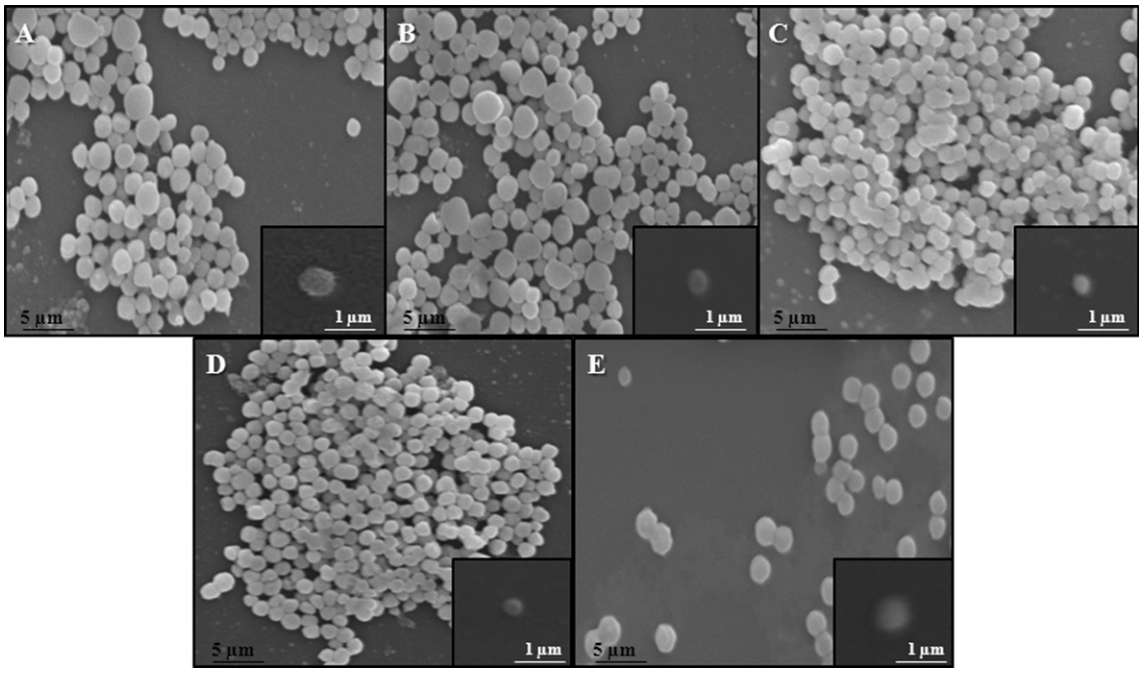

Fig. 7. Polyplexes obtained by simple complexation at pH 4.5 from commercial polymer and sRNA visualized by SEM. (A) sRNA/PEI-LMW (N/P = 3.5), (B) sRNA/PEI-HMW (N/P = 4), (C) sRNA/CS-LMW (N/P = 35), (D) sRNA/CS-MMW (N/P = 45) and (E) sRNA/PAA (N/P = 0.6).

3.5. Stability of sRNA in polyplexes

RNA must be stable to digestion by nuclease so as to have maximal activity in the cells [9]. As such, to assess if an appropriate protection of sRNA is promoted by complexation with the polycation, stability studies, for the systems displaying higher encapsulation efficiency, were performed using RNase and FBS. The results obtained are shown in Figs. 8 and 9, respectively. The UVIband—1D gel analysis software (Uvitec, Cambridge, UK) was again used as an auxiliary of the agarose electrophoresis allowing to control the degradation of sRNA.

In the case of PEI-LMW polyplexes, sRNA degradation was observed at a 10 and 100 µg/mL enzyme concentration over a period of 1 h at 37 °C, for all N/P ratios studied (Fig. 8A, lane 3–8). sRNA degradation was also observed for PAA (Fig. 8C) polyplexes at all N/P ratios in study while for PEI-HMW polyplexes, it was only observed when N/P = 4 (Fig. 8A, lane 9–14). Regarding the protection promoted in the nanoparticulated systems, it should be noted that neither sRNA in the polyplexes produced with CSs nor PEI-HMW showed signs of degradation when in contact with RNase (Fig. 8B). These results were confirmed by the intensity of the bands in each condition by value of peak volume, since the intensity peaks correspond to degraded RNA. PEI-LMW/sRNA complexes were less stable than PEI-HMW complexes at all charge ratios, with 59% maximal dissociation achieved with 100 µg/mL RNase. Therefore, PEI-HMW/sRNA complexes were more stable than the PEI-LMW/sRNA complexes, with 9.5% maximal dissociation achieved with 100 µg/mL RNase for N/P = 4. PAA/sRNA complexes achieved 16% dissociation, and, therefore, were less stable than the PEI-HMW/sRNA complexes. Thus, the structure of sRNA seems to be complexed more loosely in PEI-LMW polyplexes and, hence, RNase partially degrades the sRNA in the two enzyme concentrations, whereas PEI-HMW and CSs provide a complete protection (Fig. 8A and B).

Similar results were obtained when the polyplexes were incubated with 10% of FBS at 37 °C for 30 and 60 min (Fig. 9A–C). As shown in Fig. 9A, the degraded sRNA was visualized by the appearance of the sRNA bands in the lanes 3–8 of the PEI-LMW/sRNA

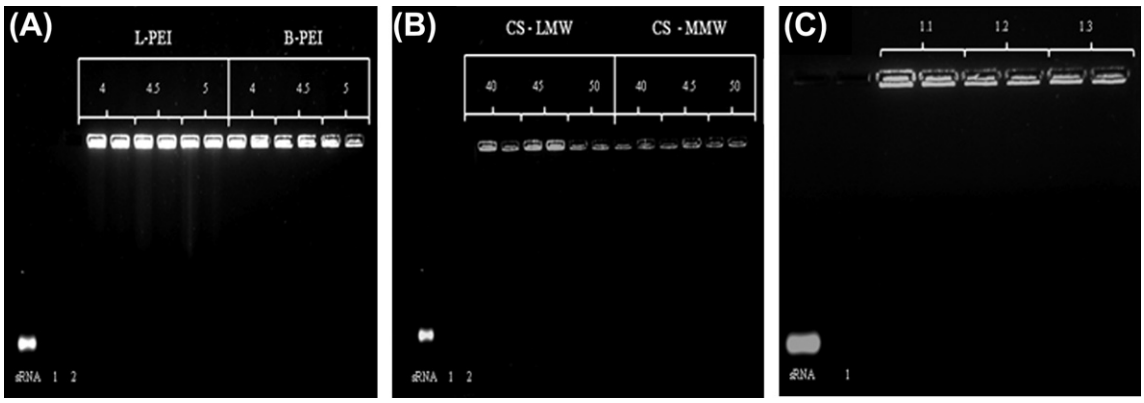

Fig. 8. Agarose gel electrophoresis of the nanoparticle following incubation with RNase (10 and 100 μg/mL) for 1 h at 37 °C. (A) sRNA/PEI-LMW and sRNA/PEI-HMW, (B) sRNA/CS-LMW and sRNA/CS-MMW and (C) sRNA/PAA. Lane 1 – sRNA + RNase (10 μg/mL) and lane 2 – sRNA + RNase (100 μg/mL). The electrophoresis presents the data of three times independents experiments.

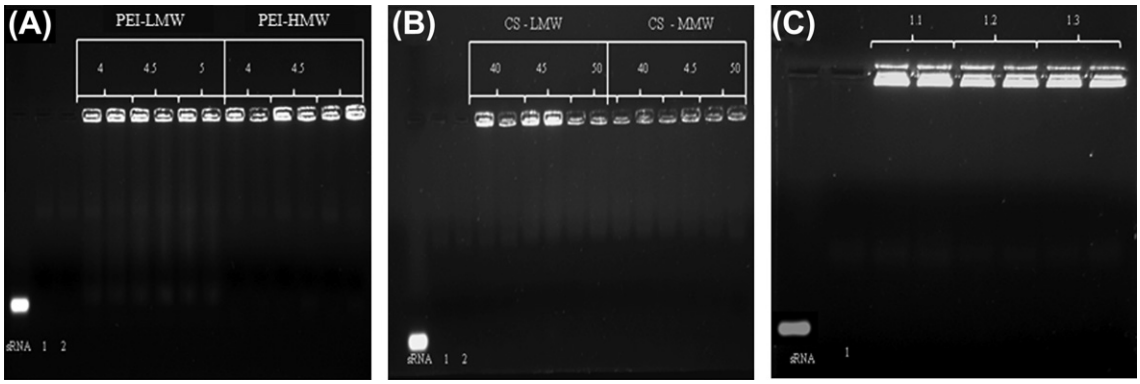

Fig. 9. Agarose gel electrophoresis of the nanoparticle protection of sRNA following incubation with FBS for 30 and 60 min. (A) sRNA/PEI-LMW and sRNA/PEI-HMW, (B) sRNA/CS-LMW and sRNA/CS-MMW and (C) sRNA/PAA. Lane 1 – FBS (10%); lane 2 – sRNA + FBS (10%). All experiments were performed of three times.

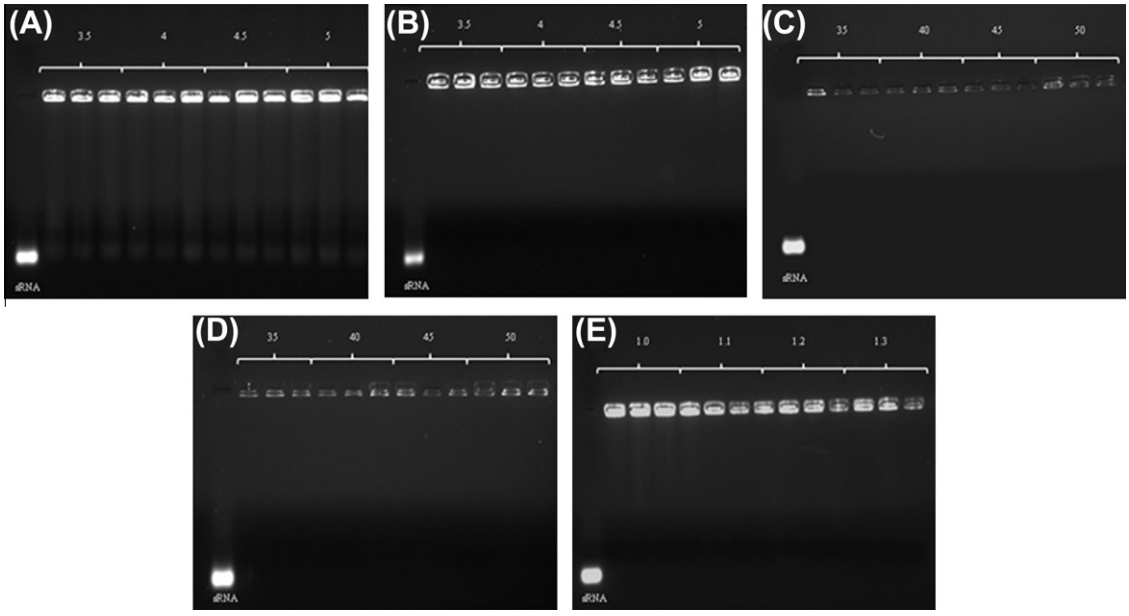

Fig. 10. Agarose gel electrophoresis of the nanocapsules following incubation with heparin (0.01, 0.1 and 0.5 IU/mL) for 1 h at 37 °C. (A) sRNA/PEI-LMW, (B) sRNA/PEI-HMW, (C) sRNA/CS-LMW, (D) sRNA/CS-MMW, (E) sRNA/PAA. Lane 1 – sRNA + heparin (0.1 IU/mL) and lane 2 – sRNA + heparin (0.5 IU/mL). Each experiment was carried three times.

complexes. On the other hand, sRNA complexed with the other polymers does not show any signs of degradation, even after incubating with 10% FBS for 1 h at 37 °C, whereas the free sRNA rapidly degrades after 30 min of incubation at 37 °C (as shown by the complete absence of sRNA bands in the gel in wells 1). It should be noted that the band of the lane 2 results of FBS as shown in the control FBS gel (Fig. 9A–C, lane 2). PEI-LMW/sRNA complexes at all N/P ratios tested, from 3.5 to 5, were very sensitive to FBS with 75% maximal dissociation. In general, these results revealed that PEI-HMW, CS-LMW, CS-MMW and PAA nanoparticles are able to protect sRNA from nuclease degradation (Fig. 9A – lanes 9–15; B and C), suggesting that they are suitable delivery vehicles for *in vitro* and *in vivo* gene delivery applications.

The dissociation properties of the polyplexes were evaluated through heparin/polyanion competition assay. Polyplexes can suffer unwanted modifications when interacting with large polyanions found outside cells, such as sulfated glycosaminoglycans and proteoglycans during the transfer membrane, since they have positively charged surfaces, which may affect the integrity and the mobility of the polyplexes [13,20]. For this reason, it is important to measure the capability of complexes for sRNA delivery through the polyanion competition assay. Heparin is a polysaccharide negatively charged bearing sulfonate groups that compete with the nucleic acids, leading to dissociation. For this purpose, polyplexes are incubated with varying amounts of heparin (0.01, 0.1 and 0.5 IU/mL) to induce the decomplexation of the sRNA within the complexes, prior to separation on agarose gels (Fig. 10A–E). All the PEI-LMW/sRNA complexes are unstable in the presence of heparin (Fig. 10A). PEI-LMW/sRNA complexes achieved 10.7% maximal dissociation, after incubation with heparin. So, these results indicate that PEI-HMW/sRNA complexes are more stable than PEI-LMW/sRNA complexes at all charge ratios, in the presence of heparin (Fig. 10A and B). The results obtained are in accordance with Kwok and Hart [44]. Furthermore, sRNA maintained stable complexes with CS-LMW and CS-MMW, even in the presence of high concentrations of heparin (Fig. 10C and D). The PAA/sRNA complexes formulated at a N/P ratio of 1.0 and 1.1 dissociated even with trace amounts of heparin (Fig. 10E). For PAA/sRNA complexes formulated at N/P ratios of 1.0 and 1.1, 13.7% and 2.9% maximal dissociation was achieved, respectively, after incubation with 0.5 IU/mL heparin. Overall, the results concerning the incubation with heparin for a period of 1 h indicate that PEI-LMW and PAA complexes are more strongly affected by heparin than PEI-HMW and CS complexes, and it is also expected that they have a lower efficiency in transfer of the cell membrane. Except for that with PAA, polyplexes that are more sensitive to RNase degradation are also more prone to decompaction by heparin. Also, longer polycations seem to promote a higher degree of protection.

The ability to dissociate in the presence of heparin reveals the potential to dissociate within the cell, releasing the nucleic acid, while providing sufficient stability outside the cells to protect and preserve the size and integrity of the acid nucleic complex.

4. Conclusions

RNA interference technology is emerging as a powerful tool for *in vivo* research, both to address questions of basic biology and the needs of drug development formulations. Their successful application depends on optimizing physicochemical properties such as size, zeta potential, encapsulation efficiency and complex stability of the carriers. The PEI-LMW/sRNA complexes showed smaller sizes and a higher encapsulation efficiency (100%). However, they were not stable in the presence of RNase, FBS and heparin. On the other hand, the PEI-HMW/sRNA complexes indicate good encapsulation efficiency, small sizes and stability in the presence of FBS and heparin. The CS/sRNA particles exhibited positive zeta values in the relevant range of N/P ratios tested, with size values of ca. 200 nm, and good stability in the presence of RNase, heparin and FBS. Additionally, they display high values for the encapsulation efficiency. Finally, the PAA/sRNA polyplexes presented the smaller size, good encapsulation efficiency and high stability in mimetized physiological conditions. We recall that PAA is, however, known to be cytotoxic. Apart from the differences between the structures of the polycations used, it was observed that it is possible to produce polyplexes with similar structural properties, such as size and potential zeta. Thus, from the polyplexes developed in this work, chitosan complexes seem to be the most promising vehicles for application in RNA therapeutic.

In a more general sense, results have also shown that a longer polycation with low charge density may induce a similar degree of condensation of that of a shorter polycation with a high linear charge density. The accessibility of the positive charge and effects of charge matching may also favor an efficient condensation. These results may easily be transposed to similar systems, and guide in the optimization of sRNA particles for sRNA delivery.

Acknowledgments

The authors would like to thank Dr. Vítor Gaspar and Eng. Ana Paula Gomes for acquiring the SEM and Professor Graça Rasteiro for kindly allowing the use of the zeta potential. Patrícia Pereira and Andreia F. Jorge gratefully acknowledge Fundação para Ciência e Tecnologia (FCT), Portugal, for financial support Ph.D. Grant, Ref SFRH/BD/81914/2011 and Ref SFRH/BD/66748/2009, respectively. A. F. J. and A.A.C.C.P. acknowledge FEDER Funds through the COMPETE Program "Programa Operacional Factores de Competitividade (FCOMP-01-0124-FEDER-010831)" and by National Funds through Fundação para a Ciência e Tecnologia (FCT) under the Project: PTDC/QUI-QUI/101442/2008.

References

[1] C.H. Ahn, S.Y. Chae, Y.H. Bae, S.W. Kim, J. Control Release 80 (2002) 273.
[2] T.H. Kim, S.I. Kim, T. Akaike, C.S. Cho, J. Control Release 105 (2005) 354.
[3] S. Mao, W. Sun, T. Kissel, Adv. Drug Deliv. Rev. 62 (2010) 12.
[4] J.X. Chen, H.Y. Wang, C.Y. Quan, X.D. Xu, X.Z. Zhang, R.X. Zhuo, Org. Biomol. Chem. 8 (2010) 3142.
[5] R.R. Breaker, Nature 432 (2004) 838.
[6] C.Y. Chu, T.M. Rana, J. Cell. Physiol. 213 (2007) 412.
[7] K.M. Wassarman, A.X. Zhang, G. Storz, Trends Microbiol. 7 (1999) 37.
[8] M.S. Huh, S.Y. Lee, S. Park, S. Lee, H. Chung, Y. Choi, Y.K. Oh, J.H. Park, S.Y. Jeong, K. Choi, K. Kim, I.C. Kwon, J. Control Release 144 (2010) 134.
[9] H. Katas, H.O. Alpar, J. Control Release 115 (2006) 216.
[10] M.E. Bonnet, P. Erbacher, A.L. Bolcato-Bellemin, Pharm. Res. 25 (2008) 2972.
[11] H. Koo, G.W. Jin, H. Kang, Y. Lee, K. Nam, C. Zhe Bai, J.S. Park, Biomaterials 31 (2010) 988.
[12] S. Nimesh, R. Chandra, Eur. J. Pharm. Biopharm. 73 (2009) 43.
[13] S.Y. Lee, M.S. Huh, S. Lee, S.J. Lee, H. Chung, J.H. Park, Y.K. Oh, K. Choi, K. Kim, I.C. Kwon, J. Control Release 141 (2010) 339.
[14] V. Dehousse, N. Garbacki, S. Jaspart, D. Castagne, G. Piel, A. Colige, B. Evrard, Int. J. Biol. Macromol. 46 (2010) 342.
[15] S.C. De Smedt, J. Demeester, W.E. Hennink, Pharm. Res. 17 (2000) 113.
[16] C. Tros de Ilarduya, Y. Sun, N. Duzgunes, Eur. J. Pharm. Sci. 40 (2010) 159.
[17] H. Gao, W. Shi, L.B. Freund, Proc. Natl. Acad. Sci. USA 102 (2005) 9469.
[18] H. Aoki, M. Satoh, K. Mitsuzuka, A. Ito, S. Saito, T. Funato, M. Endoh, T. Takahashi, Y. Arai, FEBS Lett. 567 (2004) 203.
[19] D.J. Gary, N. Puri, Y.Y. Won, J. Control Release 121 (2007) 64.
[20] M. Glodde, S.R. Sirsi, G.J. Lutz, Biomacromolecules 7 (2006) 347.
[21] H. Katas, E. Cevher, H.O. Alpar, Int. J. Pharm. 369 (2009) 144.
[22] W.E. Rudzinski, T.M. Aminabhavi, Int. J. Pharm. 399 (2010) 1.
[23] A. Pathak, A. Aggarwal, R.K. Kurupati, S. Patnaik, A. Swami, Y. Singh, P. Kumar, S.P. Vyas, K.C. Gupta, Pharm. Res. 24 (2007) 1427.
[24] R. Martins, J.A. Queiroz, F. Sousa, J. Mol. Recognit. 23 (2010) 519.
[25] Y.S. Mel'nikova, B. Lindman, Langmuir 16 (2000) 5871.
[26] F. Re, RNA Methodologies – Laboratory Guide for Isolation and Characterization, fourth ed., Academic Press, York, USA, 2005.
[27] Avogadro is an open source software under the GNU GPL. It can be downloaded from <http://avogadro.openmolecules.net/wiki/MainPage>.
[28] A.K. Rappe, C.J. Casewit, K.S. Colwell, W.A. Goddard, W.M. Skiff, J. Am. Chem. Soc. 114 (1992) 10024.

[29] A.F. Jorge, J.M. Sarraguca, R.S. Dias, A.A. Pais, Phys. Chem. Chem. Phys. 11 (2009) 10890.
[30] P. Linse. Moisim, Version 4.0.8, 2007.
[31] C. Brender, M. Lax, J. Chem. Phys. 79 (1983) 2423.
[32] B. Ranjbar, P. Gill, Chem. Biol. Drug Des. 74 (2009) 101.
[33] P. Doty, H. Boedtker, J.R. Fresco, R. Haselkorn, M. Litt, Proc. Natl. Acad. Sci. USA 45 (1959) 482.
[34] L.K. Medina-Kauwe, J. Xie, S. Hamm-Alvarez, Gene Ther. 12 (2005) 1734.
[35] R.S.P. Dias, J. Chem. Phys. 119 (2003) 8150.
[36] P. Kebbekus, D.E. Draper, P. Hagerman, Biochemistry 34 (1995) 4354.
[37] P.J. Hagerman, Annu. Rev. Biophys. Biomol. Struct. 26 (1997) 139.
[38] S.C. Tan, E. Khor, T.K. Tan, S.M. Wong, Talanta 45 (1998) 713.
[39] A.F. Jorge, R.S. Dias, J.C. Pereira, A.A. Pais, Biomacromolecules 11 (2010) 2399.
[40] M.F. Pinto, M.C. Moran, M.G. Miguel, B. Lindman, A.S. Jurado, A.A. Pais, Biomacromolecules 10 (2009) 1319.
[41] M.A. Trejo-Ramos, F. Tristan, J.L. Menchaca, E. Perez, M. Chavez-Paez, J. Chem. Phys. 126 (2007) 014901.
[42] A.C. Grayson, A.M. Doody, D. Putnam, Pharm. Res. 23 (2006) 1868.
[43] H. Bysell, P. Hansson, M. Malmsten, J. Phys. Chem. B 114 (2010) 7207.
[44] A. Kwok, S.L. Hart, Nanomedicine 7 (2011) 210.
[45] S. Choosakoonkriang, B.A. Lobo, G.S. Koe, J.G. Koe, C.R. Middaugh, J. Pharm. Sci. 92 (2003) 1710.
[46] G.C. Kini, J. Lai, M.S. Wong, S.L. Biswal, Langmuir 26 (2010) 6650.

Paper IX

Recombinant pre-miR-29b for Alzheimer´s disease therapeutics

P. Pereira, J. Tomás, J. A. Queiroz, A. Figueiras, F. Sousa

(*Submitted for publication*)

Short description: Following the establishment of appropriated strategies for human pre-miR-29b biosynthesis (paper III), purification (paper VI) and delivery of RNA (paper VIII), here it is described the application of this recombinant RNA in decreasing the BACE1 expression levels and, subsequently the Aβ expression, after transfection of N2a695 cells. Primarily, all the pre-miR-29b loaded polyplexes were formulated using the method of simple complexation which is based on the electrostatic interactions that occur between polymer and pre-miR-29b. According to the results obtained in this study, we developed an integrative platform that allows biosynthesis, purification and transfection of the recombinant pre-miR-29b using polyplexes to decrease the hBACE1 and endogenous $A\beta_{42}$ expression levels. At this point, the main objective was to verify the biological activity of the recombinant pre-miR-29b, evaluated by the efficiency to knockdown BACE1.

Recombinant pre-miR-29b for Alzheimer´s disease therapeutics

Patrícia A. Pereira*, Joana F. Tomás*, João A. Queiroz*, Ana R. Figueiras*,#, Fani Sousa*

*CICS-UBI – Health Sciences Research Centre, University of Beira Interior, Avenida Infante D. Henrique, Covilhã, 6200-506, Portugal;

#CNC – Center of Neuroscience and Cell Biology, University of Coimbra, Largo Marquês de Pombal, Coimbra, 3004-517, Portugal

*Corresponding author:
Dr. Fani Sousa
Phone: +351 275 329 074
Fax: +351 275 329 099
E-mail address: fani.sousa@fcsaude.ubi.pt
Postal address: Health Sciences Research Centre, Universidade da Beira Interior, Avenida Infante D. Henrique, 6200-506 Covilhã, Portugal

Abstract

MicroRNAs are arising as the next generation of diagnostic and therapeutic tools for gene silencing. Studies demonstrated that the miR-29 expression is decreased in Alzheimer's disease (AD) patients displaying high levels of human β-secretase (hBACE1). Recent advances toward an effective therapy for AD intend to employ miR-29 to suppress hBACE1 expression and subsequent Amyloid-β (Aβ) peptide. However, delivery of mature miRNA has demonstrated modest efficacy *in vitro*; therefore, the preparation of highly pure and biologically active pre-miRNA arises as one of the most important challenges in the development of these therapeutic strategies. Recently, we described a new strategy based arginine-affinity chromatography to specifically purify the recombinant pre-miR-29b. Following this strategy, the purified pre-miR-29b was successfully encapsulated into polyplexes that were further delivered in cytoplasm. It was verified that Chitosan/pre-miR-29b and Polyethylenimine/pre-miR-29b systems efficiently delivered pre-miR-29b to N2a695 cells, thus reducing the hBACE1 protein expression (around 78% and 86%, respectively) and $A\beta_{42}$ levels (approximately 44% and 47%, respectively). Furthermore, pre-miR-29b downregulates the hBACE1 mRNA expression in 80%. Overall, it was demonstrated that the recombinant pre-miR-29b using polyplexes allowed to decrease the hBACE1 and $A\beta_{42}$ expression levels, improving the currently available methodologies of miRNA-based therapeutics.

Keywords

Alzheimer’s disease; hBACE1; Amyloid-β; Chitosan; Polyethylenimine; Polyplexes; Recombinant pre-miR-29b;

Introduction

Over the past decade, several hundred small non-coding regulatory RNA molecules, known as microRNAs (miRNAs), have been identified as potential biomarkers and therapeutic products[1,2]. Briefly, miRNAs are initially transcribed as pri-miRNAs from the regions of the genome that are subsequently processed by the Drosha into pre-miRNAs stem-loop. Then, pre-miRNAs are exported to the cytoplasm where they are converted into mature miRNAs after the removal of their loops by Dicer. Finally, one strand of the miRNA duplex (called mature miRNA sequence) is loaded onto the RNA-induced silencing complex (RISC) and, posteriorly, binds to specific sites typically present in the 3' untranslated region (3'UTR) of messenger RNA (mRNA), leading to translational inhibition with imperfect base pairing or, less frequently, to the mRNA degradation with perfect base pairing[1,3-6]. An important feature of these RNAs is that an individual miRNA can regulate multiple mRNA targets and, consequently, can induce multiple effects on the expression of several related genes families[3]. Accordingly, it is likely that miRNAs are directly involved in a variety of cellular processes, namely in cell cycle regulation, proliferation, apoptosis, differentiation, stress response and metabolism[5,9]. Thus, the unveiling of the role of several miRNAs present in cellular processes is critical to develop new diagnosis methods or drugs for understanding and treating illnesses. To date, there are over 1880 miRNAs that have been discovered in humans, among which the miR-29 remains as one of the most interesting and intriguing miRNA families, once the dysregulation of this miRNA has a strong impact on many diseases including multiple types of cancers[10-14] and neurodegenerative[15-19] disorders, suggesting that it can be a promising target in the therapeutic of these diseases.

Recently, several studies have been published concerning the expression of miR-29 in patients with Alzheimer's disease (AD)[20,25,26], suggesting that this biomolecule can play an important role in the regulation of this neurodegenerative disease. The generation and subsequent accumulation of amyloid-β peptides (Aβ) is a histological characteristic that is strongly implicated in the pathogenesis of AD[22-24]. One of the mechanisms that contribute to the accumulation of Aβ is sequential proteolytic cleavages of full-length amyloid precursor protein (APP) by β-site amyloid precursor protein cleaving enzyme 1 (BACE1), being considered as a prime drug target for therapeutic inhibition of Aβ production in AD[25]. Hence, the regulation of the proteins expression levels involved in the Aβ generation process has demonstrated to be important in AD. Several research groups showed that the miR-29 is potentially involved in the regulation of APP and BACE1 expression because *in vitro* studies revealed that in sporadic AD patients, displaying abnormally high BACE1 protein levels, the miR-29 cluster was significantly decreased[20, 23, 26]. These findings provided support for a causal relationship between miR-29 and AD, since the miR-29 suppresses the expression levels of hBACE1 and, consequently, Aβ peptides levels in neuronal cells[16]. Thus, miR-29 can be used as a potential therapeutic weapon for pharmacological intervention of AD.

Commonly, the miRNAs used for therapeutic purposes have mostly been produced by chemical synthesis (phosphoamidite chemistry, normally used for the generation of short oligoribonucleotides), enzymatic synthesis (longer RNAs can be produced by *in vitro* transcription) or via a plasmid (for miRNA expression into eukaryotic cell lines)[26]. Although these methods can be very efficient in producing miRNA, in general, additional purification protocols to remove the impurities (failure sequences, impurities of pDNA template, enzymes, nucleotides, salts or buffer) from the production process have to be employed. The presence of impurities may lead to non-targeted gene silencing, what is commonly associated with a decrease in therapeutic effectiveness and still restrict the implementation of these oligonucleotides onto clinical applications[26,27]. Furthermore, the purification methods usually employed are still expensive, difficult to scale up and can cause degradation of the RNA molecules due to the requirement of toxic solvents and use of denaturing conditions[28]. Thus, considering the rapidly growing interest on these novel biopharmaceuticals, as a result of its potential therapeutic application, novel technologies to improve their preparation are currently being pursued.

Thus, our research group recently proposed a new process for production and purification through amino acid-based affinity chromatography, of recombinant pre-miR-29b with potential therapeutic application[29]. This strategy could contribute for the establishment of reliable, simple and more cost-effective processes, easily adopted by biopharmaceutical industries, while maintaining maximal product quality and biological activity. However, in order to improve the biological effect in RNAi-based therapies it is also essential the development of an efficient miRNA delivery system capable to overcome the biological barriers, protect the integrity of miRNA and trapping miRNA in intracellular space to exert its function[30]. During the last decades, several research groups have focused on the production and characterization of polyplexes formed between sRNA and some cationic polymers such as Polyethylenimine (PEI)[31-35] and Chitosan (CS)[36-40]. In general, these vehicles can be promising systems to compact RNA for systemic delivery because they present a mean diameter of 200 nm, high stability, biocompatibility and proved to be useful in protecting the RNA against fetal bovine serum (FBS) and ribonuclease[41]. Furthermore, delivery by polyplexes has the advantage of being more cost-effective. However, the high toxicity of PEI is one of the major limiting factors especially for *in vivo* use. Polymers with low molecular weight (< 25KDa) display low toxicity, but the transfection efficiency is low as well. It is commonly believed that the most suitable molecular weight of PEI for gene transfer ranges between 5KDa and 25KDa[42,43]. Thus, the main novelty of the present study is to report the application of the recombinant pre-miR-29b in cells transfection to decrease the hBACE1 expression levels and, subsequently the Aß expression levels. Overall, the implementation of this cutting-edge approach provides the basis for the improvement of the currently available methodologies of gene silencing as a putative genetic therapy for AD and their implementation on biopharmaceutical industry.

Results

pre-miR-29b protection by polyplexes formulation and delivery to neuronal cells

The pre-miR-29 loaded polyplexes were formulated using the following conditions: CS/pre-miR-29b with N/P ratio of 30 and to PEI/pre-miR-29b with N/P ratio of 3.5 (see Methods section). Relevant parameters such as size, zeta potential and loading capacity were determined for the different polyplexes. Thus, as shown in Table 1, all of the polyplexes demonstrated high encapsulation efficiency, small sizes and exhibited a strong positive charge on their surface.

Table 1 – Characterization of polyplexes. The values of zeta potential and size were calculated with the data obtained from three independent measurements (mean ± SD, n = 3).

Polyplexes	N/P Ratio	Size (nm)	Zeta potential (mV)	Encapsulation efficiency
Chitosan	30	130.65±8.29	+24.53±2.92	90%
Polyethylenimine	3.5	118.92±5.10	+35.00±4.22	100%

In vitro characterization of the cytotoxic profile of polyplexes

The cellular cytotoxicity effect of all the synthesized formulations (polycations/pre-miR-29b) was evaluated by MTS and compared with cells treated with ethanol (positive control). As presented in Fig. 1, at 48 and 72 h after transfection, cellular viability is clearly not affected by the presence of the CS/pre-miR-29b since the majority of cells remained viable (>96% viability), suggesting that these carriers are suitable for therapeutic applications. Also, at 48 and 72 h after transfection with PEI/pre-miR-29b, the cells remained viable (>94% viability), as demonstrated in Fig. 1B.

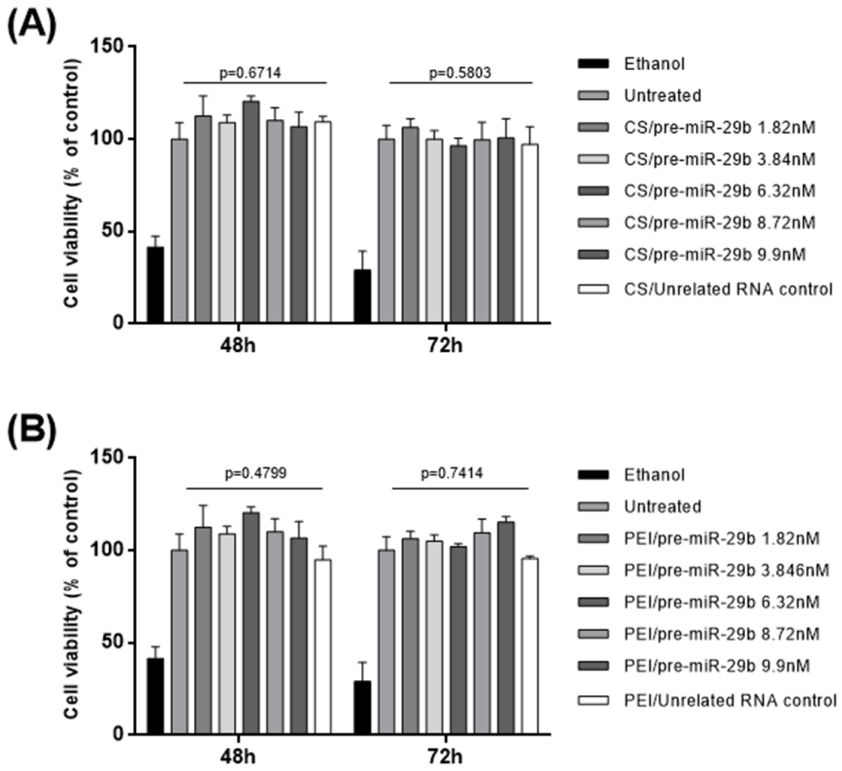

Figure 1 - MTS assays conducted in CS/pre-miR-29b **(A)** and in PEI/pre-miR-29b **(B)**, which were cultured in the presence of increasing concentrations of pre-miR-29b for 48 and 72 h. Untreated cells and cells transfected with an unrelated RNA control were used as negative controls for cytotoxicity. Ethanol treated cells were used as positive controls to induce toxicity. Mean percentage values relative to the untreated cells and standard error of the mean in 3 independent experiments are shown. ANOVA, mean ± SD.

Downregulation of human BACE1 expression induced by polyplex/pre-miR-29b

To ascertain whether recombinant pre-miR-29b could effectively suppress human BACE1 (hBACE1) expression, we used mouse neuroblastoma (N2a) cells stably transfected with cDNAs encoding human APP695 (N2a695 cells)[44]. Thus, in order to explore the effect of recombinant pre-miR-29b administration, N2a695 cells were transfected with CS/pre-miR-29b, PEI/pre-miR-29b and Lipo/pre-miR-29b using different concentrations of the pre-miR-29b (3.84, 6.32, 8.72 and 9.9 nM).

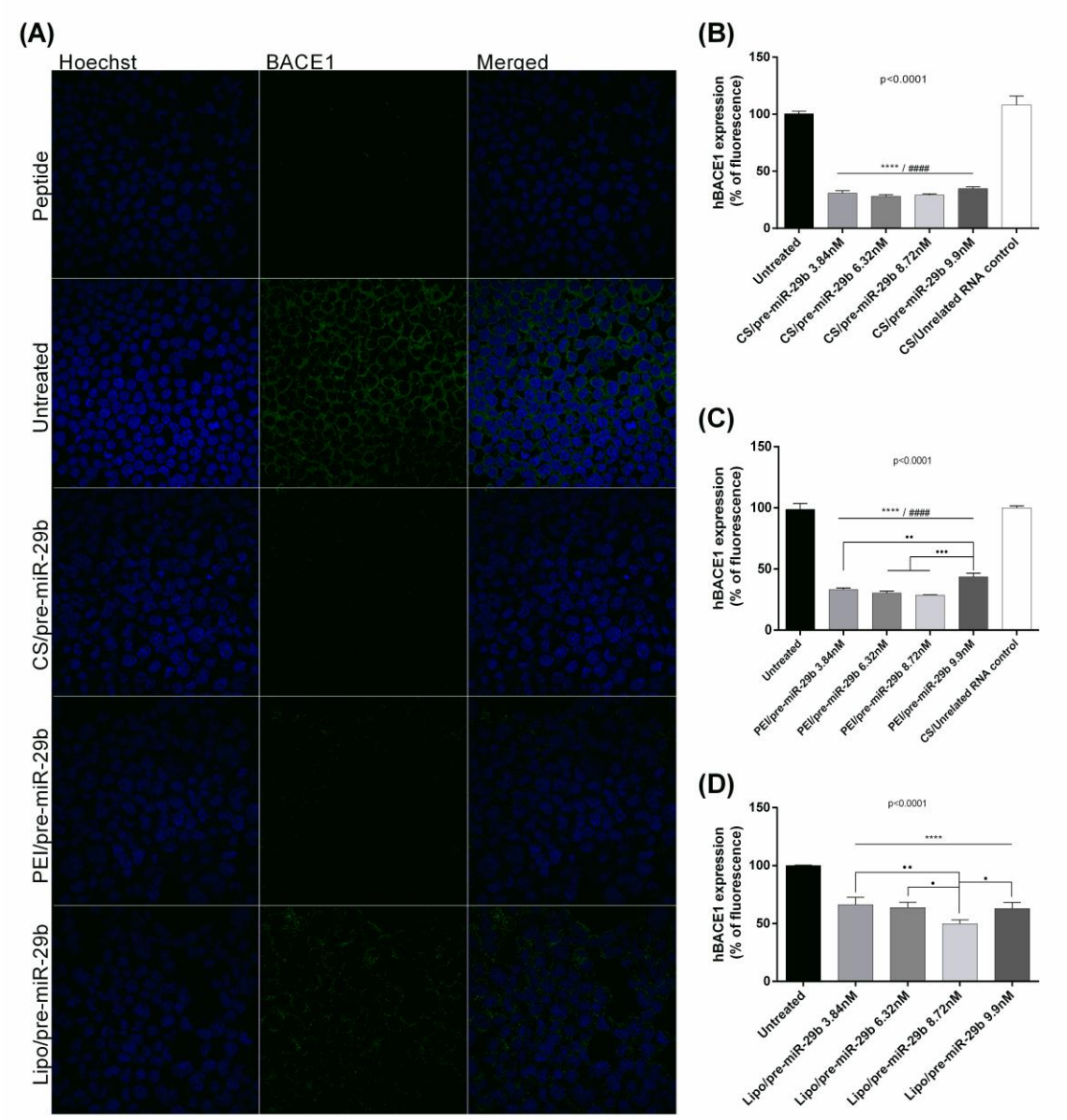

Figure 2 - Recombinant pre-miR-29b effect on BACE1 levels in N2a695 cells at different concentrations of the pre-miR-29b for 72 h. **(A)** Representative confocal microscopy images of N2a695 cells treated with CS/pre-miR-29b, PEI/pre-miR-29b and Lipo/pre-miR-29b stained against BACE1. Quantification of fluorescence intensity for BACE1 protein expression in cells transfected with: **(B)** CS/pre-miR-29b, **(C)** PEI/pre-miR-29b, and **(D)** Lipo/pre-miR-29b. All results are expressed relatively to those in untreated cells and error bars represent standard deviations derived from three or more independent experiments performed in triplicate. ANOVA, mean±SD.

Consistent with the Immunocytochemistry results, Western blot analysis revealed that endogenous hBACE1 protein levels were significantly reduced in the N2a695 cell line transfected with polyplexes containing the recombinant pre-miR-29b, compared with the untreated cells and cells transfected with an unrelated RNA control (Figs. 2 and 3), at 48 and

72 h. In addition, N2a695 cells were transfected with synthetic miR-29b (positive control) and scrambled RNA (negative control) (at a final concentration of 9.9 nM) (Fig. 3F). At 24 h after transfection, no significant changes on the endogenous levels of hBACE1 protein were detected when compared with untreated cells and cells transfected with the unrelated RNA control (data not shown). On the other hand, 72 h after transfection, hBACE1 protein expression was decreased by approximately 78% in cells transfected with CS/pre-miR-29b, and by 86% in those transfected by PEI/pre-miR-29b complexes (Figs. 2 and 3). In addition, in N2a695 cells, pre-miR-29b treatment caused concentration-dependent inhibition of hBACE1 expression (Fig. 3). Thus, hBACE1 protein expression was significantly reduced following transfection with both synthetic miR-29b (around 48% reduction) and recombinant pre-miR-29b (around 82% reduction) by comparing with the transfection of untreated cells (Fig. 3C).

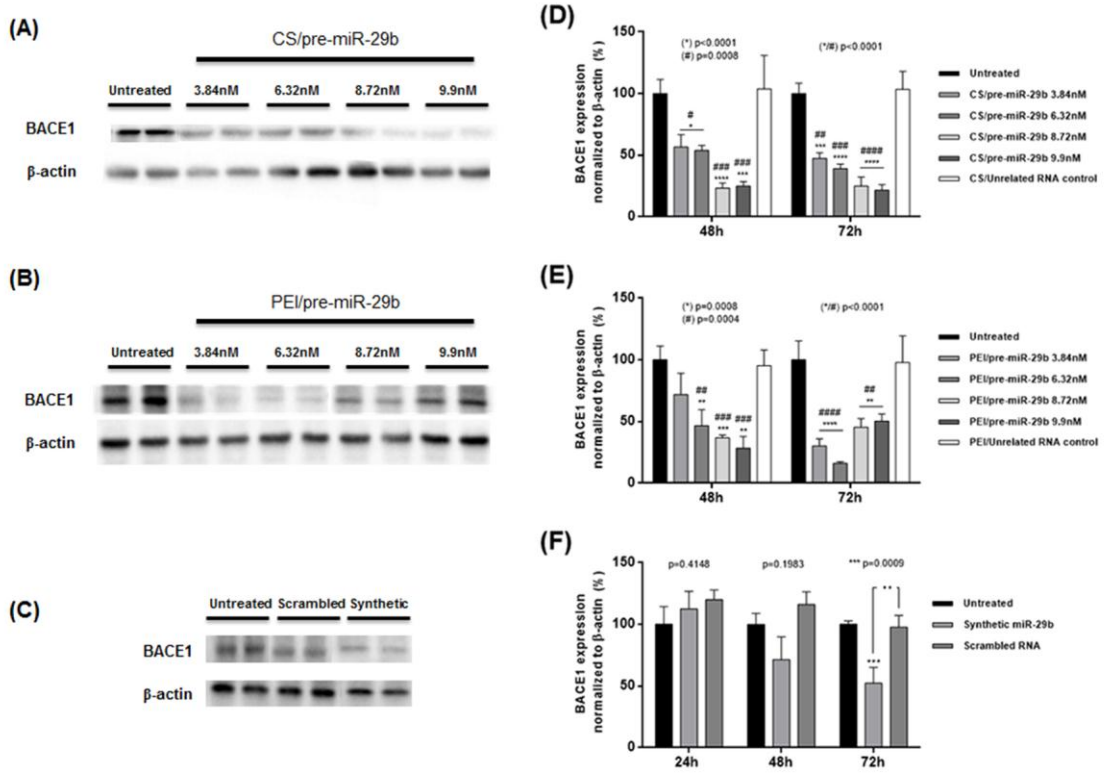

Figure 3 –Western blot analysis of endogenous hBACE1 and β-actin levels in the cell lysate of N2a695 cells treated with different concentrations of pre-miR-29b, at 24, 48 and 72 h. **(A), (B)** and **(C)**: representative images of Western blot from N2a695 cells after 72 h transfection with CS/pre-miR-29b, PEI/pre-miR-29b and Synthetic miR-29b and Scrambled RNA, respectively. **(D), (E)** and **(F)**: densitometric quantifications of hBACE1 expression from Western blot images of CS/pre-miR-29b, PEI/pre-miR-29b and synthetic miR-29b and scrambled RNA, respectively. Error bars represent standard deviations derived from three or more independent experiments performed in duplicate. ANOVA, mean±SD. (For simplicity purposes, the blots were cropped and the representative images are shown).

Therefore, endogenous hBACE1 levels are significantly inhibited by pre-miR-29b delivery in N2a695. To confirm the antibody specificity, the primary antibody anti-BACE1 was blocked with BACE1 peptide, by incubation at RT during 4 h. As demonstrated by Fig. 2A, fluorescence was not detected in the confocal microscopy image, indicating that the antibody binds to BACE1 in N2a695 cells, proving the high specificity of antibody to hBACE1.

Pre-miR-29b inhibits hBACE1 translation and affect hBACE1 mRNA level

Following the evaluation of the effect of the transfection of N2a695 cells with polyplexes loaded with recombinant pre-miR-29b on hBACE1 protein levels through Immunocytochemistry and Western-blot analysis, it was also evaluated its effect on hBACE1 mRNA levels by RT-qPCR measurements. As expected, RT-qPCR results (Fig. 4) revealed that hBACE1 mRNA levels in N2a695 cells were also significantly reduced after treatment with CS/pre-miR-29b and PEI/pre-miR-29b relatively to untreated cells and cells transfected with the unrelated RNA control (Fig. 4). As a matter of fact, miRNAs can regulate gene expression through either translational suppression, mRNA degradation or both. Data analysis showed that CS/pre-miR-29b 6.32 nM significantly decreased hBACE1 mRNA expression to 76.4±0.6% (Fig. 4A) relatively to N2a695 cells treated with PEI/pre-miR-29b 8.72 nM (77.9±4.5%), at 72 h of transfection (Fig. 4B). At 48 h after transfection, a significant reduction of hBACE1 mRNA levels was also verified, being 48.5±4.4% and 53.8±8.1%, respectively for CS/pre-miR-29b 3.84 nM and PEI/pre-miR-29b 9.9 nM (Figs. 4A and 4B). Furthermore, it was also performed RT-qPCR for RNA from N2a695 cells transfected with scrambled RNA or with synthetic miR-29b, at 24, 48 and 72 h (Fig. 4C). As expected, hBACE1 mRNA levels were also decreased in comparison with untreated control and cells transfected with an unrelated RNA control, in the cells transfected with synthetic miR-29b (41.3±3.6%), at 72 h (Fig. 4C). On the other hand, hBACE1 mRNA levels were unaffected in cells transfected with scrambled RNA (Fig. 4C). Thus, the decrease in hBACE1 protein levels is likely due to a decrease in hBACE1 mRNA stability or by reducing the transcription rate since we found by RT-qPCR that the level of hBACE1 mRNA was also decreased by recombinant pre-miR-29b and synthetic miR-29b delivery (Fig. 4)[50]. Furthermore, the correlation between hBACE1expression and pre-miR-29b provides further support for the hypothesis that pre-miR-29b contributes, at least in part, to overall changes in hBACE1 expression in AD. Taken together, these data demonstrate effective delivery of recombinant pre-miR-29b to N2a695 cells using polyplexes and that a specific suppression of hBACE1 expression occurs when these polyplexes delivered pre-miR-29b.

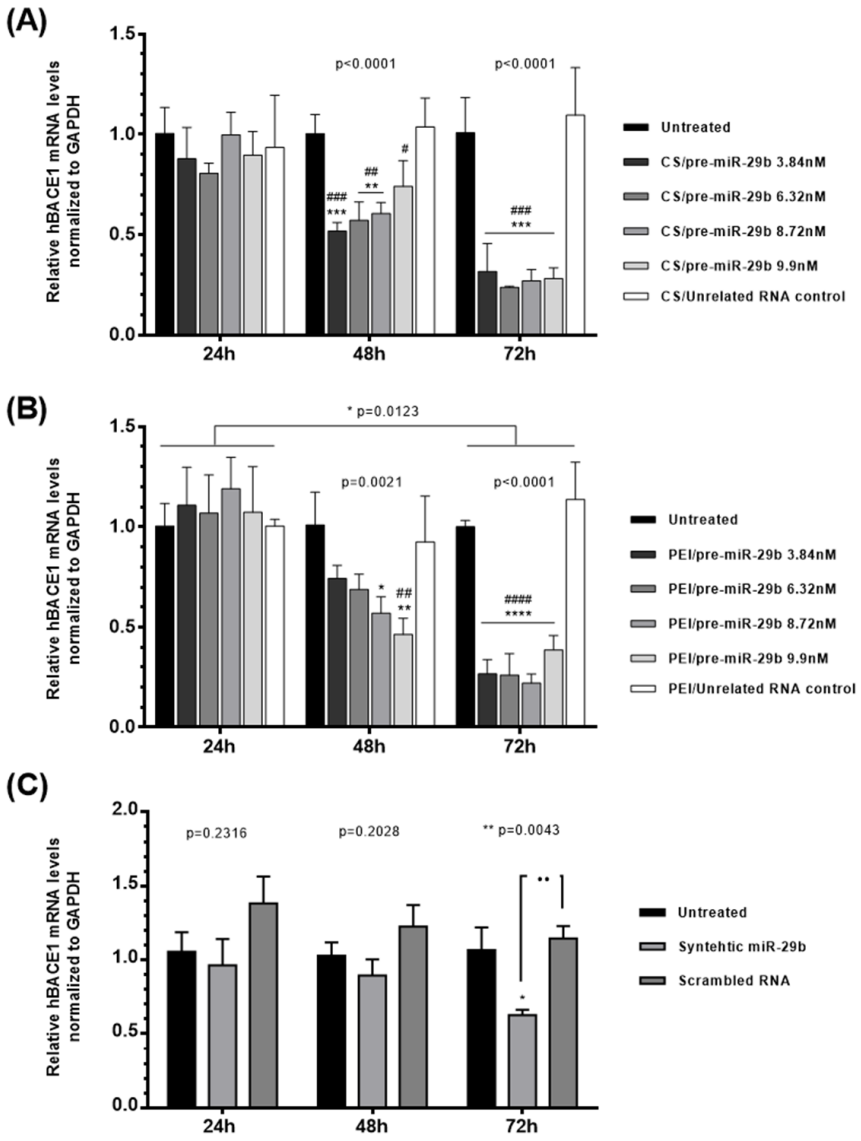

Figure 4 - Effect of recombinant pre-miR-29b on hBACE1 mRNA levels in N2a695 cells following 24, 48 and 72 h treatment with: **(A)** CS/pre-miR-29b and **(B)** PEI/pre-miR-29b **(C)** Synthetic miR-29b and Scrambled RNA. Values in the graphs are mean from triplicates of RT-qPCR threshold cycles for hBACE1 mRNA normalized to those of mRNA for GAPDH from 3 independent experiments and demonstrate significant differences across treatment conditions. ANOVA, mean ± SD.

Recombinant pre-miR-29b modulates $A\beta_{42}$ generation *in vitro*

Previous studies showed a causal relationship between miR-29b expression and BACE1 activity, and, consequently, Aβ peptides generation[16]. Interestingly, by Immunocytochemistry analysis it was found that when the endogenous $A\beta_{total}$ peptides are secreted, they accumulate around the nucleus leading to its deformation, appearing like a kidney (Fig. 5A).

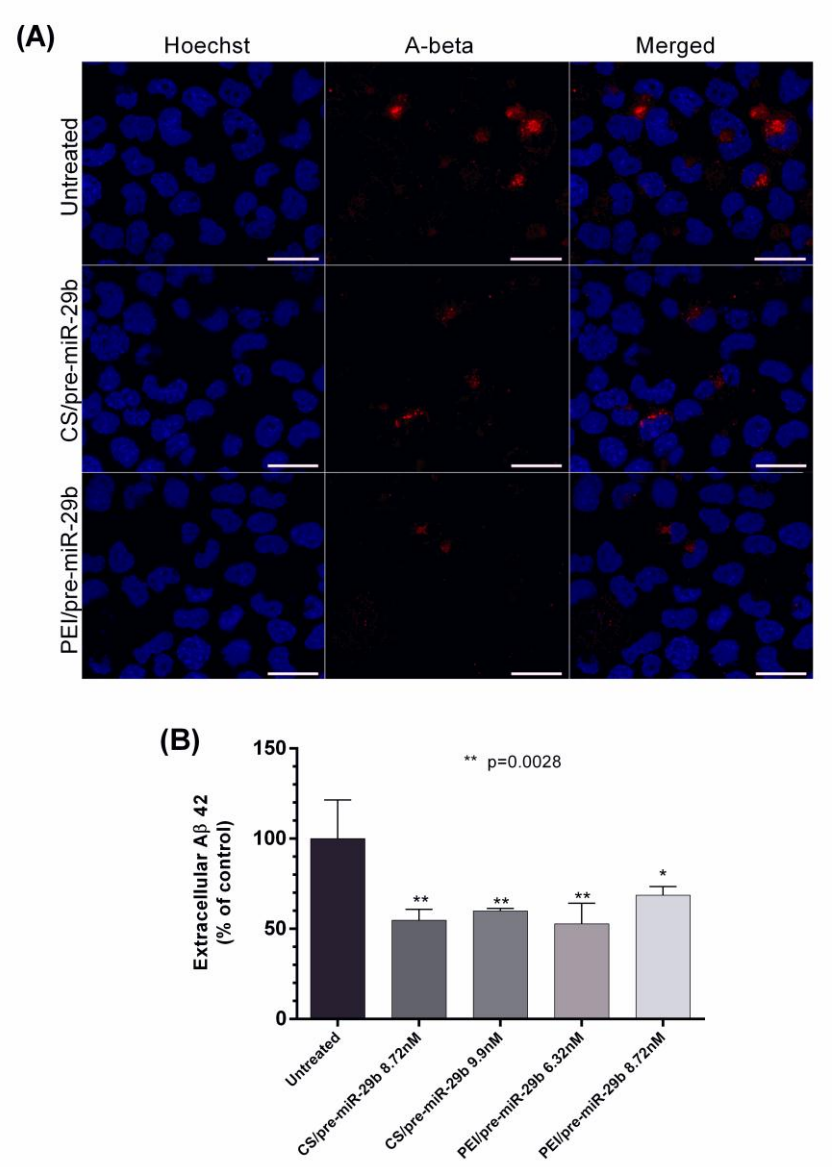

Figure 5 – Effect of recombinant pre-miR-29b on modulation of Aβ levels in N2a695 cells. **(A)** Representative confocal microscopy images of untreated N2a695 cells and cells transfected with CS/pre-miR-29b and PEI/pre-miR-29b stained against $A\beta_{total}$ peptide (scale bars 20μm). **(B)** $A\beta_{42}$ ELISA in cell lysates collected 72 h after transfection with CS/pre-miR-29b and PEI/pre-miR-29b. All results are expressed relative to those in untreated cells and presented as mean values from at least 3 independent experiments. ANOVA, mean±SD.

Thus, to directly examine whether recombinant pre-miR-29b also reduces endogenous $A\beta_{42}$ levels, the N2a695 cells (Fig. 5A) were transfected according to the best transfection conditions mentioned above (CS/pre-miR-29b and PEI/pre-miR-29b at 8.72/9.9 and 6.32/8.72 nM, respectively) to reduce the expression of hBACE1. $A\beta_{42}$ levels in culture medium and in cell lysates were analyzed using ELISA (Fig. 5B). However, it was verified that $A\beta_{42}$ could only be detected in medium but was absent in cell lysate of the transfected cells. As a result,

endogenous $A\beta_{42}$ levels were significantly reduced by 45.2±6.0% and 40.07±1.3% with CS/pre-miR-29b 8.72 and 9.9 nM, respectively. With PEI/pre-miR-29b 6.32 and 8.72 nM, the endogenous $A\beta_{42}$ levels were reduced by 47.2±11.4% and 31.31±4.7%, respectively, when compared to N2a695 untreated cells at 72 h (Fig. 5B). Therefore, endogenous $A\beta_{42}$ levels were inhibited by recombinant pre-miR-29b in this neuronal cell line. Once again, these findings indicate that recombinant pre-miR-29b regulates $A\beta_{42}$ production through mechanisms dependent of hBACE1 expression.

Discussion

BACE1 and Aβ are central players in the pathways implicated in AD, it has been established that reducing BACE1 expression has been suggested as a potential strategy for mitigating the pathological processes underlying AD[25,46]. Interestingly, the miR-29a/b-1/c cluster is significantly decreased in the brains of AD patients, and this decrease is correlated with the increased level of BACE1 protein[16,21]. Previously published studies have demonstrated the importance of using the miR-29 family as a potential major suppressor to silence BACE1 protein expression. However, the success of any therapeutic strategy depends on the development of economic, effective and efficient methods for miRNAs large-scale production (recombinant production using prokaryotic hosts) and purification, as an alternative to in vitro transcription or chemical synthesis[29]. The global interest is to produce high quantities of miRNA but also to obtain and preserve its quality, fulfilling the requirements of regulatory agencies. To accomplish this purpose, we recently described a novel purification methodology based on arginine-affinity chromatography to selectively purify the pre-miR-29b from different RNA species with high recovery yield, purity and good integrity, revealing to be an efficient and reproducible technique to obtain an appropriate RNA quality with potential applicability for transfection studies[29]. Arginine was selected because it is a conserved amino acid of the active center of the PAZ domains of the Argonaute proteins, belonging to the RISC, suggesting that they have an important role in the specific recognition of the 3'UTR of the pre-miRNA[47].

On the other hand, the development of an efficient miRNA delivery system capable to overcome the biological barriers, protect the integrity of miRNA from degradation, promote cellular uptake and, finally, release miRNA in the cytoplasmic compartment is crucial to achieve an improvement in the biological effect in RNAi-based therapies. Hence, according to previous results obtained by our research group[43], we decided to explore the possibility of using polycations-based carrier systems to efficiently deliver the recombinant pre-miR-29b to N2a695 neuronal cell line, to suppress hBACE1 expression. The polyplexes developed have not a significant cytotoxicity effect of on the selected cell line (Fig. 1). An important in vitro experimental approach in this study is the use of a stable N2a695 cell line because in these cells there is a constitutive endogenous hBACE1 expression, enabling greater sensitivity for

evaluating the direct or indirect effect of recombinant pre-miR-29b on the cellular levels of hBACE1 or on the products of its activity (Aβ42 peptides), once in biological systems over-expressing hBACE1 leads to the formation Aβ peptides[20,44,45].

Along with the role that pre-miR-29b plays in the regulation of the BACE1 levels, it was also evaluated the involvement of this miRNA in the functional regulation of the amyloid pathway. As a matter of fact, in this study and for the first time, it was demonstrated that the overexpression of recombinant pre-miR-29b induces a marked decrease in the levels of the protein hBACE1 and, consequently, a significant decrease in the level of the endogenous $A\beta_{42}$. This result suggests that the application of pre-miR-29 lead to a significant decrease in the levels of two major risk factors commonly associated with the neurodegeneration in AD. We further verified that a single treatment with CS/pre-miR-29b or PEI/pre-miR-29b dramatically decreased the amount of hBACE1 expression (suppressed in 78.5±4.5% and 86.1±1.2%, respectively) and the generation of $A\beta_{42}$ peptide (44.2±6.0% and 47.2±11.4%, respectively) by downregulating hBACE1 protein in N2a695 cells (Figs. 2, 3 and 5). These findings reinforce the fact that the ability of recombinant pre-miR-29b to regulate endogenous hBACE1 protein expression is likely direct, because it binds to the 3' UTR of hBACE1 mRNA, complementary to the miR-29b seed region (Fig. 4). Our results demonstrated that hBACE1 mRNA levels were also significantly altered following recombinant pre-miR-29b transfection, suggesting a post-transcriptional mechanism that involves direct degradation/destabilization of hBACE1 mRNA and is likely that it promotes inhibition of hBACE1 protein translation. With these results it was verified that hBACE1 is a direct target of pre-miR-29b (Figs. 2, 3 and 4), which was further validated by the downregulation of hBACE1 gene expression by polycations/pre-miR-29b *in vitro*.

Our findings, together with those from other groups, suggest a fundamental role of miR-29 in AD, and emphasize the potential application of miR-29 in prognosis prediction and AD therapy. With the successful implementation of this methodology and comparing with previously published data (~62% to miR-339-5p[46]; ~35% to miR-29c[21]; ~50% to miR-29a/b-1[16]), we obtained the highest decrease ever reported for the hBACE1 expression levels (around 78% to CS/pre-miR-29b and 86% to PEI/pre-miR-29b) in AD model cells. In addition, it was also verified a decrease of the endogenous $A\beta_{42}$ levels (approximately 44% to CS/pre-miR-29b and 47% to PEI/pre-miR-29b) in these cells. Furthermore, the concentrations of recombinant pre-miR-29b used in this study were much lower than those reported in other works using synthetic miRNA (25 to 250 nM)[16,21], thus a smaller amount of recombinant pre-miR-29b is required to obtain a higher silencing level of hBACE1. In fact, this result may be due to the fact that we are using recombinant pre-miRNA, which is more efficiently recognized and processed within the cell, instead of the mature form of miRNA or the fact that the pre-miRNA was efficiently purified and delivered to the cell through its encapsulation with polycations[48,49].

Our results suggest that recombinant pre-miR-29b can represent a novel biopharmaceutical product for the therapeutic modulation of hBACE1 levels, once this study have new implications for hBACE1 biology and offer a new perspective on the treatment of AD. According to the results obtained in this study, we developed an integrative platform that allows biosynthesis, purification and transfection of the recombinant pre-miR-29b using polyplexes to decrease the hBACE1 and endogenous $A\beta_{42}$ expression levels. In addition, this approach allowed improving the currently available methodologies of miRNA-based therapeutics, not only for neurological disorders but also for future therapeutic targets that may be of potential clinical interest.

Methods

Reagents

CS (Mw = 50–190 kDa) and cell culture reagents were purchased from Sigma–Aldrich. PEI (Mw = 10 kDa) was purchased from Polysciences. (3-(4,5-dimethylthiazol-2-yl)-5-(3-carboxymethoxyphenyl)-2-(4-sulfophenyl)-2H-tetrazolium) (MTS) was obtained from Promega. Anti-human BACE1 and BACE1 peptide (Abcam); anti-β-actin and monoclonal anti-β-Amyloid (Sigma-Aldrich); Hoechst 33342®, AlexaFluor 488® and AlexaFluor 546® (Invitrogen); Goat anti-rabbit/mouse IgG-HRP (Santa Cruz Biotechnology) were used.

Pre-miR-29b biosynthesis and purification by arginine affinity chromatography

The pre-miR-29b used in the experiments was produced in a bacterial cell culture of *Rhodovulum sulfidophilum* DSM 1374 strain (BCCM/LMG, Belgium) modified with the plasmid pBHSR1-RM containing the sequence of pre-miR-29b, as previously described by Pereira and collaborators[29]. Then, the pre-miR-29b isolation was achieved using arginine as a specific ligand in affinity chromatography[29]. The endotoxins content was also evaluated by using the ToxinSensorTM Chromogenic Limulus Amoebocyte Lysate assay kit (GenScript), being verified a considerably reduction during the chromatographic process, since the sample injected onto the arginine matrix had 0.164 EU/μg of sRNA and the final pre-miR-29b fraction presented 0.002 EU/μg of pre-miR-29b. Thus, the endotoxins level in the final pre-miR-29b sample conforms the guidelines of regulatory agencies like Food and Drug Administration (<0.06 EU/mL for the cerebrospinal fluid). In addition, the PCR product corresponding to the purified pre-miR-29b was sequenced to confirm the identity and orientation of the amplicon (Figure S1 in Supporting Information).

Formulation of polyplexes

Briefly, all the pre-miR-29b loaded polyplexes were formulated using the method of simple complexation which is based on the electrostatic interactions that occur between molar concentrations of positive charge, present in the protonated amine groups of each polycation (N), and the negative charge of the phosphate groups of RNA backbone (P), as described by

Pereira and co-workers[41]. The pre-miR-29b (a final concentration of 2 μg/mL) and polycation (a concentration of 10 mg/mL) stock solutions were prepared in sodium acetate buffer (0.1 M sodium acetate/0.1 M acetic acid, pH 4.5). In order to promote encapsulation, cationic polymer solution (100 μL) was added dropwise to the pre-miR-29b solution (400 μL), under stirring during 30 s, to particle formation[41]. The PEI/pre-miR-29b molar ratio is 0.35:1 (mol/mol) and the CS/pre-miR-29b molar ratio is 3:1 (mol/mol). The formulated polyplexes were incubated at RT for 30 min and then pelleted by centrifugation at 15000 g for 20 min. The amount of unbound pre-miR-29b was quantified by UV spectrophotometry[41]. Thus, the encapsulation efficiency (EE) was determined using the following formula: EE%=[(Total pre-miRNA amount – pre-miRNA supernatant amount)/Total pre-miRNA amount] x 100. Three repetitions of this procedure were performed for each system. The hydrodynamic diameter and zeta potential of the pre-miR-29b-loaded polyplexes were determined by dynamic light scattering (DLS) using a Zetasizer Nano ZS particle analyzer (Malvern Instruments, Worcestershire, UK), equipped with a He-Ne laser, at 25ºC. For DLS analysis particle samples were produced as before mentioned and ressuspended in ultrapure water. Size characterization was performed in fully automatic mode and with a scattering angle of 173°. Particle zeta potential measurements were performed in disposable capillary cells and computed by using Henry's [F(Ka) 1.5], and Smoluchowsky models. All the data was examined in Zetasizer software v 7.03. The experiments were performed in triplicate and an average of 30 measurements was acquired individually for each sample. As a positive control, Lipofectamine 2000 transfection reagent was used (Lipo/pre-miR-29b), according to the protocol recommended by the manufacturer.

Transfection of N2a695 cells with polyplexes/pre-miR-29b

N2a695 cells at passages 5-27 were cultured in the following medium: 1:1 mixture of Dulbecco's modified Eagle's medium (DMEM) and OptiMEM supplemented with 5% (wt/vol) heat-inactivated FBS and 1% (wt/vol) penicillin–streptomycin[48]. N2a695 cells were seeded at 3×10^4 cells/mL. When a 50 to 60% confluence was achieved, the culture medium was replaced by serum-free medium. After 12 h, CS/pre-miR-29b, PEI/pre-miR-29b and Lipofectamine/pre-miR-29b (Lipo/pre-miR-29b) were added to the cells at pre-miR-29b concentration of 3.84 to 9.9 nM and transfection was carried out during 6 h. The culture medium was replaced by fresh medium supplemented with 1% FBS and 1% antibiotic, to allow the cells to remain metabolically active, expressing hBACE1 and Aβ. Untreated cells and cells transfected with an unrelated RNA (5'-UGUGCAAAUCUAUGCAAAACUGA-3′) were used for negative controls (at a final concentration of 9.9 nM). In addition, cells were also transfected with scrambled miRNA (5′-UUCUCCGAACGUGUCACGUTT-3′; 3′-TTAAGAGGCUUGCACAGUGCA-5′) and a synthetic miR-29b in the mature form (5′-UAGCACCAUUUGAAAUCAGUGUU-3´) using CS, as controls (at a final concentration of 9.9 nM). The cells were harvested 24, 48 and 72 h after transfection. All transfection experiments were performed in triplicate.

MTS assay

The cellular cytotoxicity effect of the different formulations of polyplexes (CS and PEI/pre-miR-29b) was evaluated using the Cell Titer 96® AQueous Non-Radioactive Cell Proliferation Assay. Briefly, N2a695 cells were seeded at a density of 2×10^4 cells per well in a 96-well plate, 24 h after the cell culture medium was replaced by serum-free culture medium. Cells were then transfected as described above and the MTS assay was performed at different time points (48 and 72 h). Subsequently, the medium was exchanged, a mixture of MTS/phenazine metasulfate (PMS) was added to each well, and cells were incubated during 4 h at 37ºC in a humidified atmosphere containing 5% CO_2. Following incubation, the absorbance measurements of the soluble brown formazan produced were performed in a microplate reader (Sanofi, Diagnostics Pauster) at 492 nm. All experiments were repeated at least three times. Cells incubated with absolute ethanol were used as positive control for cytotoxicity.

Immunocytochemistry and Imaging Analysis

N2a695 cells were seeded on glass coverslips into 12-well plates, to be recovered at 24, 48 and 72 h. After transfection with either Lipofectamine 2000 or polyplexes, the cells were fixed for 10 min at RT with 4% paraformaldehyde (PFA) buffer solution, followed by permeabilization with 0.1% Triton X-100 for 5 min. Cell preparations were blocked for 1 h at RT with 20% FBS in PBS-Tween 20 (PBS-T). The cells were then incubated overnight at 4ºC with the primary anti-hBACE1 polyclonal antibody (1:100) and anti-$A\beta_{17-24}$ monoclonal antibody (1:1000). Then, cells were washed 6 times with PBS-T and incubated for 1 h at RT with the appropriate fluorescence conjugated secondary antibodies AlexaFluor 488® goat anti-rabbit or AlexaFluor 546® goat anti-mouse. After washing, the nucleus were counterstained with Hoechst 33342® (1:1000) for 10 min followed by 3 washing steps with PBS-T. Glass coverslips were mounted on slides and the preparations were visualized under a Zeiss LSM 710 laser scanning confocal microscope (Carl Zeiss SMT Inc., USA) equipped with a plane-apocromat 63×/DIC objective. Images were processed and analyzed using ImageJ software.

Western blot Analysis

Cells were rinsed in ice-cold PBS and homogenized in cell lysis buffer: 25 mM Tris-HCl buffer, pH 7.4; 2.5 mM EDTA; 1% Triton X-100; 2.5 mM EGTA; 25 mM phenylmethylsulfonyl fluoride and complete EDTA Free protease inhibitor cocktail (Roche). Once homogenized, cell extracts were centrifuged at 11500 rpm for 7 min at 4ºC. The total protein concentration in the supernatant was determined using Bradford Protein Assay (BioRad) and 50 µg of total protein from each cell extract were boiled for 10 min in reducing buffer and then fractionated by electrophoresis on 10% SDS-PAGE. After, proteins were transferred to polyvinylidene difluoride filter (PVDF) membranes and blocked with TBS-T (200 mM Tris-HCl, pH 7.4; 1.37 M NaCl; 0.1% Tween 20) supplemented with 5% BSA. Following, membranes were probed with primary antibodies recognizing the hBACE1 (1:1000 in 5% BSA in TBS-T) and β-actin (1:20000 in

TBS-T) at 4ºC overnight. After three washes with TBS-T, membranes were incubated with the HRP-labeled anti-rabbit/mouse IgG secondary antibody diluted 1:50000, followed by three washes with TBS-T. Signal detection was performed with ECL substrate (BioRad) according to manufacturer's instructions and images were acquired with the ChemiDoc™ XRS system (BioRad) and analysed with the Image Lab (BioRad).

Expression of BACE1 mRNA in N2a695 cells by RT-qPCR

Total RNA was extracted from the cells using TRIzol reagent (Invitrogen). 1 µg of total RNA was reverse transcribed using the RevertAid First Strand cDNA Synthesis Kit (Thermo Fisher Scientific Inc.), according to the manufacturer's instructions. For quantitative analysis, RT-qPCR amplification of cDNA was performed using the Maxima® SYBR Green/Fluorescein qPCR Master Mix (Thermo Fisher Scientific Inc.) in an IQ5 Cycler from BioRad. RT-qPCR efficiencies were calculated from the given slopes with MyIQ 2.0 software (BioRad). The relative quantification of the BACE1 expression was based on the comparative threshold cycle (C_T) method in which the amount of the target was determined to be $2^{-(\Delta CT \text{ target} - \Delta CT \text{ calibrator})}$, normalized to levels of glyceraldehyde-3-phosphate dehydrogenase (GAPDH) and relative to the untreated control cells. The primers used in these experiments were 5'-AGACGCTCAACATCCTGGTG-3' (forward) and 5'-CCTGGGTGTAGGGCACATAC-3' (reverse) for the amplification of human BACE (hBACE) and 5'- TGACGTGCCGCCTGGAGAAA-3' (forward), 5'-AGTGTAGCCCAAGATGCCCTTCAG-3' (reverse) for the amplification of GAPDH. Each sample was run in triplicate, and threshold cycle (C_T) values were averaged from the triplicate. The final data were averaged from 3 separately conducted experiments.

Sandwich enzyme-linked immunosorbent assay (ELISA)

The endogenous $A\beta_{42}$ levels were quantified in the culture medium and in total cell lysates using ELISA (Invitrogen), according to the manufacturer's instructions. Total cell lysates were performed as described for Western blot and the culture medium was centrifuged at 13000 rpm for 1 min to remove cell debris. Total cell lysates and culture medium were diluted 1:10 and $A\beta_{42}$ concentrations were detected with an ELISA (Invitrogen), according to the manufacturer's instructions. The results were expressed as referred to dilutions of standard synthetic control peptides. In addition, absolute $A\beta_{42}$ values (pg/ml) were measured and normalized to total protein yield of crude cell lysates.

Statistical analysis

All experiments were repeated at least three times using independent culture preparations. Data in the figures are expressed as mean ± standard error. Quantitative data were statistically analyzed by one-way analysis of variance (ANOVA), followed by pair-wise comparisons using the Fisher's least significant difference test. * indicate significant difference versus untreated cells, # indicate significant difference versus cells transfected with unrelated RNA control and ● indicate significant difference between samples, being

considered statistically significant for $p<0.05$. Statistical analysis was performed by using GraphPad Prism 6 software.

Acknowledgments

This work was supported by the Portuguese Foundation for Science and Technology (FCT), through the project EXPL/BBB-BIO/1056/2012 and Pest-OE/SAU/UI0709/2014. Patrícia Pereira acknowledges the fellowship (Ph.D. Grant, Ref SFRH/BD/81914/2011), from FCT. Joana Tomás also acknowledges the fellowship in the ambit of the project CENTRO-07-ST24-FEDER-002015. The authors also acknowledge the program Fundo Europeu de Desenvolvimento Regional (FEDER) [COMPETE [FCOMP-01-0124-FEDER-027560]]. The authors would like to thank Professor Yo Kikuchi (Division of Life Science and Biotechnology, Department of Ecological Engineering, Toyohashi University of Technology) for kindly provided of pBHSR1-RM plasmid, Prof. Wenjie Luo and Professor Cecília Santos for the kind contribution regarding the cell line N2a695 and, finally, Professor Manuel Lemos and Eduarda Coutinho for your help in sequencing.

Author's contributions

PP carried out all the experimental procedures and wrote the manuscript. PP, JT and FS conceived and designed the study. JT helped to perform the experimental procedures. All the authors contributed to the drafting of the manuscript and were responsible for the revision.

Additional information

Competing financial interests: The authors declare no competing financial interests.

References

1. Broderick, J. A.; Zamore, P. D. MicroRNA therapeutics. *Gene Ther* **18**, 1104-10 (2011)

2. Bartels, C. L.; Tsongalis, G. J. MicroRNAs: novel biomarkers for human cancer. *Clinical chemistry* **55**, 623-31 (2009)

3. Selbach, M., et al. Widespread changes in protein synthesis induced by microRNAs. *Nature* **455**, 58-63 (2008)

4. Ambros, V. The functions of animal microRNAs. *Nature* **431**, 350-5 (2004)

5. He, L.; Hannon, G. J. MicroRNAs: small RNAs with a big role in gene regulation. *Nat Rev Genet* **5**, 522-31 (2004)

6. Bartel, D. P. MicroRNAs: genomics, biogenesis, mechanism, and function. *Cell* **116**, 281-97 (2004)

7. Bartel, D. P. MicroRNAs: target recognition and regulatory functions. *Cell* **136**, 215-33 (2009)

8. Chen, F.; Hu, S. J. Effect of microRNA-34a in cell cycle, differentiation, and apoptosis: a review. *Journal of biochemical and molecular toxicology* **26**, 79-86 (2012)

9. Plaisier, C. L.; Pan, M.; Baliga, N. S. A miRNA-regulatory network explains how dysregulated miRNAs perturb oncogenic processes across diverse cancers. *Genome research* **22**, 2302-14 (2012)

10. Jiang, H.; Zhang, G.; Wu, J. H.; Jiang, C. P. Diverse roles of miR-29 in cancer (review). *Oncology reports* **31**, 1509-16 (2014)

11. Wu, Z.; Huang, X.; Zou, Q.; Guo, Y. The inhibitory role of Mir-29 in growth of breast cancer cells. *Journal of experimental & clinical cancer research : CR* **32**, 98 (2013)

12. Xiong, Y., et al. Effects of microRNA-29 on apoptosis, tumorigenicity, and prognosis of hepatocellular carcinoma. *Hepatology* **51**, 836-45 (2010)

13. Li, Y., et al. Progressive miRNA expression profiles in cervical carcinogenesis and identification of HPV-related target genes for miR-29. *The Journal of pathology* **224**, 484-95 (2011)

14. Fabbri, M., et al. MicroRNA-29 family reverts aberrant methylation in lung cancer by targeting DNA methyltransferases 3A and 3B. *Proc Natl Acad Sci U S A* **104**, 15805-10 (2007)

15. Jiao, J.; Herl, L. D.; Farese, R. V.; Gao, F. B. MicroRNA-29b regulates the expression level of human progranulin, a secreted glycoprotein implicated in frontotemporal dementia. *PloS one* **5**, e10551 (2010)

16. Hebert, S. S., et al. Loss of microRNA cluster miR-29a/b-1 in sporadic Alzheimer's disease correlates with increased BACE1/beta-secretase expression. *Proc Natl Acad Sci U S A* **105**, 6415-20 (2008)

17. Satoh, J. MicroRNAs and their therapeutic potential for human diseases: aberrant microRNA expression in Alzheimer's disease brains. *J Pharmacol Sci* **114**, 269-75 (2010)

18. Kocerha, J.; Kauppinen, S.; Wahlestedt, C. microRNAs in CNS disorders. *Neuromolecular medicine* **11**, 162-72 (2009)

19. Hebert, S. S., et al. MicroRNA regulation of Alzheimer's Amyloid precursor protein expression. *Neurobiology of disease* **33**, 422-8 (2009)

20. Bettens, K., et al. APP and BACE1 miRNA genetic variability has no major role in risk for Alzheimer disease. *Hum Mutat* **30**, 1207-13 (2009)

21. Zong, Y., et al. miR-29c regulates BACE1 protein expression. *Brain Res* **1395**, 108-15 (2011)

22. Dominguez, D. I.; Hartmann, D.; De Strooper, B. BACE1 and presenilin: two unusual aspartyl proteases involved in Alzheimer's disease. *Neuro-degenerative diseases* **1**, 168-74 (2004)

23. Cole, S. L.; Vassar, R. The Alzheimer's disease beta-secretase enzyme, BACE1. *Molecular neurodegeneration* **2**, 22 (2007)

24. Schonrock, N.; Matamales, M.; Ittner, L. M.; Gotz, J. MicroRNA networks surrounding APP and amyloid-beta metabolism-implications for Alzheimer's disease. *Experimental Neurology* **235**, 447-454 (2012)

25. Hunt, C. E.; Turner, A. J. Cell biology, regulation and inhibition of beta-secretase (BACE-1). *FEBS J* **276**, 1845-59 (2009)

26. Ponchon, L.; Dardel, F. Large scale expression and purification of recombinant RNA in *Escherichia coli*. *Methods* **54**, 267-73 (2011)

27. Sherlin, L. D., et al. Chemical and enzymatic synthesis of tRNAs for high-throughput crystallization. *RNA* **7**, 1671-8 (2001)

28. Martins, R.; Queiroz, J. A.; Sousa, F. Ribonucleic acid purification. *J Chromatogr A* **1355**, 1-14 (2014)

29. Pereira, P., et al. Purification of pre-miR-29 by arginine-affinity chromatography. *J Chromatogr B Analyt Technol Biomed Life Sci* **951-952**, 16-23 (2014)

30. Pecot, C. V.; Calin, G. A.; Coleman, R. L.; Lopez-Berestein, G.; Sood, A. K. RNA interference in the clinic: challenges and future directions. *Nat Rev Cancer* **11**, 59-67 (2011)

31. Lee, S. Y., et al. Stability and cellular uptake of polymerized siRNA (poly-siRNA)/polyethylenimine (PEI) complexes for efficient gene silencing. *J Control Release* **141**, 339-46 (2010)

32. Nimesh, S.; Chandra, R. Polyethylenimine nanoparticles as an efficient *in vitro* siRNA delivery system. *Eur J Pharm Biopharm* **73**, 43-9 (2009)

33. Kwok, A.; Hart, S. L. Comparative structural and functional studies of nanoparticle formulations for DNA and siRNA delivery. *Nanomedicine : nanotechnology, biology, and medicine* **7**, 210-9 (2011)

34. Grayson, A. C.; Doody, A. M.; Putnam, D. Biophysical and structural characterization of polyethylenimine-mediated siRNA delivery *in vitro*. *Pharmaceutical research* **23**, 1868-76 (2006)

35. Lungwitz, U.; Breunig, M.; Blunk, T.; Gopferich, A. Polyethylenimine-based non-viral gene delivery systems. *Eur J Pharm Biopharm* **60**, 247-66 (2005)

36. Sarvaiya, J.; Agrawal, Y. K. Chitosan as a suitable nanocarrier material for anti-Alzheimer drug delivery. *International journal of biological macromolecules* **72**, 454-65 (2015)

37. Howard, K. A., et al. RNA interference *in vitro* and *in vivo* using a novel chitosan/siRNA nanoparticle system. *Molecular therapy: the journal of the American Society of Gene Therapy* **14**, 476-84 (2006)

38. Holzerny, P., et al. Biophysical properties of chitosan/siRNA polyplexes: profiling the polymer/siRNA interactions and bioactivity. *J Control Release* **157**, 297-304 (2012)

39. Rudzinski, W. E.; Aminabhavi, T. M. Chitosan as a carrier for targeted delivery of small interfering RNA. *International journal of pharmaceutics* **399**, 1-11 (2010)

40. Mao, S.; Sun, W.; Kissel, T. Chitosan-based formulations for delivery of DNA and siRNA. *Advanced drug delivery reviews* **62**, 12-27 (2010)

41. Pereira, P., et al. Characterization of polyplexes involving small RNA. *J Colloid Interface Sci* **387**, 84-94 (2012)

42. Godbey, W. T.; Wu, K. K.; Mikos, A. G. Size matters: molecular weight affects the efficiency of poly(ethylenimine) as a gene delivery vehicle. *Journal of biomedical materials research* **45**, 268-75 (1999)

43. Godbey, W. T.; Wu, K. K.; Mikos, A. G. Poly(ethylenimine) and its role in gene delivery. *J Control Release* **60**, 149-60 (1999)

44. Chen, Y., et al. Antidiabetic drug metformin (GlucophageR) increases biogenesis of Alzheimer's amyloid peptides via up-regulating BACE1 transcription. *Proc Natl Acad Sci U S A* **106**, 3907-12 (2009)

45. Kobayashi, D., et al. BACE1 gene deletion: impact on behavioral function in a model of Alzheimer's disease. *Neurobiology of aging* **29**, 861-73 (2008)

46. Long, J. M.; Ray, B.; Lahiri, D. K. MicroRNA-339-5p down-regulates protein expression of beta-site amyloid precursor protein-cleaving enzyme 1 (BACE1) in human primary brain cultures and is reduced in brain tissue specimens of Alzheimer disease subjects. *J Biol Chem* **289**, 5184-98 (2014)

47. Rivas, F. V., et al. Purified Argonaute2 and an siRNA form recombinant human RISC. *Nat Struct Mol Biol* **12**, 340-9 (2005)

48. Tsutsumi, A.; Kawamata, T.; Izumi, N.; Seitz, H.; Tomari, Y. Recognition of the pre-miRNA structure by Drosophila Dicer-1. *Nat Struct Mol Biol* **18**, 1153-8 (2011)

49. Li, M. M.; Wang, W. P.; Wu, W. J.; Huang, M.; Yu, A. M. Rapid production of novel pre-microRNA agent has-mir-27b in *Escherichia coli* using recombinant RNA technology for functional studies in mammmalian cells. Drug Metab Dispos **42**, 1791-1794 (2014)

Supporting Information

Figure S1 - Sequencing of the pre-miR-29b.

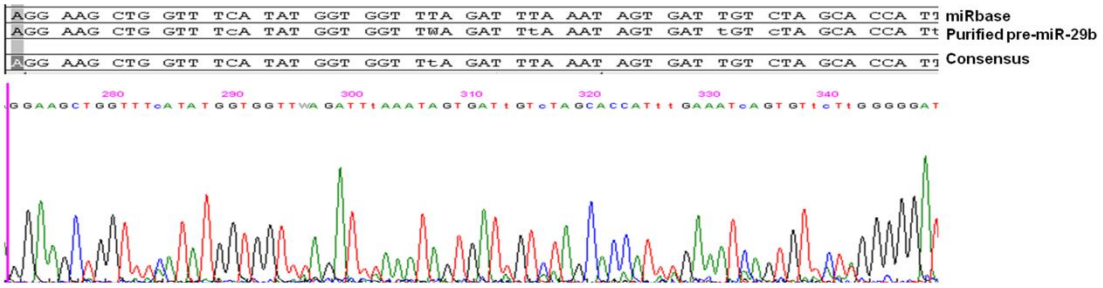

Paper X

Brain-targeting study of lactoferrin-stearic acid–Chitosan/Polyethylenimine pre-miR-29b-delivery system

P. Pereira, J. Tomás, C. Cruz, C. Santos, J. A. Queiroz, A. Figueiras, F. Sousa

(*In preparation*)

Short description: In view of the promising results previously obtained, it was necessary to develop a carrier that can cross the BBB and deliver efficient and effectively the recombinant pre-miR-29b to the brain. Thus, in this paper, the nanodevices of CS and PEI were functionalized with specific ligands, namely lactoferrin which is recognized by cell surface receptors of BBB and stearic acid which has emerged as an optimal ligand for targeting the cell membrane allowing nanoparticle endocytosis, for higher transfection yields. To observe the cellular uptake of nanodevices, cell live imaging was applied. *Ex vivo* permeation studies in brain barrier models were performed in transwell cell culture systems, in order to evaluate the delivery efficiency of the vector to the brain. Moreover, additional studies were carried out using *in vitro* models of the blood-CSF barrier (namely, Z310 cells) and BBB (Rat brain endothelial cells (RBE4) cells).

Brain-targeting study of lactoferrin-stearic acid–Chitosan/Polyethylenimine pre-miR-29b-delivery system

P. Pereira[1], J. Tomás[1], C. Cruz[1], C. Santos[1], J.A. Queiroz[1], A. Figueiras[1,2], F. Sousa[1]

[1]CICS-UBI – Health Sciences Research Centre, University of Beira Interior, Avenida Infante D. Henrique, Covilhã, 6200-506, Portugal;

[2]CNC – Center of Neuroscience and Cell Biology, University of Coimbra, Largo Marquês de Pombal, Coimbra, 3004-517, Portugal

*Corresponding author:
Dr. Fani Sousa
Phone: +351 275 329 074
Fax: +351 275 329 099
E-mail address: fani.sousa@fcsaude.ubi.pt
Postal address: Health Sciences Research Centre, Universidade da Beira Interior, Avenida Infante D. Henrique, 6200-506 Covilhã, Portugal

Abstract

The aim of the present study is to develop nanocarriers for targeted pre-miR-29b delivery across the Blood-Brain Barrier (BBB), to reach neuronal cells and inhibit the BACE1, with potential implications in Alzheimer's disease treatment. A dual-targeting drug delivery system (Chitosan (CS) or Polyethylenimine (PEI) conjugated with stearic acid (SA) and lactoferrin (Lf)) was synthesized and its BBB penetration was evaluated. Stearic acid and lactoferrin were successfully exploited as brain-targeting ligands to modify cationic polymers. The intracellular uptake of the delivery systems by neuronal cells was studied *in vitro* as well as the gene silencing efficiency of pre-miR-29b. The CS/PEI-SA-Lf systems showed very strong fluorescence in the cytoplasm and cell nucleus, and were able to deliver pre-miR-29b to N2a695 cells in 1 hour after transfection. The experiment of transport across the BBB showed that CS-SA-Lf delivered 65% of recombinant pre-miR-29b in a period of 4 hours, an higher transport ratio than the 42% found for PEI-SA-Lf in the same time. The results indicate that CS-SA-Lf can be a potential pre-miR-29b carrier for AD therapy.

Keywords

Alzheimer's disease; hBACE1; Chitosan; Polyethylenimine; Blood-Brain-Barrier; Recombinant pre-miR-29b; Lactoferrin; Stearic Acid

1. Introduction

Alzheimer's disease (AD) is the most common and devastating form of dementia in the elderly and can lead to death within 3 to 9 years after appearance of symptoms [1]. AD is pathologically characterized by the progressive neuronal loss, mainly due to the accumulation of extracellular amyloid plaques consisting of aggregates of toxic amyloid-beta (Aβ) peptides [2-4]. They are generated through sequential proteolytic cleavage of the amyloid precursor protein (APP) by β-secretase (also known as β-site APP-cleaving enzyme 1 (BACE1)) and γ-secretase, which play a pivotal role in the dysfunction and death of neurons [5-7]. Several convincing evidences suggest that the regulation of expression of proteins involved in the generation and accumulation of Aβ peptides can be extremely important in AD, since Aβ peptides play the central role in initiating and development of the pathological cascade of AD [4, 5, 8, 9]. In the last years, several research groups demonstrated that the levels and activity of BACE1 protein are elevated in sporadic AD brains, suggesting that BACE1 dysregulation is directly implicated in AD pathogenesis. For these reasons, BACE1 has been recognized as a promising drug target for the therapy of this disease, once BACE1 inhibition may decrease the formation of all forms of Aβ peptides in AD and, consequently, reduce cell death [10-12]. On the other hand, significant alterations in the expression of miR-29 family, in brains of AD patients, have been observed in most of studies [13, 14], being significantly decreased and displaying abnormally high levels of BACE1 protein. These findings raised the opportunity to use miR-29 as a possible protective therapeutic strategy for the future of AD therapy. The continued lack of progress in identifying effective diagnosis and treatment modalities also contributes to higher health care costs and social burdens that are associated with this disease [15-17].

One of the reasons limiting the development of therapies for AD is the existence of a physical barrier, the Blood-Brain Barrier (BBB), which hinders the passage of most of the therapeutic drugs from the circulating blood to the brain [18]. The BBB prevents the entry of harmful substances present in the systemic blood circulation into the brain, but allows the access of necessary nutrients and chemical signaling molecules, making of the brain a place of poor permeability to various drugs [19-22]. Its function is related to the structural characteristics, once the BBB is composed by tight intracellular junctions formed between adjacent brain capillary endothelial cells [19]. On the other hand, the BBB possesses a variety of efflux transporters, including P-glycoprotein [23], receptors for transferrin [24, 25], lactoferrin [26], insulin [27], insulin-like growth factors [28], lipoprotein receptor-related protein (LRP) [29, 30], as well as, transmembrane monocarboxylic acid transporters and fatty acid transport proteins [31], reinforcing BBB function by effectively removing drugs from the brain and pumping them back into blood.

As a result, it is strictly necessary the development of methods that promote the delivery of therapeutic drugs to the brain, safely and effectively. During the last decade, several non-

viral vectors were developed for brain targeting, including polymers (e.g. polyethyleneimine (PEI), chitosan (CS), poly(lactic-co-glycolic acid) (PLGA), poly lactic acid (PLA)), polymeric micelles, liposomes and dendrimers [32-37]. Among the vectors mentioned above, polymeric delivery systems (polyplexes) have emerged as one of the most attractive carriers to cross the BBB and increase the uptake of appropriate drugs by the brain. To accomplish this, the receptors existing on the BBB have been explored as a means to specifically target drugs to the brain. This can be achieved through the surface modification of delivery systems with a ligand (such as transferrin (Tf), lactoferrin (Lf), stearic acid (SA)) targeting to the receptor, which facilitates drug ability to interact with specific molecules expressed on the luminal side of BBB endothelial cells [38]. In the present study, the recombinant human pre-miR-29b was chosen as the therapeutic gene to be encapsulated in the polyplexes (CS or PEI) modified with Lf and SA in the surface, to bind specifically to the Lf receptors on neuronal cells, through a receptor-mediated pathway.

CS and PEI have gained much attention as delivery systems due to their advantageous properties such as, ability to encapsulate large amounts of drug, high stability in biological fluids, targeting ability, rapid cellular uptake, high transfection efficiency, biocompatibility, biodegradability, low cytotoxicity and immunogenicity, and reduced side effects by targeted delivery [39-41]. In addition, the cationic charge of CS and PEI, due to the presence of amino groups, allows the establishment of electrostatic interactions with the negatively charged RNAs, leading to an effective condensation and protection of the integrity of the RNA. In fact, the encapsulation of RNAs prevents non-specific interactions and enzymatic degradation, increasing the drug circulation in blood [39-41].

Lf is a single chain iron-binding glycoprotein that belongs to the Tf family. Its concentration in the blood plasma is low but is higher in BBB [42, 43]. Recent studies reported that the transport of Lf across the BBB monolayer model was unidirectional and that there was a strong affinity of positively charged Lf to Lf receptor, resulting in higher uptake of Lf-conjugated drug delivery systems to the brain comparing to Tf-modified NPs [26, 44]. For all these reasons, Lf has been exploited as a promising brain-targeting ligand, facilitating drug delivery into the brain. A previous study also described the ability of CS-SA for the delivery of drugs into the brain and to avoid recognition by P-glycoprotein system, yielding an efficient brain-targeting gene vector [38]. Thus, in the current study, it was explored the potential of the polyplexes CS and PEI combined with two targeting substances, Lf and SA, to encapsulate recombinant pre-miR-29b, and act as a brain-targeting delivery system. Various measurements, including ^{1}H NMR and SDS-PAGE, were used to characterize and confirm the structure of the modified polyplexes. The properties of the polyplexes CS-SA, CS-SA-Lf, PEI-SA and PEI-SA-Lf, such as the ability of transport across BBB model, the targeting effects, *in vitro* cell uptake and transfection studies were performed on N2a695, RBE4 and Z310 cells. The efficacy of these systems was finally monitored by examining the induced BACE1 inhibition.

2. Materials and Methods

2.1. Materials

Arginine–Sepharose 4B gel was acquired from Amersham Biosciences. All buffers used for the chromatographic experiments were freshly prepared with 0.05% diethyl pyrocarbonate (DEPC) treated water and were filtered through a 0.20 μm pore size membrane. Sodium chloride (NaCl) was purchased from Panreac and tris(hydroxymethyl) aminomethane (Tris) from Sigma-Aldrich. CS low molecular weight (LMW) (Mw=50–190 kDa; degree of deacetylation in the 75–85% range), Stearic acid Grade I (98.5%), Lactoferrin human, 2-Iminothiolane hydrochloride (2-IOT, 98%), 1-ethyl-3-(3-dimethylaminopropyl) carbodiimide (EDC) and all cell culture media and reagents used in cell culture procedures were purchased from Sigma–Aldrich, unless otherwise noted. PEI high molecular weight (HMW) (Mw=10 kDa) was acquired from Polysciences, Inc. (Warrington, PA). Fluorescein isothiocyanate isomer I (FITC), Hoechst 33342® and AlexaFluor 488® were obtained from Invitrogen (Carlsbad, CA, US). Mouse neuroblastoma (N2a) cells stably transfected with cDNAs encoding human APP695 (N2a695) were kindly provided by Professor Wenjie Luo (Weill Cornell Medical College). The rat brain microvascular endothelial cell line (RBE4) was provided as a gift by the laboratory of Dr. M. Aschner (Department of Pediatrics, Vanderbilt Kennedy Center, Nashville, Tennessee).

2.2. Methods

2.2.1. Synthesis and characterization of PEI and CS polyplexes conjugated with SA and Lf

The conjugation of PEI or CS to SA and Lf (designated as CS-SA-Lf and PEI-SA-Lf) was performed as previously reported by Xie and co-workers [38], with minor modifications. In brief, first, SA (2.5 mg) and EDC (25 mg, at a ratio 1:10) were dissolved in 1.0 mL anhydrous DMSO and stirred at 60ºC for 1 hour, until EDC and SA were well-dissolved and mixed. The resulting mixture (SA:EDC) was then added slowly to 1% (w/v) of CS-LMW and PEI-HMW in sodium acetate buffer (0.1 M sodium acetate/0.1 M acetic acid, pH 4.5) and the reaction solution was kept at room temperature in the dark during 24 hours, with stirring in a water bath. The amine group on PEI or CS was crosslinked with the carboxylic group of stearic acid by EDC as linker. Posteriorly, the resulting conjugate, CS/PEI-SA, was dialyzed first against phosphate buffered saline (PBS, pH 7.4) for 1 day and then against double deionized water for 2 days, using dialysis membrane (SnakeSkinTM Dialysis Tubing, MWCO 3500 Da, 22mm dry diameter, ThermoScientific). The conjugated CS/PEI-SA was isolated as a “sponge” by lyophilization, and was further characterized by ^{1}H Nuclear Magnetic Resonance (NMR) spectroscopy. All proton NMR spectra were recorded in solution of studied compounds in D_2O using a Bruker Avance III 600 MHz equipped with a QCI cryoprobe. For the preparation of CS/PEI-SA-Lf, Lf (10 mg) was dissolved in 1.0 mL aqueous solution of water and mixed with 0.5 mL aqueous solution of 2-iminothiolane hydrochloride (2-IOT, 0.7 mg) and the reaction proceed for 1 hour at room temperature, with moderate shaking. The excess of 2-IOT was removed through a column of Sephadex G 100 column (Hitrap desalting column) using PBS 1x (pH 7.0) as elution buffer. Fractions were collected according to the chromatogram obtained

by analysis of the absorbance (a peak contains about 90% of thiolated Lf) [45]. Subsequently, CS-SA or PEI-SA were dissolved in 0.5 mL PBS (pH 7.0) and then added to the PBS solution of Lf, drop by drop, for 20 hours at room temperature, in the dark. To remove unreacted Lf, the resulting mixtures were purified by dialysis (SnakeSkinTM Dialysis Tubing, MWCO 3500 Da, 22mm dry diameter, ThermoScientific) during 4 days against double deionized water and freeze dried, for further usage. The SDS-PAGE was used to characterize the carriers CS-SA-Lf and PEI-SA-Lf.

2.2.2. Formulation and characterization of CS-SA-Lf/pre-miR-29b, PEI-SA-Lf/pre-miR-29b, CS-SA/pre-miR-29b and PEI-SA/pre-miR-29b complexes

For all experiments, the human pre-miR-29b was obtained from a bacterial cell culture of *Rhodovulum sulfidophilum* DSM 1374 strain (BCCM/LMG, Belgium) modified with the plasmid pBHSR1-RM containing the sequence of pre-miR-29b. The growth was performed in a semi-defined medium containing 30 µg/mL Kanamycin. After biosynthesis, the recombinant pre-miR-29b was recovered from a complex mixture of small RNAs, through affinity chromatography by using a column of arginine, as previously described by Pereira and collaborators [46]. The quantity and quality of the purified pre-miR-29b was assessed by measuring its optical density at 260 nm and 280 nm and by polyacrylamide electrophoresis, respectively. Recombinant pre-miR-29b was covalently labeled with the fluorescent dye, FITC, when necessary. PEI-SA-Lf/pre-miR-29b, PEI-SA-Lf/pre-miR-29b, CS-Lf/pre-miR-29b and PEI-Lf/pre-miR-29b systems were formulated using the method of simple complexation through electrostatic interaction by using different amines to phosphate ratios (N/P ratios, molar ratio of CS/PEI-nitrogen atoms present in the protonated amine groups to pre-miR-29b-phosphate groups), as described by Pereira and co-workers [47]. Pre-miR-29b stock solution was prepared by pre-miRNA dissolution in sodium acetate buffer, up to a final concentration of 2 µg/mL and was kept constant in all the methods used for the characterization of the formed complexes [47]. The CS-SA-Lf, PEI-SA-Lf, PEI-Lf and CS-Lf stock solutions were also prepared in sodium acetate buffer pH 4.5 in a concentration of 10 mg/mL. Briefly, the complexes were obtained by addition of 100 µL of CS-SA-Lf, PEI-SA-Lf, PEI-Lf or CS-Lf solution, of variable concentration, dropwise to the pre-miR-29b solution (400 µL). The complexes were immediately mixed using a vortex mixer at maximum speed for 1 min. After 30 min of stabilization at room temperature, the complexes were recovered by centrifugation (15000 g, 20 min). The complexation of pre-miR-29b by CS-SA, PEI-SA, CS-SA-Lf and PEI-SA-Lf was evaluated by agarose gel electrophoresis [47].

2.2.3. Determination of the encapsulation efficiency

The encapsulation efficiency (EE) was calculated by determining free pre-miRNA concentration in the supernatant recovered after particle centrifugation (15000g, 20 min, 25ºC). The amount of unbound pre-miR-29b was quantified by UV spectrophotometry (Nanophotometer), at 260 nm. Supernatant recovered from unloaded complexes (without pre-miRNA) was used as a blank. Three repetitions of this procedure were performed for each

system. EE was determined using the following formula: EE % = [(Total pre-miRNA amount – pre-miRNA supernatant amount)/Total pre-miRNA amount] x 100 [47].

2.2.4. Cell culture

In this study, N2a695, RBE4 and Z310 choroidal epithelial cells were used. N2a695 cells (at passages 13-30) were cultured in the following medium: 1:1 mixture of Dulbecco's Modified Eagle's Medium (DMEM) and OptiMEM supplemented with 5% (wt/vol) heat-inactivated fetal bovine serum (FBS) and 1% (wt/vol) penicillin-streptomycin. In these cells there is a constitutive endogenous human BACE1 expression, enabling greater sensitivity for detecting pre-miR-29b induced changes in the human BACE1 expression at post transcriptional level. Z310 cell line (at passages 95-100) was maintained in DMEM high glucose growth medium containing 10% FBS and 1% penicillin-streptomycin [48]. On the other hand, RBE4 cultures (at passages 7-30) were grown in the following medium: Minimum Essential Medium (αMEM) and Ham's F10 Nutrient Mix (1:1 vol/vol) supplemented with 10% FBS, 1% penicillin-streptomycin, 1% L-glutamine and 0.6% Geneticin (300 µg/m). All cell lines were kept at 37ºC in a humidified atmosphere containing 5% CO_2. Cells were subcultured regularly using trypsin-EDTA [49].

2.2.5. *In vitro* transfection and expression

2.2.5.1. *In vitro* cellular uptake – Cell live imaging

In order to investigate the cellular uptake, pre-miR-29b was labeled with FITC. In brief, an aliquot of FITC-DMSO solution was added in drops to pre-miR-29b solution (8.72 nM). The resultant solution was kept under stirring for 3 hours at room temperature. Then, the final product was incubated with 3 M NaCl and 2.5 volumes of absolute ethanol ice-cold at -20ºC during 30 min. Excess FITC was removed by centrifugation at 12000g for 30 min at 4ºC. After centrifuging, the pellet was washed with 75% ethanol twice, followed by a 5 min centrifugation at 12000 g (4ºC). Finally, the FITC-pre-miR-29b was ressuspended in OptiMEM and encapsulated with CS-SA-Lf, PEI-SA-Lf, PEI-Lf and CS-Lf. N2a695 cells were seeded at a density of 2×10^4 cells/cm^2 in µ-Slide 8-well flat bottom imaging plates (Ibidi GmbH, Germany). In the following day, the medium was replaced by fresh serum-free medium and cells were stained with Hoechst 33342® nuclear probe for 20 min. Subsequently, the cells were transfected with the complexes prepared with FITC-labeled pre-miR-29b in serum-free medium. The cells were transferred to a Zeiss LSM 710 confocal laser scanning microscope (CLSM; Carl Zeiss SMT Inc., US) equipped with a plane-apocromat 63×/DIC objective and processed in Zeiss Zen (SP2, 2010) and Imaris software (Bitplane, Switzerland), in order to evaluate the cellular uptake. The fluorescence images were obtained at 63× amplification. Cells without the addition of complexes were imaged as control.

2.2.5.2. *In vitro* transfection studies

Briefly, N2a695 cells were seeded in 12-well plates at a density of 2×10^4 cells/well in 1.5 mL of complete medium. When a 50% to 60% confluence was achieved, the media was removed

and then replaced with serum-free culture medium. After 12 hours, pre-miR-29-loaded complexes and Lipofectamine/pre-miR-29b (Lipo/pre-miR-29b), previously prepared with a pre-miR-29b concentration of 8.72 nM, were added to the wells and incubated with the cells, for 4 hours. The culture medium was then replaced with 1.5 mL of fresh medium supplemented with 1% FBS and 1% antibiotic, to allow the cells to remain metabolically active, expressing human BACE1. The cells were incubated for an additional 72 hours at 37ºC. As a negative control, untreated cells were used and as a positive control, transfection with Lipo/pre-miR-29b was performed according to the manufacturer's protocol. All transfection experiments were performed in triplicate. Total RNA was recovered with TRIzol reagent (Invitrogen) and chloroform, further purified by isopropanol precipitation and washed with 75% ethanol. The concentration of total RNA was determined using a NanoPhotometer UV/Vis Spectrophotometer, and the integrity and quality of RNA was assessed by agarose gel electrophoresis. RNA was treated with DNase I to avoid genomic contamination. First-strand cDNA was synthesized using the RevertAid First Strand cDNA Synthesis Kit (Thermo Fisher Scientific Inc.) in a total volume of 20 µL containing 1 µg of total RNA, according to the manufacturer's instructions.

2.2.5.3. Expression of BACE1 mRNA in N2a695 cells by RT-qPCR

For quantitative analysis, RT-qPCR amplification of cDNA was performed using the Maxima® SYBR Green/Fluorescein qPCR Master Mix (Thermo Fisher Scientific Inc.) in an IQ5 Cycler from BioRad. PCR reaction was prepared in a final volume of 20 µL containing 10 µL of Maxima® SYBR Green/Fluorescein qPCR Master Mix, 1.2 µL each of 25 µM forward and reverse primers and 1 µL of cDNA. The cycle was performed as follows: 5 min at 95ºC, followed by 40 cycles of 30 s at 95ºC, 30 s at 62ºC, and 30 s at 72ºC. RT-qPCR efficiencies were calculated from the given slopes with MyIQ 2.0 software (BioRad). The relative quantification of the BACE1 expression was based on the comparative threshold cycle (C_T) method in which the amount of the target was determined to be $2^{-(\Delta CT \text{ target} - \Delta CT \text{ calibrator})}$, normalized to levels of glyceraldehyde-3-phosphate dehydrogenase (GAPDH) and relative to the untreated control cells. The primers used in these experiments were 5'-AGACGCTCAACATCCTGGTG-3' (forward) and 5'-CCTGGGTGTAGGGCACATAC-3' (reverse) for the amplification of human BACE (hBACE) and 5'- TGACGTGCCGCCTGGAGAAA-3' (forward), 5'-AGTGTAGCCCAAGATGCCCTTCAG-3' (reverse) for the amplification of GAPDH. Each sample was run in triplicate, and C_T values were averaged from the triplicate. The final data were averaged from 3 separately conducted experiments.

2.2.6 Transport across *in vitro* BBB model

2.2.6.1. *In vitro* BBB model

RBE4 cells and Z310 cells were established to evaluate the ability of the dual targeting complexes transpose the BBB model. RBE4 and Z310 cells were seeded in 12-well culture insert coated with type I collagen (Polycarbonate Membrane Transwell Inserts of 1.0 mm mean pore size, 1.12 cm^2 surface area, Corning, NY, USA). 0.5 mL of cell suspensions

containing 2.0 x 10^5 cells was added to the inner (donor) chamber, which was inserted into the outer (acceptor) chamber containing 1.3 mL of the same culture medium. A cell monolayer is usually formed 3-5 days after seeding, as judged by three criteria: (1) the cells formed a confluent monolayer without visible spaces between cells under a light microscope; (2) the height of the culture medium in the inner chamber had to be at least 2 mm higher than that in the outer chamber for at least 24 hours; and (3) a constant transendothelial electrical resistance (TEER) value across the cell layer was obtained [50]. The TEER was used to measure the formation of tight junctions, indicating the integrity of BBB structure for studying drug delivery to the brain. The cell monolayer integrity was monitored using an EVOM Endohmchamber (Word Precision Instruments, Inc. Sarasota, Florida, USA) to measure the TEER value of the *in vitro* BBB model. Only cell monolayers with TEER value above 100 Ωcm^2 were selected for the transport studies, which indicate that this system could be used as an *in vitro* BBB model [50]. All the permeability experiments were performed in serum-free medium at 37ºC, and the drug carriers, including CS-SA/pre-miR-29b-FITC, CS-SA-Lf/pre-miR-29b-FITC, PEI-SA/pre-miR-29b-FITC and PEI-SA-Lf/pre-miR-29b-FITC were added into the donor compartment of the above BBB model with the pre-miR-29b concentration of 8.72 nM. After 4 hours, the inserts were removed. The concentration of pre-miR-29b transported across BBB media was determined using a spectrofluorometer (Spectramax Gemini XS, Molecular Devices LLC, US), with the excitation wavelength of 480 nm and the emission wavelength at 590 nm. The BBB transport ratio of pre-miR-29b was calculated as follows: Transport ratio % = [(Total Fluorescence in the outer chamber)/ [(Total Fluorescence in the inner chamber + Total Fluorescence in the outer chamber)] x 100.

2.2.7.2. Immunofluorescence

Endothelial cells from the *in vitro* BBB model were fixed for 10 min at room temperature with 4% of paraformaldehyde (PFA) buffer solution. Cells were then washed 3 times with PBS for 10 min, followed by permeabilization with PBS containing 0.1% Triton X-100 for 15 min. After fixation, the nucleus of the endothelial cells was counterstained with Hoechst 33342® (1:1000) for 10 minutes followed by 3 washing steps with PBS-T. Cells were mounted on slides and the fluorescence images were acquired using a confocal laser scanning microscope (Zeiss LSM 710, Carl Zeiss SMT Inc., USA) equipped with a plane-apocromat 63×/DIC objective. Images were processed and analyzed using ImageJ software. All experiments were repeated at least three times, and representative images are shown.

2.8. Statistical analysis

All the experiments were repeated at least three times using independent culture preparations. Data are presented as the mean ± standard error. Statistical comparisons were performed using a one-way analysis of variance (ANOVA), followed by pair-wise comparisons using the Fisher's least significant difference test. A P value <0.05 was considered statistically significant. Statistical analysis was performed by using GraphPad Prism 6 software.

3. Results

3.1. Synthesis and characterization of CS-SA, PEI-SA, CS-SA-Lf, PEI-SA-Lf complexes

The carriers of CS/PEI-SA were synthesized by chemical reaction between the carboxyl group of SA and the amino group of CS or PEI in the presence of EDC, a carboxyl activating agent [38]. ^{1}H NMR experiments were used to characterize and confirm the chemical structure of the obtained CS/PEI-SA complexes. Also, for comparing the signals, CS and PEI spectra were also recorded without stearic acid. The ^{1}H-NMR assignment of CS was previously determined and is as follows: ^{1}H NMR (CS, D_2O) δ =5.10 (H_1), δ =3.09 (H_2), δ =3.43~3.81 (H_3, H_4, H_5, H_6), δ =1.96 ($NHCOCH_3$) ppm. The signal of H_1 was effected by the near water peak suppression of H_2O at δ=4.76. Comparing with CS ^{1}H-NMR spectrum, the triplet signals at 0.9 ppm, due to the terminal CH_3 protons of stearic acid and the new signal between 1–1.5 ppm corresponding to the CH_2 chain of acyl chain, showed that stearic acid was linked to CS. Similarly, the ^{1}H NMR spectrum of the PEI was first assignment and the proton peaks of PEI (–$NHCH_2CH_2$–) appeared at 3.2–2.0 ppm. The molecular structure of PEI-SA was then confirmed by ^{1}H NMR. ^{1}H NMR analysis indicates that the amino-groups of the PEI were acylated. The ^{1}H-NMR assignment of PEI-SA was as follows: δ (ppm): 0.86–0.89 (t, -$CH_2CH_2(CH_2)_{15}\mathbf{CH_3}$), 1.25 (br, -$CH_2CH_2(\mathbf{CH_2})_{15}CH_3$), 1.62 (br, -$CH_2\mathbf{CH_2}(CH_2)_9CH_3$), 2.18 (br, -$\mathbf{CH_2}CH_2(CH_2)_9CH_3$), 2.39–3.3 (m, -$CH_2CH_2NH$-, -$CH_2CH_2N$-, -$CH_2CH_2NHCO$-, -$CH_2CH_2NHCO$-). Although, the same chemical shifts appeared in PEI-SA, however the sharp peaks at 3.0-2.4 ppm could contribute to the chemical shifts of PEI. Moreover, the ratio of peak area at 3.0–2.4 ppm to the peak area of methyl group in PEI-SA was bigger than that of PEI. These results indicated that stearic acid was successfully link to PEI. The NMR studies also demonstrated that very few free amines are available on the CS-SA complexes comparing with PEI-SA complexes. The functionalization with Lf was obtained using a common method with 2-iminothiolane hydrochloride as the sulfhydrylization reagent [45]. After purification, thiolated protein was obtained. The SDS-PAGE was used to further confirm the surface capping of the terminal amines of the CS/PEI-SA with Lf. In the SDS-PAGE a new band above 100 KDa was observed, indicating that Lf ligand was covalently attached to the CS/PEI-SA (Figure 1). NMR experiments are current running to complement the SDS-PAGE results.

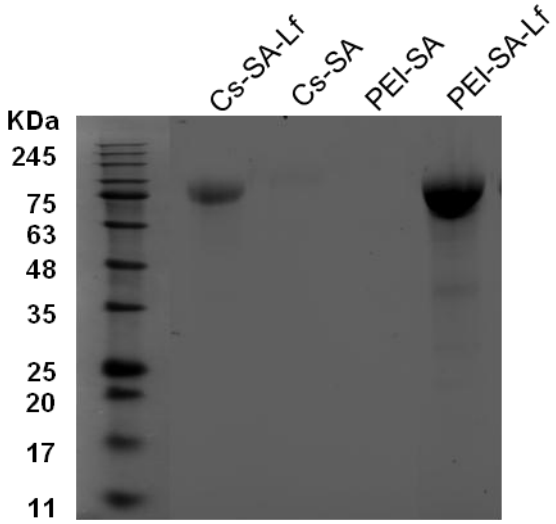

Figure 1 - SDS-PAGE of CS-SA, CS-SA-Lf, PEI-SA and PEI-SA-Lf.

3.2. Preparation of CS-SA-pre-miR-29b, PEI-SA-pre-miR-29b, CS-SA-Lf-pre-miR-29b and PEI-SA-Lf-pre-miR-29b

All pre-miR-29b-loaded complexes were prepared by electrostatic interactions that occur between the positively charged amine groups of the carriers and the phosphate groups of the pre-miR-29b [47]. The complexes were mixed with pre-miR-29b for the formation of pre-miR-29b-loaded complexes in acetate buffer at pH 4.5. In order to determine the degree of compaction between pre-miR-29b and all carriers in study, a gel retardation assay and UV spectrometry were performed (Fig. 2). As shown in Fig. 2A, the mobility of pre-miR-29b was fully retarded by all carriers, indicating that the pre-miR-29b was tightly neutralized within the carriers. It was also possible to observe that PEI-SA-pre-miR-29b and PEI-SA-Lf-pre-miR-29b moved in direction of the anode, that is, some polyplexes present an excess of positive charge, know as overcharging effects. These results are in accordance with what was observed in the encapsulation studies, in which 100% of encapsulation efficiency was achieved, indicating that pre-miR-29b was completely complexed with PEI-SA-Lf (Fig. 2B). In what concerns to the CS-based systems, CS-SA-Lf seems to be more efficient in pre-miR-29b condensation, once a value of 86% was obtained in comparison with 80% for CS-SA.

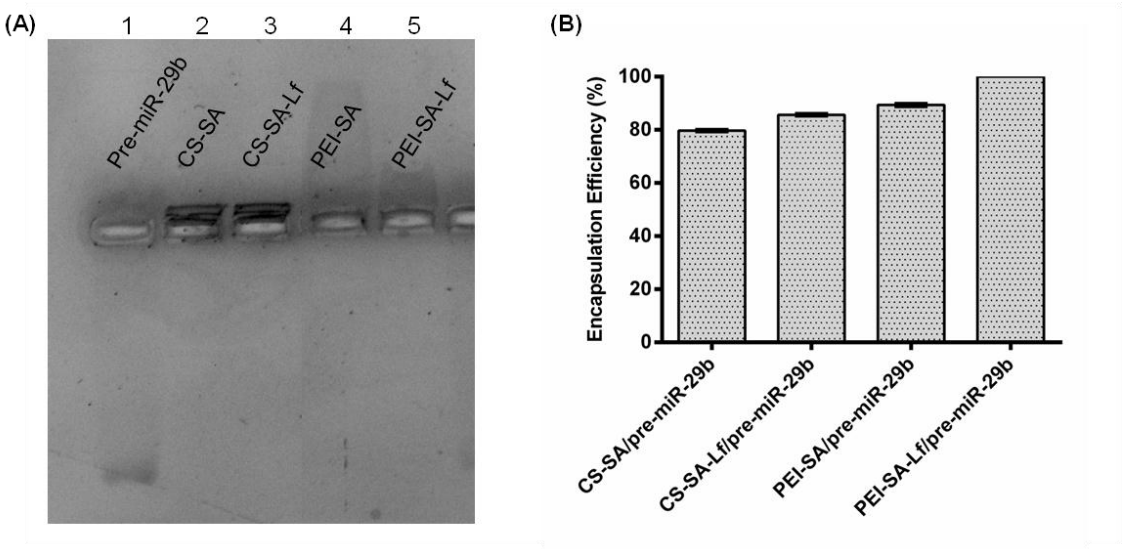

Figure 2 - Synthesis of pre-miR-29b-loaded complexes. **(A)** Agarose gel electrophoresis analysis. Lane 1: naked pre-miR-29b, lane 2-5: pre-miR-29b loaded into the different complexes, as indicated in the figure. **(B)** Encapsulation efficiency of different pre-miR-29b-loaded complexes (Data represent the mean±SD, n = 4).

3.3. *In vitro* cellular uptake and intracellular trafficking of the pre-miR-29b-loaded complexes

To evaluate the efficacy of cellular uptake of pre-miR-29b loaded onto the CS-SA-Lf and PEI-SA-Lf, laser scanning confocal microscopy was employed to quantify the uptake and to visualize the cellular distribution of pre-miR-29b (see Fig. 3 and 4). To accomplish this purpose, the pre-miR-29b was labeled with FITC to construct fluorescent complexes for their localization in N2a695 cells. Figures 3 and 4 present the confocal fluorescence microphotographs of N2a695 cells treated with CS-SA-Lf/pre-miR-29b-FITC and PEI-SA-Lf/pre-miR-29b-FITC followed during 2.5 hours, respectively. As demonstrated by serial Z-stacks of confocal images, pre-miR-29b-loaded complexes were clearly detected within the cells (see Fig. 3 and 4). After 1 hour of transfection, a homogeneous distribution of CS-SA-Lf/pre-miR-29b-FITC and PEI-SA-Lf/pre-miR-29b-FITC complexes within the cells was observed. Indeed, a significant fraction appeared in the cytoplasm near the cell nucleus (see Fig. 3 and 4), suggesting that the complexes displayed an excellent ability to cross cell membranes by cellular endocytosis. As shown in Fig. 3 and 4, after 2 hours of incubation, pre-miR-29b-loaded complexes were also present in the nuclei of cells, being visible the green fluorescence throughout the entire cytoplasm and nucleus. Following the confirmation that the pre-miR29b-loaded complexes were efficiently delivered into N2a695 cells, the expression of pre-miR-29b-FITC was also evaluated by quantitative analysis of cellular accumulation of FITC.

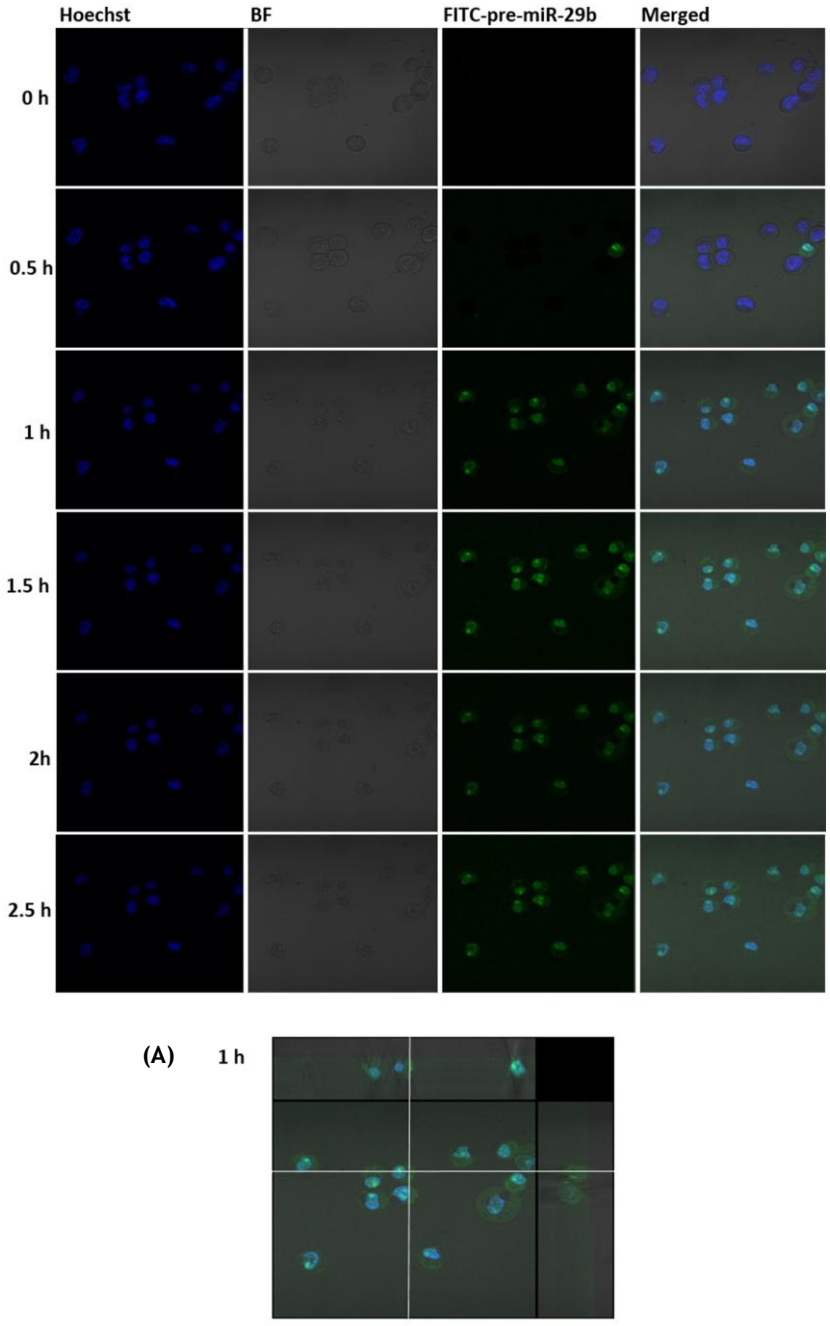

Figure 3 - Confocal laser scanning microscopy images showing the intracellular uptake of FITC-labelled CS-SA-Lf/pre-miR-29b in N2a695 cells during 0.5 to 2.5 hours. For each panel, images from left to right showed the cells with nuclear staining by Hoechst 33342® (blue); Bright field stained cell membrane; CS-SA-Lf/pre-miR-29b-FITC (green); and overlays of both images. **(A)** Representative immunostaining data showing a majority of the FITC-labelled CS-SA-Lf/pre-miR-29b localized in the cytoplasm.

Fluorescence intensity inside cells increased gradually and a significant difference in fluorescence intensity between PEI-SA-Lf/pre-miR-29b-FITC and CS-SA-Lf/pre-miR-29b-FITC was observed during the 2.5 hours of incubation. The results obtained with quantitative

analysis were extremely similar to those obtained with fluorescence imaging. Interestingly, no significant differences were found in the mean fluorescence intensity at 1.5 or 2.5 hours, indicating that a plateau was achieved after 1.5 hours of incubation, in the cells transfected with CS-SA-Lf (data not shown).

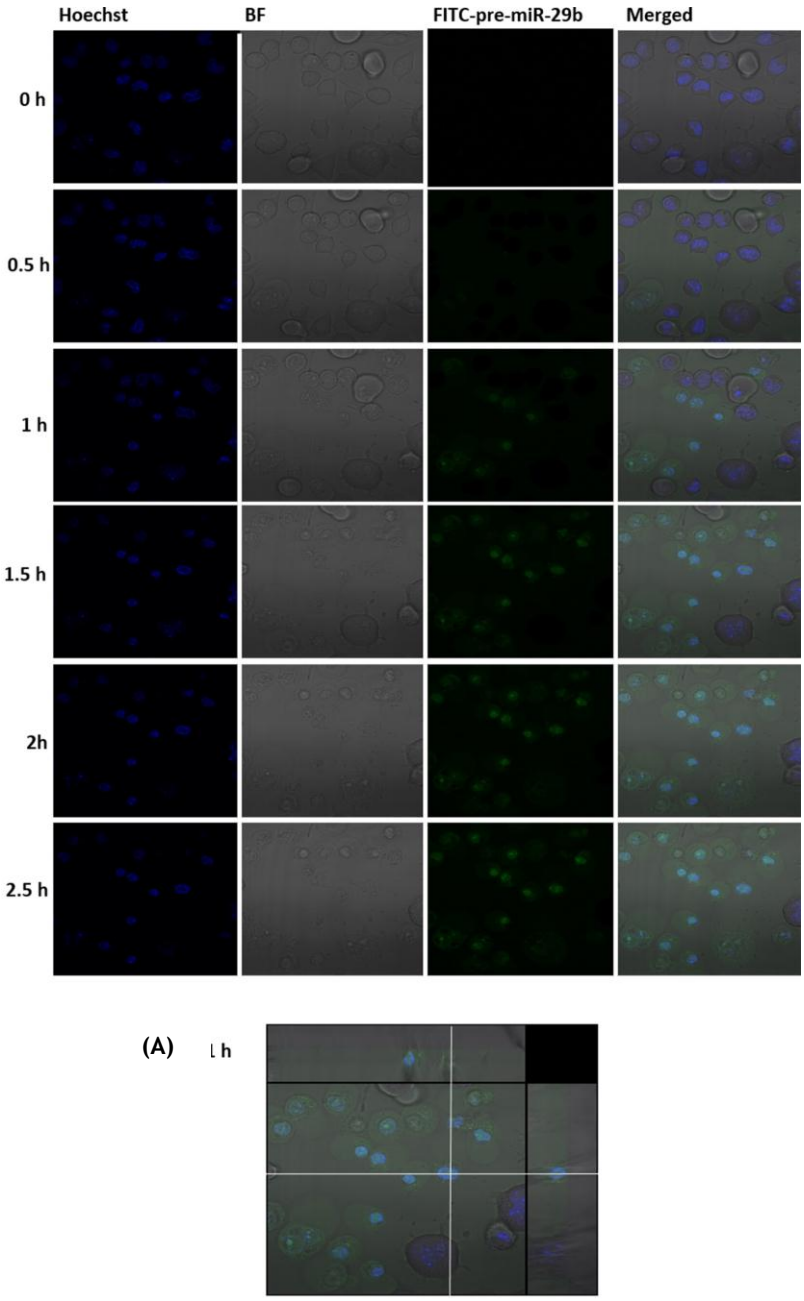

Figure 4 - Confocal laser scanning microscopy images showing the intracellular uptake of FITC-labelled PEI-SA-Lf/pre-miR-29b in N2a695 cells during 0.5 to 2.5 hours. For each panel, images from left to right showed the cells with nuclear staining by Hoechst 33342® (blue); Bright field stained cell membrane; PEI-SA-Lf/pre-miR-29b -FITC (green); and overlays of both images. **(A)** Representative immunostaining data showing a majority of the FITC-labelled PEI-SA-Lf/pre-miR-29b localized in the cytoplasm.

In contrast, the mean fluorescence intensity of the PEI-SA-Lf/pre-miR-29b complexes increased during the 2.5 hours of incubation, while CS-SA-Lf/pre-miR-29b increased until 1.5 hours of incubation and then kept stable until the end of transfection period (data not shown). These results indicate that the release of pre-miR-29b from the CS-SA-Lf complexes was faster than that from the PEI-SA-Lf.

3.4. Evaluation of human BACE1 gene knockdown induced by pre-miR-29b-loaded complexes

To investigate the effect of recombinant pre-miR-29b on hBACE1 mRNA expression levels, RT-qPCR measurements were performed. To accomplish this purpose, N2a695 cells were transfected with CS-SA-Lf/pre-miR-29b, PEI-SA-Lf/pre-miR-29b and Lipo/pre-miR-29b with 8.72 nM of the target miRNA. After 72 hours of transfection, it was verified that the overexpression of recombinant pre-miR-29b induces a notably decrease in the endogenous hBACE1 mRNA levels, in comparison with the untreated cells (Fig. 5). In particular, hBACE1 mRNA expression was decreased by approximately 77% in cells transfected with CS-SA-Lf/pre-miR-29b, and by 69% in those transfected with PEI-SA-Lf/pre-miR-29b complexes, when compared with untreated cells (Fig. 5). This reduction on mRNA hBACE1 expression was also significantly higher than the silencing (around 40%) achieved in cells transfected with Lipo/pre-miR-29b, the positive control (Fig. 5). Thus, in comparison to Lipofectamine 2000, CS-SA-Lf demonstrated a higher efficacy in delivering pre-miR-29b once it was achieved a 2 fold reduction of BACE1 mRNA levels.

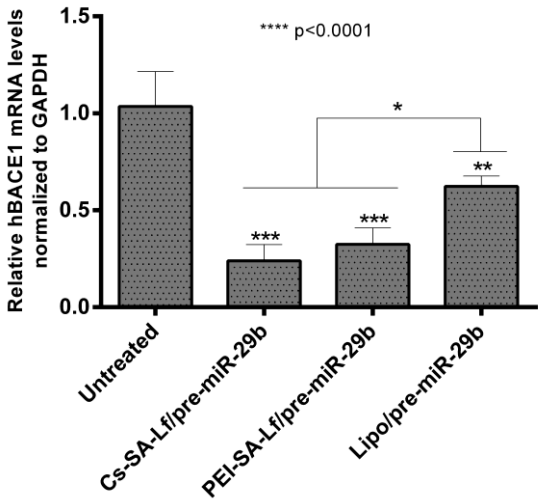

Figure 5 - *In vitro* gene silencing effect of recombinant pre-miR-29b on hBACE1 mRNA levels in N2a695 cells following 72 hours treatment with CS-SA-Lf/pre-miR-29b, PEI-SA-Lf/pre-miR-29b and Lipo/pre-miR-29b. Values in the graph are mean from triplicates of RT-qPCR threshold cycles for hBACE1 mRNA normalized to those of mRNA for GAPDH from 3 independent experiments and demonstrate significant differences across treatment conditions. ANOVA, mean±SD.

Although the functionalized CS presents a slightly lower encapsulation efficiency (86%) compared with the unmodified CS (90%), it shows a higher transfection efficiency, and consequently leads to higher hBACE inhibition, very similar to those obtained for the unmodified CS (77% to CS-SA-Lf and 76.4% to CS). These results show that the functionalization did not affect the delivery of recombinant pre-miR-29b to the cells and its biological activity continues to exceed the synthetic miR-29b. Furthermore, the PEI functionalized demonstrates a decrease in the inhibition of hBACE1 (69%) compared to the unmodified PEI (78%) what may be due to their structural characteristics after functionalization.

3.5. Permeability across the BBB using CS-SA/pre-miR-29b, PEI-SA/pre-miR-29b, CS-SA-Lf/pre-miR-29b and PEI-SA-Lf/pre-miR-29b

In order to evaluate the ability of all the systems to cross the BBB, *in vitro* BBB model was established using RBE4 cells [49], which were transfected with CS-SA/pre-miR-29b-FITC, CS-SA-Lf/pre-miR-29b-FITC, PEI-SA/pre-miR-29b-FITC and PEI-SA-Lf/pre-miR-29b-FITC. The fluorescence intensity in the inner and outer chambers of the transwell was determined, in order to evaluate the targeting effect of Lf and SA in the CS and PEI polymers to cross the BBB. Fig. 6A shows the transport ability of different complexes to cross BBB model at the same concentration of pre-miR-29b. After 4 hours of incubation, the transport ratios were of about 12.28, 41.61, 64.56 and 64.93% for PEI-SA, PEI-SA-Lf, CS-SA and CS-SA-Lf, respectively. These results indicated that the dual-targeting complexes have enhanced transport ability to cross the BBB compared to the complexes with only one targeting group. Fig. 6A shows also the immunostaining microphotographs of CS-SA-Lf and PEI-SA-Lf internalized in RBE4 cells. As revealed in Fig. 6A, the strong green intensity in cytoplasm of RBE4 cells suggested that complexes were internalized by endocytosis through the cells. Z310 cells were used as *in vitro* blood-cerebrospinal fluid barrier model for evaluating the dual-targeting effects (Fig. 6B).

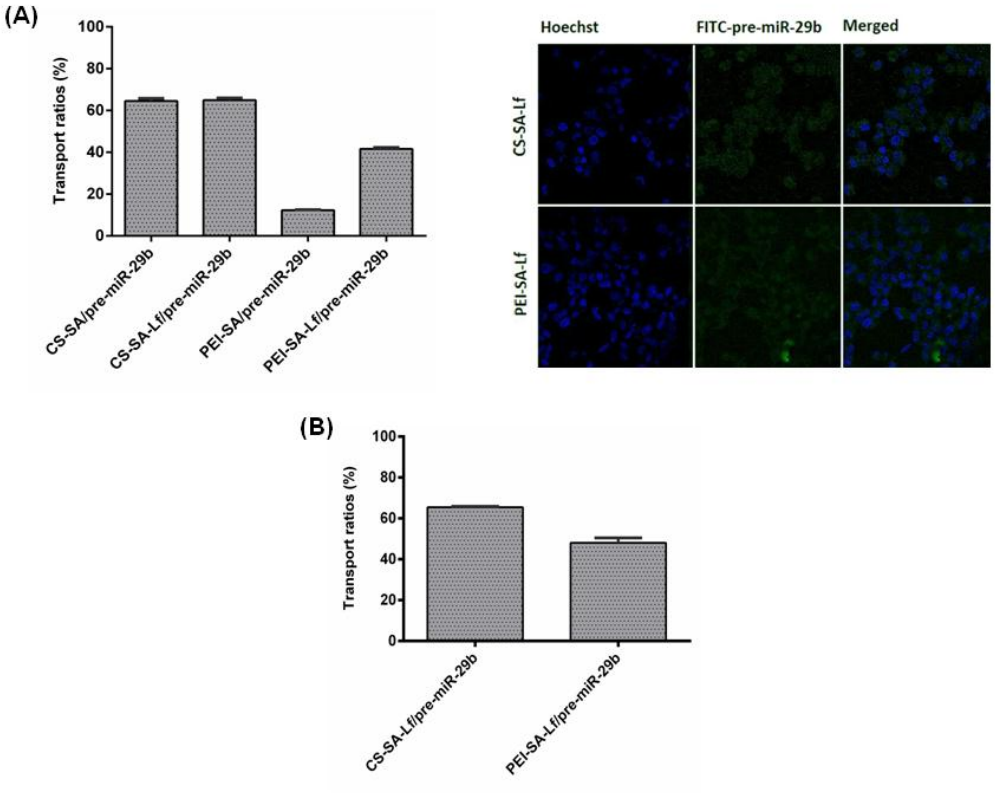

Figure 6 - The transport ratio of pre-miR-29b across the BBB during 4 hours in RBE4 cells **(A)** and Z310 cells **(B)**. Data were presented as the mean ± standard deviation. **(A)** Intracellular trafficking in RBE4 cells after treating with CS-SA-Lf/pre-miR-29b-FITC and PEI-SA-LF/pre-miR-29b-FITC. The fluorescence signals were collected by LSCM with three channels: blue fluorescence from nuclei stained with Hoechst 33258, green fluorescence from FITC labeled pre-miR-29b and the merged images of three channels.

With the same incubation time and pre-miR-29b concentration, the different formulations were internalized by Z310 cells in the following order: CS-SA-Lf/pre-miR-29b > PEI-SA-Lf/pre-miR-29b, with transport ratios of 65.49% and 48.08%, respectively. These results are in agreement with the BBB transportation result. These findings demonstrated that the dual targeting complexes (PEI/CS-SA-Lf) could mediate the recognition via Lf receptors and fatty acid transporter(s)/low-density lipoprotein receptor expressed by RBE4 and Z310 cells, allowing the transport of exogenous pre-miR-29b into the brain, probably via the pathway of receptor-mediated transcytosis (RMT). In addition, Lf is a competent protein that intensifies the interaction between complexes and RBE4 and Z310 cells. On the other hand, these results can also be explained due to the positive charge of the cationic polymers, which could promote electrostatic interactions with the negatively charged RBE4 and Z310 cell membranes, activating the cellular uptake through the pathway of adsorptive-mediated transcytosis (AMT) [38]. The internalization of CS-SA and CS-SA-Lf by RBE4 cells was higher than that of PEI-SA and PEI-SA-Lf. Thus, it was found that the chitosan improved the delivery

efficacy both in terms of targeting at an earlier time point as well as in the accumulation in cells. These results can be related to some characteristics of CS that can transiently open tight junctions, enabling the transport of components via a paracellular pathway through the epithelial barrier.

Conclusion

In conclusion, the present *in vitro* study demonstrated that CS-SA-Lf and PEI-SA-Lf could efficiently cross the BBB and thus, deliver the recombinant pre-miR-29b as a therapeutic agent to the neuronal cells. The pre-miR-29b induced the inhibition of BACE1 mRNA. Specifically, the *in vitro* cellular uptake study showed that lactoferrin and stearic acid conjugated with chitosan are highly efficient in cell transfection (about 65%) and pre-miRNA intracellular delivery, and consequently, in the silencing of the BACE1 mRNA in comparison to PEI-SA-Lf. These results suggest that chitosan conjugated with stearic acid and lactoferrin can represent a potentially promising and interesting therapeutic strategy for targeting recombinant pre-miR-29b to neuronal cells, aiming the development of effective strategies to treat AD.

Acknowledgments

This work was supported by the Portuguese Foundation for Science and Technology (FCT), through the project EXPL/BBB-BIO/1056/2012 and Pest-OE/SAU/UI0709/2014. Patrícia Pereira acknowledges the fellowship (Ph.D. Grant, Ref SFRH/BD/81914/2011), from FCT. Joana Tomás also acknowledges the fellowship in the ambit of the project CENTRO-07-ST24-FEDER-002015. The authors also acknowledge the program Fundo Europeu de Desenvolvimento Regional (FEDER) [COMPETE [FCOMP-01-0124-FEDER-027560]]. The authors would like to thank Professor Yo Kikuchi (Division of Life Science and Biotechnology, Department of Ecological Engineering, Toyohashi University of Technology) for kindly provided of pBHSR1-RM plasmid and Professor Wenjie Luo for the kind contribution regarding the cell line N2a695.

References

[1] Isik AT (2010) Late onset Alzheimer's disease in older people. Clin Interv Aging 5, 307-311.

[2] Blennow K, de Leon MJ, Zetterberg H (2006) Alzheimer's disease. Lancet 368, 387-403.

[3] Hardy, J, Selkoe, DJ (2002) The amyloid hypothesis of Alzheimer's disease: progress and problems on the road to therapeutics. Science 297, 353-356.

[4] Mullane K, Williams M (2013) Alzheimer's therapeutics: continued clinical failures question the validity of the amyloid hypothesis-but what lies beyond? Biochem Pharmacol 85, 289-305.

[5] Glenner GG (1989a) Amyloid beta protein and the basis for Alzheimer's disease. Prog Clin Biol Res 317, 857-868.

[6] Kim DH, Yeo SH, Park JM, Choi JY, Lee TH, *et al*. (2014) Genetic markers for diagnosis and pathogenesis of Alzheimer's disease. Gene 545, 185-193.

[7] Ghiso J, Frangione B (2002) Amyloidosis and Alzheimer's disease. Adv Drug Deliv Rev 54, 1539-1551.

[8] Provost P (2010a) Interpretation and applicability of microRNA data to the context of Alzheimer's and age-related diseases. Aging 2, 166-169.

[9] Schonrock N, Matamales M, Ittner LM, Gotz J (2012) MicroRNA networks surrounding APP and amyloid-beta metabolism-implications for Alzheimer's disease. Exp Neurol 235, 447-454.

[10] Vassar R, Kovacs DM, Yan R, Wong PC (2009) The beta-secretase enzyme BACE in health and Alzheimer's disease: regulation, cell biology, function, and therapeutic potential. J Neurosci 29, 12787-12794.

[11] Cole SL, Vassar R (2007) The Alzheimer's disease beta-secretase enzyme, BACE1. Mol Neurodegener 2, 22

[12] Hunt CE, Turner AJ (2009) Cell biology, regulation and inhibition of beta-secretase (BACE-1). FEBS J 276, 1845-59

[13] Zong Y, Wang H, Dong W, Quan X, Zhu H, *et al*. (2011) miR-29c regulates BACE1 protein expression. Brain Res 1395, 108-115.

[14] Hebert SS, Horre K, Nicolai L, Papadopoulou AS, Mandemakers W, *et al*. (2008) Loss of microRNA cluster miR-29a/b-1 in sporadic Alzheimer's disease correlates with increased BACE1/beta-secretase expression. Proc Natl Acad Sci U S A 105, 6415-6420.

[15] Dunkel P, Chai CL, Sperlagh B, Huleatt PB, Matyus P (2012) Clinical utility of neuroprotective agents in neurodegenerative diseases: current status of drug development for Alzheimer's, Parkinson's and Huntington's diseases, and amyotrophic lateral sclerosis. Expert Opin Investig Drugs 21, 1267-1308.

[16] Suehs BT, Davis CD, Alvir J, van Amerongen D, Pharmd NC, *et al*. (2013) The clinical and economic burden of newly diagnosed Alzheimer's disease in a medicare advantage population. Am J Alzheimers Dis other Demen 28, 384-392.

[17] Qiu C, Kivipelto M, von Strauss E (2009) Epidemiology of Alzheimer's disease: occurrence, determinants, and strategies toward intervention. Dialogues Clin Neuros 11, 111-128.

[18] Edwards RH (2001) Drug delivery via the blood-brain barrier. Nat Neurosci 4, 221-2.

[19] Alam MI, Beg S, Samad A, Baboota S, Kohli K, *et al*. (2010) Strategy for effective brain drug delivery. Eur J Pharm Sci 40, 385-403.

[20] Egleton RD, Davis TP (1997) Bioavailability and transport of peptides and peptide drugs into the brain. Peptides 18,1431-9.

[21] Pangalos MN, Schechter LE, Hurko O (2007) Drug development for CNS disorders: strategies for balancing risk and reducing attrition. Nat Rev Drug Discov 6, 521-32.

[22] Pardridge WM (2005) The blood-brain barrier: bottleneck in brain drug development. NeuroRx 2, 3-14.

[23] Kusuhara H, Sugiyama Y (2001) Efflux transport systems for drugs at the blood-brain barrier and blood-cerebrospinal fluid barrier (Part 1). Drug Discov Today 6,150-6.

[24] Descamps L, Dehouck MP, Torpier G, Cecchelli R (1996) Receptor-mediated transcytosis of transferrin through blood-brain barrier endothelial cells. Am J Physiol 270, H1149-58.

[25] Visser CC, Stevanovic S, Heleen Voorwinden L, Gaillard PJ, Crommelin DJ, *et al*. (2004) Validation of the transferrin receptor for drug targeting to brain capillary endothelial cells *in vitro*. J Drug Target 12, 145-50.

[26] Fillebeen C, Descamps L, Dehouck MP, Fenart L, Benaissa M, *et al*. (1999) Receptor-mediated transcytosis of lactoferrin through the blood-brain barrier. J Biol Chem 274, 7011-7.

[27] Duffy KR, Pardridge WM (1987) Blood-brain barrier transcytosis of insulin in developing rabbits. Brain Res 420, 32-8.

[28] Reinhardt RR, Bondy CA (1994) Insulin-like growth factors cross the blood-brain barrier. Endocrinology 135, 1753-61.

[29] Candela P, Gosselet F, Miller F, Buee-Scherrer V, Torpier G, *et al*. (2008) Physiological pathway for low-density lipoproteins across the blood-brain barrier: transcytosis through brain capillary endothelial cells *in vitro*. Endothelium 15, 254-64.

[30] Dehouck B, Fenart L, Dehouck MP, Pierce A, Torpier G, *et al*. (1997) A new function for the LDL receptor: transcytosis of LDL across the blood-brain barrier. J Cell Biol 138, 877-89.

[31] Edmond J (2001) Essential polyunsaturated fatty acids and the barrier to the brain. J Mol Neurosci 2, 181-193

[32]Kabanov AV, Batrakova EV, Alakhov VY. (2002) Pluronic block copolymers as novel polymer therapeutics for drug and gene delivery. J Control Release 82, 189-212.

[33] Chen J, Xie J (2012) Progress on RNAi-based molecular medicines. Int J Nanomedicine 7, 3971-80.

[34] Gao K, Huang L (2009) Nonviral Methods for siRNA Delivery. Mol Pharm 6, 651-8.

[35] Morille M, Passirani C, Vonarbourg A, Clavreul A, Benoit JP (2008) Progress in developing cationic vectors for non-viral systemic gene therapy against cancer. Biomaterials 29, 3477-96.

[36] Yin H, Kanasty RL, Eltoukhy AA, Vegas AJ, Dorkin JR, *et al*. (2014) Non-viral vectors for gene-based therapy. Nat Rev Genetics 15, 541-55.

[37] Zhang Y, Wang Z, Gemeinhart RA (2013) Progress in microRNA delivery. J Control Release 172, 962-74.

[38] Xie Y-T, Du YZ, Yuan H, Hu F-Q (2012) Brain-targeting study of stearic acid-grafted chitosan micelle drug-delivery system. Int J Nanomedicine 7, 3235-3244.

[39] Huwyler J, Wu D, Pardridge WM (1996) Brain drug delivery of small molecules using immunoliposomes. Proc. Natl. Acad. Sci. U.S.A. 93, 14164–14169.

[40] Swami A, Goyal R, Tripathi SK, Singh N, Katiyar N, *et al*. (2009) Effect of homobifunctional crosslinkers on nucleic acids delivery ability of PEI nanoparticles. Int J Pharm 374(1–2), 125–38.

[41] Sarvaiya J, Agrawal YK (2015) Chitosan as a suitable nanocarrier material for anti-Alzheimer drug delivery. Int J Biol Macromol 72, 454-465.

[42] Ward PP, Paz E, Conneely OM (2005) Multifunctional roles of lactoferrin: a critical overview. Cell Mol Life Sci 62, 2540–2548.

[43] Huang RQ, KeWL, Qu YH, Zhu JH, Pei YY, *et al*. (2007) Characterization of lactoferrin receptor in brain endothelial capillary cells and mouse brain. J Biomed Sci 14, 121–128.

[44] Ji B, Maeda A, Higuchi M, Inoue K, Akita H, *et al*. (2006) Pharmacokinetics and brain uptake of lactoferrin in rats. Life Sci 78, 851–855.

[45] Huang R, Ke W, Han L, Liu Y, Shao K, *et al*. (2009) Brain-targeting mechanisms of lactoderrin-modified DNA-loaded nanoparticles. J Cerebral Blood Flow & Metabolism 29, 1914-1923.

[46] Pereira P, Sousa A, Queiroz JA, Correia I, Figueiras A, *et al*. (2014) Purification of pre-miR-29 by arginine-affinity chromatography. J Chrom B Analyt Technol Biomed Life Sci 16-23, 951-952.

[47] Pereira P, Jorge A, Martins R., Pais ACCC, Sousa F, *et al*. (2012) Characterization of polyplexes involving small RNA. J Colloid Interface Sci 387, 84-94.

[48] Shi LZ, Li GJ, Wang S, Zheng W (2008) Use of Z310 cells as an *in vitro* blood-cerebrospinal fluid barrier model: Tight junction proteins and transport properties. Toxicology in Vitro 22, 190-199

[49] Balbuena P, Li W, Ehrich M (2011) Assessments of tight junction proteins occludin, claudin 5 and scaffold proteins ZO1 and ZO2 in endothelial cells of the rat blood-brain barrier: Cellular responses to neurotoxicants malathion and lead acetate. NeuroToxicology 32, 58-67

[50] Re F, Cambianica I, Zona C, Sesana S, Gregori M, *et al*. (2011) Functionalization of liposomes with ApoE-derived peptides at different density affects cellular uptake and drug transport across a blood-brain barrier model. Nanomed: Nanotech, Biol, Med 7, 551-559

Chapter 4

Concluding remarks

Over the recent years, the study and application of miRNAs has been considered useful and promising for the diagnosis and treatment of several diseases, in particular Alzheimer's disease. Most miRNAs employed in the development of these therapeutic approaches are produced either by enzymatic or chemical synthesis methods. Although, the synthesis process is efficient for large scale production, several limitations have been found regarding the use of synthetic miRNAs, once the isolation of these formulations are based on methods that employ chemical solvents and denaturing agents. Consequently, the final product is not suitable to be biologically applied, because of the health risks associated, and thus strongly compromise the success of several RNA based-procedures in the clinical field. Aiming to overcome some of these limitations, this project was centered on the establishment of a new strategy to biosynthesize and to purify the recombinant pre-miR-29b, also focusing on the preparation of suitable non-viral systems to efficiently deliver the pre-miR-29b to the cell. In addition, it was demonstrated the efficiency of the recombinant pre-miR-29b in BACE1 knockdown, using *in vitro* neuronal cells lines.

The recombinant production of pre-miR-29b was performed using the bacterium *R. sulfidophilum* DSM 1374, harboring a plasmid encoding for human pre-mir-29b. Regarding the growth conditions, and conversely to what was previously described for this bacterium, it was possible to develop an original approach for the aerobic growth of *R. sulfidophilum*, which resulted in a cellular growth improvement (higher growth rates, higher optical densities and a shorter cultivation time) followed by an enhanced production of intracellular (about 358 µg/L) and extracellular (approximately 182 µg/L) pre-miR-29b. In addition, the results indicated that the extracellular medium is not highly contaminated with genomic DNA, proteins or endotoxins, which is an important parameter concerning the integrity, stability and activity of the pre-miRNA (Paper III). In general, the use of this alternative strategy, based on the secretion of the pre-miRNA, avoids time-consuming and laborious RNA extraction methods that frequently induce RNA denaturation and, simultaneously suppresses the use of organic solvents and extremely toxic chemicals which are biologically hazardous. Despite this great advantage, in the course of this thesis it was difficult to recover the pre-miRNA from the extracellular medium, due to the high dilution factor, and the purification experiments were developed by using the RNAs recovered from the cells.

Considering the previous knowledge that pre-miR-29b can be successfully obtained by a simple, fast and economic process using the *R. sulfid*ophilum host, it is required the development and implementation of an adequate and efficient purification method that allows to overcome the challenges of the already existing chromatographic techniques, for the purification of miRNAs. In this project, it is suggested that amino acid-based affinity chromatography can be considered as a promising chromatographic strategy, to specifically

and efficiently purify the pre-miR-29b, eliminating the host impurities (small RNAs, proteins and endotoxins) by exploiting the specific interactions occurring between the $_L$-lysine and $_L$-arginine ligands and the pre-miRNA. Thus, it was developed an initial study to characterize the binding of pre-miR-29b onto the amino acids-based agarose supports using Surface Plasmon Resonance (Paper IV). The understanding of the conditions favoring these interactions was essential to control, manipulate, determine and establish the selective binding/elution chromatographic conditions (such as the composition and ionic strength of elution buffer and temperature), in order to improve the binding specificity of the pre-miR-29b onto the amino acids-based supports, preserving their structural stability and integrity. Considering the equilibrium dissociation constant, it was verified that the recombinant pre-miR-29b binds more strongly to $_L$-arginine (K_D between 10^{-6} and 10^{-7} M) than to $_L$-lysine (K_D between 10^{-5} and 10^{-7} M). This study also disclosed that the structure of the pre-miR-29b is sensitive to changes in the physical and chemical environmental conditions. In general, the results obtained provide valuable information for the optimization and implementation of $_L$-lysine and $_L$-arginine amino acids as chromatographic ligands, in order to improve the efficiency of pre-miR-29b purification.

Lysine-agarose matrix was the first support to be tested for the purification of pre-miR-29b. Due the presence of the amine groups in its structure, it is suggested that the main interactions established between nucleic acids and the $_L$-lysine amino acid are electrostatic. Thus, initial experiments were performed to choose the best binding/elution conditions for pre-miR-29b, using sodium chloride gradients. However, under these conditions the RNA binding was not effective and the selective purification of pre-miRNA was not achieved. Therefore, the retention behavior of pre-miR-29b was evaluated using an ammonium sulfate stepwise gradient (Paper V), in order to achieve higher specificity. Despite the effectiveness of lysine-based methodology in the purification of pre-miR-29b, the requirement for high salt concentration can be seen as a disadvantage, especially with regard to biotechnological and clinical applications.

To overcome this limitation and to improve pre-miR-29b purification, the arginine-agarose matrix was used. The application of arginine as specific ligand allowed the pre-miR-29b recovery under mild salt conditions, using sodium chloride gradients, showing that this matrix can be a good alternative to purify pre-miR-29b (Paper VI). The arginine ligand allowed the purification of the pre-miR-29b using three different elution strategies, namely by using sodium chloride (90% of purity and 97% of yield using a low salt concentration) and ammonium sulfate (33% of purity and requires high salt concentrations) gradients, or by establishing a competitive elution strategy with arginine (98% of purity and 57% of yield). Although electrostatic interactions are most prevalent in the arginine matrix, it was verified the presence of other interactions due the binding and elution conditions used. Moreover, the quality control analysis revealed high integrity of pre-miR-29b preparations as well as high purity degree and recovery yields, eliminating *R. sulfidophilum* impurities (proteins and

endotoxins) as well as other species of small RNAs, which can origin adverse effects and inflammatory response to the patients.

Taking into account that the structure of the chromatographic supports is continuously optimized to afford rapid and efficient separations, it was also tested a monolithic support to purify the pre-miR-29b, in order to overcome the limitations associated with the conventional supports in the purification of miRNAs. The application of the agmatine monolithic support for pre-miR-29b purification revealed a specific recognition of the pre-miR-29b that was totally isolated from other small RNAs, which represented an advantage to obtain highly pure RNA in a short time (Paper VII). These results were useful for the implementation of a new affinity chromatographic strategy using monoliths immobilized with specific ligands, such as agmatine, to efficiently and selectively purify the pre-miR-29b. In addition, this strategy allowed an efficient pre-miR-29b separation without flow rate dependence using similar binding and elution strategies to those used with arginine-agarose. With this study it was verified that the dynamic binding capacity for RNA molecules is dependent of the feed concentration and the characterization of the modified monolith revealed that a maximum binding capacity of 8.08 mg/mL was reached to a RNA concentration of 0.25 mg/mL. Moreover, the dissociation constant value obtained was 2.6×10^{-7} M, revealing a good affinity interaction between the agmatine ligand and pre-miR-29b. The quality control analysis in the final pre-miR-29b sample revealed that the removal of host impurities (proteins and small RNAs) was efficient. In fact, this new monolithic support arises as a powerful instrument on the miRNA purification to be used in further clinical applications, providing a more rapid and economical purification platform, resulting in a short contact time with pre-miR-29b molecules, which preserves the structural stability and integrity of target molecules.

Thus, the results and conclusions obtained in these studies suggest that the mechanism inherent to the purification of the pre-miR-29b results from the occurrence of multiple non-covalent interactions, including electrostatic, hydrophobic, hydrogen bonds, van der Waals forces and cation–π interactions, which combined induce a specific biorecognition of the pre-miR-29b by arginine, lysine and agmatine amino acids. In general, the application of amino acids-based affinity chromatography allowed the selective, efficient and specific isolation of the target pre-miRNA from the complex biological mixture of other sRNAs with high recovery yield, integrity and good purity, demonstrating thus the potential and versatility of these ligands in the purification of pre-miR-29b, in a single unit operation. Furthermore, the purification of the pre-miR-29b using the amino acids-based affinity chromatography showed several improvements over the currently used purification methods, thus proving to be an interesting option for the downstream processing of miRNA therapeutic products.

After the purification of the target pre-miRNA, the project was focused on the development of delivery systems able to encapsulate, protect and promote the delivery of pre-miR-29b to the target cells. Initially, as described in paper VIII, a systematic study of three polymers,

polyethylenimine (PEI), chitosan (CS) and poly(allylamine), with different structural characteristics (such as molecular weights, charge densities and backbone structure) was performed, in order to design a successful non-viral delivery system for small RNAs. The polymers of PEI and CS stood out in the condensation of small RNA as well as in relation to its physicochemical characteristics, namely size, zeta potential, morphology, encapsulation efficiency and complex stability.

In the previous papers it was possible to develop efficient methodologies to recover pre-miR-29b with a high purity degree, in particular with arginine-agarose matrix. Thus, in the paper IX, is described how the recombinant pre-miR-29b was condensed and some systems were prepared and characterized to encapsulate and protect the pre-miR-29b activity. All of the polyplexes demonstrated high loading capacity, small sizes and exhibited a strong positive charge on their surface. Moreover, the results showed that the levels of human BACE1 protein expression were significantly decreased, by approximately 80%, in cells transfected with polyplexes loaded with recombinant pre-miR-29b relatively to untreated cells and cells treated with scrambled RNA and miR-29 synthetic. Consequently, endogenous $A\beta_{42}$ levels were also significantly reduced in about 45%. It is important to highlight that the therapeutic effect of pre-miR-29b in BACE1 mRNA silencing was also achieved, with a mRNA reduction of approximately 77% in cells transfected with CS-SA-Lf/pre-miR-29b and 69% in those transfected by PEI-SA-Lf/pre-miR-29b. Overall, these results showed that the miR-29b can induce the suppression of the expression levels of Aβ peptides in neuronal cells, showing a causal relationship between miR-29b expression and BACE1 activity, and, consequently, Aβ generation. Considering the application of the pre-miR-29b in the brain, the delivery systems previously characterized were functionalized with ligands, to facilitate their access and interaction with specific molecules expressed on the surface of BBB endothelial cells. In the paper X, it was demonstrated that CS functionalized with lactoferrin and stearic acid cross the BBB quickly and with high transfection efficiency, causing an increase of the pre-miRNAs concentration in the brain.

According to the results obtained in this doctoral research work and comparing with previously published data, it was developed a biotechnological platform that allows biosynthesis, purification and transfection of the recombinant pre-miR-29b using polyplexes. With the successful implementation of this methodology it was obtained the highest decrease ever reported for the hBACE1 and endogenous $A\beta_{42}$ expression levels in AD model cells. Overall, the development and implementation of these cutting-edge approaches allows obtaining high quantities of pure pre-miR-29b, in its biologically active form, for further application in many molecular biology subjects. This approach also provides the basis for the improvement of the currently available methodologies of microRNA-based therapeutics, not only for neurological disorders but also for other diseases, and can be translated to additional therapeutic targets that may be of potential clinical interest in the future.

Future trends

Overall, it can be asserted that the main aims of this research work were fulfilled. However several challenging questions arisen that can be addressed as future perspectives. The integration of innovative affinity chromatographic strategies in the global bioprocess of pre-miR-29b biosynthesis and purification will be required for removing the host contaminants from the extracellular pre-miR-29b. Thus, the development of a selective strategy for efficiently isolate the extracellular pre-miR-29b will allow recovering this target miRNA directly from the culture medium without cells lysis and, consequently, without employing organic solvents and other harmful reagents.

Following the work already performed, more studies can be developed to motivate the improvement of the already implemented chromatographic techniques or the establishment of new purification approaches. In this way, in order to improve the specificity, selectivity and throughput of the bioseparation methodology for purification of the target pre-miRNAs, other affinity purification strategies can be implemented, using other immobilized amino acids, its derivatives or peptides or even testing other specific ligands like complementary nucleotide sequences to pre-miRNAs. These ligands could be immobilized onto different chromatographic matrices, such as agarose-based and monoliths to purify pre-miRNAs from the constituents of culture medium, expecting the improvement of the process performance, namely considering the purification degree and recovery yield.

Likewise, it is extremely necessary to understand the phenomenon of biorecognition, since the identification of the interactions involved in the isolation of pre-miRNA can be very important, allowing the control and manipulation of the chromatographic conditions responsible for the recognition of the pre-miRNA molecules. Accordingly, to characterize the binding recognition, as well as the thermodynamic parameters underlying the main interaction mechanism between pre-miRNAs and the different affinity ligands, and to determine the magnitude of kinetics and/or affinity constants, it could be used Nuclear Magnetic Resonance (NMR) spectroscopy, Flow Microcalorimetry (FMC) and Surface Plasmon Resonance (SPR), respectively. Furthermore, in order to fully characterize and compare the novel supports, dynamic binding capacity studies with target pre-miRNAs can be performed under different operation conditions (e.g. feed concentration, flow rate, pH and salt concentration), allowing the establishment of the best ligands and conditions to purify the target pre-miRNAs.

On the other hand, to improve the delivery of pre-miRNA therapeutics to the cells and the cellular response, different delivery systems based on polymers, such as polymeric nanoparticles (e.g. Poly(lactic-co-glycolic acid)) and poloxamer micelles (Pluronic® block copolymers) can be developed and characterized. Moreover, as these systems are so

versatile, they can be functionalized with brain-targeting molecules, either on their surface or on the polymeric network, to be recognized by cell surface receptors of BBB, and promote targeting to specific cells and tissues.

With the successful implementation of these methodologies, it could be further evaluated the therapeutic function of the recombinant pre-miRNA in *in vivo* studies and test its efficacy in improving cognition and biochemical hallmarks of disease, using mice models of AD (3xTg and APPswe/PSEN1ΔE9). To accomplish this objective, several studies are required to establish the range of doses and administration routes to be employed in the pharmacological studies (biodistribution/pharmacokinetics and toxicity studies). Finally, it could also be evaluated and compared the performance of recombinant pre-miRNAs and conventional therapeutic drugs. These studies should be first performed *in vitro*, but the development of some *in vivo* studies could bring important insights about the efficacy and safety of gene therapy, either used separately or in combination with conventional drugs, opening a new prospect of cure, due to the possible synergistic effect.